

Polycarbonate to Polyether Conversions

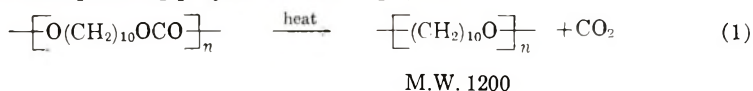
K. C. STUEBEN, *Union Carbide Corporation, Plastics Division, Research and Development Department, Bound Brook, New Jersey*

Synopsis

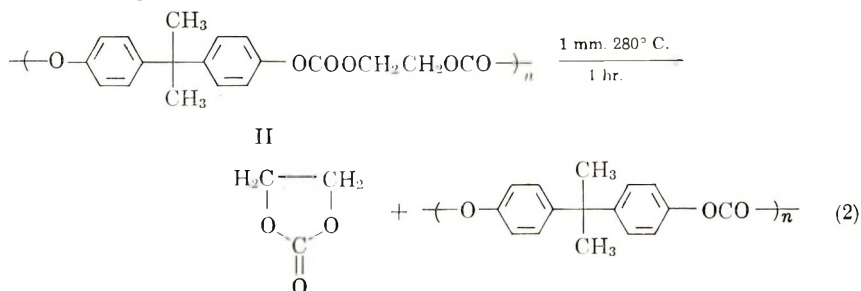
The preparation of aromatic polycarbonates via the base-catalyzed disproportionation of suitable alkyl-aryl carbonates (Alkyl-OCOO-Aryl-OCOO-Alkyl) was found to be accompanied by the formation of alkyl-aryl ethers. Substitution of a poly(alkyl aryl carbonate) in place of the monomeric species resulted in the formation of a poly(alkyl aryl ether). Thus, it was possible to convert a copolymer of ethylene glycol and 2,2-bis(4-hydroxyphenyl)propane to the corresponding poly(alkyl aryl ether) with only slight loss of molecular weight. The structure of this polyether and a partially converted poly(carbonate ether) were established by analytical and degradative techniques. Conversions of other poly(alkyl aryl carbonates) were also achieved but with less success because of competing reactions. A possible mechanism for these conversions is presented.

INTRODUCTION

The pyrolysis of organic carbonates to ethers and carbon dioxide is a well documented reaction.¹⁻⁶ In general, this reaction has been limited to small organic molecules, but occasional references^{7,8} to its occurrence in polymer systems have appeared. Hill⁸ noted that some low molecular weight poly(decamethylene oxide) formed during the thermal depolymerization of the corresponding polycarbonate [eq. (1)]:



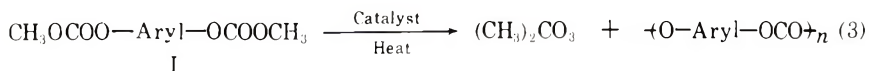
No attempts were made to extend this finding until recently, when Sweeney heated the copolycarbonate(II) of ethylene glycol and bisphenol A [2,2-bis(4-hydroxyphenyl) propane] under vacuum in an effort to prepare the corresponding poly(alkyl aryl ether). However, instead of the desired product, cyclic ethylene carbonate and bisphenol A polycarbonate were obtained [eq. (2)].



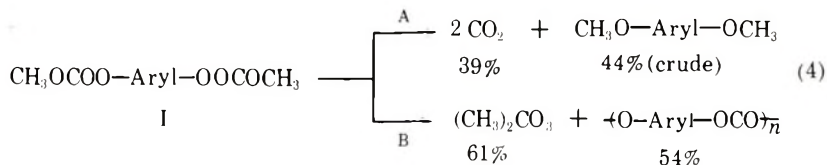
Recent work in these laboratories indicated that the desired conversion might be achieved if different conditions were employed.

DISCUSSION

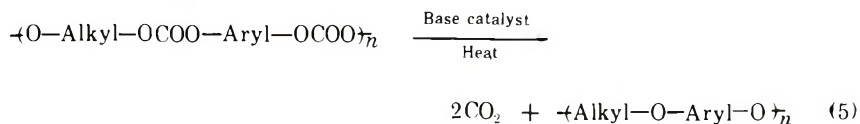
One of the many routes available for the preparation of aromatic polycarbonates is the disproportionation of bis(alkyl) aryl carbonates (I) [eq. (3)]



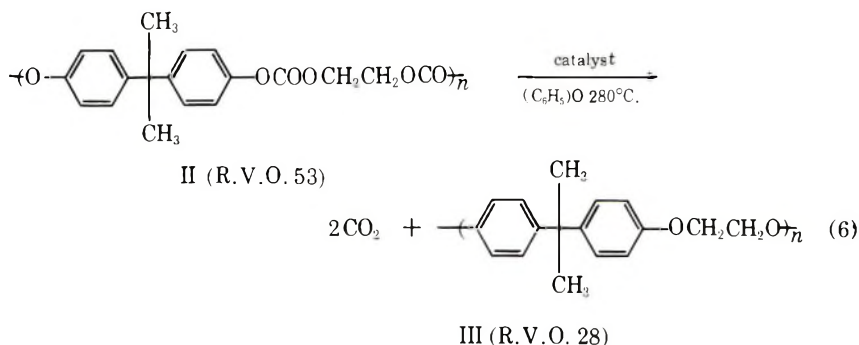
A catalyst¹⁰ comprised of sodium methylate and tetrabutyl titanate was employed for this reaction recently and was found to give only low molecular weight polymer. The failure to form high polymer was traced to the formation of nonpolymerizable by-products subsequently identified as alkyl aryl ethers. Closer examination revealed that the competing side reaction (A) accounted for 40% of the products while the desired ester exchange (B) only 60% [eq. (4)]



The ease with which the ether formation occurred and the apparent absence of other products suggested that the side reaction itself might be useful for the preparation of poly(alkyl aryl ethers). This might be achieved [eq. (5)] by starting with a poly(alkyl aryl carbonate) in place of the monomeric carbonate(I)

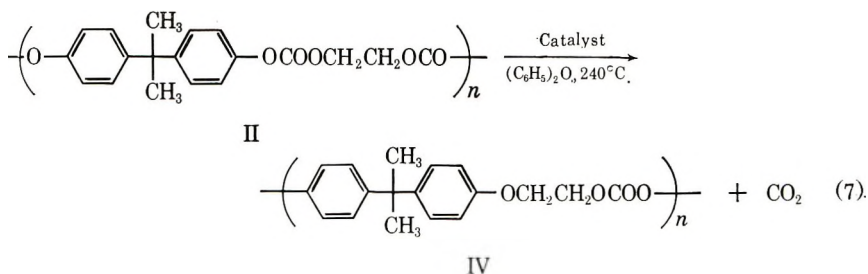


The copolymer(II) of ethylene glycol and bisphenol A studied earlier by Sweeney⁹ was chosen for the initial experiments. When heated together with an alkaline catalyst at 280°C. at atmospheric pressure, this copolymer evolved 98% of its carbonyl group as carbon dioxide. The product of this reaction (III), isolated in 67% yield, was still polymeric, although its reduced viscosity had decreased to half of the starting value [eq. (6)]. Thus, virtually every one of the connecting linkages broken during the elimination of carbon dioxide had reformed in the polyether product.

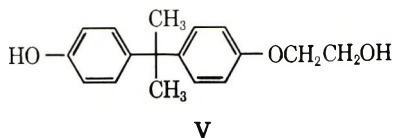


Verification that the product was indeed the desired polyether(III) was obtained by elemental analysis and infrared and NMR spectra.

When the copolycarbonate(II) was heated at a lower temperature (i.e., 240°C.), the evolution of carbon dioxide continued until only 50% complete, and then ceased. Isolation of the product afforded an 87% yield of polymer with a reduced viscosity (R.V.) of 0.28. The diminished carbonyl activity in the infrared and elemental analysis of the product indicated its structure to be the 1:1 ether-carbonate(IV).

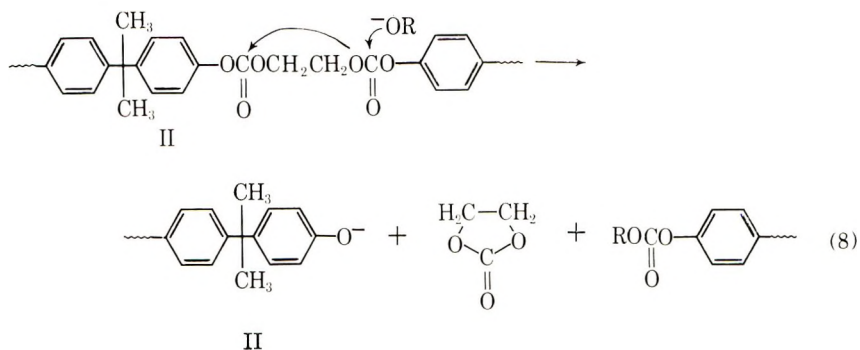


Because of the possibility of ester exchange preceding the ether-forming reaction, the alkyl and bisphenol groups might be randomly distributed throughout the molecule rather than alternating as shown. In order to gain more information about the structure of this polymer (IV), it was degraded by a combination of ammonia and aqueous caustic. Analytical data (elemental analysis, molecular weight, infrared, and NMR) on the hydrolyzate were in accord with the average structure (V). In addition, gas chromatographic

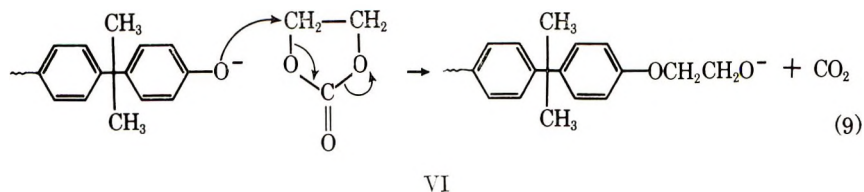


examination of the hydrolyzate (as the acetate) revealed the presence of bisphenol A residues as well as the related bis(β -hydroxyethoxy) derivative. No evidence was found for the presence of ethylene glycol or diethylene glycol residues in the hydrolyzate.

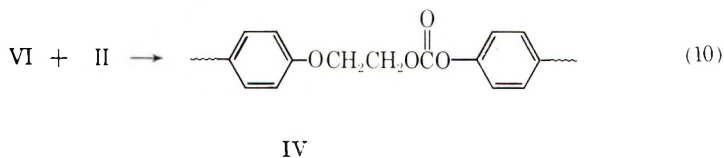
A possible mechanism for these polymer conversions which is consistent with the available evidence is given in eqs. (8)–(11). Attack of phenoxide or alkoxide ion (^-OR) at the ester carbonyl readily generates cyclic ethylene carbonate [eq. (8)].



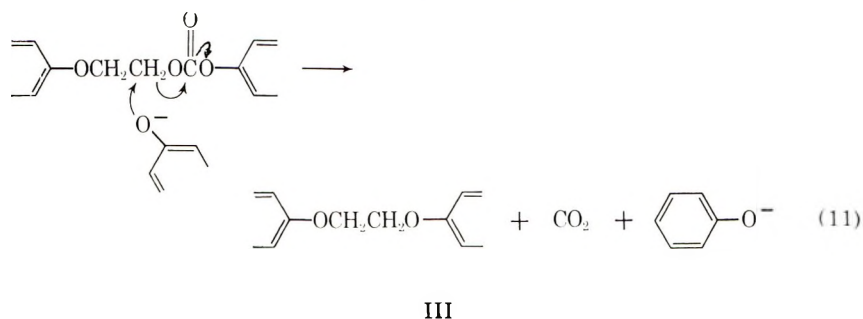
Under the conditions used in the present work, this reactive carbonate combines with the phenolate anion [eq. (9)¹¹] to form the alkyl aryl ether (VI)



and one mole of carbon dioxide. Further reaction of the anion (VI) with the starting alkyl aryl carbonate leads to the copoly(carbonate ether) (IV) as shown in eq. (10):



Elimination of the second mole of carbon dioxide from the copolymer (IV) is more difficult than step (9) and requires higher temperature, thus accounting for the two-step nature of the process.



Despite the possibility for various termination reactions such as olefin formation,¹² chain cleavage by catalyst, decomposition of the bisphenol moiety,¹³ and others,⁷ a surprisingly small amount of degradation was encountered in this particular case. This finding prompted an extension of this study to polymers incapable of forming reactive cyclic carbonates.

A copolymer of bisphenol A and diethylene glycol was found to liberate 86% of its carbon dioxide on heating to 220–245°C. for 8.5 hr. The product obtained in 65% yield possessed a reduced viscosity of 0.34 (orig. 0.23) and an elemental analysis which was in reasonable accord with that expected. In addition, the infrared spectrum of the product showed a considerably diminished carbonyl absorption. The copolycarbonate of bisphenol-A and 1,4-cyclohexanedimethanol required temperatures of approximately 295°C. before carbon dioxide was liberated, possibly because of increased steric hindrance. After 72% of the carbon dioxide had been evolved, the product was isolated and found to have an elemental analysis in accord with the expected structure. The remaining carbonyl groups apparently underwent other changes during this treatment, however, as evidenced by a shift of the carbonyl absorption in the infrared from 1740 cm.^{-1} to 1690 cm.^{-1} . Further elucidation of the structure was not undertaken because the reduced viscosity of the polymer had decreased from 0.67 to 0.22. The conversion was also attempted with other alkyl aryl copolycarbonates but in these cases, the reactions proved erratic and degradation too pronounced to warrant further effort.

Attempts were made to find less vigorous conditions for carrying out these reactions which would cause less degradation. Examination of other catalysts, including lithium chloride, alumina, sodium phosphate, and sodium and potassium carbonates, did not result in any improvement. The use of other solids,¹⁴ such as powdered glass, was also investigated briefly and found to have little effect. When tetramethylene sulfone was employed as solvent, the rate of carbon dioxide evolution did increase, possibly due to increased solubility of the catalyst but this also failed to eliminate the degradation process.

Certain alkyl aryl carbonates liberate carbon dioxide very readily, and this may limit their use as monomers in melt polymerizations. Thus, attempts to polymerize bisphenol-A with the bis(phenyl) carbonate of *p*-xylylene glycol at 200–240°C. with a lithium acetate catalyst resulted in the formation of low molecular weight polymer (R.V. 0.09) and an 87% yield of carbon dioxide. In this particular instance the expulsion of carbon dioxide took place readily, perhaps by a different mechanism¹⁵ (SNi) than those already suggested.

EXPERIMENTAL

Dimethyl-6,6'-3,3',5,5'-tetramethyl-1,1'-spirobiindane Carbonate

This compound was prepared by allowing 0.1 mole of the dihydroxy-spiroindane¹⁶ in 30 ml. of pyridine to react with 0.21 mole of methyl chloro-

formate at 10–15°C. Work up followed by crystallization from methanol afforded the crude product (48%), m.p. 150–160°C. Recrystallization from isopropanol raised the melting point to 171–173°C.

ANAL. Calcd. for $C_{22}H_{28}O_6$: C, 70.91%; H, 6.65%; Found: C, 70.91%, H, 6.80%.

Ether Formation during Polycarbonate Preparation

In a flask was placed 3.4730 g. (0.0088 mole) of the spiroindane methyl carbonate and 0.07 g. of sodium methoxide. The flask was sparged with dry nitrogen, the exit gases passing through a receiver cooled in Dry Ice then through a tube filled with Ascarite. On heating to 205–235°C., simultaneous evolution of gas and formation of dimethyl carbonate began and continued for 30 min. After an additional 25 min. at 245–260°C., vacuum (0.35 mm.) was applied followed by further heating at 270–297°C. for 15 min. During the vacuum application, an oily distillate (1.1978 g.) came over which was readily crystallized from 50:50 ethanol–water to yield 0.86 g. of a low-melting solid. Further recrystallizations gave product with m.p. 116.5–117°C.

ANAL. Calcd. for $C_{23}H_{28}O_2$: C, 82.1%; H, 8.4%; O, 9.5%; mol. wt. 336. Found: C, 80.90%; H, 7.93%; O, 10.85%; mol. wt. 306.

The infrared and NMR spectra indicate the material to be the dimethyl ether of the spiroindane, a known compound, m.p. 118°C. (reported,¹⁶ 118°C.). Also isolated from the reaction were 0.2761 g. of carbon dioxide (38.5%), 0.452 g. of dimethyl carbonate (61%), and 1.4839 g. residue polymer (54%). A total 98% of starting weight was accounted for.

Preparation of the Alkyl Aryl Polycarbonates

The general interfacial procedure used for the preparation of poly(alkyl aryl carbonates) is illustrated by the preparation of poly(ethylene-bisphenol-A carbonate). A solution of 6.85 g. (0.03 mole) of bisphenol A, 3.0 g. (0.075 mole) of sodium hydroxide, 15 drops of triethylamine, and 150 ml. of water was placed in a Morton flask along with 90 ml. of methylene chloride. Then a solution of 5.6 g. (0.03 mole) of freshly distilled ethylene glycol bischloroformate in 90 ml. of methylene chloride was added over a 15-min. period with stirring. An additional 15 drops of triethylamine were added at this point, and stirring was continued for an additional 10 min. The organic layer was removed and then washed by stirring for 10–15 min. each in the following sequence: 20 ml. water (2×), 200 ml. water containing 2 ml. H_3PO_4 , 200 ml. water (4×). Finally, the organic layer was coagulated in 1 liter of isopropanol, the polymer removed by filtration and dried in a vacuum oven at ca. 50°C. The reduced viscosity (0.2 g./100 ml. chloroform) at 25°C. was 0.53; the yield was 7.82 g.

Other polymers similarly prepared include the copolycarbonates of diethylene glycol-bisphenol-A.

ANAL. Calcd. for $(C_{21}H_{22}O_7)_n$: C, 65.27%; H, 5.74%; O, 28.99%. Found: C, 64.36%; H, 5.77%; O, 27.37%.

The copolycarbonate from 1,4-cyclohexanedimethanol-bisphenol-A was also prepared.

ANAL. Calcd. for $(C_{25}H_{28}O_6)_n$: C, 70.73%; H, 6.65%; O, 22.62%. Found: C, 71.54%; H, 6.91%; O, 20.22%.

Conversion of Poly(ethylene-bisphenol-A Carbonate) to the Corresponding Ether

In a side-arm test tube fitted with a gas inlet tube was placed 1.0 g. (0.00292 mole) of the ethylene glycol-bisphenol-A copolycarbonate(II) (reduced viscosity at 25°C. in chloroform = 0.53), 2 ml. of diphenyl ether, and 0.01 g. of the disodium salt of bisphenol A. (The hexahydrate was employed here. The small amount of water present volatilizes immediately under the conditions used and apparently does no harm. Use of the anhydrous form gave substantially the same results.) Argon was bubbled through the mixture and then into Drierite and tared Ascarite tubes. The reaction mixture was heated at 280°C., and the evolution of carbon dioxide with time followed by the increase in weight of the Ascarite; results are shown in Table I.

TABLE I

Time, min.	Wt. CO ₂ , g.	% CO ₂
30	0.0963	37.5
40	0.1212	47.2
50	0.1352	52.5
70	0.1452	56.5
90	0.1542	60.0
130	0.1702	66.0
250	0.1882	73.5
490	0.2313	86.5
595	0.2473	96.0
670	0.2503	97.4
760	0.2503	97.4

At this time the reaction mixture was light brown in color and still viscous. It was diluted with several milliliters of methylene chloride, treated with charcoal and then coagulated in isopropanol (coagulation was often facilitated by first cooling the isopropanol with Dry Ice) to give 0.5 g. (67%) of fibrous, ivory-colored polymer having a reduced viscosity of 0.28 in chloroform at 25°C. Careful drying under high vacuum was necessary to remove solvent. The product began to soften and flow at 80°C.

ANAL. Calcd. for $(C_{17}H_{18}O_2)_x$: C, 80.3%; H, 7.1%; O, 12.6%. Found: C, 79.34%; H, 6.95%; O, 13.62%.

A solution spectrum of this polymer in chloroform (5%) was consistent with the polyether structure. Very little carbonyl was evident.

An NMR spectrum (Varian A-60) run on the polymer was also consistent with the proposed polyether structure. The chemical shift (relative to

tetramethylsilane) relative areas, and assignments are: 96 cycles/sec., 5.70 ($(\text{CH}_3)_2\text{C}$); 256 cycles/sec., 3.75 ($-\text{CH}_2\text{CH}_2-$); and 402–438 cycles/sec. (4 peaks), 8.55 (aromatic H).

Partial Conversion of Poly(ethylene-bisphenol-A Carbonate) to the Poly(carbonate Ether)(IV)

By a procedure similar to that described above, a mixture of 4.0 ml. of diphenyl ether, 0.02 g. of the disodium salt of bisphenol-A hexahydrate, and 4.0 g. of the copolycarbonate(II) was heated in a stream of argon. After heating 15 min. at 224–240°C., the sample had evolved 0.4336 g. (42%) of carbon dioxide, while a blank yielded only 0.02 g. (1.9%). Further heating at 233–247°C. for 4 hr. raised the total carbon dioxide evolved from the sample to 0.5450 g. (52.9%) and that from the blank to 0.3522 g. (34.4%). The infrared spectrum of the blank showed presence of ethylene carbonate at this point. Coagulation of the sample in isopropanol as above afforded 3.01 g. (87%) of polymer having a reduced viscosity (25°C., CHCl_3) of 0.28.

ANAL. Calcd. for 1:1 carbonate-ether ($\text{C}_{15}\text{H}_{18}\text{O}_4$)_n: C, 72.5%; H, 6.08%; O, 21.4%. Found: C, 73.88%; H, 6.27%; O, 20.23%.

Ammonolysis of Poly(carbonate Ether)

Ammonia degradation of the poly(carbonate ether) prepared above was carried out by contacting 1.0 g. of the polymer with a solution of 8 ml. of methanol and 8 ml. of concentrated ammonium hydroxide. After standing for 2 days at room temperature with occasional stirring, the original solid had been converted to a tan oil. The reaction mixture was then poured onto ice and acidified with dilute hydrochloric acid. The oily layer formed was extracted into methylene chloride, dried with magnesium sulfate, and then evaporated to yield 0.92 g. of a viscous liquid whose infrared spectrum showed strong $-\text{OH}$ absorption and carbonyl absorption at 1695 cm^{-1} (urethane). (Under these same conditions, bisphenol-A polycarbonate is completely cleaved to bisphenol-A.)

Further hydrolysis was achieved by refluxing 15 min. with a solution of 1 g. of potassium hydroxide in 5 ml. of methanol. The methanol was removed *in vacuo*, replaced with 25 ml. of water, and the mixture then acidified with hydrochloric acid. The resultant oil was extracted into ether (four times), dried, and concentrated to give ca. 0.8 g. of viscous liquid. The infrared spectrum showed strong $-\text{OH}$, no carbonyl and was consistent with a material having the average structure $\text{HOC}_6\text{H}_4\text{C}(\text{CH}_3)_2\text{C}_6\text{H}_4\text{OCH}_2\text{CH}_2\text{OH}$.

ANAL. Calcd. for $\text{C}_{17}\text{H}_{20}\text{O}_3$: C, 74.97%; H, 7.4%; O, 17.63%; mol. wt. 272. Found: C, 75.76%; H, 7.59%; O, 17.01%; mol. wt. 282 \pm 2 (vapor phase osmometer).

The NMR spectrum of this material displayed absorptions consistent with the average structure above (Table II). The lack of any difference in chemical shift for the methylene protons is somewhat unusual. Acetylation, however, resolved these peaks.

TABLE II

Type	Chemical shift, cycles/sec.	Area	
		Found	Calcd.
CH ₃ -C-CH ₃	95	5.70	6
ArOCH ₂ -	236	4.2	4
HOCH ₂ -	236		
ArH-	400-440	8	8

Acetylation was accomplished by conventional means. The acetate had an NMR showing the absorptions given in Table III, again consistent with the average structure:

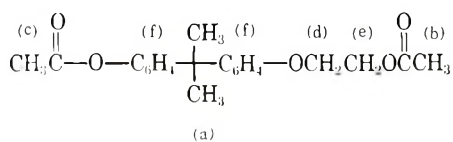


TABLE III

H	Type	Chemical shift, cycles/sec.	Area
a	CH ₃ -C-CH ₃	97	6.35
b	AcOCH ₂ -	118	2.71
c	AcOAr	130	2.81
d	-CH ₂ OAr	247	3.84
e	-CH ₂ OAc	257	
f	ArH	400-440	8.30

Gas chromatographic analysis of this acetate on a silicone-rubber column at 310°C. demonstrated the presence of bisphenol-A diacetate and the bis-(β-acetoxyethoxy) derivative.¹⁷

Partial Conversion of Poly(1,4-bisphenol-A-cyclohexanedimethylene) Carbonate to its Ether Carbonate

A mixture of 1.0 g. of poly(bisphenol-A, 1,4-cyclohexane-dimethylene) carbonate (R. V. 0.67), 1.0 ml. of diphenyl ether, and 0.01 g. of sodium methylate was heated together in a stream of argon for 7.5 hr. at 291-298°C. During this treatment, a total of 72% of the carbonyl present in the original polymer was evolved as carbon dioxide. After removing some gel species by filtration, the product was isolated by coagulation in isopropanol in 54% yield and had a reduced viscosity of 0.22 in chloroform at 25°C. An infrared spectrum of the product in chloroform showed considerable similarity to the starting polymer but otherwise had greatly reduced carbonyl intensity (from 10% to 50% transmission) and had undergone a shift from 1740 cm.⁻¹ to 1690 cm.⁻¹.

ANAL. Calcd. for C₂₃H₂₈O₂(C₂O₄)_{0.28}: C, 78.30%; H, 7.82%; O, 13.82%. Found: C, 77.67%; H, 7.77%; O, 14.49%.

The author is indebted to Miss O. Garty for performing the gas chromatographic work and to Dr. W. Beach and G. Hellerman for the NMR data.

References

1. Searles, S., *J. Am. Chem. Soc.*, **82**, 2928 (1960).
2. Malkemus, J. D., V. A. Currier, and J. B. Bell, U. S. Pat. 2,856,413 (Oct. 14, 1958).
3. Reynolds, D. O., and K. R. Dunham, U. S. Pats. 2,789,967; 2,789,969 (April 23, 1957).
4. Ritchie, P. D., *J. Chem. Soc.*, **1935**, 1056.
5. Gomberg, M., *Ber.* **46**, 225 (1913).
6. Einhorn, A., *Ber.*, **42**, 2237 (1909).
7. Schnell, H., *Angew. Chem.*, **68**, 633 (1956).
8. Hill, J. W., *J. Am. Chem. Soc.*, **57**, 1131 (1935).
9. Sweeny, W., *J. Appl. Polymer Sci.*, **5**, S15 (1961).
10. Bestfamil'nyĭ, I. B., V. N. Kotrelev, and T. D. Kostryukova, U.S.S.R. Pat. 138,030; *Chem. Abstr.*, **56**, 4956* (1962).
11. Carlson, W. W., and L. H. Cretcher, *J. Am. Chem. Soc.*, **69**, 1952 (1947).
12. Smith, G. G., *J. Org. Chem.*, **28**, 3547 (1963).
13. Schnell, H., and H. Krimm, *Angew. Chem.*, **75**, 662 (1963).
14. Newman, M. S., and E. G. Calfisch, Jr., *J. Am. Chem. Soc.*, **80**, 862 (1958).
15. Kice, J. L., and R. A. Burtch, *Tetrahedron Letters*, **25**, 1693 (1963).
16. Curtis, R. F., *J. Chem. Soc.*, **1962**, 415.
17. Coleman, G. H., B. C. Hadler, and R. W. Sapp, U. S., Pat. 2,359,622, (Oct. 3, 1944).

Résumé

On a trouvé que la préparation des polycarbonates aromatiques par disproportionnement, catalysée par les bases, des alcoyl-arylcarbonates (Alcoyl—OCOO—Aryl—OCOO—Alcoyl) est accompagnée de la formation d'éthers alcoyl-aryliques. La substitution d'une espèce monomérique par un polycarbonate alcoyl-arylique entraîne la formation d'un éther poly alcoyl-arylique. Il est donc possible de transformer un copolymère de l'éthylène glycol et du 2,2-bis (4-hydroxyphényl)-propane en poly (alcoyl aryl éther) correspondant avec seulement une diminution de poids moléculaire très petite. On a déterminé la structure de ce poly-éther et d'un éther polycarbonate partiellement transformé par des techniques analytiques et des techniques de dégradation. La transformation d'autres poly-alcoyl aryl-carbonates a aussi été faite, mais avec moins de succès à cause des réactions de compétitions. On présente un mécanisme possible pour ces transformations.

Zusammenfassung

Die Darstellung aromatischer Polykarbonate durch basenkatalysierte Disproportionierung geeigneter Alkyl-Arylkarbonate (Alkyl—OCOO—aryl—OCOO—alkyl) war von der Bildung von Alkyl-Aryläthern begleitet. Ersatz des Monomeren durch ein Poly(alkylarylkarbonate) führte zur Bildung eines Poly(alkylaryläthers). So war es möglich, ein Kopolymeres aus Äthylenglykol und 2,2-Bis(4-hydroxyphenyl)propan mit nur geringem Molekulargewichtsverlust in den entsprechenden Poly(alkylaryläther) umzuwandeln. Die Struktur dieses Polyäthers und eines partiell umgewandelten Poly(Karbonat-äthers) wurde analytisch und durch Abbau ermittelt. Die Umwandlung anderer Poly(alkylarylkarbonate) war ebenfalls, aber wegen auftretender Konkurrenzreaktionen mit weniger Erfolg, möglich. Ein Mechanismus für diese Umwandlungen wird angegeben.

Received December 16, 1964

Revised March 27, 1965

Prod. No. 4715A

Study of the Orientation of Light-Sensitive Tetrazonium Salt in Poly(vinyl Alcohol)

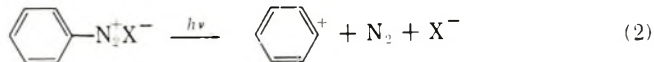
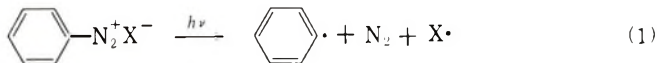
TAKAHIRO TSUNODA and TSUGUO YAMAOKA, *Faculty of
Engineering, Chiba University, Chiba, Japan*

Synopsis

$\nu(N\equiv N)$ band of the diazo or tetrazonium salt, derived from *p*-methoxyaniline, *p*-hydroxyaniline, benzidine, or *o*-dianisidine shows perpendicular dichroism in the stretched poly(vinyl alcohol) film. This means that these salts are directing their longer axes perpendicularly to the direction of the stretching. However, that of the diazonium salt from *p*-aminodiphenyl or *o*-anisidine shows no dichroism. From the above facts, it is concluded that the interactions between the polar groups of poly(vinyl alcohol) and those on the both ends of the diazo or tetrazonium salt such as diazo, methoxy, and hydroxy group result in the perpendicular orientation of the diazo or tetrazonium molecule.

INTRODUCTION

Most aromatic diazonium salts are sensitive to light, and decompose photochemically according to the two primary processes represented by eqs. (1) and (2).¹



Some diazonium salts in polymers, when they are decomposed on irradiation, insolubilize them in their solvents.² We studied the insolubilizing effects of several diazonium salts for poly(vinyl alcohol), and found the tetrazonium salts were more effective than the diazonium salts. From an infrared spectroscopical study, it was concluded that the tetrazonium salt crosslinked the chain molecules of poly(vinyl alcohol) on irradiation with light. In the present paper we report results of a study of the infrared dichroism of the tetrazonium and diazonium salts in stretched poly(vinyl alcohol) film to determine interactions between poly(vinyl alcohol) and these salts.

EXPERIMENTAL

Materials

The diazonium salts used were synthesized from the corresponding amines and purified by repeated salting out.

Poly(vinyl alcohol) was obtained from Nippon Gosei Chemical Co., Ltd. The average degree of polymerization was 2600 and the saponification was over 99.5%. We used this material after further saponification and purification.

Measurement of the Infrared Dichroism

The sample for determination of the infrared dichroism was prepared in the following way. A 10-g. portion of poly(vinyl alcohol) was dissolved in 100 ml. of water on a steam bath, and then 0.5 g. of the diazonium salt was added in 10 ml. of this solution. This mixture was poured onto a nicked plate having a smooth surface. After drying, the film was stripped from the plate, attached with adhesive tape on the stretching apparatus shown in Figure 1, and stretched to about six times the initial length. The dichroism was measured with a Hitachi EPI-2S infrared spectrophotometer equipped with sodium chloride prism and a silver halide polarizer.

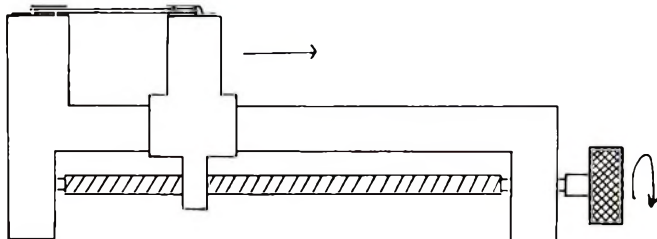


Fig. 1. Apparatus used for stretching the sample film.

RESULTS

In Figure 2, the spectrum of the tetrazonium salt derived from benzidine is shown. The band in the 2100–2300 cm.^{-1} region appears in all spectra of the diazonium salts used. This band has been attributed by Whetsel, Hawkins, and Johnson³ and by Aroney, LeFevre, and Werner⁴ to the triple bond of the diazonium group. All spectra show a strong band at 1595–1575 cm.^{-1} too, though the assignment of this band is not completely understood. However, when the diazonium salts are decomposed photo-

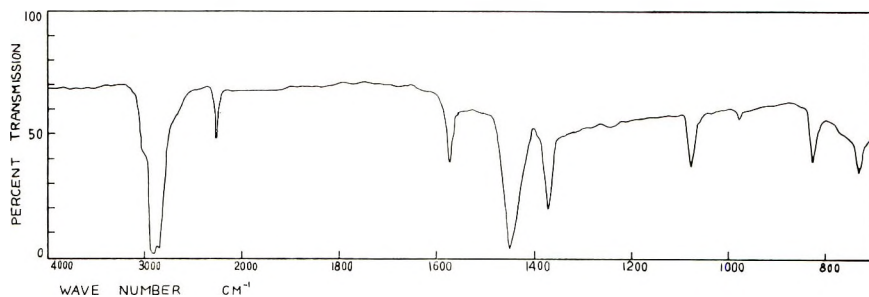


Fig. 2. Infrared spectrum of the tetrazonium salt derived from benzidine (Nujol mull).

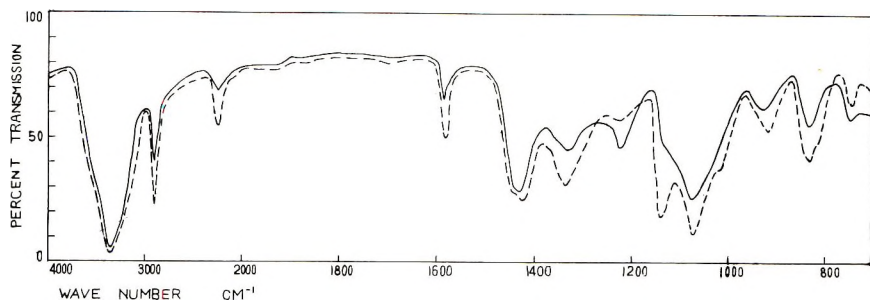


Fig. 3. Infrared spectra of tetrazotized benzidine in stretched poly(vinyl alcohol) film: (—) electric vector of polarized incident radiation parallel to direction of stretching; (---) electric vector perpendicular to the direction of stretching.

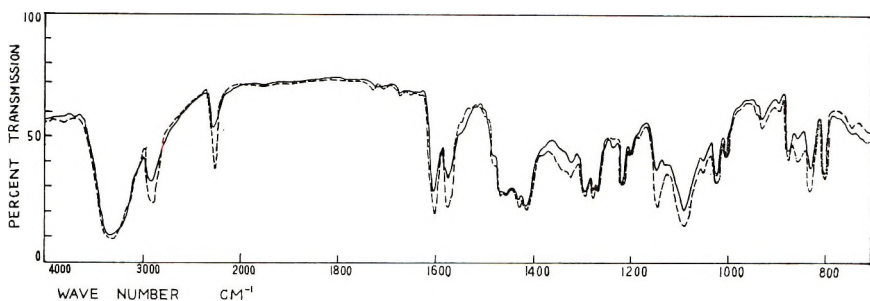


Fig. 4. Infrared spectra of tetrazotized *o*-dianisidine in stretched poly(vinyl alcohol) film: (—) electric vector parallel to direction of stretching; (---) electric vector perpendicular to direction of stretching.

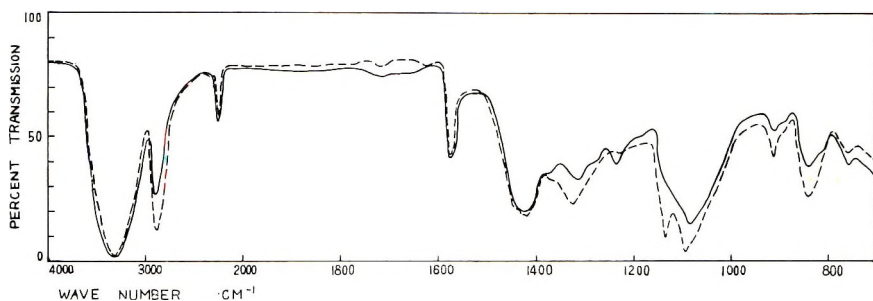


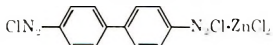
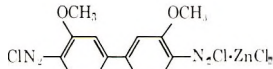
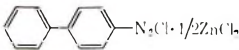
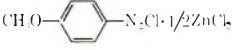
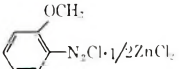
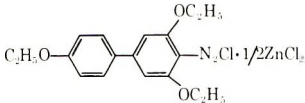
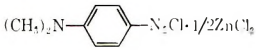
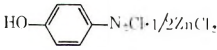
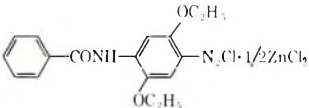
Fig. 5. Infrared spectra of diazotized *p*-aminodiphenyl in stretched poly(vinyl alcohol) film: (—) electric vector parallel to direction of stretching; (---) electric vector perpendicular to direction of stretching.

chemically or thermally, this band decreases at the same rate as that of decrease of the $\nu(\text{N}\equiv\text{N})$ band, and the direction of the transition moment of this band is same as that of $\nu(\text{N}\equiv\text{N})$ band. Judging from the above facts, this band may be attributed to the stretching vibration of the C—N bond between the aromatic ring and the nitrogen of the diazonium group. Figures 3 and 4 show the infrared dichroism spectra of the tetrazonium salts of benzidine and *l*-dianisidine in the stretched poly(vinyl alcohol) film.

According to these spectra, the $\nu(\text{N}\equiv\text{N})$ band of the diazonium group and the $\nu(\text{C}-\text{N})$ band have perpendicular dichroism and their R_d values are about the same. On the other hand, the $\nu(\text{N}\equiv\text{N})$ band of *p*-diazodiphenyl chloride does not show perpendicular dichroism, although it is similar to tetrazotized benzidine in structure (Fig. 5).

In Table I, the dichroic ratios of the $\nu(\text{N}\equiv\text{N})$ band of diazo and tetrazonium salts in stretched poly(vinyl alcohol) film are listed. The dichroic ratio R_d is represented by the equation: $R_d = D_{\parallel}/D_{\perp} = \log(I_0/I_{\parallel})/\log(I_0/I_{\perp})$ where I_0 is the intensity of the incident radiations, I_{\parallel} and I_{\perp} are the intensity of parallel and perpendicular radiations, respectively, after passage through the sample, and D_{\parallel} and D_{\perp} are the respective absorbances. The dichroic ratio is greater than unity for parallel bands, and

TABLE I
Infrared Dichroism of Diazo and Tetrazonium Salts in Stretched Poly(vinyl Alcohol) Film

Diazo and tetrazonium salt	Di- chroism	R_d value of $\nu_{as}(\text{CH}_2)$ of poly- (vinyl alcohol)	R_d value of $\nu(\text{N}\equiv\text{N})$
	\perp	0.55	0.40
	\perp	0.53	0.60
	—	0.45	1
	\perp	0.37	0.75
	—	0.25	1
	—	0.42	1
	\perp	0.45	0.63
	\perp	0.40	0.60
	—	0.45	1

smaller than unity for perpendicular bands. In order to indicate the extent of the orientation of polymer molecules, the R_d values for the 2945 cm.^{-1} band assigned to $\nu_{as}(\text{CH}_2)$ of poly(vinyl alcohol) was measured.

DISCUSSION

Table I shows that $\nu(\text{N}\equiv\text{N})$ bands of tetrazotized benzidine and *o*-dianisidine have the dichroism perpendicular to the chain axis of the oriented poly(vinyl alcohol) molecule. Figure 6 shows a simple molecular orbital diagram of tetrazotized benzidine.

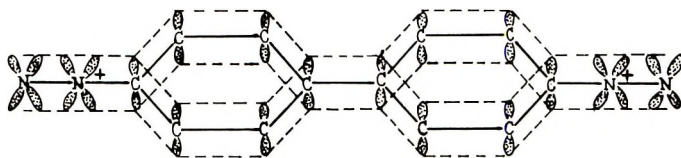


Fig. 6. Molecular orbital diagram of tetrazotized benzidine.

As the nitrogens in conjugation with phenyl rings release one p electron and forming four covalent bonds, the σ bonds of these nitrogens consist of sp hybrid orbitals.

Accordingly, the direction of the $-\text{N}\equiv\text{N}^+$ bond and of its transition moment is in the direction of the long axis of the diazo or tetrazonium molecule.

When the poly(vinyl alcohol) film is stretched, the diazonium molecules in the film will also be oriented in the direction of stretching by the physical stress. So, the perpendicular dichroism of the $\nu(\text{N}\equiv\text{N})$ band of the tetrazonium salts indicates that the tetrazonium molecules are directing their longer axes perpendicular to the polymer chains.

p-Diazodiphenyl chloride, which resembles tetrazotized benzidine in its structure except that it has only one diazonium group, shows no perpendicular dichroism at the $\nu(\text{N}\equiv\text{N})$ band; $\nu(\text{N}\equiv\text{N})$ of *o*-methoxybenzediazonium chloride shows parallel dichroism, while that of *p*-methoxybenzediazonium chloride shows perpendicular dichroism.

Thus, Table I indicates that the compounds which have the polar groups on the both ends of the longer axis of the molecule show perpendicular dichroism at $\nu(\text{N}\equiv\text{N})$ band. This would mean that the interactions of polar groups of the diazo or tetrazonium salts with those of poly(vinyl alcohol) molecules result in perpendicular orientation of these salts.

2,4,5-Trimethoxydiphenyl-4-diazonium chloride shows no perpendicular dichroism, probably because of the effects of the methoxy groups in the *ortho* and *meta* positions.

In Figures 7 and 8, the R_d values of $\nu(\text{N}\equiv\text{N})$ are plotted against the extent of the orientation of the polymer molecules. As the degree of orientation of the polymer increases, the R_d value of $\nu(\text{N}\equiv\text{N})$ also increases.

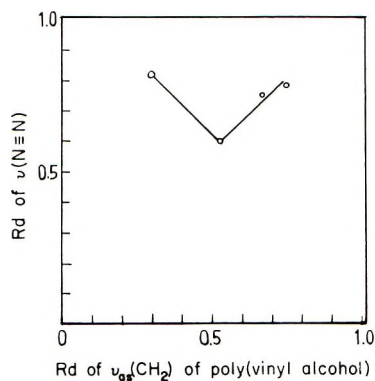


Fig. 7. R_d of $\nu(\text{N}\equiv\text{N})$ of tetrazotized *o*-dianisidine vs. the extent of orientation of poly(vinyl alcohol) film.

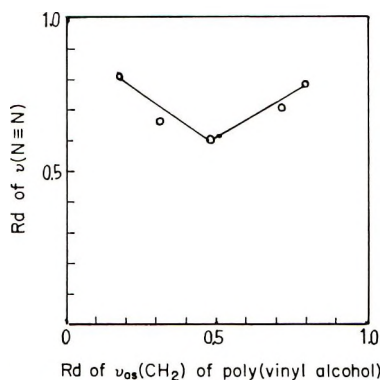


Fig. 8. R_d value of $\nu(\text{N}\equiv\text{N})$ of diazotized *p*-aminodimethylaniline vs. the extent of orientation of poly(vinyl alcohol) film.

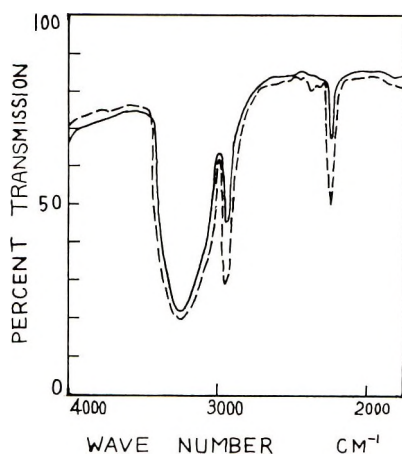


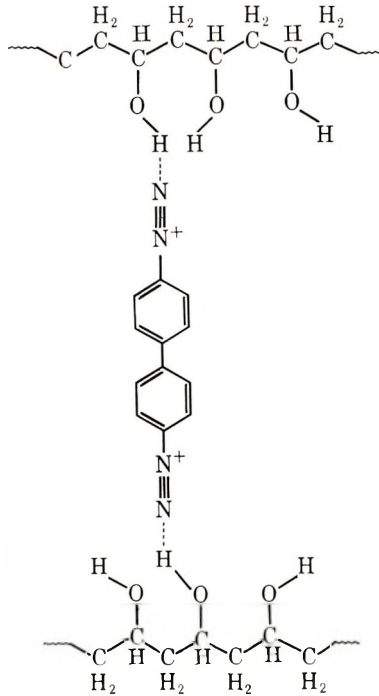
Fig. 9. Infrared dichroism of $\nu(\text{N}\equiv\text{N})$ of tetrazotized *o*-dianisidine absorbed in stretched poly(vinyl alcohol) film.

However, R_d values of $\nu(\text{N}\equiv\text{N})$ begin to decrease when the extent of the orientation of the polymer goes over a certain point. This might mean that the interactions between the diazonium groups and poly(vinyl alcohol) molecules are reduced by the further stretching of the film.

Figure 9 represents the spectrum of the stretched poly(vinyl alcohol) film in which the tetrazonium salt was absorbed by dipping it in an aqueous solution of tetrazotized *o*-dianisidine. In this case, there is no physical stress acting on the tetrazonium molecules, and the $\nu(\text{N}\equiv\text{N})$ band also shows perpendicular dichroism.

The nature of the interaction between poly(vinyl alcohol) and the diazo or tetrazonium molecule is not completely clear. However, from the molecular structure of the compounds it is presumable that the hydrogen bonds are formed between $-\text{OH}$ groups of poly(vinyl alcohol) and the polar groups of the diazo or tetrazonium salts such as diazo groups and hydroxy or methoxy groups.

For example, in the case of poly(vinyl alcohol) and tetrazotized benzidine, model I is proposed.



References

1. Lee, W. E., J. G. Calvert, and E. W. Malmberg, *J. Am. Chem. Soc.*, **83**, 1928 (1961).
2. Tsunoda, T., and T. Yamaoka, *J. Appl. Polymer Sci.*, **8**, 1379 (1964).

3. Whetsel, K. B., G. F. Hawkins, and F. E. Johnson, *J. Am. Chem. Soc.*, **78**, 3360 (1956).

4. Aroney, M., R. J. W. LeFevre, and R. L. Werner, *J. Chem. Soc.*, **1955**, 276.

Résumé

Les bandes $\nu(\text{N}\equiv\text{N})$ des sels de diazonium ou de tétrazonium dérivés de la *p*-méthoxyaniline, de la *p*-hydroxy aniline, de la benzidine ou de l'*o*-dianisidine montrent un dichroïsme perpendiculaire dans des films d'alcool polyvinylique étirés. Cela signifie que ces sels dirigent leur plus grand axe perpendiculairement à la direction d'étirement. Cependant, les sels de diazonium de *p*-aminodiphényle et de la *o*-anisidine ne montrent pas de dichroïsme. De ces faits, on conclut que les interactions entre les groupements polaires de l'alcool polyvinylique et ceux des deux extrémités des sels de diazonium et de tétrazonium tels que les groupements diazoïques, méthoxyles et hydroxyles provoquent une orientation perpendiculaire des molécules de diazoïques et de tétrazoïques.

Zusammenfassung

Die $\nu(\text{N}\equiv\text{N})$ Bande des von *p*-Methoxyanilin, *p*-Hydroxyanilin, Benzidin, oder *o*-Dianisidin abgeleiteten Diazo- oder Tétrazoniumsalzes zeigt senkrechten Dichroismus in gestrecktem Poly(vinylalkohol) film. Das bedeutet, dass diese Salze ihre längere Achse senkrecht zur Streckungsrichtung ausrichten. Die Band des Diazoniumsalzes von *p*-Aminodiphenyl oder *o*-Anisidin zeigt jedoch keinen Dichroismus. Aus den angeführten Ergebnissen wird geschlossen, dass die Wechselwirkung zwischen den polaren Gruppen von Poly(vinylalkohol) und denjenigen an den beiden Enden des Diazo- oder Tétrazoniumsalzes, wie die Diazo-, Methoxy- und Hydroxygruppe, zur senkrechten Orientierung des Diazo- oder Tétrazoniummoleküls führen.

Received December 24, 1964

Revised March 11, 1965

Prod. No. 4718A

Terpolymerization of Olefins and *cis, cis*-1,5-Cyclooctadiene with Sulfur Dioxide and Carbon Monoxide

A. H. FRAZER, *E. I. du Pont de Nemours & Company, Inc., Pioneering Research Laboratory, Experimental Station, Wilmington, Delaware*

Synopsis

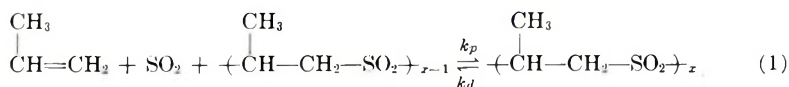
The terpolymerization of propylene, 1-butene, isobutene, and *cis, cis*-1,5-cyclooctadiene with sulfur dioxide and carbon monoxide at elevated temperatures and pressures has been studied. With the α -olefins, at carbon monoxide pressures of 1000 and 3000 atm. and temperatures above the ceiling temperature of the particular olefin-sulfur dioxide system, terpolymers of the olefin, sulfur dioxide, and carbon monoxide were obtained. With the diene, at these carbon monoxide pressures over a broad temperature range, similar terpolymers were obtained. All of these systems exhibited a ceiling temperature. The properties of these terpolymers were determined, and the structures and mechanism for the preparation of such structures postulated.

INTRODUCTION

Copolymers of olefins and sulfur dioxide have been known for fifty years. For simple olefins, these products¹⁻⁴ appear to be the 1:1 copolymer, regardless of olefin/sulfur dioxide feed composition.

Another characteristic of these systems is the ceiling temperature (T_c),⁵ the temperature above which no reaction occurs, and Dainton⁶ has shown that this is a consequence of the polymerization's being an exothermic process accompanied by a large loss in entropy.

From copolymerization theory and the work of Dainton⁶ and Walling,⁷ it may be shown that for the polymerization of an olefin such as propylene with sulfur dioxide

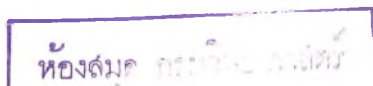


at the ceiling temperature (T_c), $k_p = k_d$ and so

$$T_c = \Delta H = \Delta H / (\Delta S^\circ + R \ln [\text{olefin}] [\text{SO}_2]) \quad (2)$$

It is apparent from the above that increasing the pressure on such a polymerization system will, in turn, increase the T_c .

Similarly, it has been shown that the copolymerization of carbon monoxide with an olefin proceeds by a similar mechanism, involving the reversible addition of carbon monoxide to the growing chain.⁸



Thus, it was of interest to study the effect of carrying out the olefin-sulfur dioxide copolymerization at or above the T_c under carbon monoxide pressures and determine the nature of the products obtained.

DISCUSSION

Polymerization

The copolymerization experiments of sulfur dioxide with propylene under monoxide pressure at various temperatures are detailed in Table I and summarized in Figure 1. The ceiling temperature (T_c) of the propylene-sulfur dioxide system has been reported to be 86–89°C. Inspection of Figure 1 shows that at 1000 atm. the T_c of this system is 100–125°C. and at 3000 atm., 120–135°C. The spread in T_c with reactant concen-

TABLE I
Propylene-SO₂-CO Polymerization^a

Pressure, atm.	SO ₂ , g.	Temp., °C.	Catalyst type ^b	Amt. catalyst, g.	Yield, g.	η_{inh}	S, % ^c
3000	50	70	A	1.5	80	1.1	30.1
"	"	90	A	"	70	1.2	28.9
"	"	115	A	"	50	1.98	28.4
"	"	135	B	2.0	5	1.2	28.0
"	"	150	B	"	—	—	—
"	25	70	A	1.0	33	1.3	30.1
"	"	90	A	"	30	1.0	28.7
"	"	115	A	"	25	1.3	28.9
"	"	135	B	1.5	3	0.95	28.1
"	"	140	B	"	—	—	—
"	10	70	A	0.5	15	1.1	30.1
"	"	90	A	"	13	0.95	28.9
"	"	125	B	"	3	0.83	28.1
"	"	130	B	"	—	—	—
1000	50	70	A	1.5	53	1.2	30.0
"	"	90	A	"	43	1.5	28.7
"	"	115	A	"	24	1.0	28.5
"	"	125	B	2.0	2	0.85	28.1
"	"	135	B	"	—	—	—
"	25	70	A	1.0	18	1.5	30.0
"	"	90	A	"	15	1.3	28.2
"	"	115	A	"	4	1.1	28.1
"	"	125	B	1.5	—	—	—
"	10	70	A	0.5	8	2.2	30.1
"	"	90	A	"	3	1.8	29.0
"	"	100	A	"	—	—	—

^a Propylene charge = 50 g.

^b A = α,α -azobisisobutyronitrile; B-*tert*-butyl peroxide. A change in initiator *per se*, does not cause a decrease in polymer yield (see Table IV).

^c Theory for propylene-SO₂ copolymer, S = 30.2%.

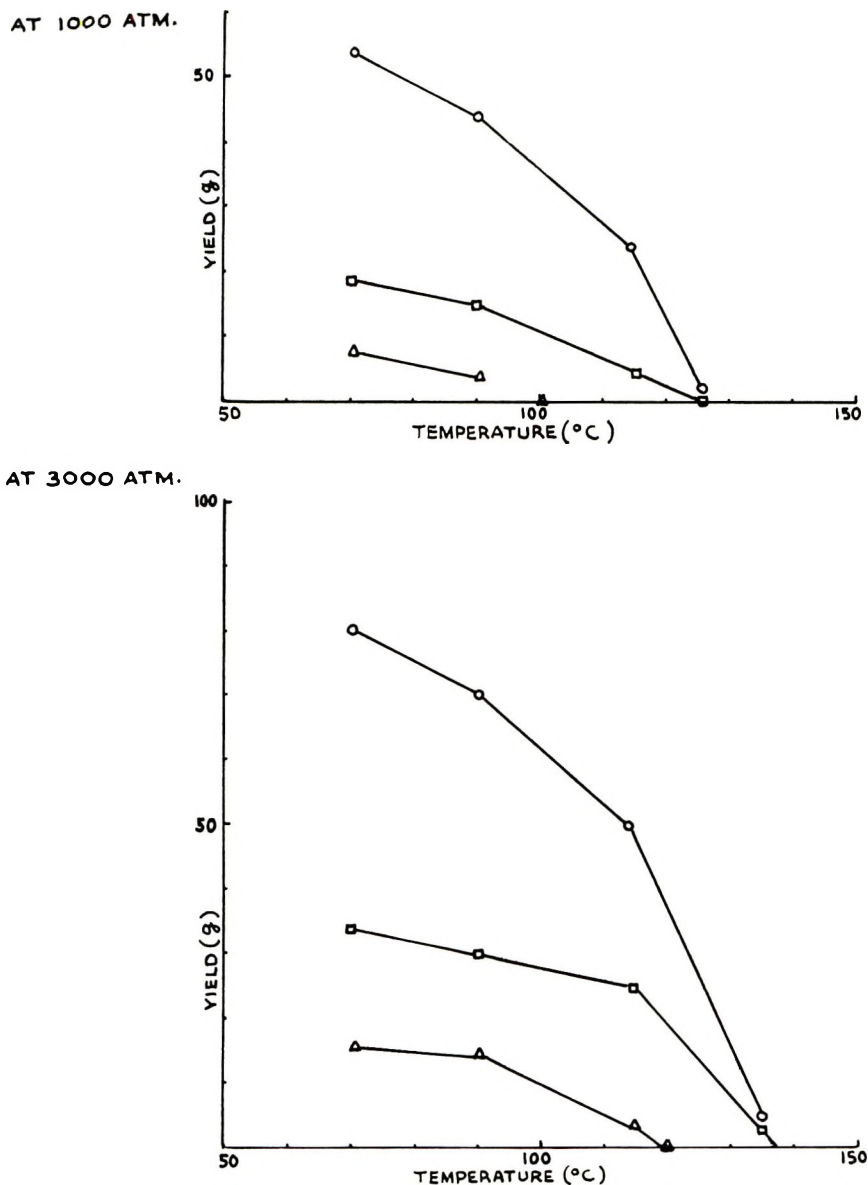


Fig. 1. Propylene-SO₂-CO polymerizations: (O) initial charge, 50 g. SO₂/50 g. olefin; (□) initial charge, 25 g. SO₂/50 g. olefin; (Δ) initial charge, 10 g. SO₂/50 g. olefin.

tration [more accurately, activity, see eq. (2)] is consistent with predicted behavior.

For the copolymerization of sulfur dioxide with 1-butene, the reported T_c is 63–66°C. As summarized in Table II and Figure 2, this system under carbon monoxide pressure of 1000 atm. exhibited a T_c of 90–100°C., and at 3000 atm., T_c was 100–110°C.

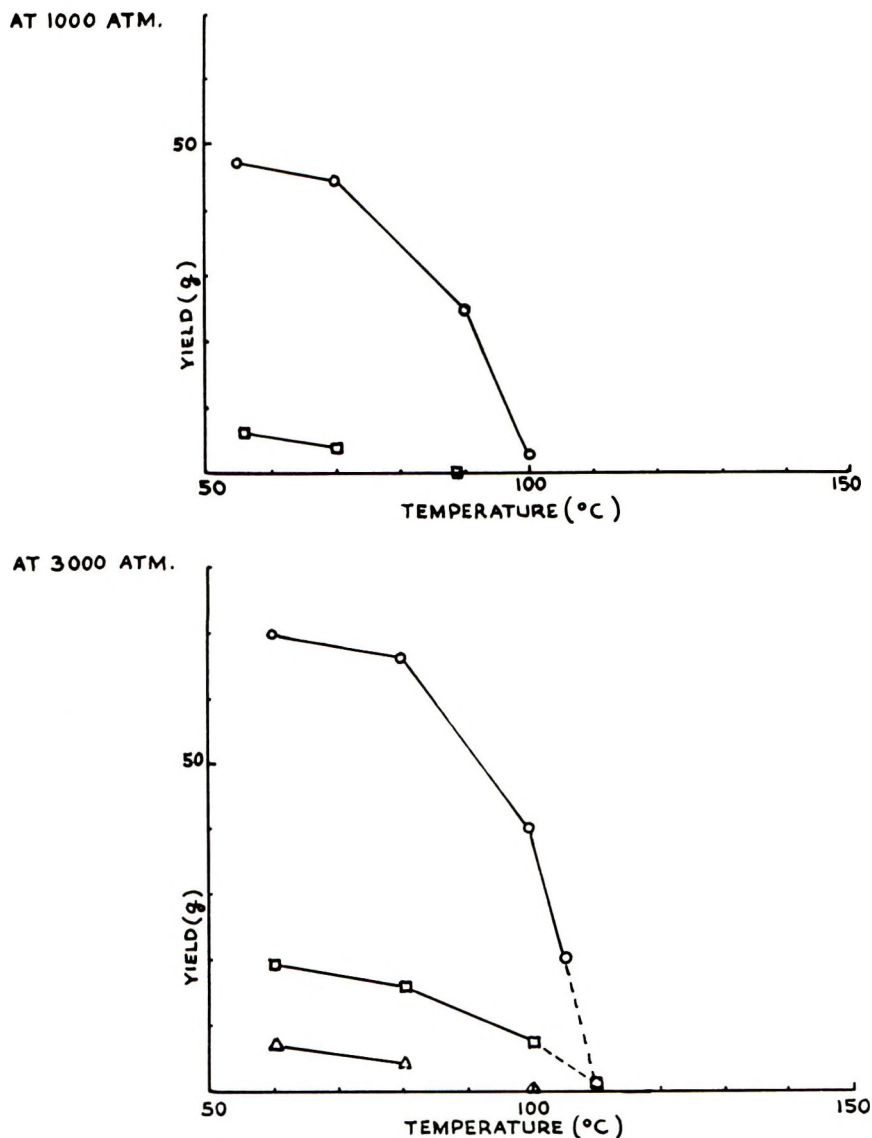


Fig. 2. 1-Butene-SO₂-CO polymerizations: (O) initial charge, 50 g. SO₂/50 g. olefin; (□) initial charge, 25 g. SO₂/50 g. olefin; (△) initial charge, 10 g. SO₂/50 g. olefin.

For the isobutene-sulfur dioxide system, the T_c has been variously reported to be from 5 to 25°C. For this system under carbon monoxide pressure at 1000 atm., the T_c is 50–55°C., and at 3000 atm., 65–70°C. (see Table III and Fig. 3). Based on the effects observed with the propylene-sulfur dioxide system and the 1-butene-sulfur dioxide system, it would appear that the T_c for the isobutene-sulfur dioxide system at autogenous pressures is at the upper end of the reported range of values.

TABLE II. 1-Butene-SO₂-CO Polymerizations^a

Pressure, atm.	SO ₂ , g.	Temp., °C.	Amt. catalyst, g. ^b	Yield, g.	η_{inh} (DMSO)	S, % ^c
3000	50	60	1.5	70	1.2	26.6
"	"	80	"	66	1.3	25.9
"	"	100	"	40	1.0	25.2
"	"	105	"	20	1.0	25.0
"	"	110	"	—	—	—
"	25	60	1.0	18	1.3	26.3
"	"	80	"	15	1.5	25.7
"	"	100	"	8	1.0	25.0
"	"	110	"	—	—	—
"	10	60	0.5	7	1.2	26.2
"	"	80	"	4	1.3	25.1
"	"	100	"	—	—	—
1000	50	55	1.5	47	1.1	26.3
"	"	70	"	44	1.4	26.1
"	"	90	"	25	1.3	25.5
"	"	100	"	3	1.0	25.3
"	"	115	"	—	—	—
"	25	55	1.0	7	1.1	26.3
"	"	70	"	3	1.3	25.3
"	"	90	"	—	—	—

^a 1-Butene charge = 50 g.^b α, α' -Azobisisobutyronitrile.^c Theory for 1-butene-SO₂ copolymer, S = 26.67%.TABLE III. Isobutene-SO₂-CO Polymerizations^a

Pressure, atm.	SO ₂ , g.	Temp., °C.	Catalyst type ^b	Amt. catalyst, g.	Yield, g.	η_{inh} ^c	S, % ^d
3000	50	20	A	1.5	69	1.3	26.3
"	"	40	A	"	65	1.8	25.9
"	"	60	B	"	40	1.5	25.8
"	"	70	B	"	3	0.85	25.5
"	"	90	B	"	—	—	—
"	25	20	A	1.0	20	1.4	26.5
"	"	40	B	"	15	1.9	25.9
"	"	60	B	"	5	1.1	25.6
"	"	80	B	"	—	—	—
1000	50	20	A	1.5	40	1.3	26.3
"	"	40	A	"	25	1.8	25.5
"	"	50	B	"	7	0.85	25.3
"	"	60	B	"	—	—	—
"	25	20	A	1.0	8	1.2	26.6
"	"	40	A	"	4	0.75	25.3
"	"	50	B	"	—	—	—

^a Isobutene charge = 50 g.^b A = α, α' -azobis(α, γ -dimethylvaleronitrile); B = α, α' -azobisisobutyronitrile.^c Determined in H₂SO₄.^d Theory for isobutene-SO₂ copolymer, S = 26.67%.

For the copolymerization of sulfur dioxide with *cis, cis*-1,5-cyclooctadiene, which yields a polybicyclosulfone as product and involves the copolymerization of two moles of sulfur dioxide with one of the diene, the T_c has not been determined. Polymerization has been reported⁹ to occur up to

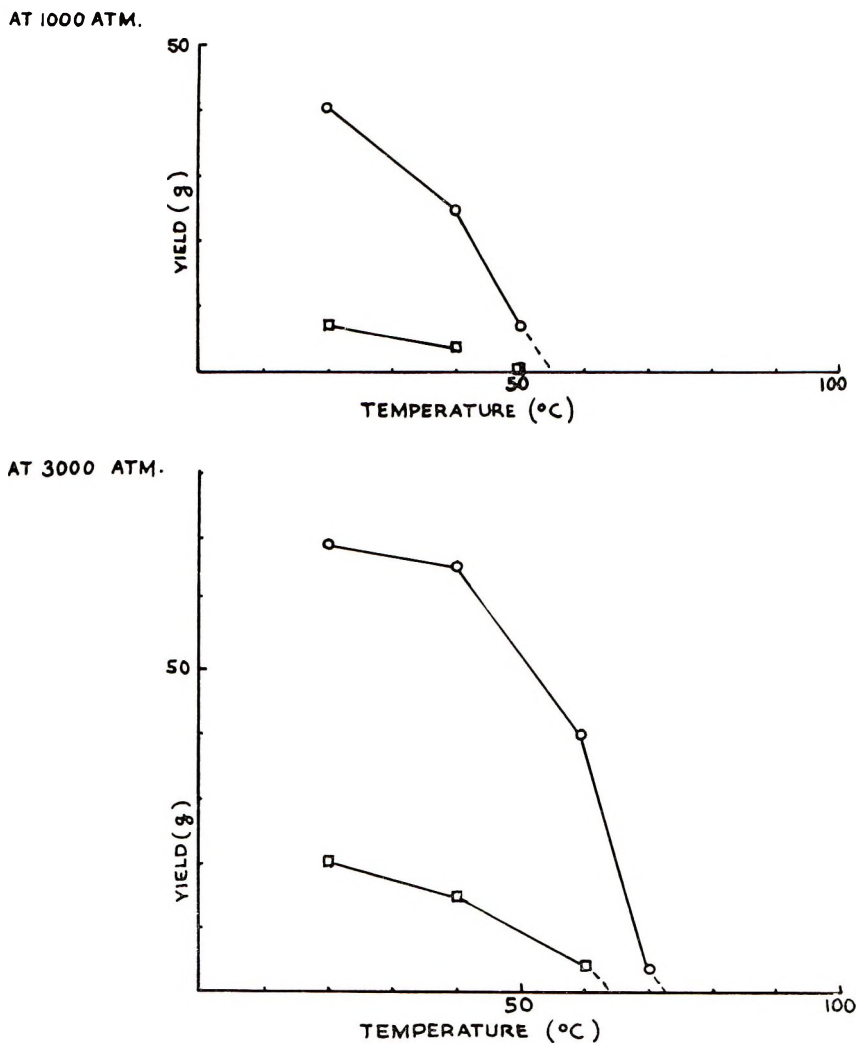


Fig. 3. Isobutene-SO₂-CO polymerizations: (○) initial charge, 50 g. SO₂/50 g. olefin; (□) initial charge, 25 g. SO₂/50 g. olefin.

temperatures as high as 135°C. As shown in Figure 4 and Table IV, at 1000 atm. the T_c , by extrapolation, is 150–160°C., and at 3000 atm., 155–175°C. At these elevated temperatures, these data are somewhat in doubt, since side reactions (redox reactions involving sulfur dioxide and the diene) do occur, and products other than the copolymer⁹ are obtained.

TABLE IV
cis,cis-1,5-Cyclooctadiene-SO₂-CO Polymerizations^a

Pressure, atm.	SO ₂ , g.	Temp., °C.	Catalyst type ^b	Amt.		Yield, g.	η _{inh}	S, % ^c
				catalyst, g.	g.			
3000	50	50	A	2.0	59	1.3	26.2	
"	"	90	A	"	55	1.5	25.8	
"	"	135	B	1.5	50	1.7	25.9	
"	"	160	B	"	47	0.85	25.5	
"	"	170	B	"	20	0.65	25.5	
"	"	180	B	"	—	—	—	
"	25	50	A	1.5	26	1.3	26.3	
"	"	90	B	"	25	1.7	25.9	
"	"	120	B	1.0	24	1.7	25.9	
"	"	150	B	"	23	0.80	25.5	
"	"	160	B	"	5	0.60	25.3	
1000	50	70	A	2.0	40	1.3	26.5	
"	"	110	B	1.5	37	1.8	25.8	
"	"	150	B	"	33	0.75	25.9	
"	"	155	B	"	20	0.45	25.8	
"	"	160	B	"	3	0.45	25.3	
"	"	170	B	"	—	—	—	
"	25	70	A	1.5	8	1.3	26.7	
"	"	110	B	"	7	1.6	26.1	
"	"	145	B	"	6	0.53	25.5	
"	"	150	B	"	2	0.53	25.5	
"	"	160	B	"	—	—	—	

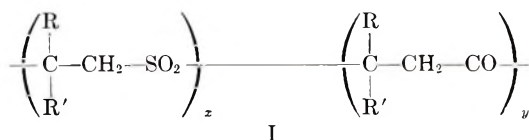
^a *cis,cis*-1,5-Cyclooctadiene charge = 50 g.

^b A = α,α'-azobisisobutyronitrile; B = *tert*-butyl peroxide.

^c Theory for *cis,cis*-1,5-cyclooctadiene-SO₂, S = 26.68%.

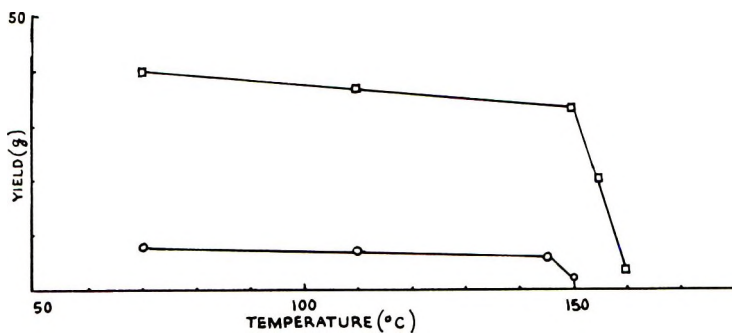
Polymers

For simple olefins such as propylene, 1-butene, and isobutene, the products obtained at temperatures up to the normal T_c of the system were poly(olefin sulfones). At temperatures in excess of the reported T_c , the products were terpolymers of the olefin, carbon monoxide, and sulfur dioxide. Based on past work on olefin-sulfur dioxide copolymerization¹ and olefin-carbon monoxide copolymerization,^{7,8} these copolymers would appear to have the structure I:



Based on elemental analyses, the amount of olefin-carbon monoxide linkages incorporated in the polymer chain was at the most 10 mole-%. At this level of modification, these terpolymers are practically identical with the parent polyolefin sulfone in such properties as polymer melt temperature solubility, density, etc. (see Table V).

AT 1000 ATM.



AT 3000 ATM.

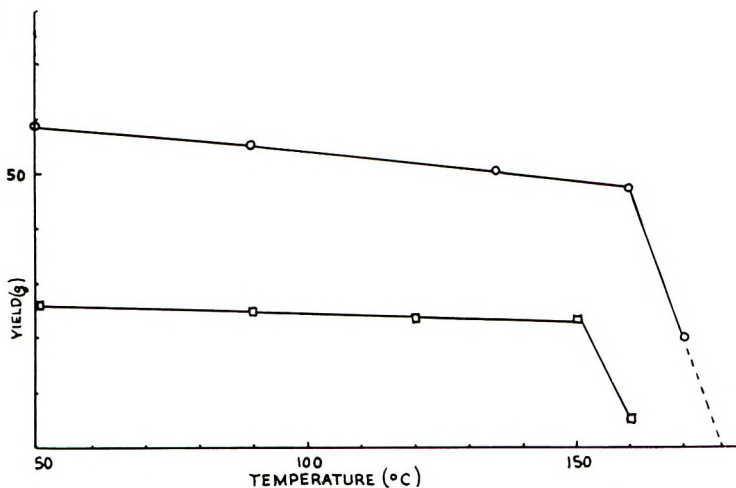


Fig. 4. *cis,cis*-1,5-Cyclooctadiene-SO₂-CO polymerizations: (O) initial charge, 50 g. SO₂/50 g. diene; (□) initial charge, 10 g. SO₂/50 g. diene.

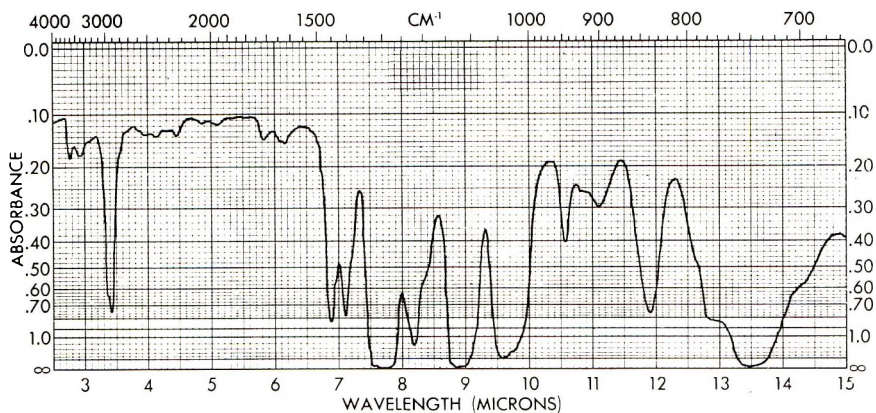


Fig. 5. Infrared spectrum of propylene-SO₂-CO terpolymer.

TABLE V
Comparative Properties of Copolymers and Terpolymers

Polymer	PMT, °C.	η_{inh}	S, %	Density, g./cc.	Water absorption, % on film	Solvents ^a
Propylene-SO ₂	280 (dec.)	1.24 ^b	30.1	1.4568	7.2	DMSO, TMS NMP, H ₂ SO ₄
Propylene-SO ₂ -CO	280 (dec.)	1.51 ^b	28.7	1.4564	6.8	DMSO, TMS NMP, H ₂ SO ₄
1-Butene-SO ₂	150 (dec.)	150 ^b	26.6	1.2453	5.5	DMSO, TMS NMP, H ₂ SO ₄
1-Butene-SO ₂ -CO	150 (dec.)	1.32 ^b	25.9	1.2480	5.8	DMSO, TMS NMP, H ₂ SO ₄
Isobutene-SO ₂	230 (dec.)	1.42 ^c	26.5	1.4061	—	H ₂ SO ₄
Isobutene-SO ₂ -CO	230 (dec.)	1.52 ^c	25.8	1.4075	—	H ₂ SO ₄
C ₈ H ₁₂ -SO ₂ ^d	260 (dec.)	2.10 ^b	26.6	1.5211	5.3	DMSO, TMS NMP, H ₂ SO ₄
C ₈ H ₁₂ -SO ₂ -CO ^d	260 (dec.)	1.81 ^b	25.8	1.5294	5.7	DMSO, TMS NMP, H ₂ SO ₄

^a DMSO = Dimethyl sulfoxide; TMS = tetramethylene sulfone; NMP = *N*-methylpyrrolidone; H₂SO₄ = concentrated sulfuric acid.

^b Solvent = DMSO.

^c Solvent = H₂SO₄.

^d C₈H₁₂ = *cis,cis*-1,5-cyclooctadiene.

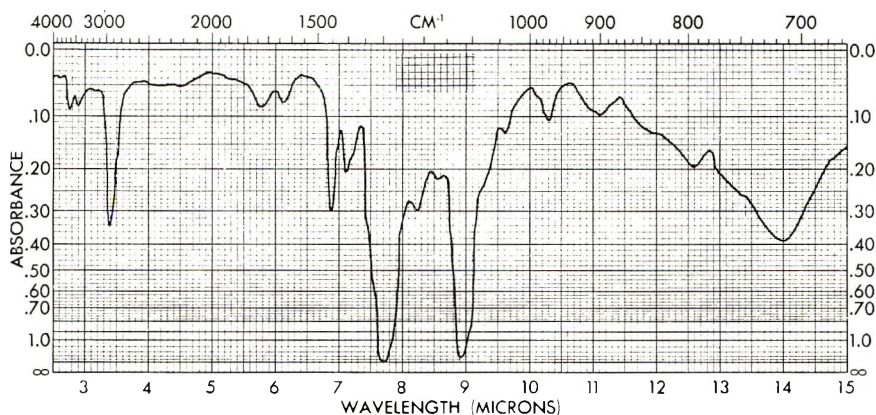


Fig. 6. Infrared spectrum of 1-butene-SO₂-CO terpolymer.

The infrared spectra of thin films of the terpolymers derived from propylene and 1-butene, in addition to the absorptions arising from the poly(olefin sulfone) structure, have the expected carbonyl absorption at 5.8–5.9 μ but, in addition, have absorption bands at 2.9 μ (hydroxyl) and 6.15 μ (unsaturation) (see Figs. 5 and 6). An inspection of the spectra of olefin-carbon monoxide copolymers shows no such absorptions at these

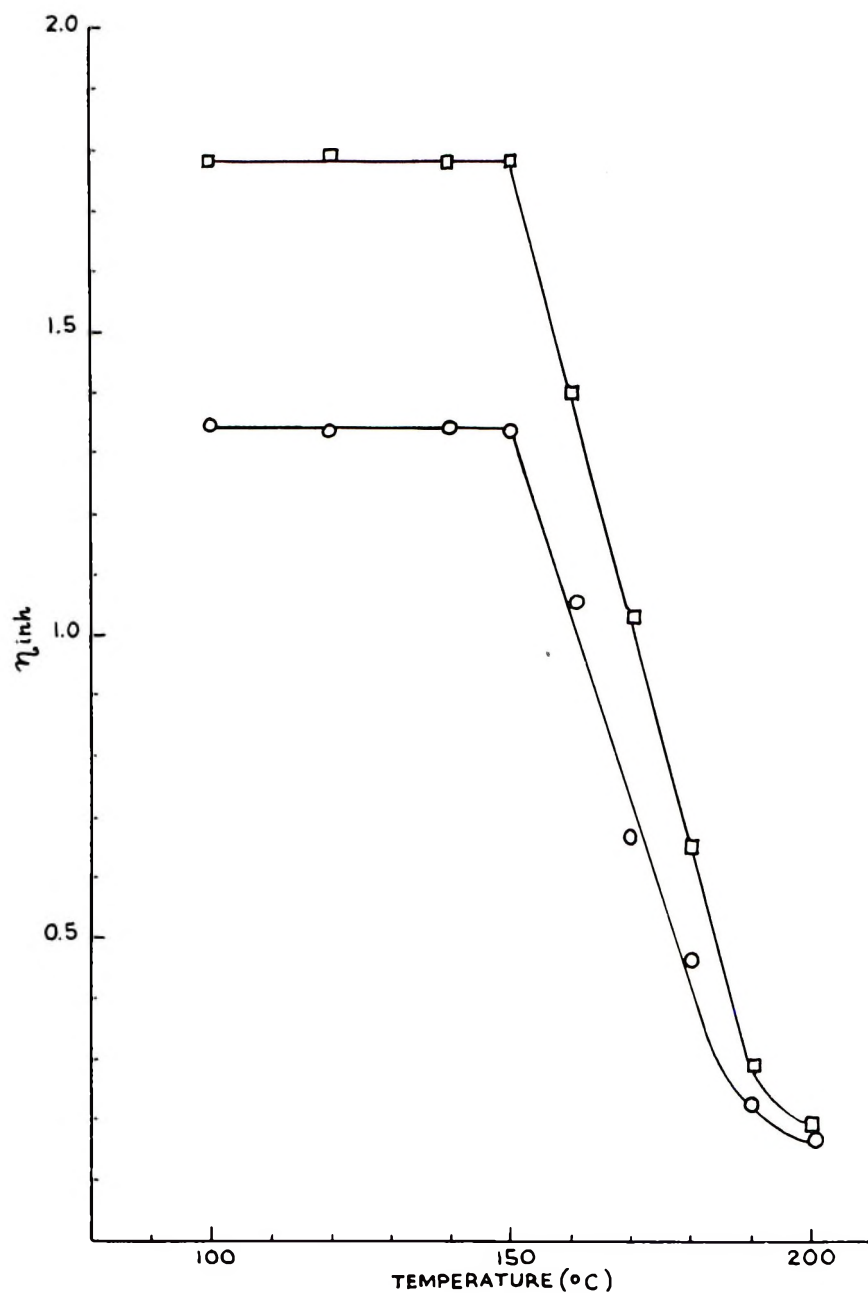


Fig. 7. Thermal degradation of copolymer and terpolymer after 1 hr. at indicated temperature under N_2 : (□) propylene sulfone copolymer; (○) propylene- SO_2 -CO terpolymer.

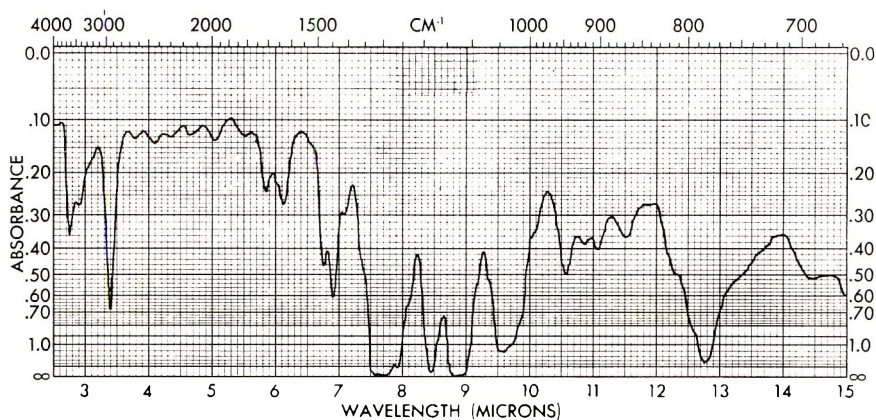
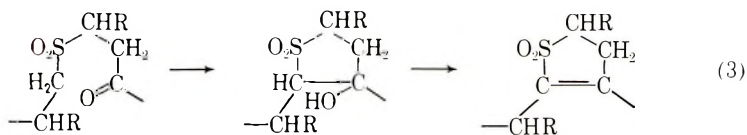


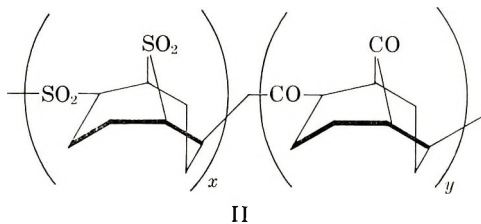
Fig. 8. Infrared spectrum of $C_3H_{12}-SO_2-CO$ terpolymer.

wavelengths.⁸ A possible reaction sequence which could give rise to structures which would have these bands is outlined in eq. (3).



The similarity in the thermal stability of these terpolymers and the normal polyolefin sulfones is illustrated in Figure 7. In this figure are plotted the inherent viscosities of a terpolymer of propylene, sulfur dioxide, and carbon monoxide at 10 molc-% modification after 1 hr. heating at the temperature indicated. Essentially, there is no change in inherent viscosity for such heating times up to temperatures of 150°C . Above this temperature, there is a precipitous drop in inherent viscosity. As can be seen from the companion curve for a "normal" poly(propylene sulfone), the behaviors are identical.

Products from the polymerization of *cis,cis*-1,5-cyclooctadiene and sulfur dioxide under carbon monoxide pressure at all temperatures investigated were terpolymers of the diene, sulfur dioxide, and carbon monoxide. If, as in the case of the diene sulfone polymerization, it is assumed that the carbon monoxide added to the growing radical chain in the same manner as the sulfur dioxide, the product would be a polybicyclopentane, and the terpolymer structure would contain two moles of carbon monoxide per diene, as indicated in the structure II:



As in the case of the simple olefins, based on elemental analyses, the amount of diene-carbon monoxide linkages incorporated in the polymer chain was at the most 10 mole-%. At this level of modification, these terpolymers are identical in properties with the poly(diene sulfone). The infrared spectra of thin films of these terpolymers show absorption bands at 9.2μ (hydroxyl) 5.8 – 5.9μ (carbonyl), and 6.15μ (unsaturation) (Fig. 8). All of the terpolymers, whether derived from propylene, 1-butene, or *cis-cis*-1,5-cyclooctadiene, yielded brittle, flammable, thermally and hydrolytically unstable films on casting from dimethyl sulfoxide solution. This behavior is like that observed for the normal poly(olefin sulfones) and poly(diene sulfones).

EXPERIMENTAL

Preparation of Olefin/SO₂/CO Terpolymers

The synthesis of a typical terpolymer is illustrated by the following experiment. To a 300 ml. stainless steel shaker tube capable of withstanding pressures of 3000 atm. was charged 1.5 g. of α, α' -azobisisobutyronitrile. The tube was evacuated to less than 1 mm. pressure, purged with nitrogen, and re-evacuated to less than 1 mm. pressure. The tube was chilled in Dry Ice-acetone and 50 g. of propylene and 50 g. of sulfur dioxide distilled in. The tube was then pressured with carbon monoxide to 3000 atm. and the temperature brought to 115°C . These conditions were maintained for 4 hr. After allowing the reactor to cool, the excess gas was bled off and the contents of the tube washed repeatedly with methanol to remove all traces of monomer and catalyst residue. After drying overnight at 100°C . *in vacuo*, 50 g. of polymer having a composition corresponding to 9 mole-% modification of propylene-carbon monoxide linkages with polymer melt temperature greater than 265°C . and an inherent viscosity in dimethyl sulfoxide of 1.98 was obtained.

ANAL. Calcd. for $[\text{CH}(\text{CH}_3)\text{CH}_2\text{SO}_2]_{0.91}[\text{CH}(\text{CH}_3)\text{CH}_2\text{C}=\text{O}]_{0.09}$: C, 36.11%; H, 5.69%; S, 28.42%; O, 29.78%. Found: C, 36.20, 36.15%; H, 5.69, 5.65%; S, 28.45, 28.40%; O, 29.80, 29.71%.

This procedure was varied in the following manner. When liquid monomer was used (*cis-cis*-1,5-cyclooctadiene), the initiator and monomer were charged to the reactor before evacuation and purging with nitrogen. In some runs, in order to assure the onset of polymerization at the temperature indicated, sulfur dioxide and initiator alone were charged to the reactor, the reactor pressured with carbon monoxide, this mixture raised to reaction temperature, and then olefin pressured in at that temperature. Since there was no difference in the yield, inherent viscosity, or nature of the products obtained by this procedure, the original more convenient, procedure was used for carrying out most of these polymerizations.

Polymer Characterization

Density. The density of the products was determined by comparison with solutions of known specific gravity. Water-methanol, water-methanol-potassium iodide mixtures, and water were used. Test solutions were maintained at $23 \pm 1^\circ \text{C}$. Samples were dropped into test solutions and the rise or fall of specimens noted. The density of the test solution was then adjusted until the polymer particles neither rose nor fell.

Polymer Melt Temperature. Polymer melt temperature (PMT) was determined by the methods outlined by Sorenson and Campbell.¹⁰

Infrared Absorption Spectra. The infrared absorption spectra were determined by using a Perkin-Elmer Model 21 recording infrared spectrophotometer on thin films (less than 1 mil) of the polymer prepared from dimethyl sulfoxide solutions.

Inherent Viscosity. Inherent viscosity, $\eta_{inh} (\ln \eta_{rel}/c)$, for 0.5 g. polymer/100 ml. of dimethyl sulfoxide solution was determined at 30°C . by using an Ostwald-Fenske viscometer.

The author wishes to express his appreciation for the work of the late Mr. Miller Nelson in carrying out the high pressure experiments and to Mr. W. F. Holley for his excellent technical assistance.

References

1. Mathews, F. E., and H. M. Elder, Brit. Pat. 11,635 (1915).
2. Frederick, D. S., H. D. Cogan, and C. S. Marvel, *J. Am. Chem. Soc.*, **56**, 1815 (1934).
3. Hunt, M., and C. S. Marvel, *J. Am. Chem. Soc.*, **57**, 1691 (1935).
4. Staudinger, H., and B. Ritzenthaler, *Ber.*, **63**, 455 (1935).
5. Snow, R. D., and F. E. Frey, *J. Am. Chem. Soc.*, **65**, 2417 (1943).
6. Dainton, F. S., and K. J. Ivin, *Proc. Roy. Soc. (London)*, **212**, 96 (1952).
7. Walling, C., *J. Polymer Sci.*, **16**, 315 (1955).
8. Brubaker, M. M., D. D. Coffman, and H. H. Hoehn, *J. Am. Chem. Soc.*, **74**, 1509 (1953).
9. Frazer, A. H., and W. P. O'Neill, *J. Am. Chem. Soc.*, **85**, 2613 (1963).
10. Sorensen, W. R., and T. W. Campbell, *Preparative Methods of Polymer Chemistry*, Interscience, New York, 1961.

Résumé

On a étudié la terpolymérisation du propylène, du 1-butène, de l'isobutène et du *cis,cis*-1,5-cyclooctadiène en présence d'anhydride sulfureux et de monoxyde de carbone à températures et pressions élevées. On obtient des terpolymères de l'oléfine, de l'anhydride sulfureux et du monoxyde de carbone dans le cas des α -oléfines à des pressions de 1000 et de 3000 atmosphères de monoxyde de carbone et à des températures supérieures à la température "plafond" critique pour le système particulier oléfine-anhydride sulfureux. On obtient des terpolymères semblables au départ de diènes, aux mêmes pressions de monoxyde de carbone et dans le même domaine de température. Tous ces systèmes ont une température "plafond" critique. On a déterminé les propriétés de ces terpolymères et on propose des structures et un mécanisme pour l'obtention de telles structures.

Zusammenfassung

Die Terpolymerisation von Propylen, 1-Buten, Isobuten und *cis,cis*-1,5-Cyclooctadien mit Schwefeldioxyd und Kohlenmonoxyd wurde bei erhöhten Temperaturen und Drucken untersucht. Mit den α -Olefinen wurden bei Kohlenmonoxyddrucken von 1000 und 3000 atm und Temperaturen oberhalb der Ceilingtemperatur des betreffenden Olefin-Schwefeldioxyd-systems Terpolymere des Olefins, Schwefeldioxyds und Kohlenmonoxyds erhalten. Mit dem Dien wurden bei diesen Kohlenmonoxyddrucken in einem breiten Temperaturbereich ähnliche Terpolymere erhalten. Alle Systeme besaßen eine Ceilingtemperatur. Die Eigenschaften der Terpolymeren wurden bestimmt, sowie deren Struktur und ein Mechanismus für die Darstellung solcher Strukturen vorgeschlagen.

Received February 16, 1965

Revised March 29, 1965

Prod. No. 4720A

Studies on Alcohol-Modified Transition Metal Polymerization Catalysts. I. Infrared Studies

R. H. MARCHESSAULT, H. CHANZY, S. HIDER, W. BILGOR, and J. J. HERMANS, *Cellulose Research Institute and Chemistry Department, State University College of Forestry, Syracuse, New York*

Synopsis

The interaction of titanium tetrachloride and alcohols in benzene and carbon tetrachloride has been studied by means of infrared spectroscopy. A "continuous variation" study of various absorption bands has allowed establishment of two different interactions: one involving a 1:1 alcohol-titanium tetrachloride ratio and another at 3:1. High-resolution spectroscopy in the $3\ \mu$ region for the latter indicates well-defined hydrogen bonding of the intramolecular kind. This has been interpreted in terms of the alcohols being both reacted and coordinated in a titanium complex. Significantly, polymerization activity of the titanium compound decreases sharply when alcohol is in molar excess and goes to zero at a 3:1 ratio. The effect of added aluminum triethyl on the infrared spectrum of the propanol-titanium tetrachloride 3:1 complex in the $3\ \mu$ region was observed. Significant changes in the OH stretching modes were noted. Interaction spectra of propanol-methyl titanium trichloride were also recorded.

INTRODUCTION

The present study is aimed, first of all, at understanding the purely chemical changes that can occur when polymerization catalysts of the transition metal type¹ are prepared in the presence of alcohols. Aside from the fact that esters of titanium are known cocatalysts for ionic polymerizations, there has been relatively little incentive for the study of alcohol-modified stereospecific catalysts. It was early realized in the studies on such systems that monomers bearing polar or reactive groups tend to deactivate the highly electrophilic catalyst components. Nevertheless, the whole field of so-called Ziegler-Natta catalysts which usually involve reactive halide groupings is very susceptible to alcohol modification.

From a practical point of view, the adsorption of catalyst component TiCl_4 onto cellulosic substrates is an example of such modification. This has proven useful for bringing about a selective polymerization of nonpolar monomers at the fiber surface.² The potential for surface modification of this type is quite broad. For example, a recent article³ describes the use of BF_3 as a surface-selection polymerization catalyst for butadiene on paper.

Basically, such chemical modification would appear to rest on the fact that typical catalysts or catalyst components such as TiCl_4 can react with an

alcohol molecule to yield a product of the form $\text{TiCl}_{4-n}(\text{OR})_n$. Most typical, is a compound with $n = 1$ or $n = 2$. In addition to the reaction, coordination of alcohol can occur, and a crystalline product of formula $\text{TiCl}_2(\text{OR})_2 \cdot \text{ROH}$ has been isolated.⁴ As far as polymerization is concerned, excess alcohol obviously will deactivate the catalyst by occupying all the coordination sites. There is, however, a region of tolerance where even some catalytic benefit could be achieved by addition of alcohol. For example, Sigwalt and Vairon⁵ attribute their success in obtaining high molecular weight product from cyclopentadiene to the decreased acidity of their titanium halide catalyst as achieved by replacing one chlorine with a *n*-butoxy group. Such an effect, along with the above-mentioned application² which results in an "encapsulation" of cellulose fibers with a polyolefin coating, provided incentive for undertaking the following studies. In this report, the infrared spectra of TiCl_4 -alcohol mixtures were recorded and various auxiliary experiments were performed in order to assist in tentative band assignments. Finally the results of the infrared study were related to the polymerization of styrene by TiCl_4 - $\text{Al}(\text{Et})_3$ in the presence of added alcohol.

EXPERIMENTAL

Preparation of Materials

Titanium tetrachloride obtained from Matheson, Coleman and Bell and labelled 99.5% pure was used. On analysis, a Cl/Ti ratio of 3.95 was obtained. Infrared spectra of this chemical were comparable with those obtained in the literature.⁶

n-Propyl alcohol was desiccated over anhydrous CaSO_4 and distilled on a spinning band column over magnesium propoxide. The fraction boiling at 96.5–97.5°C. was collected and stored in a ground glass-stoppered flask inside a desiccator over P_2O_5 .

Other alcohols were prepared similarly.

Benzene was Fisher reagent grade, thoroughly treated with H_2SO_4 until no further coloration was present in the acid layer. It was stored over CaCl_2 and then distilled in an efficient column; the fraction boiling at 79.5–80.5°C. was collected. Benzene was then stored over sodium wire which was added until bubbles of hydrogen were no longer evolved.

Carbon tetrachloride was Fisher reagent grade, washed with hot alcoholic potassium hydroxide and then with H_2SO_4 until no further coloration was found in the acid layer. It was then distilled over P_2O_5 , and the fraction boiling at 76.5°C. was collected. The purity was checked spectroscopically.

n-Heptane was Eastman Chemical Company reagent grade, washed with H_2SO_4 until no further coloration was obtained inside the acid layer. It was then stored over anhydrous CaCl_2 and distilled on an efficient column. The fraction boiling at 98°C. was collected and stored over sodium wire.

Triethyl aluminum was received from Ethyl Corporation as a solution in inert solvent (toluene or heptane). Infrared studies were performed with

solutions of 10% by weight of AlEt_3 in heptane. Polymerizations were performed with solutions of 20% by weight of AlEt_3 in toluene. Aluminum determinations (cf. below) served to establish the reagent concentration.

Methyltitanium trichloride was received from Orgmet and stored in Dry Ice until it was used. After resublimation, solutions of it were made in heptane as well as in CCl_4 . Fresh solutions had to be used rapidly because of instability.

Solution Preparation and Analysis

Solution preparation as well as filling of infrared cells was performed in a sealed dry box in dry nitrogen atmosphere. Alcohols were measured volumetrically and not titrated. Other chemicals were titrated.

Titanium was precipitated as $\text{TiO}_2 \cdot x\text{H}_2\text{O}$ with ammonium hydroxide solution. This precipitate was incinerated for 4 hr. at 900°C . Another method involving sodium hydroxide usually yielded somewhat higher results. This was attributed to sodium retention in the precipitate.

Chlorine was determined by the Volhard method. Again, a procedure involving addition of excess water and titration of HCl with sodium hydroxide usually yielded low results. This is probably due to loss of HCl .

Aluminum was determined by the method of Watts.⁷

Infrared Spectroscopy

The spectra were recorded on a Baird Atomic double-beam spectrophotometer, Model 4-55. When the two cells could be matched closely enough, the double beam technique was used. Otherwise, operation was single-beam in the region where the solvent was transparent. Cell thickness was variable from 0.1 to 15 mm.

Spectra were recorded with a NaCl prism from 4000 to 625 cm^{-1} . High resolution was obtained with a LiF prism in the region $2000\text{--}6000\text{ cm}^{-1}$.

In each run a careful calibration was performed: a polystyrene film was used for calibration between 4000 and 625 cm^{-1} and 1,2,4 trichlorobenzene was used in the region $6000\text{--}4000\text{ cm}^{-1}$.

Polymerization in the Presence of Alcohols

Styrene polymerization was performed under nitrogen atmosphere by using 0.001 mole of titanium tetrachloride, 3 cc. of freshly distilled styrene, and 0.001 mole of AlEt_3 in 100 cc. of benzene containing the appropriate amount of alcohol. The order of addition was as presented above. Polymerization occurred readily and was allowed to proceed for 1 hr.; then it was terminated by addition of methanol until the solution became slightly cloudy. The reaction mixture was added dropwise to a solution of 10 cc. HCl in 300 cc. of methanol, and the resulting precipitate was then washed with 1N HCl , water, and methanol before being dried in a vacuum oven at $50\text{--}55^\circ\text{C}$.

RESULTS AND DISCUSSION

Continuous Variation for the *n*-Propanol-TiCl₄ System in Benzene

The method of continuous variation, due to Job⁸ was used to study the interaction of TiCl₄ and propanol in benzene. In this method the recorded variable was the optical density of infrared absorption bands in the region 625-5000 cm.⁻¹. Low-resolution spectra with a fairly high concentration of the two stock solutions (0.228*M*) and high-resolution spectra where a lower concentration (0.0575*M*) in *n*-propanol eliminates most of the intermolecular hydrogen bonding are shown in Figures 1 and 2.

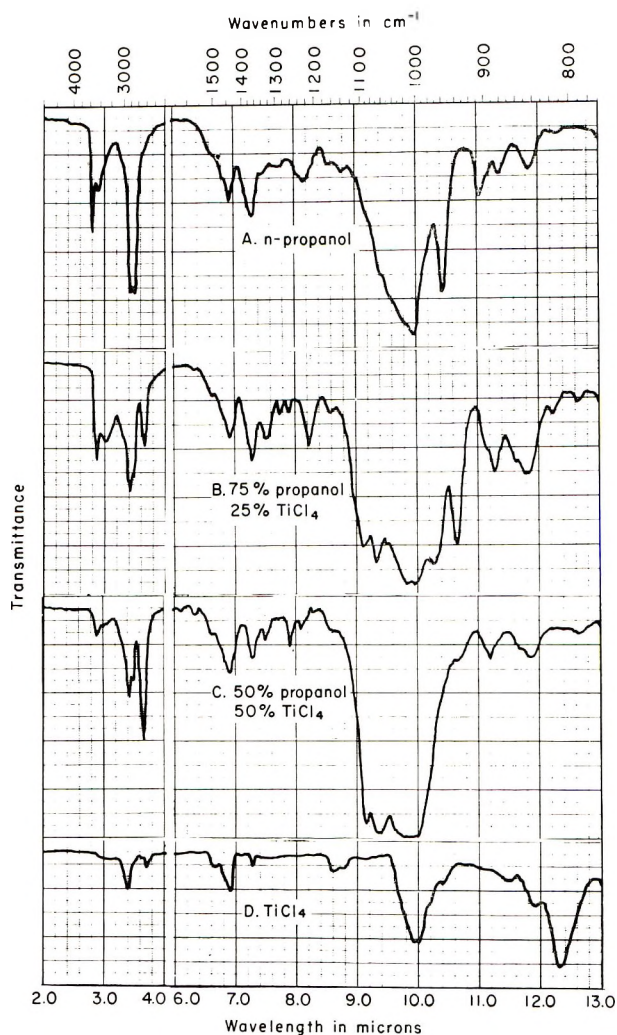


Fig. 1. Low-resolution infrared spectra of the interaction of 0.228*M* solution of TiCl₄ in benzene and 0.228*M* solution of *n*-propanol in benzene.

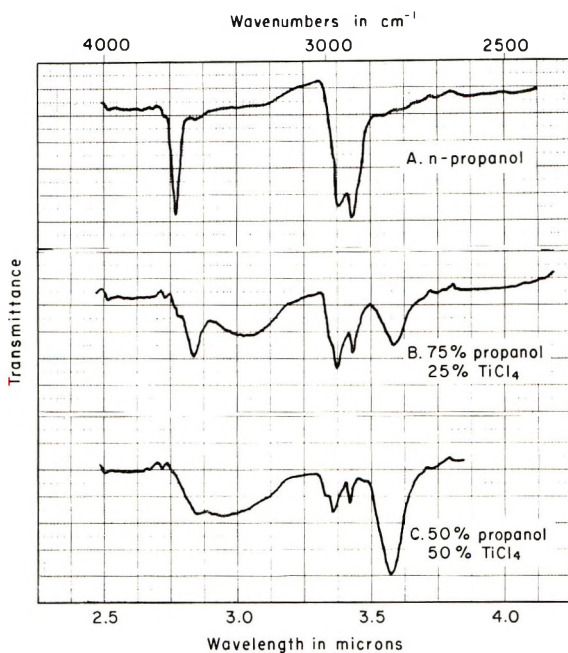


Fig. 2. High-resolution infrared spectra of the interaction of $0.0575M$ solution of $TiCl_4$ in benzene and $0.0575M$ solution of n -propanol in benzene.

If one surveys the spectra from 5000 to 625 cm.^{-1} after each variation in the proportions of the two stock solutions, one finds that the absorption bands can be classified into four groups (Table I) according to their behavior. Some show a constant decrease in their intensity with increasing

TABLE I
Continuous Variation in Infrared Absorption Bands for $TiCl_4$ - n -Propanol in Benzene

Absorption bands, cm.^{-1}			
Optical density constantly decreases with mole fraction of $TiCl_4$	Optical density constantly increases with mole fraction of $TiCl_4$	Optical density maximum when $\frac{n\text{-propanol}}{TiCl_4} = 1$	Optical density maximum when $\frac{n\text{-propanol}}{TiCl_4} = 3$
2920	815	2750	3530
2860			3330
1450		1070	1218
1370		1100	940
3600			882
1225			884
958			
906			

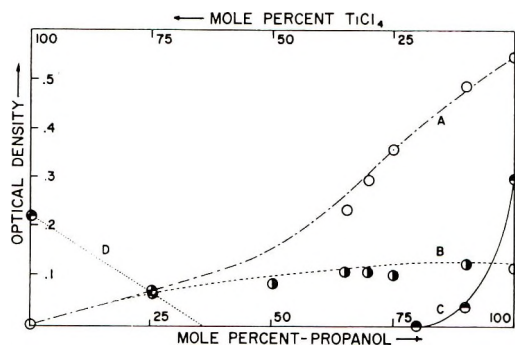


Fig. 3. Interaction of TiCl_4 and n -propanol: variation of optical density with the mole per cent at (A) 2920 cm.^{-1} , (B) 1450 cm.^{-1} , (C) 3600 cm.^{-1} , and (D) 815 cm.^{-1} for benzene solvent.

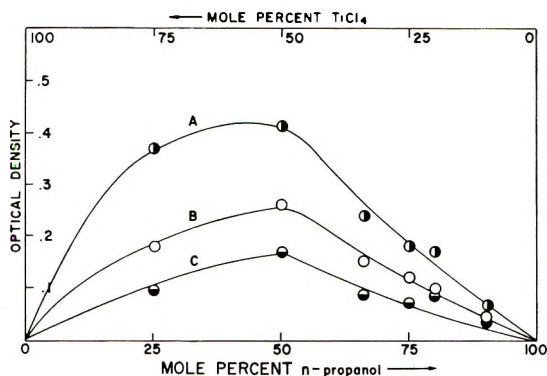


Fig. 4. Interaction of TiCl_4 and n -propanol: variation of optical density with the mole per cent of n -propanol at (A) 1070 cm.^{-1} , (B) 1100 cm.^{-1} , and (C) 2750 cm.^{-1} for benzene solvent.

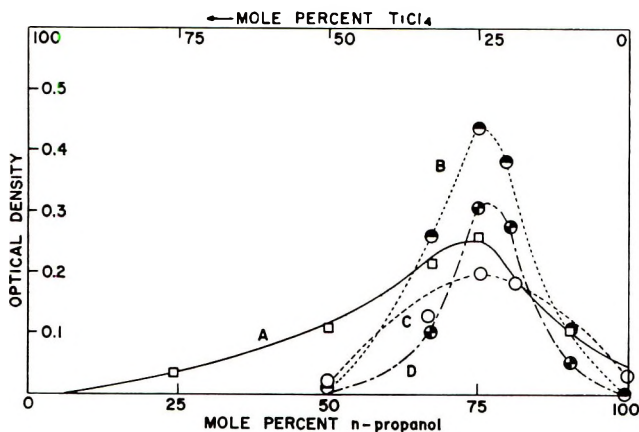


Fig. 5. Interaction of TiCl_4 and n -propanol: variation of optical density with mole per cent of n -propanol at (A) 882 cm.^{-1} , (B) 940 cm.^{-1} , (C) 3330 cm.^{-1} , and (D) 844 cm.^{-1} for benzene solvent.

proportion of alcohol whereas some show a constant increase. Finally, others show a maximum at definite ratios of *n*-propanol/TiCl₄.

To illustrate this, the optical density of several bands has been plotted versus increasing amount of alcohol (Figs. 3-5). In Figure 3, curves *A*, *B*, *C* correspond to bands the optical density of which increases constantly on increasing proportion of alcohol, whereas *D* decreases under the same conditions. Figure 4 relates to some of the bands recorded in the third column of Table I, and it is seen that the intensities of these bands have maxima when the ratio *n*-propanol/TiCl₄ is 1:1. In Figure 5, corresponding to some of the bands recorded in the fourth column of Table I, one sees that the intensities of these bands have maxima when the ratio *n*-propanol/TiCl₄ is 3:1. From the continuous variation theory, it is known that the product giving an absorption whose intensity is maximum when the two starting materials are mixed in equal amounts corresponds to a product with 1:1 stoichiometry. If on the other hand, a maximum occurs when the ratio is 3:1, the stoichiometry must be 3:1. Thus with the data of Table I and a correct band assignment it should be possible to deduce the structure of the complex.

In reviewing all the absorption bands recorded in Table I, a tentative band assignment based on group frequency data was made as follows.

In the first group are found bands the intensities of which decrease constantly when the mole fraction of TiCl₄ is increased (Fig. 3). These bands correspond to CH₃ and CH₂ stretching frequencies (2920 and 2860 cm.⁻¹) and deformation frequencies (1450 and 1370 cm.⁻¹). Others represent the free OH stretching (3600 cm.⁻¹) and deformation (1225 cm.⁻¹) modes. These assignments are similar to the ones made by Stuart,⁹ who used CCl₄ as solvent. The bands at 906 and 958 cm.⁻¹ were not assigned. It is to be noticed that optical density of bands corresponding to CH vibration frequencies are not very reliable due to almost complete absorption by the solvent at these frequencies.

In the second group there is a band at 815 cm.⁻¹ which increases with mole fraction of TiCl₄ (Fig. 3). This band does not correspond to any particular absorption of TiCl₄⁶ but, as Elliott et al. have reported¹⁰ the formation of a 1:1 complex between TiCl₄ and benzene, it may be postulated that this band relates to this complex.

In the third group are absorption bands due to the product of the reaction, since they do not exist in the starting material and develop on reaction to a maximum at a *n*-propanol/TiCl₄ ratio of 1:1 (Fig. 4). Thus the 2750 cm.⁻¹ band is the stretching mode for HCl in benzene according to the studies of Josien.¹¹ Two bands at 1070 and 1100 cm.⁻¹ have been tentatively assigned to the Ti—O—C vibration based on knowledge of the similar C—O—C bands.

The fourth group also includes bands corresponding to the product of the reaction. These bands have maximum intensities for a *n*-propanol/TiCl₄ ratio of 3:1 (Fig. 5). At 3530 and 3330 cm.⁻¹ are found the hydrogen-bonded OH stretching frequencies. The 1218 cm.⁻¹ peak seems to relate

to the 1225 cm^{-1} and the 940 and 882 cm^{-1} bands seem to be similarly related to 958 and 906 cm^{-1} bands. They may also correspond to shifts due to formation of hydrogen bonds, since it is known that absorption bands corresponding to C—O—H vibration will be shifted to lower wave numbers by hydrogen bonding.⁹

From these data the following scheme is proposed. Since there is a maximum in the HCl curves at a 1:1 ratio of TiCl_4 and *n*-propanol, then



and this reaction must prevail at high mole fractions of TiCl_4 . Titanium trichloride propylate is a well known compound the isolation of which has been reported by Nesmeyanov,¹² and its preparation requires an excess of TiCl_4 .

In the case where *n*-propanol is in excess, another reaction must be considered in order to account for the absorption bands, listed in the fourth column of Table I, which maximize at a 3:1 ratio. Since this group of bands includes hydrogen bonded OH modes, and since even at a high mole ratio of *n*-propanol some HCl is still found, reaction (2) or (3) seems most plausible, the complexed *n*-propanol being hydrogen-bonded.



A decision in favor of either reaction (2) or (3) does not appear to be justified. It may be shown that the optical density curves shown in Figure 4 should be symmetrical hyperbolae if reactions (1) and (2) were occurring, whereas they should show two maxima if reactions (1) and (3) were occurring. Neither extreme is found and a combination of the various reactions, each one weighted according to its own equilibrium constant is most probable. It is worth noting that $\text{TiCl}_2\text{OR}_2 \cdot \text{ROH}$ has been isolated by Jennings and co-workers.⁴

To the above equilibria must be added the formation of association complexes, as shown in eqs. (4) and (5).



The latter is considered to be particularly important from the catalytic point of view, since HCl is considered as a potential poison. Thus solvent could be a determining factor in reactivity on the basis of reaction (5).

Continuous Variation for the *n*-Propanol— TiCl_4 System in Carbon Tetrachloride

To illustrate the solvent effect, the data shown in Figure 6 were collected by use of the spectroscopically neutral solvent, carbon tetrachloride. Although only the high resolution spectra are shown, the results were essentially the same as for benzene solvent, except that some bands were shifted to higher wave numbers. These were OH and HCl modes, which

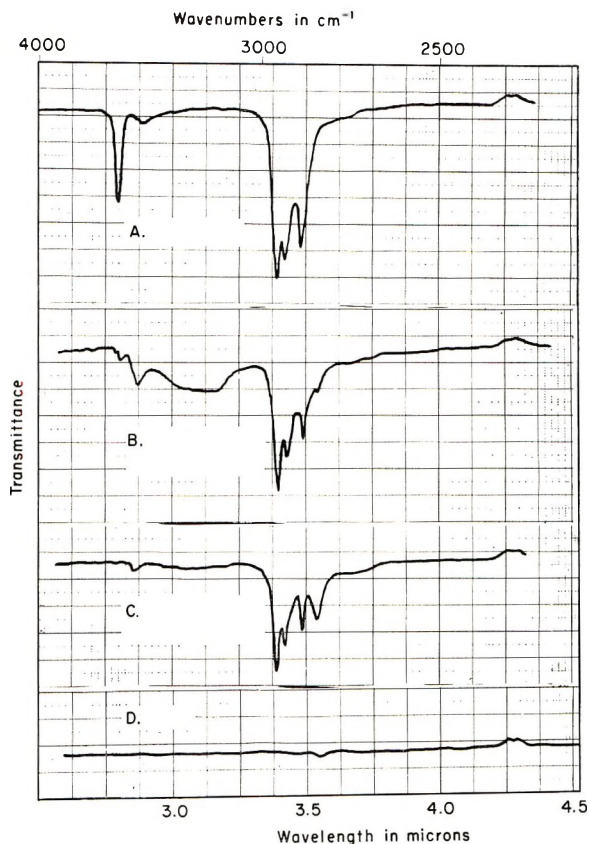


Fig. 6. High-resolution infrared spectra for the interaction of 0.0624M solution of TiCl_4 in CCl_4 and 0.0624M solution of *n*-propanol in CCl_4 ; A, *n*-propanol; B, 75% propanol, 25% TiCl_4 ; C, 50% propanol, 50% TiCl_4 ; D, TiCl_4 .

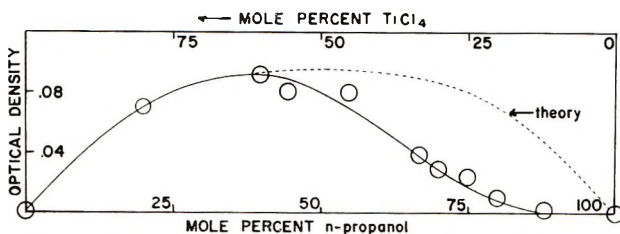


Fig. 7. Interaction of TiCl_4 and *n*-propanol: variation of optical density with mole per cent of *n*-propanol at 2831 cm^{-1} for CCl_4 solvent.

represent the well-established solvent effects for these groups.^{11,14} Although Figures 2 and 6 are not directly comparable, the shape and intensity of the HCl bands appear to be distinctly different in the two figures. It was also noted that the optical density of the free HCl band in Figure 6 at 2831 cm^{-1} , when plotted against mole per cent *n*-propanol (Fig. 7), was

more asymmetric at higher *n*-propanol mole fractions than for the equivalent curve in Figure 4.

Study of Hydrogen Bonding at High Resolution

As mentioned above, when TiCl_4 is mixed with an excess of *n*-propanol, three moles of *n*-propanol are linked to one of TiCl_4 . According to reactions (2) or (3), out of three molecules of *n*-propanol, one or two can react and give HCl whereas two or one are linked to the product and involved in a hydrogen bond. To add to our knowledge concerning the latter, several experiments were performed at high resolution and in carbon tetrachloride as solvent.

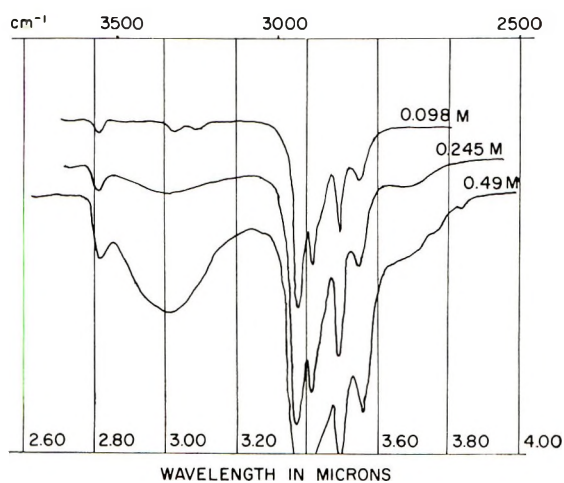


Fig. 8. High-resolution infrared spectra of equimolar amounts of TiCl_4 and propanol in CCl_4 at different concentrations.

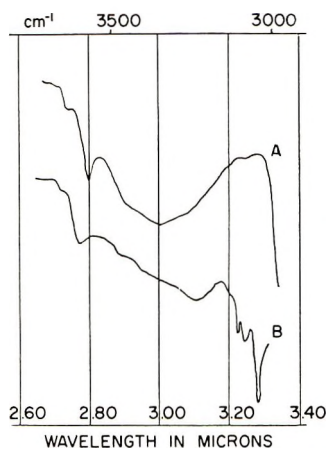


Fig. 9. High-resolution infrared spectra of mixtures containing 3 moles of *n*-propanol per mole of TiCl_4 at various dilutions in CCl_4 .

Dilution Experiment. In a first experiment a $0.49M$ solution of $TiCl_4$ was mixed with a $0.49M$ solution of n -propanol in 1:1 ratio. The solution was then diluted several times and the corresponding spectra were recorded. Figure 8 shows the 3000 cm.^{-1} region of four spectra corresponding to four dilutions. In the OH stretching region a band at 3365 cm.^{-1} disappears completely on dilution, whereas another one at 3560 cm.^{-1} is unaffected. This is the standard criterion for distinguishing intermolecular and intramolecular hydrogen bonds, hence it is concluded the 3560 cm.^{-1} band corresponds to an intramolecular hydrogen bond between complexed alcohol and the partial titanate.

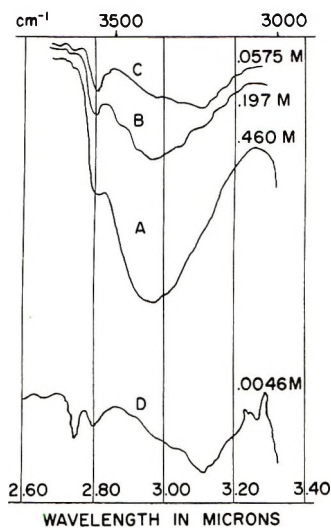
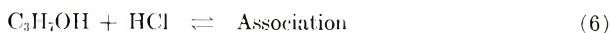


Fig. 10. High-resolution infrared spectra of $0.1M$ solutions of n -propanol and $TiCl_4$ in CCl_4 before and after addition of $0.1M$ triethyl aluminum: (A) 3:1 ratio of n -propanol/ $TiCl_4$; (B) 3:1:1 ratio of n -propanol/ $TiCl_4/Al(Et)_3$.

In a second experiment, a $0.46M$ solution of $TiCl_4$ was mixed with an excess of $0.46M$ n -propanol, the ratio of n -propanol to $TiCl_4$ being 3. Again, several dilutions were performed, and the corresponding spectra are recorded in Figure 9. As before, the two bands at 3365 and 3560 cm.^{-1} are found in the more concentrated solutions. On dilution, the band at 3365 cm.^{-1} disappears, whereas that at 3560 cm.^{-1} remains and a new band at 3220 cm.^{-1} appears. The latter is unaffected by dilution but seems to be overlapped at higher concentration by the intense, broad band at 3365 cm.^{-1} . It should be remembered that for n -propanol in CCl_4 , dimeric and polymeric associations of OH absorb at 3500 and 3300 cm.^{-1} ,¹³ which is different from what is observed in these experiments. Here again it may be said that the 3220 and 3560 cm.^{-1} bands seem to represent intramolecular hydrogen bonding corresponding to the coordinated n -propanol, whereas the 3365 cm.^{-1} band which disappears on dilution seems to be of the intermolecular hydrogen-bonding type.

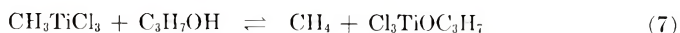
On the basis of these two experiments, as well as the observed dissymmetry in the HCl curves of Figure 4 and more particularly Figure 7, it was hypothesized that some HCl produced in the reaction of TiCl_4 and *n*-propanol was associated with some unreacted *n*-propanol. This has the effect of limiting the availability of the latter for reaction with TiCl_4 . This association of OH and HCl could then give rise to the absorption at 3365 cm^{-1} which corresponds to intermolecular hydrogen bonding. If this is correct, it should then be possible to detect this association in the HCl region, also, since the associated HCl should absorb at lower wave number. In Figure 8, it can be seen that around 2740 cm^{-1} the HCl absorption peak shows a marked shoulder which tends to disappear on dilution and could correspond to the association of HCl and *n*-propanol. For this situation, the following reaction can be written:



Other evidence of this equilibrium was found in the following cases.

Addition of AlEt_3 . AlEt_3 reacts readily with labile hydrogen to give ethane.¹⁵ One expects, *a priori*, that AlEt_3 will react faster with HCl than with *n*-propanol, hence if a small amount of the former is added to a mixture of TiCl_4 and propanol, only HCl should react. An infrared trace before and after addition of AlEt_3 is shown in Figure 10. The absorption band at 3365 cm^{-1} has disappeared, and the band at 3220 cm^{-1} has developed in accordance with the proposed reaction paths.

Replacement of TiCl_4 by CH_3TiCl_3 . If C_3HTiCl_3 is reacted with *n*-propanol, reaction (7) can be written:¹⁶



As before then, one or two alcohol molecules can be coordinated and one or none reacted:



or

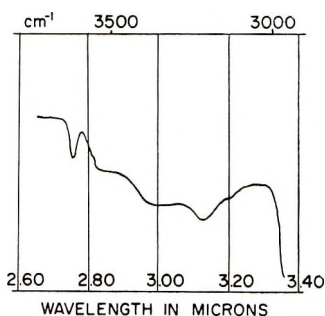


Fig. 11. High-resolution infrared spectra of a mixture of 20 mole-% CH_3TiCl_3 in CCl_4 and 80 mole-% *n*-propanol in CCl_4 . Both solutions were 0.17*M*.

If reaction (9) occurs, most of the HCl would be streamed away by the profuse methane evolution and, as for the addition of AlEt_3 , little or no HCl should be present in the reaction mixture. Here again, as shown in Figure 11, the band at 3365 cm.^{-1} has disappeared and is replaced by a band at 3220 cm.^{-1} . The observation is readily explained if the 3365 cm.^{-1} band is assigned to HCl-*n*-propanol association.

Effect of Alcohols on Polymerization Initiated by Transition Metal Catalysts

The foregoing complexing studies can be related to polymerization by a study of the effect of added alcohol on the polymer yield in a $\text{TiCl}_4\text{-Al}(\text{Et})_3$ system. Polymerizations of styrene at various $\text{TiCl}_4\text{-alcohol}$ mole ratios were performed, and the results are plotted in Figure 12 for the *n*-propanol system. Several other alcohols were also studied in detail: *n*-propanol, 1,3-butanediol, and 2,3-butanediol. In all cases results were essentially the same, i.e., the presence of alcohol has little effect on the amount of polymer formed up to an alcohol content of 1 mole/mole of titanium. Beyond this there is a sharp decrease in the amount of polymer formed, and the yield was zero when the mole fraction of alcohol was greater than 0.75 (three alcohols per titanium).

The broken curve in Figure 12 represents the optical density in benzene at 940 cm.^{-1} . It will be remembered that this was one of the absorption bands which was maximum at a 3:1 alcohol/titanium ratio (Table I). It would appear, therefore, that the complexing reactions is detrimental to catalyst activity only when the alcohol is present in excess. This suggests that a compound of the type postulated as the product of reaction (1) is capable of undergoing normal interaction with $\text{Al}(\text{Et})_3$. However, the products of reactions (2) or (3), where the coordinating valences of titanium are occupied by alcohol, no longer can undergo the requisite interaction with organometallic compound.

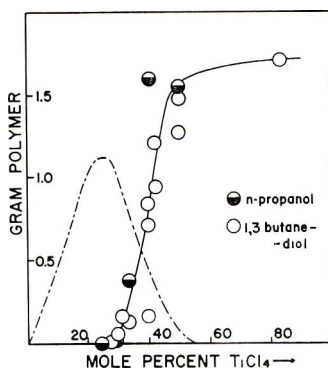


Fig. 12. Polymer yield as a function of the added alcohol for styrene polymerization with 1:1 $\text{TiCl}_4\text{-Al}(\text{Et})_3$ catalyst system. Broken curve is the optical density at 940 cm.^{-1} in the system $\text{TiCl}_4\text{-alcohol}$.

Aside from the fact that the point at which no polymer was formed in diol systems was at a titanium/alcohol mole ratio about 5% higher than for *n*-propanol, the diols showed surprisingly similar behavior. This suggests that there are some steric requirements in the formation of the complex which do not allow easy participation from the added hydroxyl grouping in the same molecule. Attempts to study the TiCl_4 -diol system by infrared spectroscopy were frustrated by the formation of a solid precipitate. The latter yielded on analysis a 2:1 ratio of diol to titanium under conditions of excess diol, which correlates well with the ratio of reactants when polymerization yield dropped to zero.

Although a detailed evaluation of the polymeric product of the various experiments was not undertaken, viscosity molecular weights were evaluated. In all cases it was found that the product was of low molecular weight ($\bar{M}_v = 3000$). There was no effect of titanium/alcohol ratio or catalyst concentration, up to 0.01 mole/100 ml., on the observed molecular weights.

CONCLUSION

In an actual polymerization system, a complex series of equilibria and reactions will be involved when alcohols are present with catalyst components such as titanium tetrachloride and aluminum triethyl. Nevertheless, it seems possible to state that with excess titanium tetrachloride.



excess of alcohol will lead to:



or



The latter reaction represents the deactivating aspect of the interactions.

The polymerization data show a clear correlation with the infrared results and indicate that catalyst deactivation comes about through occupancy of the titanium *d* orbitals by alcohols.

In addition, the several secondary complexes involving solvent, co-catalyst, or reaction product can significantly modify the relative concentrations of the primary complexes. Qualitatively the interactions are the same, but quantitatively the extent of the various primary processes could be considerably changed as a result of changing solvent or adding a proton acceptor to the system.

In conclusion it should be emphasized that with excess alcohol, titanium is involved in a soluble hydrogen-bonded complex without catalytic activity. At equivalent titanium-alcohol concentrations, a well-defined compound of limited solubility is formed but with complete retention of normal catalytic activity.

References

1. Bawn, C. E. H., and A. Ledwith, *Quart. Rev.*, **16**, 321 (1962).
2. Orsino, J. A., and D. F. Herman, U. S. Pat. 3,121,698 (1964).
3. Rausing, G., and S. Sunner, *Tappi*, **45**, 203A (1962).
4. Jenning, J. S., W. Wardlaw, and W. J. R. Way, *J. Chem. Soc.*, **1936**, 637.
5. Sigwalt, P., and J. P. Vairon, *Bull. Soc. Chim. France*, **1964**, 482.
6. Codell, M., *Analytical Chemistry of Titanium Metals and Compounds*, Interscience, New York-London, 1959, p. 307.
7. Watts, H. L., *Anal. Chem.*, **30**, 967 (1958).
8. Job, P., *Ann. Chim. (Paris)* [10], **9**, 113 (1928).
9. Stuart, A. V., and G. B. B. M. Sutherland, *J. Chem. Phys.*, **24**, 563 (1956).
10. Elliott, B., A. G. Evans, and E. D. Owen, *J. Chem. Soc.*, **1962**, 689.
11. Josien, M. L., and G. Sourisseau, *Bull. Soc. Chim. France*, **1955**, 178.
12. Nesmeyanov, A. N., R. Kh. Freidlina, and O. V. Nogina, *Izv. Akad. Nauk SSSR, Otd. Khim. Nauk*, **1951**, 518.
13. Stuart, A. V., *J. Chem. Phys.*, **21**, 1115 (1953).
14. Pimentel, G. C., and A. L. McClellan, *The Hydrogen Bond*, Freeman, San Francisco-London, 1960, p. 80.
15. Technical Information, Ethyl Corporation, Chemical Sales Div., Baton Rouge, La. (1961).
16. Beermann, C., and H. Bestian, *Angew. Chem.*, **71**, 618 (1959).

Résumé

On étudie l'interaction du tétrachlorure de titane et des alcools dans le benzène et le tétrachlorure de carbone par spectroscopie infrarouge. Une étude par "variation continue" des différentes bandes d'absorption a permis d'établir deux interactions différentes: l'une impliquant un rapport alcool-tétrachlorure de titane de 1/1 et l'autre de 3/1. La spectroscopie à haute résolution dans la région de $3\ \mu$ pour le dernier rapport indique une liaison-hydrogène bien définie, de nature intra-moléculaire. On interprète ceci en fonction des alcools qui sont à la fois entrés en réaction et coordonnés dans le complexe de titane. L'effet sur la polymérisation du composé de titane décroît fortement quand l'alcool est en excès molaire et tombe à zéro pour un rapport 3/1. On observe l'effet de l'addition de triéthyl-aluminium sur le spectre infra-rouge du complexe propanol-tétrachlorure de titane 3/1 dans la région de $3\ \mu$. On note des changements importants dans les modes de vibration OH. On mentionne aussi le spectre d'interaction du propanol-trichlorure de méthyltitane.

Zusammenfassung

Die Wechselwirkung zwischen Titan-tetrachlorid und Alkoholen in Benzol und Tetrachlorkohlenstoff wurde infrarotspektroskopisch untersucht. Eine Untersuchung der verschiedenen Absorptionsbanden durch "kontinuierliche Variation" erlaubte die Feststellung zweier verschiedener Wechselwirkungen: eine mit einem Alkohol-Titan-tetrachlorid-Verhältnis von 1:1 und einem anderen mit einem solchen von 3:1. Hochauflösungsspektroskopie im $3\text{-}\mu$ -Bereich zeigt bei letzterer eine gute definierte intramolekulare Wasserstoffbindung. Dies wurde als Reaktion und Koordination der Alkohole in einem Titan-Komplex interpretiert. Bezeichnenderweise nimmt die Polymerisationsaktivität der Titan-Verbindung bei molarem Alkoholüberschuss scharf ab und geht beim Verhältnis 3:1 gegen null. Der Einfluss von zugesetztem Aluminiumtriäthyl auf das Infrarotspektrum des Propanol-Titan-tetrachlorid-3:1-Komplexes wurde im $3\text{-}\mu$ -Bereich untersucht. Charakteristische Änderungen der OH-Valenzfrequenz wurden festgestellt. Schliesslich wurden die Wechselwirkungsspektren von Propanol und Methyltitan-tetrachlorid aufgenommen.

Received February 18, 1965

Revised April 14, 1965

Prod. No. 4744A

Penultimate Effect in Stereospecific Polymerization by Ionic Mechanism

Y. OHSUMI, T. HIGASHIMURA, and S. OKAMURA, *Department of
Polymer Chemistry, Kyoto University, Kyoto, Japan*

Synopsis

To clarify the penultimate effect in the stereospecific polymerization by ionic catalysts, the relationship between the steric structure of the polymer and polymerization conditions was studied for α -methylstyrene (α MS), methyl vinyl ether (MVE), and methyl methacrylate (MMA) from our result and literature results. Two possible probabilities of an isotactic addition considering the penultimate effect, P_{ii} and P_{si} , are compared. We define the α value as $P_{si} = \alpha P_{ii}$. The greater the deviation of the α -value is from unity, the greater the penultimate effect. It is shown that the α value in a given monomer is constant for a wide range of tacticity in the various conditions. In α MS, the α value is unity and there is no penultimate effect. Otherwise, in the MVE-BF₃-O(C₂H₅)₂ system, α is 0.7 and the penultimate effect is present. When MMA is polymerized by alkali alkyl, the α value is changed by the kind of alkali metal, that is, α values in toluene solution are 0.45, 0.65, and 0.75 for Li, Na, and K, respectively.

I. INTRODUCTION

Many experimental data on the stereospecific polymerization of vinyl monomers by an ionic mechanism have been published. Although many reaction mechanisms have been proposed for a heterogeneous catalyst, the mechanism for a homogeneous catalyst has not been so actively discussed as that for a heterogeneous catalyst. Bawn and Ledwith¹ summarized the mechanism of a homogeneous polymerization in their review, and they proposed a reaction mechanism for the stereospecific polymerization of a monomer having a polar substituent, e.g., methyl methacrylate (MMA) and vinyl ethers, by a homogeneous catalyst. These mechanisms take into account not only the effect of an end unit of a growing chain but also that of a penultimate unit in determining the steric structure of an attacking monomer.

For MMA, it was confirmed from the NMR spectra that the steric configuration of an attacking monomer is controlled only by the last unit at the growing end in the radical polymerization, but not in anionic polymerization.²⁻⁵ These experimental results provided the basis of the reaction mechanisms proposed at present.

Although the necessity of the penultimate effect for isotactic polymerization has been confirmed in the case of a polar monomer such as MMA, it is not clear whether the penultimate effect is necessary for formation of

isotactic polymer for all monomers. Bywater et al.⁶ reported that the penultimate effect was not noted in the syndiotactic polymerization of α -methylstyrene (α MS). It is very important for the elucidation of the mechanism of the stereospecific polymerization to know the conditions under which a penultimate unit affects the steric configuration of an attacking monomer. Therefore, we want to know the steric structure of polymers obtained from a polar and a nonpolar monomer by cationic polymerization. Fortunately, the steric structure of poly(methyl vinyl ether) (PMVE)⁷ obtained by $\text{BF}_3 \cdot \text{O}(\text{C}_2\text{H}_5)_2$ and that of poly- α -methylstyrene ($\text{P}\alpha\text{MS}$)^{6,8} polymerized by various catalysts have already been studied by NMR spectra.

In the present paper report the use of various solvents in the homogeneous polymerization of α MS catalyzed by $\text{BF}_3 \cdot \text{O}(\text{C}_2\text{H}_5)_2$. In previous papers^{6,8} many kinds of catalysts were used for the polymerization of α MS, but the effect of a solvent is just as important as well as that of catalysts for the stereospecific polymerization in the cationic mechanism.⁹ In this paper, we have also tried to present a quantitative measure of the penultimate effect. It is found that a penultimate effect can be recognized in the two polar monomers, MMA and methyl vinyl ether (MVE), and that the penultimate effect in the polymerization of MMA in BuLi-catalyzed polymerization is greater than that in polymerization of MVE. No penultimate effect is noted in cationic polymerization of the nonpolar monomer, α MS, or in the radical polymerization of MMA.

EXPERIMENTAL

Polymerization and purification of materials were carried out by the same procedures as in the previous paper.^{10,11}

NMR spectra of $\text{P}\alpha\text{MS}$ were measured by using a chloroform solution (15%, w/v) in a sealed tube at 60 Mcycles/sec. (Varian Associates HR-60).

RESULTS AND DISCUSSION

Polymerization of α MS by $\text{BF}_3 \cdot \text{O}(\text{C}_2\text{H}_5)_2$

α MS was polymerized in a chloroform-*n*-hexane mixed solvent by $\text{BF}_3 \cdot \text{O}(\text{C}_2\text{H}_5)_2$ at -70°C . As already reported, polymer yield increased as chloroform in the mixed solvent was increased. The molecular weight of the resultant polymer increased with increasing content of chloroform and attained a maximum value at 40–60 vol.-% of chloroform.^{10,11} Also, $\text{P}\alpha\text{MS}$ obtained in mixed solvent of high chloroform content was only slightly soluble in benzene, and the x-ray diffraction pattern of this polymer was sharper than that of ordinary $\text{P}\alpha\text{MS}$.¹² It was later found that the steric structure of $\text{P}\alpha\text{MS}$ could be analyzed by NMR spectra.^{6,8} Therefore, the relationship between polymerization conditions and the steric structure of $\text{P}\alpha\text{MS}$ was re-examined by NMR spectra.

The NMR spectrum of $\text{P}\alpha\text{MS}$ obtained in *n*-hexane was clearly different from that obtained in chloroform, as shown in Figure 1. The proton

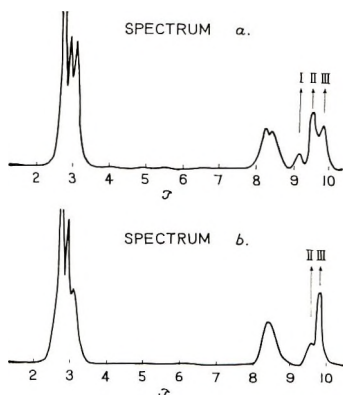


Fig. 1. NMR spectra of poly- α -methylstyrene in chloroform solutions: (a) polymer prepared with $\text{BF}_3 \cdot \text{O}(\text{C}_2\text{H}_5)_2$ in *n*-hexane at -70°C .; (b) polymer prepared with $\text{BF}_3 \cdot \text{O}(\text{C}_2\text{H}_5)_2$ in chloroform at -70°C .

resonances with chemical shifts of $\tau = 9.82, 9.57$, and 9.08 were assigned to isotactic, heterotactic, and syndiotactic triads, respectively. These positions of peaks of α -methyl group agree with those reported by Bywater et al.,⁶ Braun et al.,¹³ and Sakurada et al.⁸

The interpretation of the NMR spectrum of $\text{P}\alpha\text{MS}$ has not been decided yet, but we tentatively adopted the interpretation of Sakurada et al.¹⁴ because they analyzed the crystalline structure of $\text{P}\alpha\text{MS}$ obtained in the cationic mechanism on the basis of x-ray data as well as NMR spectra. The fiber identity period of this $\text{P}\alpha\text{MS}$ was 6.6 \AA ., and the structure of the crystalline material was rhombohedral, as is the case in isotactic polystyrene. The dimensions of the hexagonal unit were $a = 23.7 \text{ \AA}$. and $c = 6.6 \text{ \AA}$., and these values are very similar to those of isotactic polystyrene ($a = 21.9 \text{ \AA}$., $c = 6.65 \text{ \AA}$.). This is why we chose the isotactic structure for $\text{P}\alpha\text{MS}$ obtained by $\text{BF}_3 \cdot \text{O}(\text{C}_2\text{H}_5)_2$. Even if the assignments for isotactic and syndiotactic triad are reversed, this does not invalidate the following discussion on the penultimate effect.

Therefore, the fraction (or the probability of addition) of diad and triad of the isotactic structure, P_i and P_{ii} , is given by eqs. (1) and (2), respectively (from Fig. 1).

$$P_i = \frac{1/2(\text{Area of peak II}) + (\text{area of peak III})}{(\text{Area of peak I}) + (\text{area of peak II}) + (\text{area of peak III})} \quad (1)$$

$$P_{ii} = \frac{(\text{Area of peak III})}{1/2(\text{Area of peak II}) + (\text{area of peak III})} \quad (2)$$

The fractions of a syndiotactic and heterotactic part were similarly calculated from the peak area of Figure 1 corresponding to each structure.

Figure 2 shows the relationship between the steric structure of $\text{P}\alpha\text{MS}$ obtained from NMR spectra and solvent composition. The isotactic

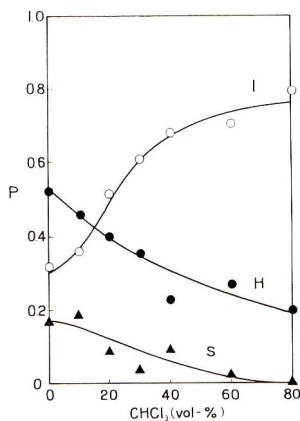


Fig. 2. Relationship between solvent composition of polymerization and fraction P of poly- α -methylstyrene in the *n*-hexane-chloroform system: (○) isotactic I; (●) heterotactic H; (▲) syndiotactic S. Monomer concentration 20 vol.-%; $\text{BF}_3 \cdot \text{O}(\text{C}_2\text{H}_5)_2$ concentration: (0.24 mole/l.; polymerization temperature: -70°C .; polymerization time: 90 min.

fraction increased with increasing chloroform in the solvent. This result agrees with our previous results from solubility and x-ray diffraction data.¹²

Similar relationships were observed in mixed solvents of *n*-hexane-toluene and *n*-hexane-methylene chloride.¹⁵ Atactic P α MS was obtained in *n*-hexane, which is a poor solvent for P α MS and the isotactic content of P α MS was increased by addition of good solvents for P α MS, independent of the polarity of the solvents. In the homogeneous polymerization of vinyl ethers by cationic catalysts, the isotacticity of the resultant polymer decreases markedly on addition of a polar solvent.⁹ The difference between these monomers will be reported in detail in a separate paper. We were able to obtain P α MS having various tacticities by merely changing solvent compositions.

Method of Estimation of the Penultimate Effect

When σ is defined as the probability that an attacking monomer gives the same configuration as that of the last unit at its growing end and there is no penultimate effect, according to Bovey et al.,² the following relationships are valid:

$$\begin{aligned} I &= \sigma^2 \\ S &= (1 - \sigma)^2 \\ H &= 2\sigma(1 - \sigma) \end{aligned} \quad (3)$$

where I , S , and H are a fraction of triad for isotactic, syndiotactic, and heterotactic structure, respectively. Johnsen et al.³ found the following relationships:

$$I = P_i P_{ii} = P_{si} P_{ii} / (P_{is} + P_{si}) \quad (4)$$

$$H = P_i P_{is} + P_s P_{si} = 2P_{si} P_{is} / (P_{is} + P_{si}) \quad (5)$$

$$S = P_s P_{ss} = P_{is} P_{ss} / (P_{is} + P_{si}) \quad (6)$$

where P_{ii} is the probability of l -addition of a monomer to an ll growing chain end or a d -addition to a dl growing chain end. P_{ss} , P_{is} , and P_{si} are similarly defined. Also, P_i is the probability that a monomer unit will add to a growing end and give the same configuration as that of the last unit of the growing end, and therefore $P_s = 1 - P_i$ (P_i is the same as Bovey's σ).

When a penultimate unit does not affect the steric configuration of the entering monomer and the steric configuration of that is controlled only by the last unit of a growing chain, $P_i = P_{ii} = P_{si} = \sigma$ and $P_s = P_{ss} = P_{is} = 1 - \sigma$. Therefore, eqs. (4)–(6) reduce to eq. (3). When there is a penultimate effect, P_{ii} should differ from P_{si} , and we can consider that this difference will show the degree of the penultimate effect. To show quantitatively the penultimate effect, we define an α value as follows:

$$P_{si} = \alpha P_{ii} \quad (7)$$

That is, the penultimate effect does not exist in the case of $\alpha = 1$, and the greater the difference of α from unity, the greater the penultimate effect.

If we put eq. (7) into eqs. (4)–(6), I , H , and S are presented as a function of only P_{ii} and α as shown in eqs. (8)–(10).

$$I = P_i P_{ii} = \alpha P_{ii}^2 / [1 - (1 - \alpha) P_{ii}] \quad (8)$$

$$H = P_i P_{is} + P_s P_{si} = 2\alpha P_{ii} (1 - P_{ii}) / [1 - (1 - \alpha) P_{ii}] \quad (9)$$

$$S = P_s P_{ss} = (1 - P_{ii})(1 - \alpha P_{ii}) / [1 - (1 - \alpha) P_{ii}] \quad (10)$$

From these equations, we can obtain a simple relationship between P_i or P_s and P_{ii} as follows:

$$1/P_i = (1/\alpha)(1/P_{ii}) - [(1 - \alpha)/\alpha] \quad (11)$$

$$1/P_s = [\alpha/(1 - P_{ii})] + (1 - \alpha) \quad (12)$$

As P_i and P_{ii} can be measured for various polymers by NMR spectra, we can easily obtain the α value for various systems.

Calculation of α from Experimental Results

α -Methylstyrene. For $P\alpha$ MS obtained in various mixed solvents at -70°C . by $\text{BF}_3 \cdot \text{O}(\text{C}_2\text{H}_5)_2$ catalyst, $1/P_i$ was plotted against $1/P_{ii}$ according to eq. (11). A straight line through the origin was obtained for a whole range of P_{ii} , as shown in Figure 3. The α value is clearly unity from this line for this system over a wide range of tacticity. In Figure 4 the theoretical curve ($\alpha = 1$) and experimental results are plotted for P_{ii} . This figure is essentially the same as Bovey's σ plot. Thus, we conclude that P_i is equal to P_{ii} in the system $\alpha\text{MS}-\text{BF}_3 \cdot \text{O}(\text{C}_2\text{H}_5)_2$ for all mixed solvents. Bywater et al.⁶ reported that the steric structure of $P\alpha$ MS obtained by various catalysts was represented by a single σ value, that is, there is no

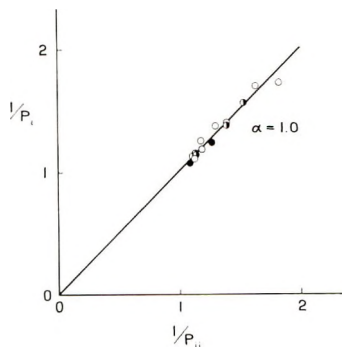


Fig. 3. Plot of $1/P_i$ vs. $1/P_{ii}$ of poly- α -methylstyrene prepared with $\text{BF}_3 \cdot \text{O}(\text{C}_2\text{H}_5)_2$ in various solvents: (O) *n*-hexane-chloroform; (◐) *n*-hexane-toluene; (●) *n*-hexane-methylene chloride.

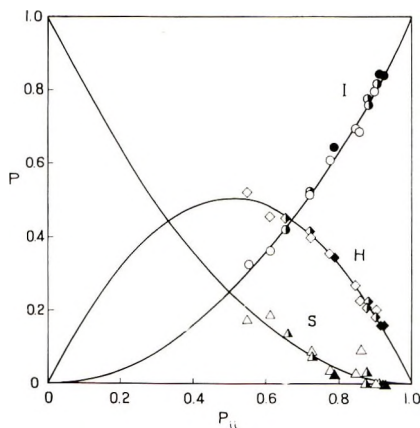


Fig. 4. Plot of P vs. P_{ii} for (O, ◐, ●) isotactic, (◊, ◑, ◆) heterotactic, and (Δ, ▲, ◆) syndiotactic fraction of poly- α -methylstyrenes prepared with $\text{BF}_3 \cdot \text{O}(\text{C}_2\text{H}_5)_2$ in various solvents: (O, ◊, Δ) *n*-hexane-chloroform; (◐, ◑, ▲) *n*-hexane-toluene; (●, ◆, ▲) *n*-hexane-methylene chloride.

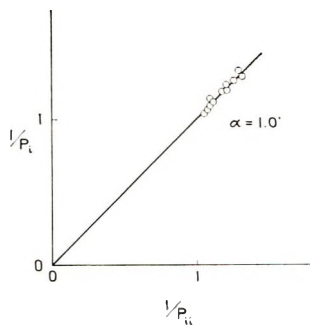


Fig. 5. Relationship between $1/P_{ii}$ and $1/P_i$ for poly- α -methylstyrene prepared with various catalysts. Data of Sakurada and Nishioka.⁸

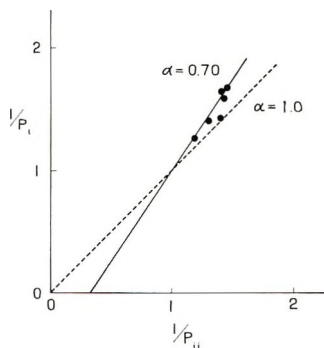


Fig. 6. Plot of $1/P_i$ vs. $1/P_{ii}$ for poly(methyl vinyl ether).⁷

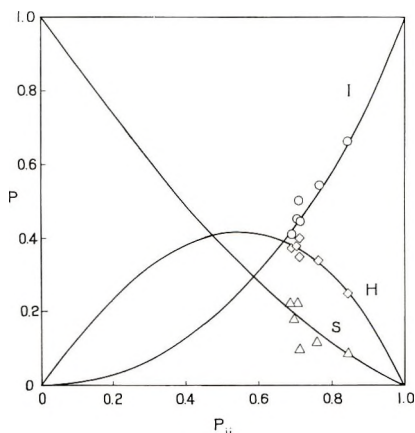


Fig. 7. Plot of P vs. P_{ii} for poly(methyl vinyl ether):⁷ (○) isotactic; (◇) heterotactic; (△) syndiotactic.

penultimate effect for α MS. To confirm this conclusion, Sakurada's results were plotted by eq. (11). As shown in Figure 5, the value of α was unity for all catalysts, and this result agrees with Bywater's result except for a reverse relationship between an isotactic and syndiotactic assignment.

Recently, Braun et al.¹³ reported the structure of $P\alpha$ MS obtained by various initiators. We also calculated the α value from these results by the same method; exactly the same result was obtained for cationic $P\alpha$ MS, that is, the α value was unity. Otherwise, α values of anionic $P\alpha$ MS slightly deviated from unity. This deviation may be due to experimental errors, because the tacticity of anionic $P\alpha$ MS was low.

Methyl Vinyl Ether. Brownstein's data for PMVE produced by $\text{BF}_3 \cdot \text{O}(\text{C}_2\text{H}_5)_2$ catalyst were analyzed by eq. (11). These data indicated that the configuration of PMVE can not be represented by a single parameter σ . A plot of $1/P_i$ against $1/P_{ii}$ showed a good linear relationship over a whole range of a tacticity, as shown in Figure 6. We can calculate the α

value from the inclination and an intercept of this straight line. Figure 7 shows the plot of fractions of each triad (P) against P_{ii} in the case of $\alpha = 0.70$. It is very important that the α value is constant for a wide tacticity range independent of polymerization conditions.

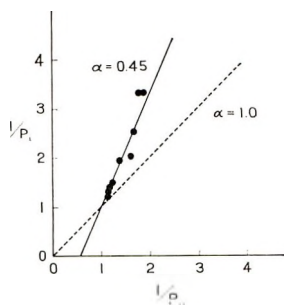


Fig. 8. Plot of $1/P_i$ vs. P_{ii} for poly(methyl methacrylate) prepared with BuLi in toluene and dimethoxyethane.^{2,3}

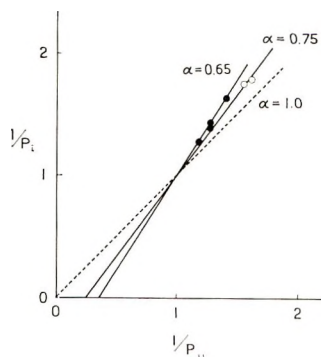


Fig. 9. Plot of $1/P_i$ vs. $1/P_{ii}$ for poly(methyl methacrylate) prepared with various catalysts in hydrocarbon solvents: (●) *n*-amyl Na; (○) *n*-octyl K.

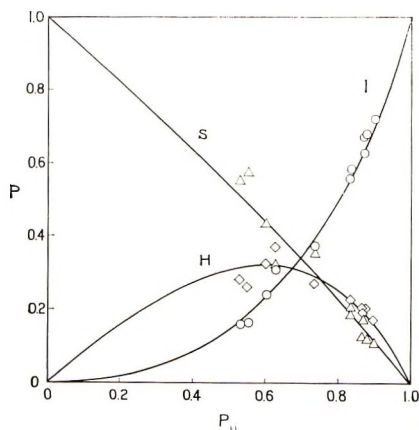


Fig. 10. Plot of P vs. P_{ii} for poly(methyl methacrylate) prepared with BuLi in toluene and dimethoxyethane: (○) isotactic; (◇) heterotactic; (△) syndiotactic.

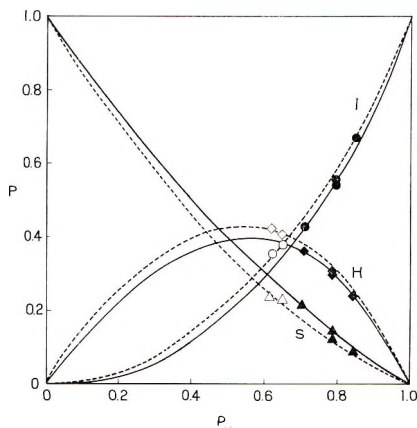


Fig. 11. Plot of P vs. P_i for (○, ●) isotactic, (◇, ◆) heterotactic, and (△, ▲) syndiotactic poly(methyl methacrylate) prepared with various catalysts in hydrocarbon solvents:³ (●, ◆, ▲) *n*-amyl Na; (○, ◇, △) *n*-octyl K.

Methyl Methacrylate. MMA has been polymerized in many kinds of solvents by various alkali alkyl catalysts, and the steric structure of the resultant polymers have been determined by NMR spectra by many researchers.²⁻⁴ When these results were plotted in accord with eq. (11), each alkali metal showed a distinct pattern. We obtained good linear relationships, as shown in Figures 8 and 9. Theoretical curves and experimental results obtained by using these α values are shown in Figures 10 and 11. In the case of Li alkyl, the α value was constant over a wide tacticity range except the case of an addition of pyridine and tetrahydrofuran. Although there are few data for about Na and K alkyls, it is clearly shown that α values with these catalysts are greater than that with BuLi catalyst.

DISCUSSION

From these results, it is concluded that we can obtain a constant α value for a wide tacticity range when a given monomer is polymerized at various conditions. The α values for several monomers and several catalysts are summarized in Table I.

TABLE I
Summary of α Values for Various Monomers

Monomer	Catalyst	Solvent	α	Ref.
α MS	$\text{BF}_3 \cdot \text{O}(\text{C}_2\text{H}_5)_2$	Various	1.0	
"	Various	Mainly hydrocarbon	1.0	6, 8
MVE	$\text{BF}_3 \cdot \text{O}(\text{C}_2\text{H}_5)_2$	Various	0.70	15
MMA	BuLi	Toluene	0.45	3
"	Amyl Na	"	0.65	3
"	Octyl K	"	0.75	3

Table I shows that the monomer having a polar side group generally gives an α value smaller than unity. However, for a nonpolar monomer, such as α MS produced an isotactic polymer by the ionic polymerization, the α value is unity and the penultimate effect does not exist. This is true not only for polymers obtained with $\text{BF}_3 \cdot \text{O}(\text{C}_2\text{H}_5)_2$ catalyst but with other catalysts, such as Ziegler and anionic catalysts also. Szwarc et al.¹⁶ reported a penultimate effect for the α -methyl group in α MS on the basis of the propagation rate constant of anionic homopolymerization and copolymerization. It, therefore, appears that the meaning of the penultimate effect in the stereospecific polymerization is a little different from that of rate of polymerization.

In MMA and MVE, the α value is smaller than unity, and a penultimate effect can be recognized. The smaller the α value, the greater the penultimate effect is. Therefore, the penultimate unit of a growing chain of MMA greatly affects an attacking monomer.

A comparison of the kind of alkali metal used in the polymerization of MMA shows that a counterion which is of a small size and high electronegativity shows a small α value and a large penultimate effect. This result seems to support the mechanism of Bawn et al.¹ according to which the lithium atom as a counterion coordinates with the carbonyl oxygen of the penultimate monomer unit. However, the α value for an isotactic PMVE obtained in a nonpolar solvent, is the same as the α value for atactic PMVE produced in a polar solvent. It is generally considered that the counter ion is solvated by a solvent molecule in a polar solvent and that the penultimate effect thus is decreased in this system. Therefore, the constant of the α value in various solvents cannot be interpreted according to Bawn's mechanism. This point is presently being investigated by studies on other vinyl monomers.

Of course, the penultimate effect is not the only reason for producing an isotactic polymer. It should be noted that atactic or syndiotactic polymer is also produced in systems in which the penultimate effect operates.

The authors thank The Research Institute of Kureha Spinning Co. Ltd. and Central Research Laboratories of Toyo Rayon Co. for the measurement of NMR spectra.

References

1. Bawn, C. E. H., and A. Ledwith, *Quart. Rev.*, **16**, 361 (1962).
2. Bovey, F. A., and G. V. D. Tiers, *J. Polymer Sci.*, **44**, 173 (1960).
3. Brawn, D., M. Hermer, U. Johnsen, and W. Kern, *Makromol. Chem.*, **51**, 15 (1962).
4. Nishioka, A., H. Watanabe, I. Yamaguchi, and H. Shimizu, *J. Polymer Sci.*, **45**, 232 (1960); *ibid.*, **48**, 241 (1960).
5. Miller, R. L., *J. Polymer Sci.*, **56**, 375 (1962).
6. Brownstein, S., S. Bywater, and D. J. Worsfold, *Makromol. Chem.*, **48**, 127 (1961).
7. Brownstein, S., and D. M. Wiles, *J. Polymer Sci.*, **A2**, 1901 (1964).
8. Sakurada, Y., and A. Nishioka, *J. Polymer Sci.*, **B1**, 633 (1963).
9. Higashimura, T., T. Kodama, and S. Okamura, *Kobunshi Kagaku*, **17**, 163 (1960).
10. Okamura, S., Y. Imanishi, and T. Higashimura, *Kobunshi Kagaku*, **16**, 69 (1959).

11. Imanishi, Y., T. Higashimura, and S. Okamura, *Kobunshi Kagaku*, **17**, 236 (1960).
12. Okamura, S., T. Higashimura, and Y. Imanishi, *J. Polymer Sci.*, **33**, 491 (1958); *Kobunshi Kagaku*, **16**, 129 (1959).
13. Braun, D., G. Heufer, V. Johnsen, and K. Koble, *Z. Physik. Chem.*, **68**, 959 (1964).
14. Sakurada, Y., Doctoral Thesis (Kyoto University), 1964; Japan. Pat. 11540 (1962).
15. Ohsumi, Y., and T. Higashimura, unpublished data.
16. Bhattacharyya, D. N., C. L. Lee, J. Smid, and M. Szwarc, *J. Am. Chem. Soc.*, **85**, 533 (1963).

Résumé

On a pour but d'éclaircir l'influence de l'unité pénultième au cours de la polymérisation stéréospécifique au moyen de catalyseurs ioniques. La relation entre la structure stérique du polymère et les conditions de polymérisation a été étudiée à partir de nos résultats et de ceux de la littérature pour l' α -méthylstyrène (α MS), l'éther méthylvinyle (MVE) et le méthacrylate de méthyle (MMA). On compare les deux probabilités possibles d'une addition isotactique tenant compte de l'influence de l'unité pénultième, P_{ii} et P_{si} . Nous définissons la valeur α par l'équation $P_{si} = \alpha P_{ii}$. Plus la déviation de la valeur de α est grande par rapport à l'unité, plus l'influence de l'unité pénultième est importante. On montre que la valeur de α pour un monomère donné est constante dans un large domaine de tacticité et dans diverses conditions. Pour α MS, la valeur de α est égale à l'unité et il n'y a pas d'influence de l'unité pénultième. D'un autre côté, dans le système, MVE - $\text{BF}_3 \cdot \text{O}(\text{C}_2\text{H}_5)_2$, la valeur de α est égale à 0,7 et l'influence de l'unité pénultième est reconnue. Lorsque MMA est polymérisé par un alcool-alcalin, la valeur de α est changée par la nature du métal alcalin. Les valeurs de α sont 0,45, 0,65, et 0,75 pour Li, Na, et K respectivement.

Zusammenfassung

Zur Aufklärung des Einflusses des vorletzten Bausteins bei der stereospezifischen Polymerisation mit ionischen Katalysatoren wird die Beziehung zwischen der räumlichen Struktur des Polymeren und den Polymerisationsbedingungen für α -Methylstyrol (α MS), Methylvinyläther (MVE) und Methylmethacrylat (MMA) aus eigenen Ergebnissen und solchen aus der Literatur untersucht. Zwei mögliche Wahrscheinlichkeiten für eine isotaktische Addition unter Berücksichtigung des Einflusses der vorletzten Gruppe, P_{ii} und P_{si} werden verglichen. Ein α -Wert wird durch $P_{si} = \alpha P_{ii}$ definiert. Je grösser die Abweichung des α -Werts von eins ist, umso grösser ist der Einfluss der vorletzten Gruppe. Es wird gezeigt, dass der α -Wert bei einem gegebenen Monomeren für einen weiten Taktizitätsbereich unter verschiedenen Bedingungen konstant ist. Bei α MS beträgt der α -Wert eins und es besteht kein Einfluss der vorletzten Gruppe. Dagegen ist der α -Wert im MVE- $\text{BF}_3 \cdot \text{O}(\text{C}_2\text{H}_5)_2$ -System 0,7 und ein Einfluss der vorletzten Gruppe ist nachweisbar. Bei der Polymerisation von MMA durch Alkaliäthyl ist der α -Wert, hängt von der Art des Alkalimetalls ab, sodass die α -Werte für Li, Na bzw. K 0,45; 0,65 bzw. 0,75 betragen.

Received February 25, 1965

Revised May 11, 1965

Prod. No. 4753A

Poly(chloroaldehydes). III. Poly(dichloroacetaldehyde)

IRVING ROSEN and C. L. STURM, *T. R. Evans Research Center, Diamond Alkali Company, Painesville, Ohio*

Synopsis

Although dichloroacetaldehyde has only one chlorine less than chloral, the polymerization and polymer characteristics are quite different. Dichloroacetaldehyde is readily polymerized by Lewis acid catalysts to polymer with terminal hydroxyl groups. The catalyst $\text{BF}_3 \cdot \text{Et}_2\text{O}$, at 0°C ., produces very high molecular weight polymer, in bulk polymerization. A $\overline{\text{DP}}_n$ of about 400 is readily attainable. The characteristics of the polymerization indicate a cationic type, with greater dependence of $\overline{\text{DP}}$ upon chain termination rather than chain transfer. The polymer is readily end-capped by acetic anhydride, with a pyridine catalyst, to increase its thermal stability. Melting point, infrared spectra, and x-ray diffraction measurements confirm that the polymer produced under these conditions is amorphous. Cast films of the polymer could be only partially oriented. The polymer is soluble in many common organic solvents.

INTRODUCTION

Around 1870, dichloroacetaldehyde (DCA) was noted to polymerize on standing, as well as in the presence of traces of acid.^{1,2} Since then, only one new report has appeared, which describes the spontaneous polymerization of DCA to a block of soft, transparent material.³ The polymer formed is crystalline, soluble in acetone, but insoluble in water and alcohol. The dearth of information on the polymerization of DCA becomes evident in a perusal of recent review articles on polyacetals.^{4,5}

The DCA polymers described in the literature have been of low degree of polymerization ($\overline{\text{DP}}$). This report deals with attempts to obtain high polymer, predominantly by means of cationic initiators.

EXPERIMENTAL

Two sources of DCA were used in this work. One was DCA trimer which may be decomposed thermally to a monomer of 99.3% purity. The other was commercially available (FMC Corp.) and contained about 6% of chloroacetaldehyde, 3% of chloral, 90% of DCA, and 2000-3000 ppm of H_2O . Drying of this crude DCA over P_2O_5 and careful distillation produced DCA of 95% purity with chloral as the single major impurity. Because of its greater availability, this monomer was used in several of the screening and polymerization experiments. The results compared favorably with

those carried out with the purer monomer. Later work showed that the polymer produced did not contain any detectable chloral comonomer.

The polymerizations were carried out in small resin kettles which were dried at 120°C. and kept under a dry nitrogen atmosphere as they cooled. Addition of reagents was made by means of dried hypodermic syringes. After the polymerization was completed, the polymer was ground in a Waring Blendor in the presence of acidic methanol to remove the catalyst.

The relative molecular weight of the polymer was determined by viscosity measurement in tetrahydrofuran. A limited number of measurements were made in a Mechrolab membrane osmometer to obtain some estimates of the relationship between \overline{DP}_n and the viscosity.

As a matter of convenience, the reduced viscosity, η_{sp}/c , was the solution property most often determined by measuring the flow time of a solution of 0.1 g. of polymer in 100 ml. of tetrahydrofuran at 25.0°C. In many instances, uncapped polymer gave low viscosity values because of gradual decomposition of the polymer in solution. End-capped polymers usually tended to higher values because of their stability, and possibly because a portion of the low molecular weight fraction may have been lost by decomposition during the capping reaction.

The structure of the polymer was investigated by means of infrared spectroscopy and x-ray diffraction. The infrared spectrum was obtained from film cast from a tetrahydrofuran solution, with the use of a Perkin-Elmer Infracord or Perkin-Elmer Model 21 spectrometer (NaCl prism). For work near the OH region, Nujol mulls and a calcium fluoride prism were used. Fiber-type diffraction patterns were obtained from polymer films with the use of nickel-filtered copper $K\alpha$ radiation.

RESULTS

Catalyst Screening

Several reagents, covering anionic, neutral, and cationic types, were screened as DCA polymerization catalysts. The screening was carried out without a solvent at 0°C., and with 0.1–1 mmole of catalyst with 10 ml. of DCA. The object was to determine which catalysts might be the most efficient in producing high molecular weight polymer.

Many Lewis acid catalysts were particularly effective, forming good yields of polymer within 1–2 hr. after the catalyst was added, e.g., SnCl_4 , NbCl_5 , AlCl_3 , AlBr_3 , $\text{BF}_3 \cdot \text{Et}_2\text{O}$. Basic and neutral catalysts, such as tertiary amines, tertiary phosphines, and quaternary ammonium salts, formed either very small amounts or no polymer, even after prolonged standing at both 0°C. and ambient temperature.

Polymerization

The catalyst $\text{BF}_3 \cdot \text{Et}_2\text{O}$ was utilized in most of the bulk polymerizations because it conveniently yielded high conversions of high molecular weight polymers which were readily freed from the catalyst residue.

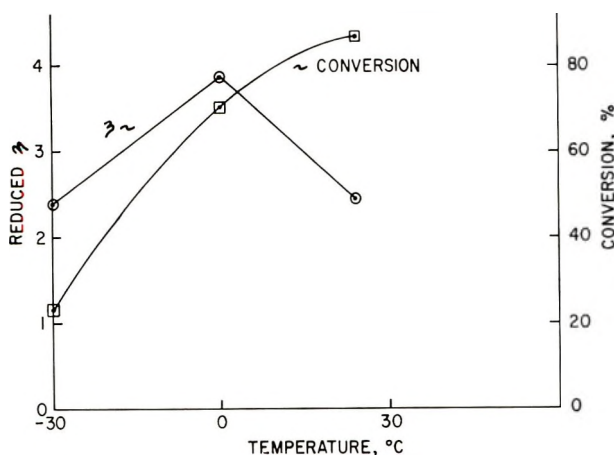


Fig. 1. Influence of polymerization temperature on (○) polymer viscosity and (□) conversion in the bulk polymerization of DCA. (0.16 mmole $\text{BF}_3 \cdot \text{Et}_2\text{O}$ /mole DCA).

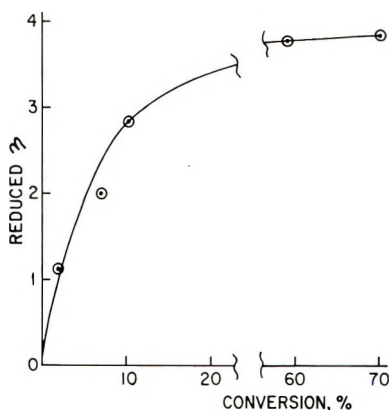


Fig. 2. Variation of polymer viscosity with conversion in $\text{BF}_3 \cdot \text{Et}_2\text{O}$ -catalyzed polymerization of DCA at 0°C .

The polymerization temperature has the most marked influence on the polymer molecular weight and conversion (Fig. 1). Although the conversion of monomer to polymer increases with the polymerization temperature, the optimum molecular weight is obtained at about 0°C .

During polymerization, samples of the reaction mass were withdrawn to determine the effect of the degree of conversion on the polymer molecular weight. In the early stages of the bulk polymerization, up to about 10% conversion of monomer to polymer, there is considerable chain termination (Fig. 2). Beyond this point, the variation of molecular weight with conversion is considerably reduced and is very small in the 50–70% conversion range.

Increase of catalyst concentration results in only a slight decrease in polymer molecular weight (Fig. 3). The average rate of conversion of DCA

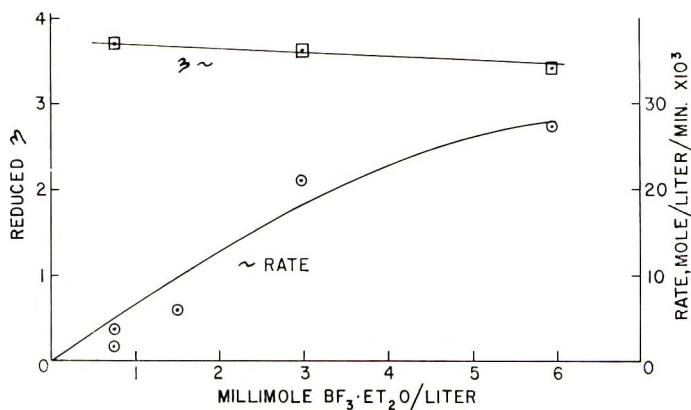


Fig. 3. Variation of (□) polymer viscosity and (○) average rate of conversion of DCA to polymer with $\text{BF}_3 \cdot \text{Et}_2\text{O}$ concentration, at 0°C . Polymerizations carried out to 50–70% conversions.

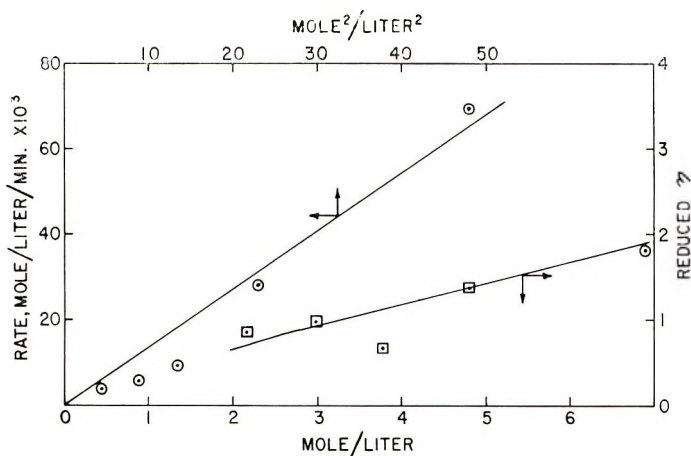


Fig. 4. Plots (□) polymer viscosity and (○) polymerization rate as functions of monomer concentration and $[\text{monomer concentration}]^2$, respectively. AlBr_3 -catalyzed polymerization in CH_2Cl_2 .

to polymer, however, is significantly increased. The polymers were compared at the 50–70% conversion level.

Hydrocarbon solvents cause a considerable reduction in the polymer molecular weight and conversions (Table I). With an AlBr_3 catalyst, it was possible to achieve 50–70% conversions over a wide range of solvent concentrations, but the polymer molecular weight decreases with increasing dilution (Fig. 4).

Polymer Stabilization

The thermal stability of the polydichloroacetaldehyde is poor, and decomposition appears to begin at low temperatures. To improve the

TABLE I
 Solvent Effect on DCA Polymerization at 0°C.

Solvent ^a	Catalyst (BF ₃ ·Et ₂ O) concentration, mmole/mole solution	Polymeriza- tion time, hr.	Conversion, %	η_{sp}/c
None	0.24	5	70	3.8
Heptane	0.24	5	36	1.25
"	0.12	5	15	^b
Toluene	0.12	28	Trace	—
Cyclohexane	0.12	28	23	1.27

^a Equimolar amounts of solvent and DCA were employed.

^b Product was predominantly liquid, and methanol soluble.

thermal stability, the terminal groups of the polymer were end-capped by esterification with acetic anhydride. The stabilization procedure involves contact of the polymer with refluxing acetic anhydride and catalytic quantities of pyridine for 15 min. The polymer is filtered, washed with methanol, dried, and the uncapped polymer removed by heating in dimethylformamide at 130°C. for 30 min. Uncapped polymer is substantially completely decomposed to monomer by the dimethylformamide treatment. The yields of capped polymer ranged from 60 to 95% and appeared to depend upon the molecular weight of the polymer; that is, the higher the molecular weight, the greater the conversion to capped polymer. The low molecular weight polymer tends to decompose more readily under the conditions used in the end-capping procedure.

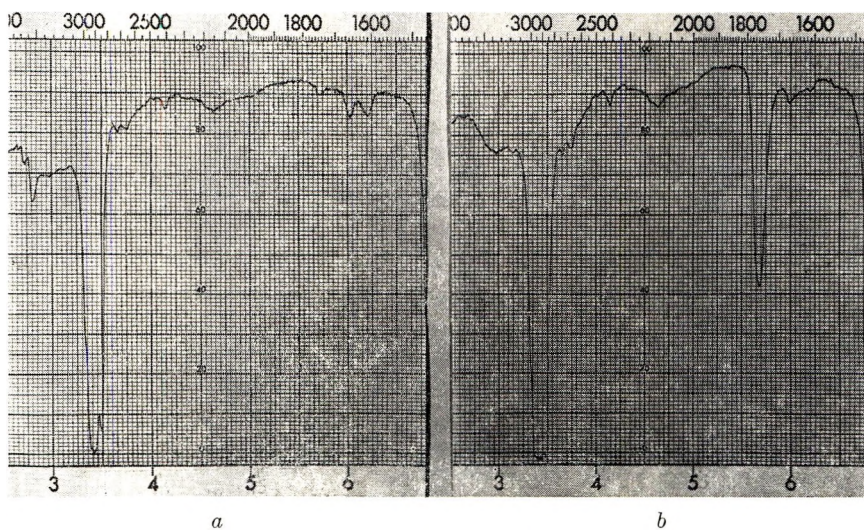


Fig. 5. Infrared spectrum of low molecular weight PDCA (a) before and (b) after end-capping.

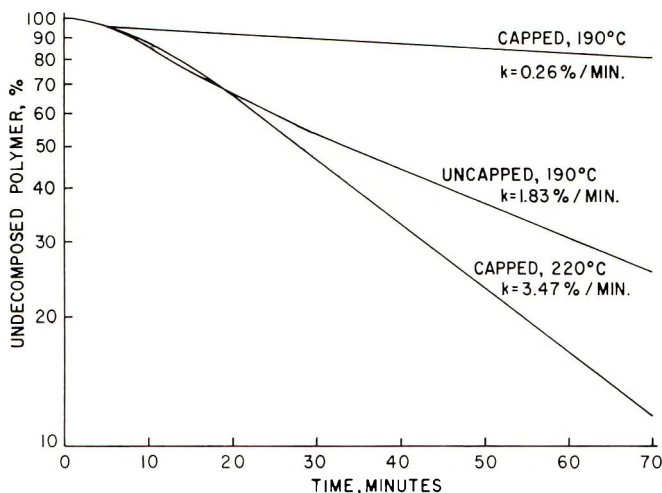


Fig. 6. Thermogravimetric analysis of PDCA under nitrogen.

The use of acid chlorides as end-capping agents, such as were used with polychloral,⁶ resulted in lower yields of capped polymer and a concomitant reduction in the molecular weight of the polymer.

The change in the chemical character of the polymer after end-capping is easily discernible in the infrared spectrum of low molecular weight polymer (Fig. 5). The absorption due to OH stretching at 3550 cm.^{-1} in the polymer disappears after end-capping. A new absorption band due to the carbonyl in the ester group appears at 1760 cm.^{-1} . Neither the C—OH nor carbonyl absorption is readily detectable with the high molecular weight polymers.

After treatment with the end-capping reagents there is a marked increase in the thermal stability of the polymer, which indicates that end-capping has been achieved (Fig. 6). The rate of decomposition under nitrogen is considerably reduced at 190°C . At higher temperatures (220°C), even the capped polymer decomposes fairly rapidly. The activation energy for thermal decomposition of the end-capped polymer is calculated to be about 40 kcal./mole .

The end-capping appears to take place with minimal degradation of the high molecular weight polymer. Recovery of polymer stable in hot dimethylformamide is usually 96% or better. As additional evidence for nondegradation and for end-capping, the viscosity of the polymer is about the same after the treatment compared with before. However, many times sufficient difference was observed as to render unreliable the determination of the viscosity of the uncapped polymer.

Polymer Characterization

The high molecular weight end-capped polymer did not have any detectable melting or softening point below its decomposition point. Observation

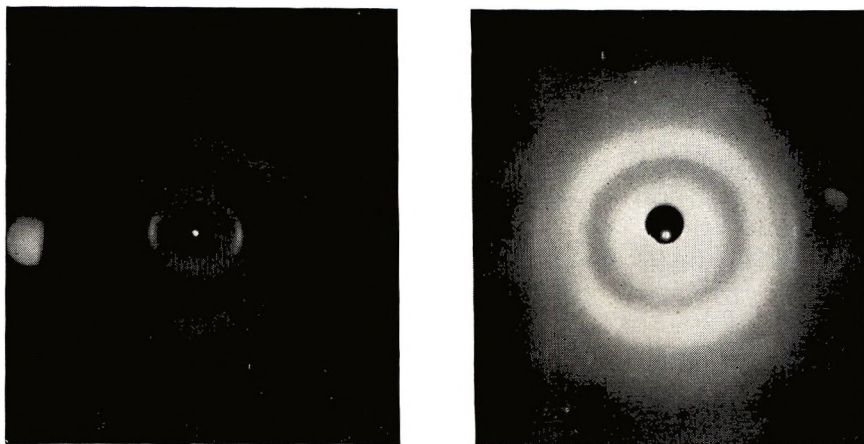


Fig. 7. X-ray diffraction pattern of PDCA film, stretched $3\times$. Shorter exposure on left.

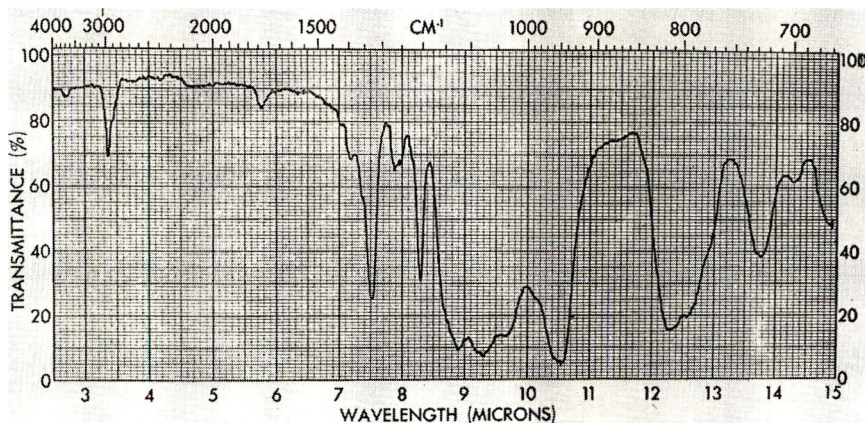


Fig. 8. Infrared spectrum of high molecular weight PDCA, from Perkin-Elmer Infracord.

with the Perkin-Elmer differential scanning calorimeter (DSC-1), polarized light microscope, and melting point block indicated that decomposition started at about 230°C . No melting point was observed up to 240°C ., with the microscope.

The powder x-ray diffraction pattern of the high molecular weight polymer is amorphous in nature. A threefold stretching of a cast film swollen in diethyl ether developed some orientation, but the crystallinity remained low. The x-ray diffraction patterns after exposures of 8 and 24 hrs. are shown in Figure 7. Equatorially oriented lines are located at 8.4 and 3.13 Å.; a meridionally oriented line is at 4.5 Å. After a 32 hr. exposure, the "ring" at 4.5 Å. shows signs of splitting along the equator. These lines are in a very heavy background and, therefore, are difficult to see. They have approximate spacings of 4.37 and 3.91 Å. Low molecular weight end-capped polymer, on the other hand, produces a more crystalline pattern,

with d spacings similar to those reported by Novak and Whalley for a low molecular weight PDCA.³

The infrared spectrum of a film of high molecular weight PDCA has essentially the same absorption features as those of the low molecular weight polymer reported by Novak and Whalley (Fig. 8).³ A notable difference appears in the broadening of the absorptions in the CO stretching region from 900 to 1200 cm.^{-1} . Also, the high molecular weight polymers exhibited little or no absorption at about 3500 cm.^{-1} , which band is assigned to OH stretching. Some of the lower molecular weight polymers were soluble in methanol and had somewhat narrower absorption bands in the 900–1200 cm.^{-1} region, especially at 1040 and 1087 cm.^{-1} .

The polymer is soluble in tetrahydrofuran, acetone, and dimethylformamide. It is insoluble in aliphatic hydrocarbons and certain chlorinated hydrocarbons, such as carbon tetrachloride. Clear films of PDCA are readily cast from solutions of the polymer in tetrahydrofuran or methyl ethyl ketone.

The Huggins viscosity constant k' is about 0.43, which is close to the usual range of 0.35–0.40 for most polymers. The $\overline{\text{DP}}$ of the polymer is fair, but the molecular weight is high because of the high weight of each monomer unit (Table II).

TABLE II
Viscosity–Molecular Weight Relationship

$\eta_{sp}/0.1\%$	$[\eta]$	k'	$\overline{\text{DP}}_n$
2.15	1.97	0.44	190
4.36	3.77	0.42	440

DISCUSSION

Acids catalyze the polymerization of the three chlorinated aldehydes.^{1–3} Very strong acids are required to polymerize chloral, but only polymer of low $\overline{\text{DP}}$ is formed.⁶ DCA, on the other hand, is readily polymerized to polymer of high $\overline{\text{DP}}$ by a variety of acid catalysts. The observations may be most simply attributed to the difference between the inductive effects of the CCl_3 and CHCl_2 groups on the polarizability of the carbonyl group. Because of a lower inductive effect, the oxygen of the carbonyl in DCA is more negative and thus can be more prone to attack by an acid. The difference in the ease of protonation of the two monomers is shown in the difference of the dissociation constants of the corresponding acids, where the proton of the trichloroacetic acid is much more readily ionized.

In general, cationic polymerizations are characterized by high rates at low temperatures. With DCA, however, the reverse is true. Both the $\overline{\text{DP}}$ and rate increase as the temperature rises to about 0°C., and then the $\overline{\text{DP}}$ decreases with further rise in temperature. The behavior of the $\overline{\text{DP}}$ is contrary to that normally expected but could be associated with the lower

conversions obtained at the lower temperatures, at which point the growing polymer is more easily terminated (Fig. 2).

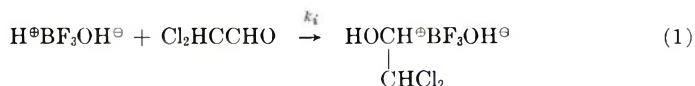
At high conversions, the \overline{DP} of the polymer varies so little with the catalyst concentration as to be virtually independent (Fig. 3). The overall rate of the polymerization, however, is dependent upon the catalyst concentration. In a solvent, there is a considerable diminution of the rate as the solvent concentration increases, with the overall rate approximately proportional to the square of the monomer concentration. Because of the dependence of \overline{DP} on the monomer concentration, the polymerization probably does not involve chain transfer to any extent, but instead, termination predominates. The observations can be accounted for by the scheme outlined in eqs. (1)–(4), assuming steady-state kinetics, wherein the rate of polymerization,

$$V_p = (k_i k_t / k_{tr}) [\text{Cat}] [\text{DCA}]^2$$

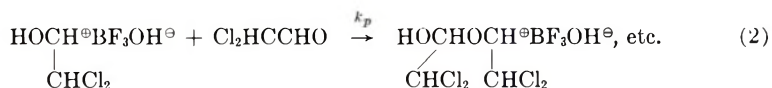
and in the case where $k_t \gg k_{tr}$,

$$\overline{DP} = (k_p / k_t) [\text{DCA}]$$

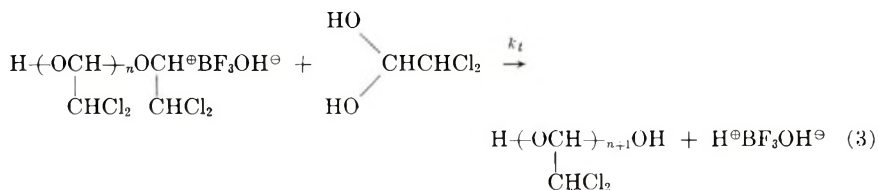
Initiation:



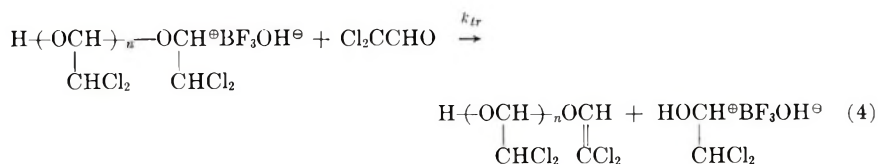
Propagation:



Termination:



Transfer:



The presence of OH endgroups on the polymer is confirmed by the increased thermal stability imparted to the polymer after acylation. Neither PDCA nor end-capped PDCA is as thermally stable under nitrogen as the corresponding polychloral. Since the thermal decompositions of these

materials are fairly close to first-order, the implication is that the mechanisms are about the same. Assuming that in both cases thermal decomposition occurs by unravelling of the main chain, the added Cl atom in the polychloral side unit provides added stability in two possible ways. It imparts steric hindrance to attack of the chain by reactive species generated during the decomposition. Alternatively, the increased inductive effect reduces the electron density around the O atom, which should reduce the comparative ease of any C—O cleavage.

The end-capping of PDCA is quite different from that in polychloral, where basic catalysts resulted in degradation of the polymer.⁶ It was expected, on the basis of similarity of structure, that PDCA would be as sensitive to base as polychloral. However, such was not the case, and the base-catalyzed end-capping proceeds smoothly. This is attributed to the lower inductive effect of only two chlorines on the PDCA unit, which reduces the tendency for proton abstraction from the end of the chain and anion formation. Here again, the ionization constants of di- and trichloroacetic acid may be invoked to demonstrate the marked difference induced by one Cl atom.

The amorphous nature of the x-ray diffraction patterns and only moderate success at orientation imply a fairly disordered, or atactic structure in the polymer. Confirmation of this is obtained by the broad absorption bands in the region from 900 to 1200 cm^{-1} as well as by the lack of a crystalline melting point. In some of the polymerizations, methanol-soluble polymer fractions were obtained which exhibited a bit greater crystallinity and sharper infrared absorption bands. These polymers were of lower molecular weight than the methanol-insoluble polymers, so that the crystallinity appeared to increase as the molecular weight decreased. Whether or not the increased crystallinity could also be attributed to increased polymer stereoregularity has not yet been determined.

We thank C. L. Sieglaff for his generous aid in the molecular weight determinations, and T. S. Wang and K. O'Leary for the infrared and x-ray investigations.

References

1. Paterno, *Z. Chem.*, **1868**, 668.
2. Jacobsen, O., *Ber.*, **8**, 87 (1875).
3. Novak, A., and E. Whalley, *Can. J. Chem.*, **37**, 1722 (1959).
4. Bevington, J. C., *Brit. Plastics*, **35**, 75 (1962).
5. Chistyakova, M. V., *Russ. Chem. Rev. (Engl. Transl.)*, **31**, 224 (1962).
6. Rosen, I., D. E. Hudgin, C. L. Sturm, G. H. McCain, and R. M. Wilhelm, *J. Polymer Sci.*, **A3**, 1535 (1965).

Résumé

Bien que la dichloroacétaldéhyde possède seulement un chlore en moins que le chloral, la polymérisation et les caractéristiques du polymère sont tout à fait différentes. Le dichloroacétaldéhyde polymérise facilement au moyen des catalyseurs acides de Lewis pour former un polymère possédant des groupements hydroxyles terminaux. Le catalyseur $\text{BF}_3 \cdot \text{Et}_2\text{O}$ à 0°C produit un polymère de très haut poids moléculaire par polymérisa-

tion en bloc. Un \overline{DP}_n d'environ 400 est facilement obtainable. La polymérisation est du type cationique caractéristique, avec une dépendance plus grande du \overline{DP} de la terminaison de chaîne que du transfert de chaîne. Le polymère est facilement protégé en fin de chaîne par l'anhydride acétique au moyen d'un catalyseur pyridinique afin d'augmenter sa stabilité thermique. Des mesures du point de fusion, infrarouge, et de diffraction aux rayons-X confirment que le polymère produit dans ces conditions est amorphe. Des films coulés du polymère seraient seulement partiellement orientés. Le polymère est soluble dans plusieurs solvants organiques habituels.

Zusammenfassung

Obwohl Dichloroacetaldehyd nur ein Chloratom weniger besitzt als Chloral, sind doch seine Polymerisation und die Polymercharakteristika völlig verschieden. Dichloroacetaldehyd wird durch Lewis-Säuren als Katalysator leicht zu einem Polymeren mit endständigen Hydroxylgruppen polymerisiert. $BF_3 \cdot Et_2O$ als Katalysator bildet bei 0°C bei Polymerisation in Substanz sehr hochmolekulare Polymere. Ein \overline{DP}_n von etwa 400 kann leicht erreicht werden. Der Verlauf der Polymerisation entspricht einem kationischen Typ mit stärkerer Abhängigkeit des \overline{DP} vom Kettenabbruch als von der Kettenübertragung. Das Polymere kann zur Erhöhung seiner thermischen Stabilität leicht durch Essigsäureanhydrid mit einem Pyridinkatalysator mit schützenden Endgruppen versehen werden. Schmelzpunkts-, Infrarot- und Röntgenbeugungsmessungen bestätigen, dass das unter den gewählten Bedingungen erzeugte Polymere amorph ist. Gegossene Polymerfilme konnten nur teilweise orientiert werden. Das Polymere ist in vielen gebräuchlichen Lösungsmitteln löslich.

Received March 9, 1965

Prod. No. 4755A

Polymerization and Telomerization Reaction of Olefins with a Tertiary Amine-Coordinated Lithiumalkyl Catalyst

G. G. EBERHARDT and W. R. DAVIS, *Research and Development
Division, Sun Oil Company, Marcus Hook, Pennsylvania*

Synopsis

Tertiary amine-chelated alkyllithium compounds were investigated as catalyst systems for the reactions of olefinic hydrocarbons. Ethylene is polymerized in paraffinic hydrocarbon solution to a high-melting, low molecular weight polyethylene wax having terminal olefinic unsaturation. A chain-transfer reaction is interpreted in terms of an olefin displacement reaction. Other olefins with available allylic hydrogen are metallized in this position. The C₄ olefins in conjunction with ethylene were found to undergo a telomerization reaction, involving the olefin as telogen and ethylene as taxogen. The structure and the mechanism of formation of these telomeric olefins are discussed.

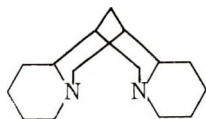
INTRODUCTION

It was reported earlier¹ that amine-coordinated organolithium compounds catalyze the telomerization of aromatic hydrocarbons (e.g., benzene, toluene, xylene) with ethylene. *n*-Butyllithium in conjunction with the chelating *N,N'*-tetramethylethylenediamine (TMED) was found to be a particularly active catalyst. Thus, benzene as solvent and telogen reacted with ethylene under moderate pressure and temperature to yield 1-phenylalkanes in a statistical distribution:



A concurrent transmetalation and ethylene propagation step was suggested as the mechanism of this telomerization reaction. The results reported here deal with the reactions of olefins induced by this catalyst system in the absence of aromatic reactants.

The factors involved in the activity of the tertiary amine/alkyllithium catalyst system have been discussed before.¹ The catalyst system pre-



I

ferred here contains the alkaloid sparteine ($C_{15}H_{26}N_2$) as the tertiary amine ligand(I). This amine has two tertiary nitrogens in a chelating arrangement and in a fixed bridgeheaded position which gives the catalyst complex an increased stability. Moreover, the exchange of the aromatic for a paraffinic or olefinic solvent introduced considerable difficulties as to the catalyst solubility, which could be overcome to the best degree with sparteine as the amine ligand. The catalyst system used here contains *n*-butyllithium/sparteine in a molar ratio of 1:1.

RESULTS

Polymerization of Ethylene

The formation of long *n*-alkyl side chains in the reported telomerization reaction of aromatic hydrocarbons with ethylene points to the ability of the catalyst system to promote the polymerization of ethylene. In the absence of "acidic" hydrocarbons such as benzene or toluene, a chain-transfer reaction via transmetallation to the aromatic hydrocarbon cannot occur, and the formation of ethylene polymers would be expected. Indeed, *n*-butyllithium/sparteine and *n*-butyllithium/TMED dissolved in octane were found to be very active catalyst systems for the polymerization of ethylene under mild pressure and temperature conditions (Table I).

TABLE I
Polymerization of Ethylene with the *n*-Butyllithium/Sparteine (1:1) Catalyst System at a Catalyst Concentration of 0.03*M* in Octane

Ethylene pressure, psi	Temperature, °C.	Initial rate of polymerization, mole C_2H_4 /mole BuLi/hr.	Number-average molecular weight ^a	Melting range, °C. ^b
400	110	120	1390	106-122
800	110	275	1360	104-109

^a Measured by ebulliometry in benzene.

^b Endothermic maxima of the differential thermal analysis heating curve.

The high melting range, in spite of the low average molecular weight of the product, suggests a complete linearity of the polymer chain. Also, its high crystallinity of 92% measured by x-ray diffraction and the typical infrared absorption bands at 13.7 and 13.9 μ associated with the linear arrangement of solid paraffinic carbon chains^{2,3} is in agreement with the assignment of a linear carbon chain structure for the polyethylene wax. Moreover, a molten film of the polyethylene wax shows an infrared absorption pattern in the 7.25 μ region similar to that of an authentic sample of polymethylene as reported in the literature.^{2,3} Furthermore, the infrared spectrum of a molten polyethylene sample reveals the presence of a terminal olefinic unsaturation.

The catalyst system is not stable, and the rates indicated in Table I are only observed initially. The rate of decomposition of the catalyst system depends on the reaction temperature, which is for optimal results kept in the range of 100–120°C. Catalyst yields on the order of 300 g. of polymer/g. butyllithium at 800 psi ethylene pressure were obtained, which corresponds to approximately 14 moles of polymer produced per mole of catalyst. The conditions were not optimized as to a maximum catalyst yield.

Telomerization of Olefins with Ethylene

The replacement of ethylene by other olefins, e.g., propylene, did not yield a polymerization reaction with the catalyst system employed. Instead, solid to oily precipitates were obtained from the paraffinic solvent, which were shown to be allylic metallation products. For instance, the system *n*-butyllithium/sparteine in hexane reacted with propylene to give a crystalline allylic metallation derivative:



Analogous allylic metallation products were obtained from systems involving different olefins or different chelating (TMED) or bridgehead tertiary amine ligands. The metallation of olefins in allylic positions is known to occur readily with sodium alkyls.⁴ In this case the transmetallation reaction also leads to isomerization of terminal olefins to 2-olefins. The *n*-butyllithium/sparteine catalyst system, however, isomerized 1-octene only to a small degree even after several hours of heating to 90°C. Thus, olefins with available allylic hydrogens, analogous to the alkyl aromatic hydrocarbons, yield to proton abstraction by the amine-coordinated alkyl lithium base. The olefins react, however, in the presence of this catalyst system, with ethylene to yield liquid to waxy olefinic products.

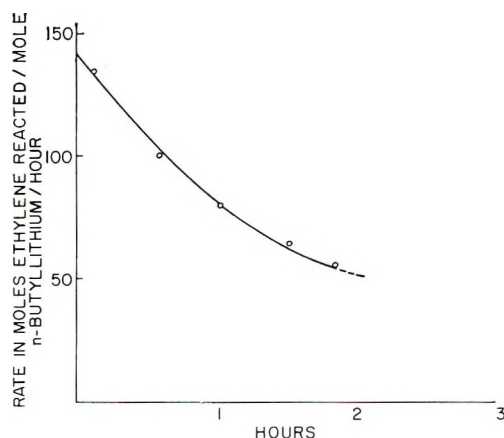


Fig. 1. Rate decay in the catalytic telomerization of isobutylene with ethylene (400 psi partial pressure). Catalyst system, *n*-butyllithium/sparteine (1:1); catalyst concentration, 0.05 *M*; temperature, 110°C.

TABLE II
Telomerization of C₄ Olefins with Ethylene, with *n*-Butyllithium/Sparteine (1:1) as Catalyst System at a Catalyst Concentration of 0.05*M* in Excess Telogen

Telogen	Ethylene partial pressure, psi	Temperature, °C.	Initial rate, mole C ₂ H ₄ /mole BuLi/hr. ^a	β^b	Structure of olefinic telomerization products ^c
Isobutylene	600	110	182	0.12	Olefinic telomers (80% of product): 2-methyl-1-pentene + homologs
	400	110	123	0.15	
	200	110	27	0.22	
	400	100	75	0.18	
<i>cis</i> -2-Butene	400	110	146	0.20	Olefinic telomers (70% of product): 3-methyl-1-pentene and 2-hexene and higher homologs in a ratio of 1.6:1
<i>trans</i> -2-Butene	400	110	123	0.15	Olefinic telomers (70% of product): 3-methyl-1-pentene and 2-hexene and higher homologs in a ratio of 1.5:1
1-Butene	400	110	290	0.10	Olefinic telomers (70% of product): 3-methyl-1-pentene and 2-hexene and higher homologs in a ratio of 0.5:1

^a The initial rate decays rapidly.

^b Rate of transmetalation/rate of propagation.

^c The nonolefinic telomerization products are cycloparaffin derivatives, which were structurally not identified.

While the aromatic hydrocarbons, as described earlier,¹ react with ethylene under these conditions with fast initial rates, the replacement of the aromatic hydrocarbons by a paraffinic or olefinic solvent effected a considerable decrease in the initial rates of reaction, which is thought to be caused by increased catalyst association or limited solubility. The system propylene/ethylene did not yield to an investigation because of the catalyst insolubility. The results reported here involve the C₄ olefins (isobutylene, 1- and 2-butene) in conjunction with ethylene. The C₄ olefins, which are liquid under the reaction conditions, are used in excess as reactants and solvents. A typical rate behavior of such a reaction is illustrated in Figure 1. The liquid or waxy reaction products show on gas chromatographic analysis a distribution pattern typical for a telomerization reaction. The C₆ and C₈ telomer fractions were isolated, and the structure of their olefinic components was determined (Table II). The telomers of high molecular weight are assumed to be homologs of the C₆ and C₈ telomer

fractions, differing by a successive number of ethylene units. The infrared spectrum of the total telomerization product is consistent with this assumption.

EXPERIMENTAL

Reagents

The *n*-butyllithium was used in the form of a 10% solution in pentane. A commercial sample of the alkaloid sparteine was vacuum distilled, and redistilled from molten sodium. Both materials were stored under nitrogen in rubber-sealed glass bottles and handled with syringe techniques. The olefinic reactants (C.P. commercial grade) were liquefied over small amounts of *n*-butyllithium and distilled therefrom before use. The ethylene (C.P. grade) was passed over activated molecular sieves before entering the reactor.

Equipment

A 150-cc. stainless steel bomb was used as a reactor. The bomb was closely fitted in an aluminum block for heating. The temperature was measured by a thermocouple placed inside the bomb. Agitation was provided by rocking. For the purpose of rate measurements, the ethylene pressure was set by means of a diaphragm regulating valve. The ethylene uptake was measured via incremental pressure decrease in a reservoir cylinder. The pressure increments were standardized independently in weight units.

Polymerization of Ethylene

A 150-cc. well dried stainless bomb was charged with 50 cc. octane 0.1 g. *n*-butyllithium (in 10% hexane solution) and 0.36 cc. sparteine under a blanket of purified nitrogen. The reactor was assembled and heated under rocking agitation. During the heating period (5–10 min.), the ethylene pressure was slowly increased to 800 psi at 110°C. The reaction was continued at this temperature and pressure for 2.5 hr. At this point, the reaction was interrupted by releasing the ethylene pressure and destroying the residual, but still active catalyst, with 1 cc. of isopropyl alcohol. The hot solution of the polymer was then removed from the reactor. On cooling, the polymer precipitated from the hydrocarbon solution. The polymer was filtered and washed several times with isopropyl alcohol. The white and powdery material was dried in vacuum; the yield was 20 g. The combined washing solutions were evaporated, yielding 1 g. of a residue containing the sparteine, besides some polymeric materials.

The olefinic unsaturation was qualitatively identified from the spectrum of a molten film as mainly terminal vinyl from the absorption bands at 915 cm.^{-1} .

Metallation of Olefins

A 50-cc. stainless steel bomb was charged with 0.25 g. (0.039 mole) *n*-butyllithium in 10 cc. hexane, and 0.8 cc. of sparteine was added with a syringe under nitrogen protection. The reactor was closed, and 5 g. propylene was introduced. The closed reactor was now heated up to 70°C. and shaken for 2 hr. at this temperature. Thereafter, the excess propylene was vented and a solution of 0.59 g. fluorenone in 25 cc. hexane was added to the solid reaction product. After a few minutes of vigorous shaking, a small amount of dilute hydrochloric acid was added, and the hydrocarbon layer was worked up, yielding 0.66 g. (88% yield), m.p. 116.7–117°C. of 9-allyl fluoren-9-ol. The melting point after one recrystallization from hexane was 117–118°C. (lit.:⁶ 118°C.).

Telomerization of Isobutylene with Ethylene

A 150-cc. stainless steel bomb was charged with 30 cc. pentane, 0.25 g. *n*-butyllithium, and 0.9 cc. sparteine. The reactor was assembled, and 28 g. purified isobutylene was condensed in the autoclave. The reactor was then heated up under rocking agitation. An increasing ethylene pressure was applied to the system so that at 110°C. a total pressure of 600 psi was reached, corresponding to an ethylene partial pressure of ca. 400 psi in the reactor. The reaction was continued at this temperature and pressure for 1.5 hr. (see Fig. 1 for the rate of ethylene uptake). At this point, the reaction was interrupted and cooled to room temperature. The unreacted gases were vented. The residual catalyst was destroyed with a small amount of methanol. The product had the appearance of a waxy slurry. The total product was distilled first at atmospheric pressure and then up to 150°C. at 3 mm.; 17 g. of a white, waxy residue remained. The distillate was washed with 2*N* HCl and water, and the pentane solvent was distilled off in a 50-plate column; 3 g. of liquid olefinic telomers remained.

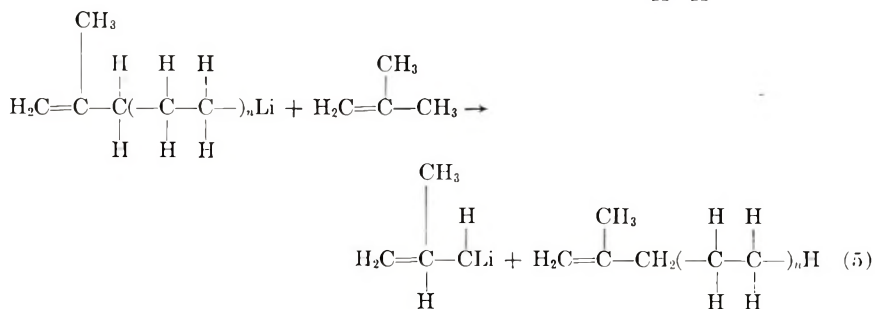
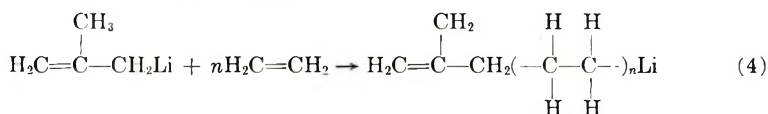
Analyses

Determination of β Values. β values were obtained from vapor-phase analysis by means of a temperature-programmed gas chromatograph. The entire telomeric product was separated on a 3.60 \times 0.56 m. O.D. column with 5% SF96 on Chromosorb P. The column temperature was programmed from 75 to 225°C. at 4.6°C./min. at a flow rate of 70 cc./min. The β values were obtained by comparing the peak areas of the consecutive carbon numbers and relating them mathematically as described in the discussion.

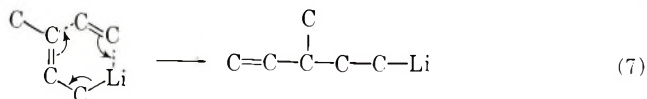
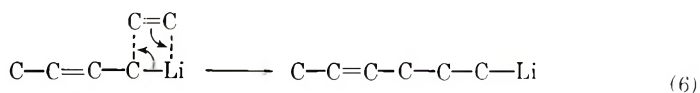
Identification of Olefinic Compounds. The pure olefinic compounds were isolated by collecting them at the gas exhaust of the gas chromatograph. A 300 \times 0.56 cm. O.D. column with 15% didecyl phthalate on Chromosorb P was used for these separations. The C₆ and C₅ compounds were separated and collected at column temperatures of 75 and 110°C., respectively. A flow rate of 60 cc./min. was used in both cases. The individual compounds

The terminal unsaturation of the polymer was confirmed by infrared analysis. The possibility of a chain transfer via metallation of ethylene in the vinyl position cannot be excluded, since recent studies⁸ involving sodium alkyls have shown that such a metallation can occur. The ethylene addition step can be interpreted as an insertion of the ethylene molecule between an amine-coordinated lithium cation and a carbanionic residue. This insertion reaction necessarily leads to the formation of a linear paraffinic carbon chain, which is in accordance with the experimental findings.

The replacement of ethylene by propylene leads to a metallation of the olefin in allylic position. This fact is not surprising in the light of the well-demonstrated metallating power of the catalyst system towards aromatic hydrocarbons,¹ which readily form the corresponding benzylic or phenylic metallation products. The olefins, however, readily undergo a catalytic reaction in the presence of ethylene. The products appear in a distribution typical for a telomerization reaction and analogous to the product distribution obtained from the reaction of aromatic hydrocarbons with ethylene using the same catalyst system. On the basis of the demonstrated ability of the catalyst system to metallate olefins in the allylic position and to propagate the polymerization of ethylene, we interpret the reaction as a telomerization characterized by a competitive transmetallation and ethylene polymerization reaction.



In accordance with this reaction scheme, the structure of the telomeric olefins obtained from isobutylene and ethylene were found to be homologs of 2-methyl-1-pentene. The expected telomers derived from 2-butene or 1-butene as telogens should be the homologs of 2-hexene and 3-methyl-1-pentene, respectively. Indeed, these olefins are present among the telomeric products (Table II). Surprisingly, however, the main products derived from 2-butene are homologs of 3-methyl-1-pentene and the ones derived from 1-butene are homologs of 2-hexene. This fact points to the possibility that two different mechanisms may be competing in the formation of the telomeric products. We suggest the following explanation as a mechanistic interpretation of these results. The telomerization of 2-butene with ethylene is used as a specific illustration.



The first reaction pathway, eq. (6), involves a four-centered ethylene insertion, while the second pathway, eq. (7), involves a six-centered ethylene addition reaction. Products of both pathways are observed among the 2-butene/ethylene telomers. The predominant formation of 3-methyl-1-pentene from 2-butene suggests the six-centered reaction pathway is the preferred one. The unique product structure of the olefinic telomers derived from isobutylene as a telogen can also be easily understood on the basis of the scheme proposed, because in this case both reaction pathways would yield the same product: 2-methyl-1-pentene and its homologs. Similar reaction sequences are expected to occur with other olefinic telogens.

The chain-transfer reaction (5), here a transmetalation step, is independent of the ethylene partial pressure. The average number of ethylene units (\bar{n}) incorporated into the telomer product is, therefore, a function of the ethylene partial pressure for a given system. The ratio β (rate of chain transfer/rate of propagation) thus becomes smaller with increasing ethylene pressure (see Table II). The number \bar{n} is related to β by the equation:⁹

$$\bar{n} = (1 + \beta)/\beta$$

The values of β may be readily determined experimentally by comparing the relative mole fractions of the telomer product at any successive values of n :

$$\beta = (N_n/N_{(n+1)}) - 1$$

where N_n is moles/fraction.

The value of β determined in this manner may be used to calculate the mole fraction of product at all values of n :

$$N_n = \beta/(1 + \beta)n$$

TABLE IV
 β Values Observed with Four Different Telogens under Equivalent Reaction Conditions^a

Telogen	β
Toluene	0.75 ^b
Benzene	0.45 ^b
Isobutylene	0.15
1-Butene	0.1

^a Ethylene partial pressure, 400 psi, temperature, 110°C.

^b β values obtained from previous publication.¹

In this connection, it is interesting to compare the β values of various hydrocarbon telogens under equivalent reaction conditions (Table IV).

These values reflect the differences in the rate of transmetallation of the hydrocarbons.

The rapid catalyst decomposition limits the catalyst yields. The decomposition rate of the catalyst depends on the temperature and on the substrate involved. The polymerization of ethylene in a paraffinic hydrocarbon solvent results in high catalyst yields, while the telomerization of isobutylene (see Fig. 1) or particularly of 1-butene shows a much more rapid catalyst decay. A more detailed study of the mechanism of the catalyst decomposition may yet result in the development of more stable systems.

The investigations of the analytical department of Sun Oil Company, particularly of Mrs. J. Duswalt, are gratefully acknowledged. The authors also wish to thank the Sun Oil Company for permission to publish this research.

References

1. Eberhardt, G. G., and W. A. Butte, *J. Org. Chem.*, **29**, 2928 (1964).
2. Krimm, S., C. Liang, and G. Sutherland, *J. Chem. Phys.*, **25**, 549 (1956).
3. Bryant, W., and R. Voter, *J. Am. Chem. Soc.*, **75**, 6113 (1953).
4. Morton, A. A., and E. J. Lampher, *J. Org. Chem.*, **20**, 839 (1955).
5. Chiang, R., *J. Polymer Sci.*, **36**, 91 (1959).
6. Wittig, G., H. Doeser, and J. Lorenz, *Ann.*, **562**, 192 (1949).
7. Ziegler, K., and H. Gellert, *Ann.*, **567**, 195 (1950).
8. Broaddus, C., T. Logan, and T. Flautt, *J. Org. Chem.*, **28**, 1174 (1963).
9. Wesslau, H., *Ann.*, **629**, 198 (1960).

Résumé

On a envisagé l'emploi de composés du type amine tertiaire-alcoyl-lithium chélaté comme systèmes catalytiques pour les réactions des hydrocarbures oléfiniques. L'éthylène a été polymérisé en solution dans un hydrocarbure paraffinique et a fourni une cire de polyéthylène de faible poids moléculaire, à point de fusion élevé et possédant une insaturation terminale oléfinique. On interprète une réaction de transfert de chaîne comme réaction de déplacement oléfinique. D'autres oléfines possédant un hydrogène allylique disponible ont été métallisées dans cette position. On a trouvé que les oléfines en C₄ en combinaison avec l'éthylène conduisaient à une réaction de télomérisation, impliquant l'oléfine comme télogène et l'éthylène comme taxogène. On discute de la structure et du mécanisme de formation de ces oléfines télomérisés.

Zusammenfassung

Mit tertiärem Amin chelierte Alkylolithiumverbindungen wurden auf ihre Brauchbarkeit als Katalysatoren bei den Reaktionen olefinischer Kohlenwasserstoffe untersucht. Athylen wird in paraffinischer Kohlenwasserstofflösung zu einem hochschmelzenden niedermolekularem Polyäthylenwachs mit endständigen Doppelbindungen polymerisiert. Als Kettenübertragungsreaktion wird eine Olefinverschiebungsreaktion angenommen. Andere Olefine mit einem verfügbaren Allylwasserstoff werden in dieser Stellung metalliert. Die C₄-Olefine gehen mit Athylen eine Telomerisierungsreaktion ein, wobei das Olefin als Telogen und das Athylen als Taxogen fungiert. Struktur und Bildungsmechanismus dieser telomeren Olefine werden diskutiert.

Received April 26, 1965

Prod. No. 4756A

Radiation Grafting of Vinyl Monomers to Wool. Part I.

V. STANNETT, K. ARAKI,* J. A. GERVASI, and
S. W. McLESKEY, *Camille Dreyfus Laboratory,
Research Triangle Institute, Durham, North Carolina*

Synopsis

A number of vinyl monomers have been grafted to wool by using the mutual radiation technique. Styrene has been studied in considerable detail in dioxane solution; water or methanol was found to be necessary for successful grafting. It is believed that these function as swelling agents, enabling the monomer to diffuse to the active centers created in the wool by the radiation. The rate of grafting always went through a maximum and then leveled off to a slower rate. This is believed to be due to the slow build-up of the radical population, leading eventually to a diffusion-controlled rate of grafting. Considerable post-polymerization grafting was found to take place. Acrylonitrile and a number of allyl monomers were also successfully grafted to wool by the mutual radiation method in dimethylformamide solution. Again water or methanol was found to be necessary; the grafting rate leveled off close to zero at a degree of grafting depending on the amount of swelling agent present.

Introduction

The radiation grafting of various vinyl monomers to a wide variety of natural and synthetic polymeric substrates has been investigated widely, and there is an extensive literature on the subject.¹ Cellulose fibers have been particularly well investigated in attempts to improve their mechanical, chemical, thermal, and other properties.² It is surprising, therefore, that comparatively little attention has been paid to radiation grafting to wool fibers. Burke et al.³ have used the trapped radicals in irradiated wool to graft acrylonitrile; Horio et al.⁴ have grafted styrene, methyl methacrylate, and acrylonitrile to wool using the mutual method, and Armstrong and Rutherford⁵ included wool fibers in their extensive study of radiation grafting to textile fibers by the vapor-phase technique. The importance of swelling the wool fibers to effect adequate grafting had been pointed out earlier by Puig.⁶

In this present work the direct or "mutual" method has been studied in the liquid phase. Although a number of monomers have been studied, styrene was chosen for a more detailed investigation. In earlier work on

* On leave of absence from Japanese Atomic Energy Research Institute, Takasaki, Japan.

grafting to poly(vinyl alcohol) and cellulose it was shown that water was necessary to obtain adequate grafting.⁷ Dioxane was found to be a satisfactory solvent, since it tolerated the addition of an adequate amount of water and at the same time kept the polystyrene formed by the radiation in solution. A similar grafting solution has now been investigated for wool, and in addition methanol has been studied in place of water.

EXPERIMENTAL

The wool used for all the experiments to be described consisted of fabric (J. P. Stevens style number 31200-1); the individual fibers had an average diameter of 22 μ . Before use these were extracted in a Soxhlet apparatus for 8 hr. with diethyl ether followed by 8 hr. with ethanol. The wool was then washed with distilled water and dried at room temperature under a moderate vacuum. The monomers and solvents used were all freshly distilled before use.

The grafting experiments were carried out in Pyrex tubes, 16 mm. in diameter and about 15 cm. in length. A weighed strip of wool fabric 2 \times 0.5 in. (about 0.17 g.), was placed in the tube before constricting and 8.0 cc. of a monomer-solvent-water mixture was added by hypodermic syringe under a dry nitrogen atmosphere. The styrene content was maintained at 3.06*M* in dioxane; the water or methanol content was varied as shown in the actual data. The tubes were attached to a high vacuum line, degassed by five freeze-thaw cycles at below 10⁻⁴ mm. Hg pressure, and sealed under vacuum. It was found that essentially similar results were obtained when the wool was degassed separately and degassed monomer added under high vacuum. The samples were irradiated in a 4000-curie Co⁶⁰ gamma cell (by kind cooperation of the North Carolina State University School of Textiles) at 25°C. and a dose rate of about 0.3 Mrad/hr. The tubes were then opened and the homopolymer in the solution was isolated by precipitation in methanol, filtering and drying. The wool samples were washed to constant weight with benzene and reweighed. The increase in weight divided by the original weight \times 100 was recorded as the per cent grafting.

The viscosity determinations were carried out on the styrene homopolymer in toluene at 30°C. in an Ubbelohde viscometer, and the viscosity-average molecular weight calculated by the equation:⁸

$$\log \bar{M}_v = (4.01 + \log[\eta])/0.73$$

RESULTS AND DISCUSSION

Styrene Monomer

The styrene content, in 15-fold excess over the wool, was held constant for these initial studies, and only the water or methanol content and the total dose varied. The effect of the water or methanol content on the

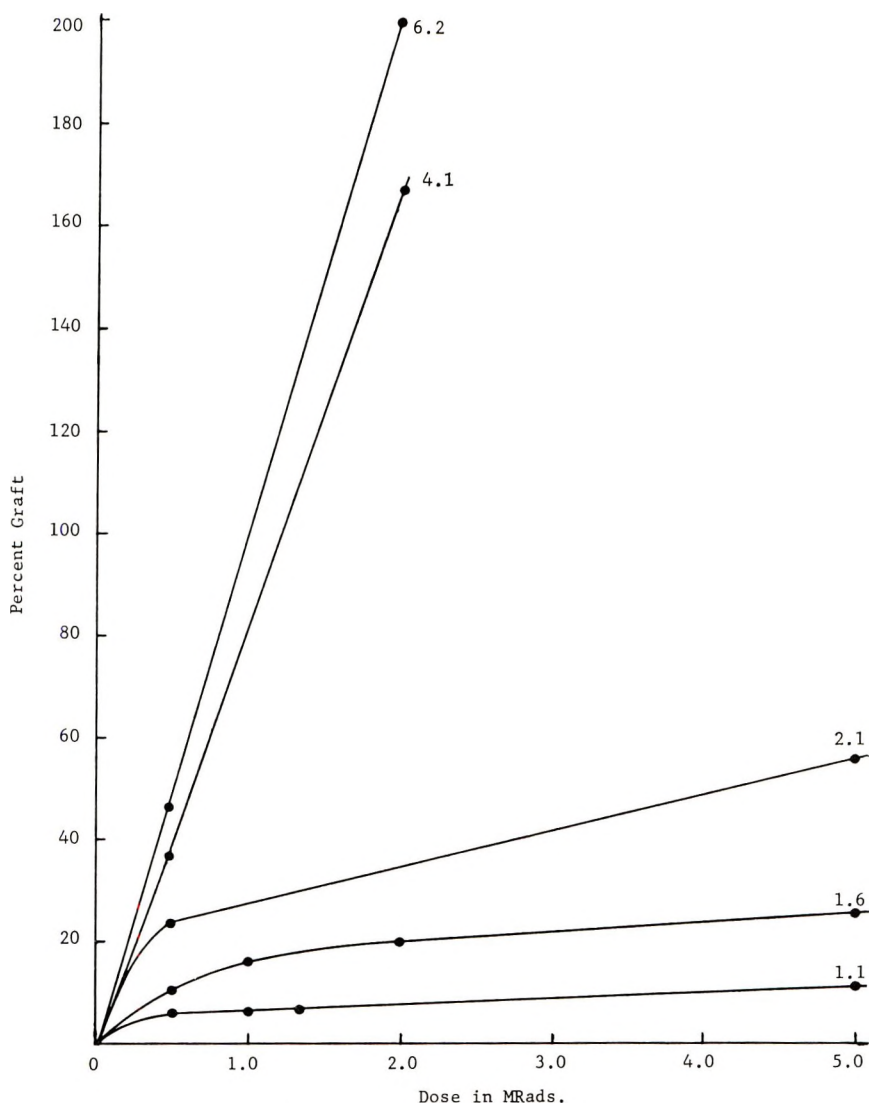


Fig. 1. Effect of radiation dose on grafting onto wool at different water contents of monomer solution. The numbers refer to the per cent water in the styrene-dioxane solution.

amount of grafting is shown in Figures 1 and 2. The dramatic effects of water and methanol are clearly displayed at all dose levels. The shapes of the grafting-dose curves are similar for both water and methanol. The high water content systems appear to be linear from the origin. However, subsequent work at higher total doses showed that leveling off began eventually, even at the highest water content. The autoacceleration shown with methanol at the earlier stages of grafting was found to occur to a much smaller extent with water. It can be seen from a comparison of

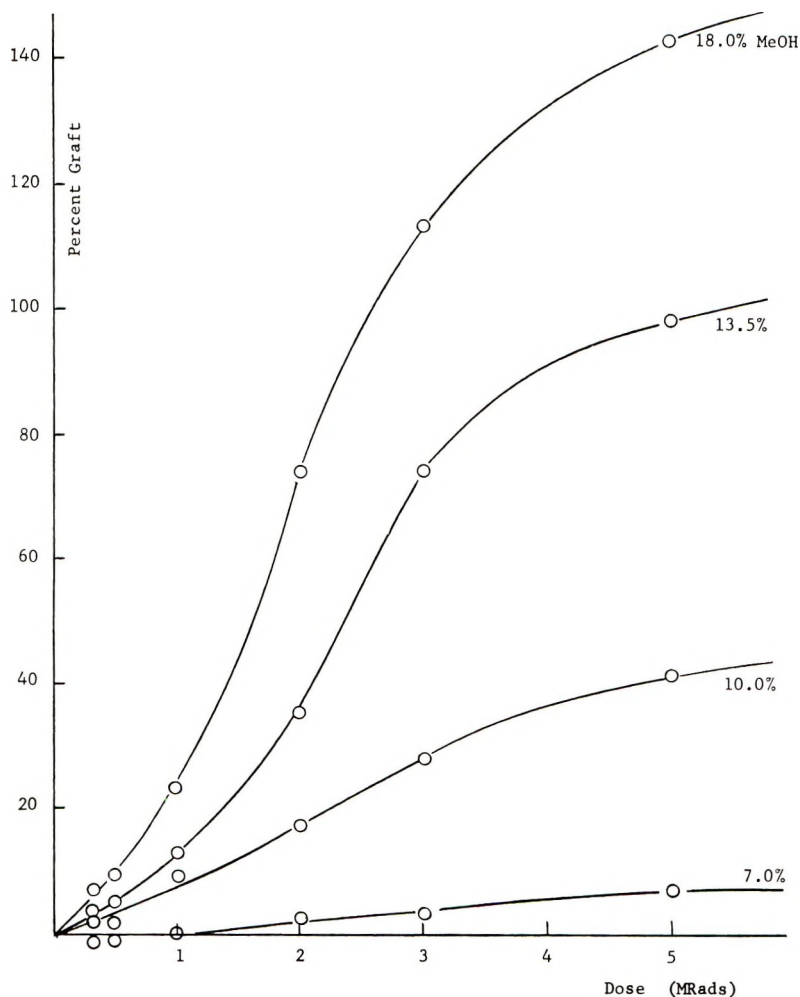


Fig. 2. Grafting of styrene vs. radiation dose at various concentrations of methanol in the monomer-dioxane solution.

Figures 1 and 2 that water is much more effective than methanol on a percentage basis, although the water and methanol sorption isotherms are quite similar, as shown in Figure 3. This is probably due to the greater hydrogen-bonding capacity of the water molecules facilitating the diffusion process. The yield of styrene homopolymer produced in the free solution has also been determined at various methanol contents, and the results are shown graphically in Figure 4. It is quite clear that the tremendous changes in grafting at different methanol concentrations are due to the fiber system and not to any special features of the radiolysis of the monomer solution.

The effect of swelling agents on the rate of grafting to swollen fibers and films has been widely interpreted as due to the faster rate of diffusion of

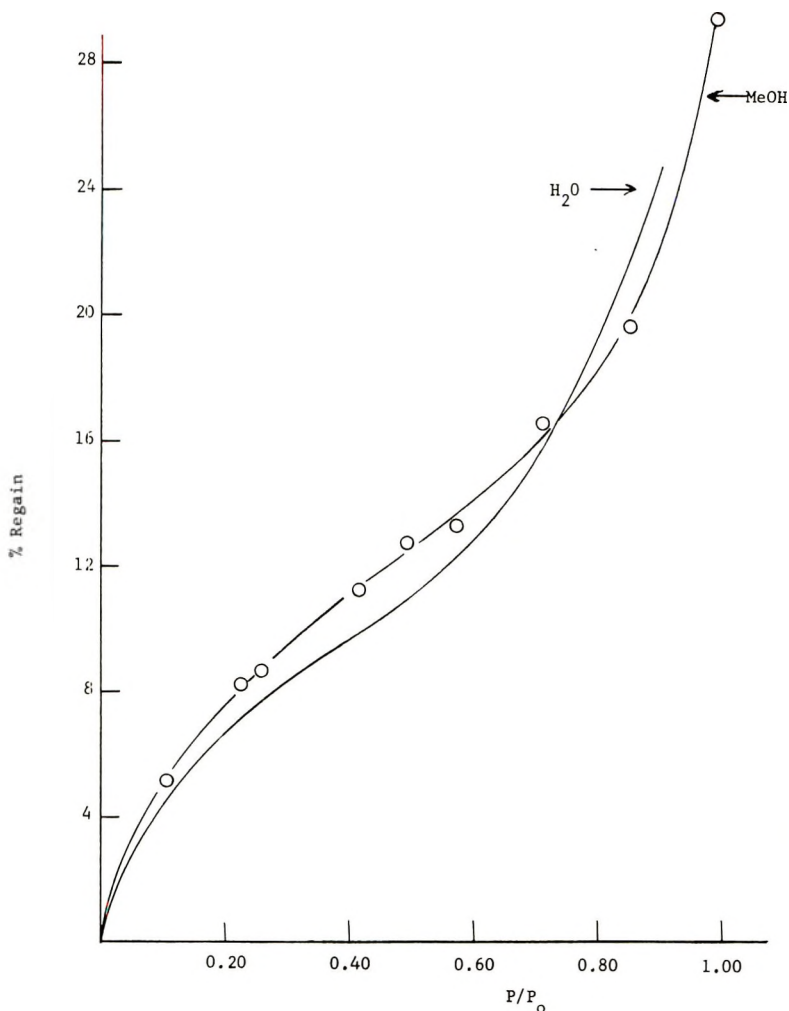


Fig. 3. Sorption isotherm of wool with methanol and water at 25°C.

monomer to the active centers formed by radiolysis of the swollen fiber. There seems little reason to doubt that a similar mechanism is operating in the present system, modified however by the complex morphology of the wool fibers. At low degrees of swelling it is probable that grafting mainly occurs in the surface regions of the fiber and the monomer never reaches the center except in such low concentration that little polymerization occurs during the course of the experiment.

The effect of time of contact between the wool fabric and the monomer solution before beginning irradiation had been investigated in experiments with 4.5% water and 12% methanol; both sets of results are presented in Figure 5. Since the amount of grafting (at zero contact time) is 68% in the case of water compared with only 9.7% with methanol, the results are pre-

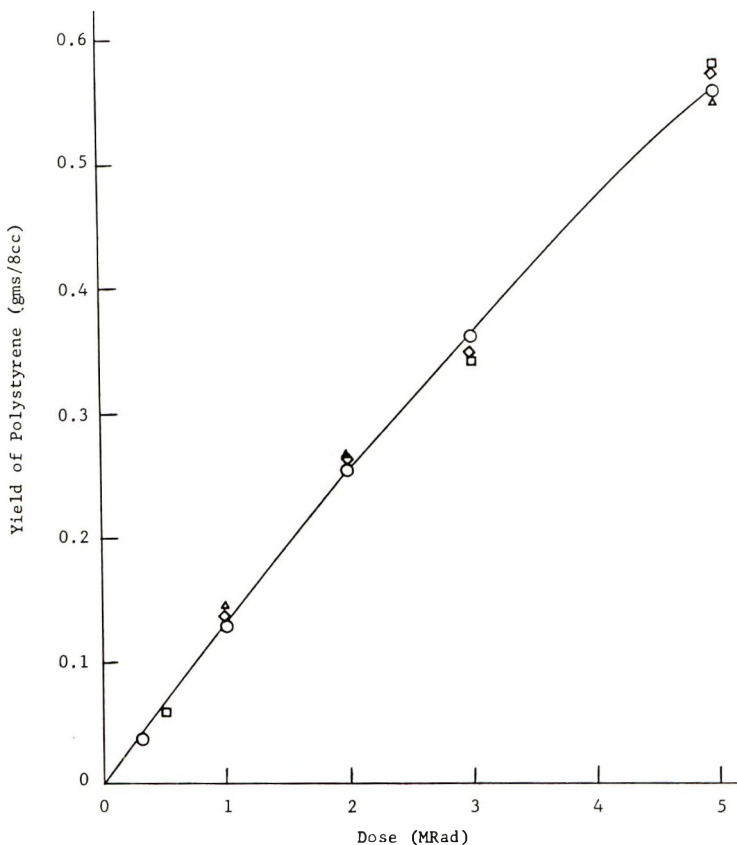


Fig. 4. Yield of polystyrene homopolymer with radiation dose at methanol concentrations of 7.0–18.0%.

sented as percentage increases in grafting as a function of contact time for 1 Mrad total radiation dose. It can be seen that there is a slow increase in grafting with soaking in the monomer solution, but at normal times the effects are small. For example, even in 24 hr. there is only a 5% increase with methanol and 6.8% in the case of water. The slow increase in grafting is probably associated with a slow relaxation of hydrogen bonds on long periods of exposure to water or methanol.

Some additional experiments have also been made by use of a 3 M.e.v. Van de Graaff electron accelerator (High Voltage Engineering Corporation, Burlington, Mass.) at a dose rate of about 3 Mrad/min.; the results obtained are shown in Figure 6. The high yields at 1 Mrad are of interest and may be due to post-polymerization effects as shown to exist in previous experiments (see Fig. 7, for example). Why this effect is not so pronounced with water is not clear, although it is quite possible that considerably lower post effects are occurring with the more active water system. This could be due, for example, to a lower radical population owing to the greater ease of termination in a more mobile, more swollen matrix. The reasons for the

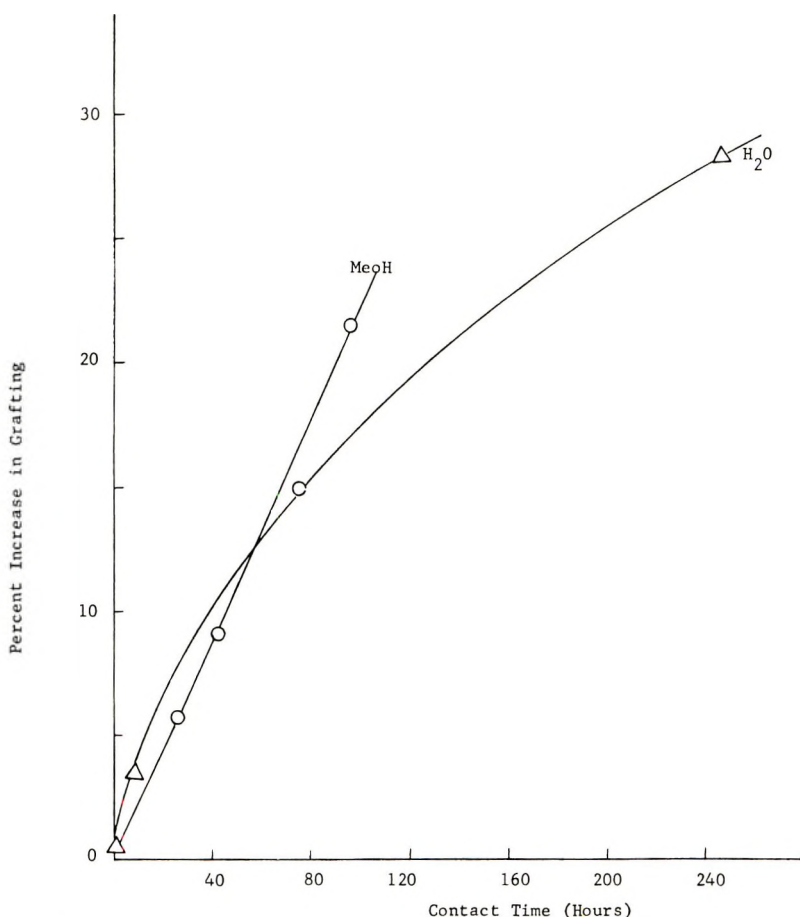


Fig. 5. Effect of contact time before grafting of styrene with 12% methanol and 4.5% water at 1.0 Mrad.

leveling off of the grafting versus radiation dose curves are not clear, and the course of the grafting process has been investigated further.

Some initial experiments were aimed at seeing if free fibers grafted in the same fashion as fabric in case some artifact was involved. A comparable set of grafting experiments for fabric and free fibers is presented in Figure 7. The same leveling off was found with the free fibers. It is interesting that a quite different rate of grafting was observed. The free fibers had an average diameter of 26.5μ compared with 22μ for those making up the fabric. This would certainly help to explain the slower rate of grafting of the free fibers, since the reaction is diffusion-controlled. Work with other wools has shown that although the general features of the grafting are identical there are definite differences in the rates of grafting for each type. Such differences are not unexpected for a complex natural fiber. It is gratifying, however, that the reproducibility as shown in Figure 7 is excellent for any given type of wool.

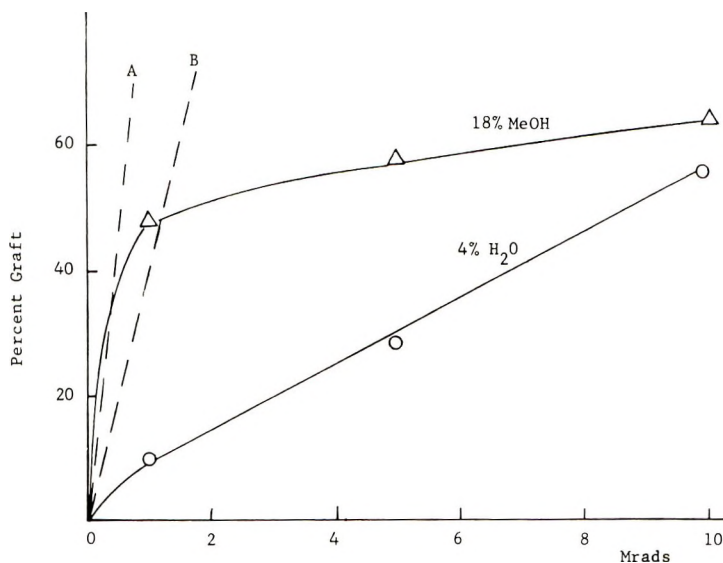


Fig. 6. Grafting vs. dose with 3 M.e.v. from a Van de Graaff source at a rate of 3 Mrad/min.; A and B are comparative rates with γ -radiation at a rate of 0.005 Mrad/min. in H₂O and MeOH, respectively.

The amount of extractable polystyrene is very small for grafted wool. Even at 130% grafting only 4% could be extracted and only 9% at 240% grafting. These figures also include small amounts of superficial polystyrene left on the wool after centrifuging. The residues from the benzene extracts of the grafted wool were also added to styrene and polymerized by radiation; no inhibition whatever was observed. The per cent homopolymer in the free solution also showed no leveling-off effect, as shown in Figure 4. This again showed that no soluble inhibitors were formed from the radiolysis of the wool.

A series of experiments was conducted in which the grafted wool was removed from the grafting solution after the leveling off (e.g., at 5 Mrads) and replaced in fresh monomer solution and reirradiated. The results are shown in Figure 8. It can be seen that the autoacceleration phase of the grafting reaction tends to disappear on regrafting. This is perhaps due to the greater swelling of the already grafted fibers or to some initial relaxation effect of the fibers on grafting connected in some way, perhaps, to the time of contact experiments. It can be seen also that the rate of grafting continued at a rate comparable to that observed before the leveling-off period and then gradually began to level off as before.

A somewhat similar set of experiments were conducted in which the grafting tubes were simply left for 3 days after the leveling-off period and then reirradiated. The results are shown in Figure 9. It can be seen that there is a very large post-irradiation effect and that further irradiation only produces minor increases in grafting. However, it can be seen that on

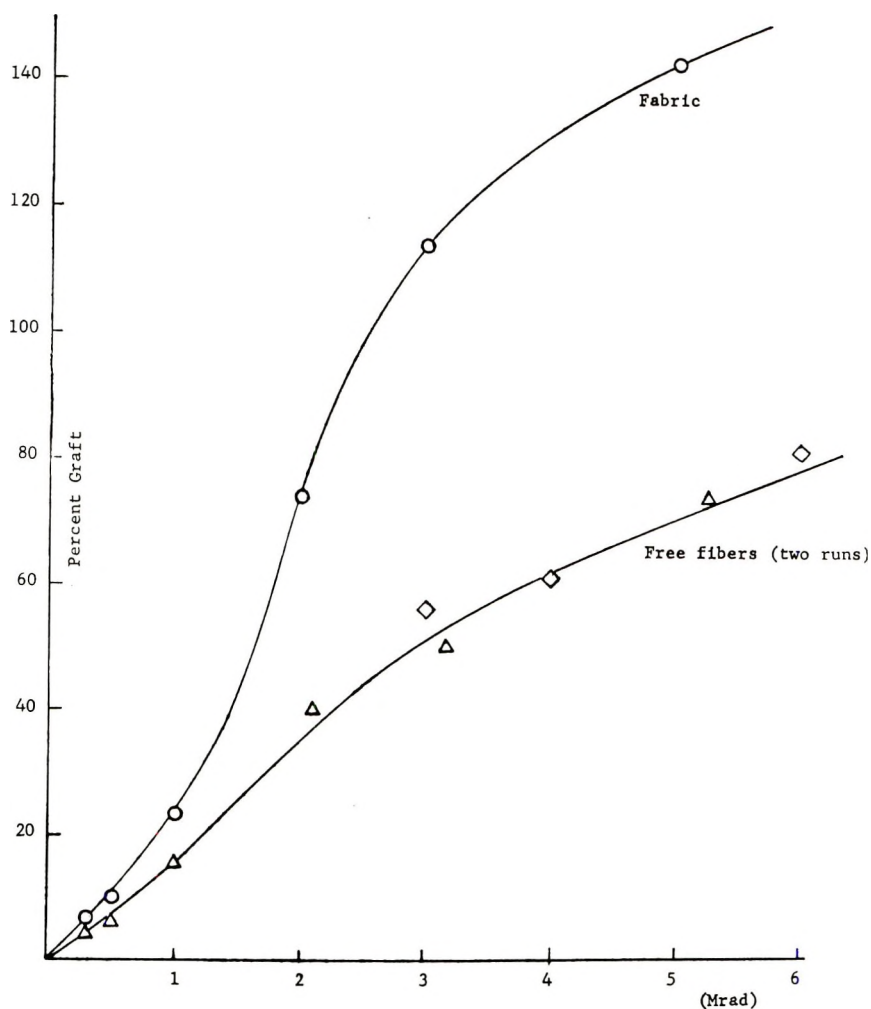


Fig. 7. Grafting of styrene to wool fabric and free fibers of different grades in 18% methanol-dioxane solution.

standing for several days, considerable post-polymerization again occurred (points *A* and *B* in Fig. 9). On reirradiating only minor grafting again occurred. It was thought that the lack of grafting with the mutual method in these cases was due to the fact that more than 240% of styrene was already grafted and that the wool structure had reached its capacity for further growth under the rather high dose rate conditions used. To check this hypothesis, a number of tubes were grafted until the levelling-off period occurred and then immediately opened to the air. It was found that under these conditions no post-grafting occurred due to inhibition, presumably, by oxygen. The remaining tubes were then degassed, sealed, and reirradiated. Under these conditions grafting continued at roughly the same rate as before and again with eventual leveling off. It should be

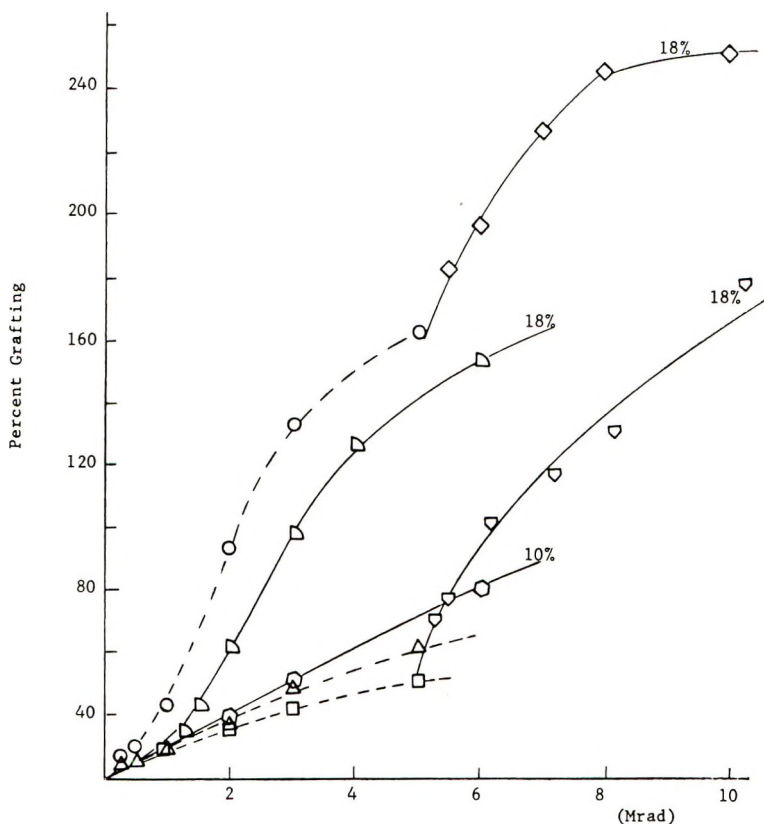


Fig. 8. Grafting followed by regrafting after washing: (\diamond) 18% MeOH second grafting after 5.0 Mrad, 18% first grafting; (\square) 18% MeOH second grafting after 1.0 Mrad, 8.5% first grafting; (∇) 18% MeOH second grafting after 5.0 Mrad, 8.5% first grafting; (\circ) 10% MeOH second grafting after 1.0 Mrad, 8.5% first grafting; (---) first graftings with (\circ) 18% MeOH, (\triangle) 10% MeOH, or (\square) 8.5% MeOH.

pointed out that in these series of experiments the same monomer solution was used showing that no inhibition or monomer exhaustion was involved in the leveling-off phenomenon. The grafting reaction is known to be diffusion-controlled; it is probable at the high dose rate used that the radical population continues to increase during at least the earlier stages of the reaction. As the radical population increases the monomer concentration in the fiber begins to decrease due to the increased consumption by polymerization. The overall effect is an initial increase in rate to a maximum and then a leveling off to a steady lower rate, i.e., exactly as observed, for example, in Figure 2. When the degree of swelling is decreased, the initial monomer content and the rate of diffusion of monomer in the fiber is less. This leads to a lower rate at the steady leveled-off stage of the grafting reaction as observed. In all cases when the radiation is interrupted and air is introduced, the trapped radicals can terminate, fresh monomer diffuses in, and a similar initial rate is obtained on reirradiating

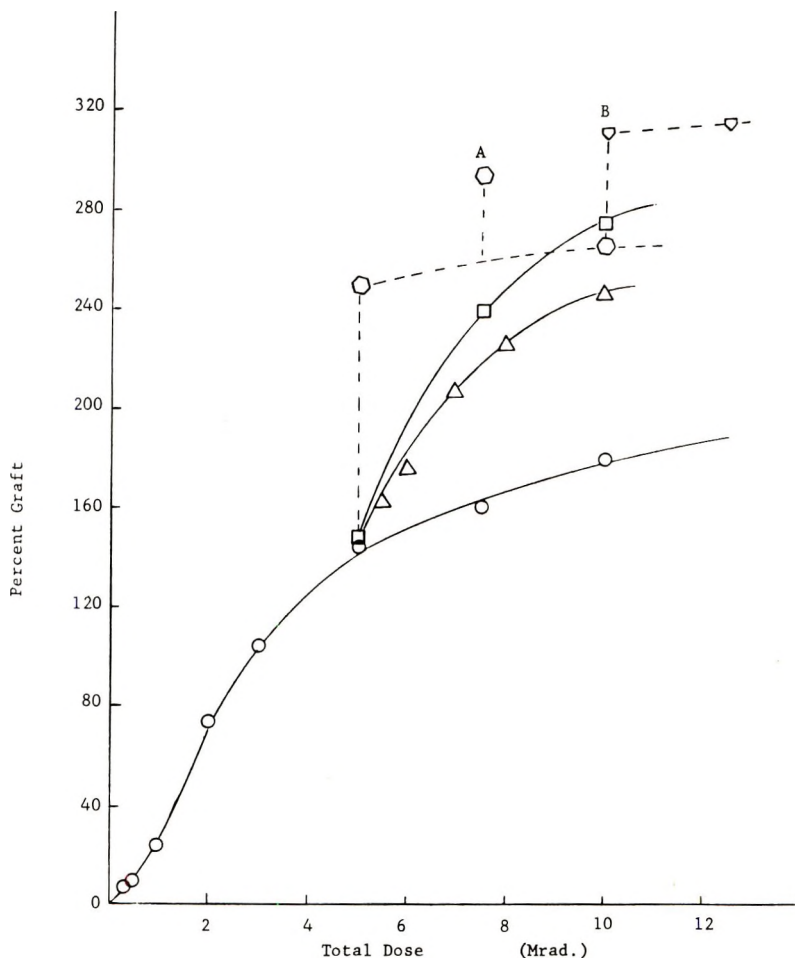


Fig. 9. Grafting of styrene to wool fabric followed by regrafting in the same monomer solution, 18% methanol in dioxane: (O) original grafting curve; (○) after 3 days *in vacuo*; (□) after 3 days in air; (△) after washing (from Fig. 8); (A,B) samples left 2 and 3 days before opening.

as shown in Figures 6 and 7. The detailed kinetics of this type of grafting reaction has been worked out and shows good agreement with the experimental results. This analysis is presented in another paper.⁹ The data of Figure 9 are presented on a time scale in Figure 10 since the course of the post-irradiation grafting can now be included. It can be seen that after a brief period the grafting begins at a similar rate as before but soon declines to a lower rate as the radical population diminishes. These data are also consistent with the explanation presented above. As the degree of swelling increases the polymerization is facilitated, and the leveling off occurs at a much higher level. Similarly, the substitution of water for methanol probably facilitates the monomer diffusion process, leading to

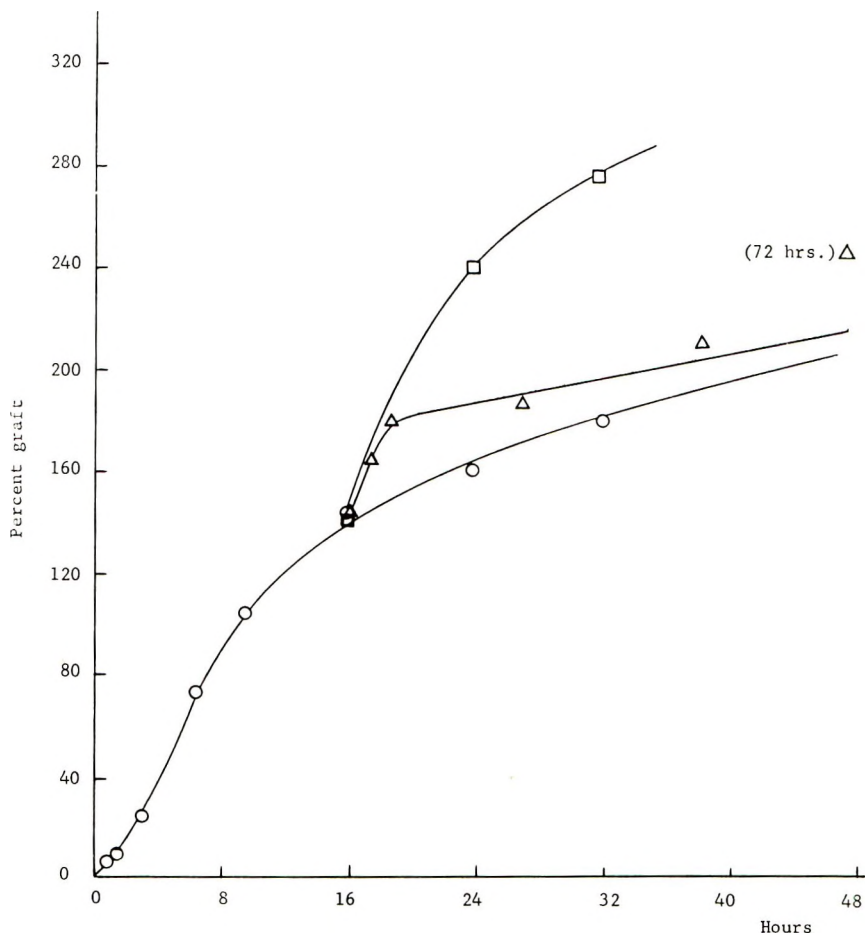


Fig. 10. Grafting of styrene to wool fabric followed by regrafting in the same monomer solution, 18% methanol in dioxane: (O) original mutual grafting curve (3.0×10^5 rad/hr.); (Δ) post-polymerization after mutual grafting; (\square) reirradiation after 3 days in air (3.0×10^6 rad/hr.).

the same effect as a high methanol content. Further studies, including fiber diameter distributions, ESR and dose rate measurements, are needed to elucidate more fully the mechanism operating during the grafting of wool fibers. These experiments are now in progress and will be reported in a later paper.

Acrylonitrile

Dimethylformamide was chosen as the solvent for the mutual grafting of acrylonitrile in order to keep the polyacrylonitrile in solution. Water or methanol was found to be necessary for appreciable grafting at the dose rate used. The course of the grafting process is shown graphically in Figures 11 and 12. Water was again found to be more effective than

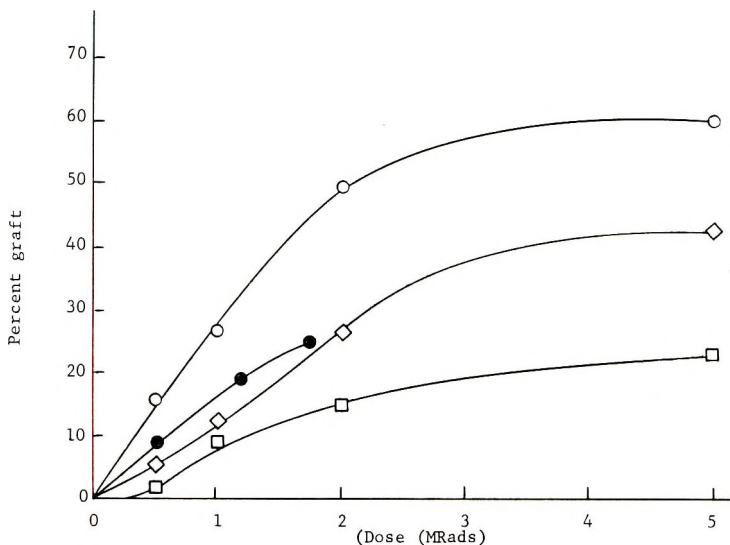


Fig. 11. Grafting of polyacrylonitrile to wool vs. radiation dose, monomer in dimethylformamide (3.06M) with added water at various concentrations: (○) 2% H₂O; (◇) 3.56% H₂O; (□) 0.43% H₂O; (●) vapor-phase grafting.

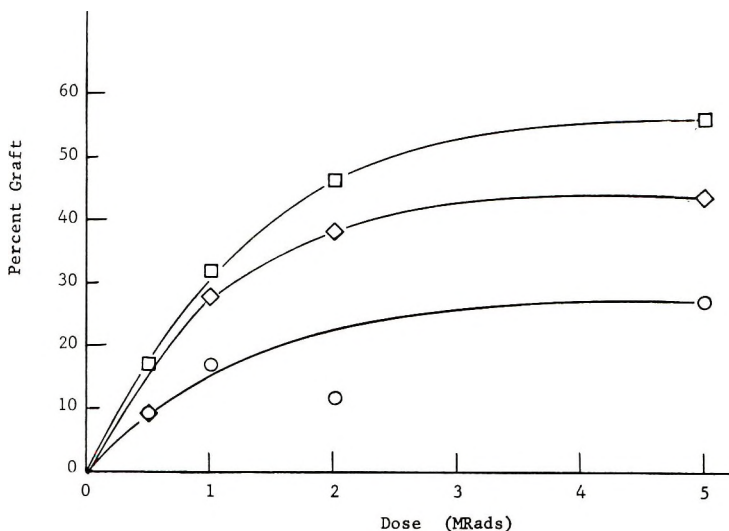


Fig. 12. Grafting of acrylonitrile to wool vs. radiation dose, monomer in dimethylformamide with added methanol at various concentrations: (□) 4.51% MeOH; (◇) 2.49% MeOH; (○) 0.50% MeOH.

methanol; however, after about 2% the rate of grafting began to drop due to the precipitation of polyacrylonitrile, preventing effective diffusion of monomer to the active centers. It is interesting that there was no acceleration period in the early stages as found with styrene, even with methanol. This is probably due to the excellent swelling of the wool by the dimethyl-

formamide itself. The leveling off in grafting is quite pronounced and is again dependent on the degree of swelling.

A few grafting experiments were also conducted using the vapor phase method developed by Armstrong and Rutherford.⁵ In this method wool cloth strips were suspended on a rack inside a one-liter stainless steel sample container. The sample container was flushed for 2 hr. with pre-purified nitrogen (1000 cm.³/min.) saturated at 75°F. and atmospheric pressure with the two-phase acrylonitrile-water system. This flushing was used to purge the system of oxygen and to allow the acrylonitrile and water time to diffuse into the wool fiber. The samples were placed in the irradiation position for various time intervals (2, 3, and 4 hr.) with the flushing continuing. After irradiation the samples were removed and the polymer addition determined by the weight gain of the sample. The acrylonitrile additions are included in Figure 11. All the acrylonitrile graftings were 60% on the weight of wool, or less, compared with several hundred per cent with styrene.

Miscellaneous Monomers

Attempts were made to graft a number of monomers which would lead to hydrophobic polymers. These included 2-ethylhexyl and stearyl methacrylates, and a number of fluorinated monomers and some allyl esters.

2-Ethylhexyl acrylate was grafted by simply padding on to the wool surface by use of a 15% and a 30% solution in methanol and irradiating to 0.3 Mrad. Weight increases after washing in methanol of 15 and 37% were found, which reduced to 5 and 30% after extraction with benzene to constant weight.

Stearyl methacrylate was grafted in pure monomer containing a few per cent of added methanol. At 0.5 Mrad, 6.6% grafted; beyond this a crosslinked mass resulted. In addition to these, 1,1-dihydroperfluoro-*n*-undecyl acrylate was studied, but crosslinked polymer resulted in each case. The acrylates and methacrylates polymerize rapidly by radiation and are not suitable for the direct method. Further experiments are in

TABLE I
Grafting of Allyl Monomers

Monomer	Water, %	Weight change at various doses, %	
		1 Mrad	5 Mrad
Allyl acetate ^a	2	4.0	4.7
	6	0	6.0
Allyl benzoate ^a	2	9.5	11.6
	6	9.7	10.6
Allyl stearate (satd., 0.97 <i>M</i>)	2	23.1	21.5
	6	15.1	16.1

^a 3.06*M* in dioxane solution.

progress using the pre-irradiation technique and will be reported in due course.

The allyl monomers grafted successfully in dioxane solution with a small percentage of added water, and the results are presented in Table I. The per cent grafting was quite small and reached a maximum at about 1 Mrad.

Examination of the Styrene Grafted Wools

Wool can be hydrolyzed away and in this way the grafted side chains can be separated and examined. Untreated wool will dissolve completely in warm 10% aqueous sodium hydroxide in about 4 hr. The styrene-grafted wools, on the other hand, were not dissolved or disintegrated even after one week of alkaline hydrolysis. However, it was found that a mixture of equal volumes of benzene and 5% potassium hydroxide, to which sufficient water had been added to form two layers, was quite effective. The wools were refluxed in this mixture for about 12 hr. Untreated wool disappeared to give two yellowish but clear layers, whereas grafted wools formed opaque emulsions. A sample of wool grafted, in 18% methanol solution in dioxane, to 140% was treated in this way. The emulsion was acidified with hydrochloric acid and poured into excess ethanol and the insoluble precipitate collected. It was found that the residue could be divided into roughly equal parts by benzene. The benzene-insoluble portion was, however, soluble in dimethylformamide. The intrinsic viscosity of the two fractions was determined in dimethylformamide and in toluene, respectively. Correcting for the difference in solvents, the viscosity-average molecular weights were found to be 49,000 and 62,000 for the benzene-insoluble and benzene-soluble fractions, respectively. The corresponding molecular weight for the polystyrene produced in the free solution was only 15,000. The molecular weight of the grafted side chains in a sample prepared in 6% water solution was about 120,000, whereas the homopolymers in the free solution also had similar molecular weights close to 15,000, as would be expected. These experiments show that, although the gel effect leads to higher molecular weights it is far less effective than in most heterogeneous grafting experiments, with cellulose acetate or cotton, for example. The reasons for this must remain obscure until more detailed investigations are made. The infrared spectrum of both polystyrene fractions showed bands normally associated with carbonyl and amide groupings. The benzene-insoluble portion showed much stronger bands than the soluble. Ninhydrin reagent also gave the characteristic blue color normally associated with the presence of proteins. The experiments described above leave little doubt that actual grafting takes place and that alkaline hydrolysis leaves behind polystyrene containing attached amino acid residues. Even prolonged acid hydrolysis failed to render the insoluble fraction soluble in benzene.

A number of efforts were made to examine the grafted fibers microscopically by using numerous staining techniques and including polarizing

microscopy, and ultraviolet and electron microscopic examination. Even with the highly grafted samples, no large discontinuous regions could be observed and it appears that the grafting was quite homogeneous in nature. Knowledge of the location of the grafted polymer is highly important for elucidation of the mechanism of the grafting process and, most important, to correlate with the properties of the grafted fibers.

A portion of this research was conducted under contract with U. S. Department of Agriculture and authorized by the Research and Marketing Act of 1946. The contract was supervised by the Wool and Mohair Laboratory of the Western Utilization Research and Development Division of Agricultural Research Service.

Reference to a company and/or product name by the Department is only for purposes of information and does not imply approval or recommendation of the product by the exclusion of others which may also be suitable.

References

1. Chapiro, A., *Radiation Chemistry of Polymeric Systems*, Interscience, New York, 1962, ch. 12.
2. Krassig, H. A., and V. Stannett, *Fortschr. Hochpolymer. Forsch.*, **4**, 111 (1965).
3. Burke, M., P. Kenny, and G. M. Nicholls, *J. Textile Inst.*, **53**, T370 (1962).
4. Horio, M., K. Ogami, T. Kondo, and K. Sekimoto, *Bull. Inst. Chem. Res., Kyoto Univ.*, **41**, 10 (1963).
5. Armstrong, A. A., and H. A. Rutherford, *Textile Res. J.*, **33**, 264 (1963); *Industrial Uses of Large Radiation Sources*, Vol. I, I.A.E.A., Vienna, 1963, pp. 257-287.
6. Puig, J. R., French Pat. 1,278,000 (Oct. 30, 1961).
7. Chapiro, A., and V. Stannett, *Intern. J. Appl. Radiation Isotopes*, **8**, 164 (1960).
8. Fox, T. G., and P. J. Flory, *J. Am. Chem. Soc.*, **73**, 1915 (1951).
9. Araki, K., H. Kiho, and V. Stannett, *Makromol. Chem.*, in press.

Résumé

On a greffé un certain nombre de monomères vinyliques à de la laine en faisant usage de la technique de l'irradiation mutuelle. L'étude du styrène en solution dans le dioxane fut très poussée; on a trouvé que l'eau et le méthanol sont nécessaires à la réussite du greffage. Nous considérons que ceus-ci font gonfler le substrat, permettant au monomère de pénétrer jusqu'aux centres actifs de la laine, produits par l'irradiation. La vitesse de greffage passe toujours par un maximum avant de se stabiliser à une vitesse moins élevée. Nous croyons que ceci est dû à la lente augmentation de la concentration en radicaux, menant en fin de compte à une vitesse de greffage régie par la diffusion. On a trouvé qu'un greffage important a lieu par post-polymérisation. L'acrylonitrile ainsi qu'un nombre considérable de monomères allyliques ont été également greffés à la laine solution dans le diméthylformamide par la méthode d'irradiation mutuelle. À nouveau la présence d'eau, et de méthanol a été trouvée nécessaire; la vitesse de greffage se rapproche de zéro à un degré de greffage qui dépend de la quantité d'agent de gonflement présent.

Zusammenfassung

Eine Anzahl Vinylmonomere wurde mit dem Verfahren der wechselweisen Bestrahlung auf Wolle aufgepfropft. Styrol wurde eingehend in Dioxanlösung untersucht; für eine erfolgreiche Aufpfropfung war die Anwesenheit von Wasser oder Methanol notwendig. Es wird angenommen, dass diese Stoffe als Quellungsmittel fungieren und eine Diffusion des Monomeren zu den aktiven, in der Wolle durch die Strahlung erzeugten Zentren ermöglichen. Die Aufpfropfungsgeschwindigkeit ging immer durch ein Maxi-

mum und strebte dann einer kleineren Geschwindigkeit als Grenzwert zu. Es wird angenommen, dass dieses Verhalten auf den langsamen Aufbau der Radikalkonzentration zurückzuführen ist, was zu einer diffusionskontrollierten Aufpfropfungsgeschwindigkeit führen kann. Es wurde gefunden, dass bei einer Pfropfpolymerisation ein beträchtlicher Nacheffekt auftritt. Weiters wurden auch Acrylnitril und eine Anzahl von Allylmonomeren nach der Methode der wechselweisen Bestrahlung in Dimethylformamidlösung erfolgreich auf Wolle aufgefropft. Auch hier erwiesen sich Wasser oder Methanol als notwendig; die Aufpfropfungsgeschwindigkeit näherte sich bei einem von der Menge des anwesenden Quellungsmittels abhängigen Aufpfropfungsgrad dem Werte 0.

Received May 20, 1965

Prod. No. 4763A

Glass Temperature and Crystal Modification of Linear Polymethylene

J. H. MAGILL, S. S. POLLACK, and D. P. WYMAN,*
Mellon Institute, Pittsburgh, Pennsylvania

Synopsis

The preparation of high molecular weight linear polymethylene is described at low temperatures. The onset of a polymorphic transformation (triclinic to orthorhombic) is observed on warming this low crystallinity ($\sim 50\%$) polymer to about -25°C . Relative rates of transformation above this temperature are also given. No significant increase in crystallinity occurs on warming the polymer up to room temperature, where some triclinic phase still persists. Annealing polymethylene at 100°C . leaves only the orthorhombic material which is approximately 80% crystalline. A glass transition temperature around -30°C ., is reported for the low crystallinity polymer.

Introduction

Numerous techniques have been employed to ascertain the glass temperature of polymethylene and diverse results for this transition have been reported in the literature.¹ The present communication briefly reports results on linear polymethylenes in the 1.4×10^5 to $1.5 \times 10^6 \bar{M}_n$ range. Most results refer to the lower molecular weight polymers in this range.

Sample Preparation

In sample preparation,² approximately 6 g. (0.143 mole) of diazomethane was generated in ether (280 cc.) from 43 g. of Diazald (*N*-methyl-*N*-nitroso-*p*-toluene-sulfonamide) by using the "alcohol-free" procedure of Deboer and Backer.³ The diazomethane ether solution was distilled as it was generated into a receiver containing 30 g. KOH pellets which acted as a drying agent. After $1/2$ hr. the solution was distilled into the 1-liter polymerization flask charged with 450 cc. of ether distilled from lithium aluminum hydride. The polymerization flask, open to an atmosphere of dry nitrogen, was submerged in a Dry Ice-acetone bath. When a 5-cc. aliquot of purified boron trifluoride etherate was added from a syringe through a serum cap, the reaction was virtually instantaneous, giving rise to a finely divided white suspension of polymethylene in ether. The suspension was rapidly filtered at Dry Ice temperatures, leaving a polymer-

* Present address: Plastics Research Laboratory, Marbon Chemical, Washington, West Virginia.

ether slush in the filter which was then transferred to a high vacuum system where the remaining ether was removed at Dry Ice-acetone temperature over a period of several days. Special care was taken to insure that certain samples were never exposed to temperatures higher than -50°C . from the time of polymerization until the time the x-ray measurements were made, as described below.

The molecular weight⁴ M_v of this polymer was estimated by viscometry in decalin at 135°C . by use of the relationship:

$$[\eta] = 4.6 \times 10^{-4} M_v^{0.73}$$

Significant is the fact that the infrared spectra of various polymethylenes prepared in this manner, at temperatures between -30 and -70°C ., showed no evidence for methyl group absorption in the infrared at 7.25μ , indicating that the polymer was devoid of short-chain branching.

X-Ray Diffraction

Flat-film x-ray diffraction photographs of this polymer were obtained from liquid nitrogen temperature up to $+30^{\circ}\text{C}$. approximately. The polymethylene as synthesized is of low crystallinity (~ 40 - 50%) and is predominantly present in the triclinic form. On a photograph, Figure 1a, made at -30°C ., d spacings ($\pm 0.05 \text{ \AA}$.) of 4.47 \AA . (m), 4.07 \AA . (w), and 3.74 \AA . (w) were measured. A small amount of the orthorhombic phase may be also present. As the sample temperature is increased stepwise, the triclinic phase starts changing into the more common orthorhombic crystalline form above -25°C . This transformation is not accompanied by a significant increase in polymer crystallinity up to and including room temperature (22°C .) where the following d spacings ($\pm 0.05 \text{ \AA}$.) were obtained: 4.55 \AA . (w), 4.12 \AA . (s), and 3.75 \AA . (m). The orthorhombic phase is predominant at room temperature, as illustrated in Figure 1b. Figure 2 shows the intensity difference between the triclinic peak at 4.5 \AA .

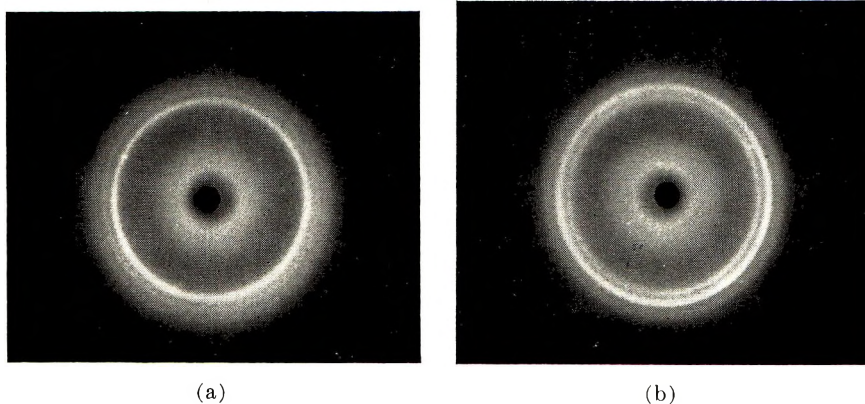


Fig. 1. X-ray diffraction patterns (a) polymethylene at -30°C .; (b) same sample after raising temperature to 22°C .

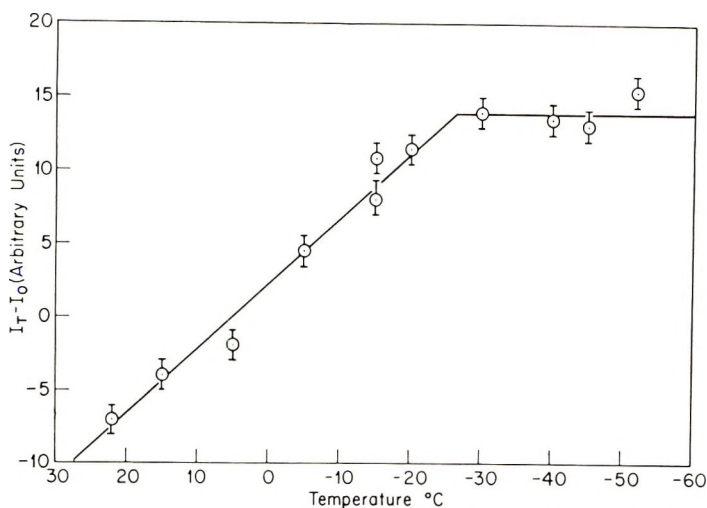


Fig. 2. Amount of polyethylene transformed expressed as the difference in intensity ($I_T - I_0$) as a function of temperature. The difference in peak heights between the triclinic peak at ≈ 4.5 Å. (I_T) and that of the orthorhombic peak at ≈ 4.1 Å. (I_0) is expressed in arbitrary units.

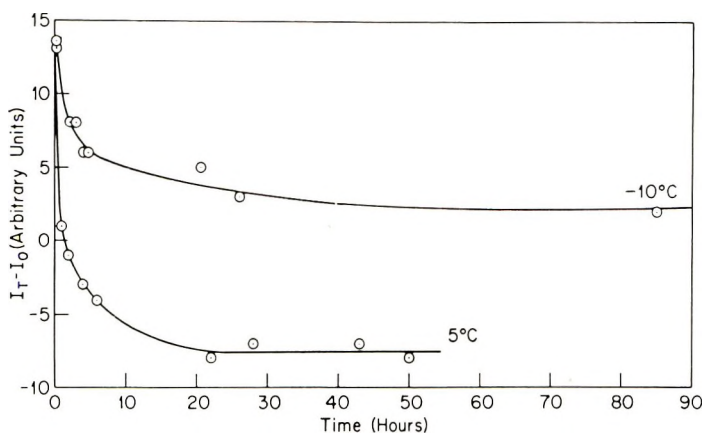


Fig. 3. Isothermal transformation rates at -10 and $+5^\circ\text{C}$. for polyethylene prepared at approximately -70°C . (Phase change is triclinic to orthorhombic.)

and the orthorhombic peak at about 4.1 Å., as a function of increasing temperature. A distinct transition is observed between -20 and -30°C . The actual slope of the line in Figure 2 at temperatures above -20°C . approximately will be somewhat dependent on the time scale of the measurements, but the position of the transition will not be altered significantly. The change from the triclinic to the more symmetric orthorhombic form was not reversed on a sample which had been raised to room temperature and then held for 18 hr. in liquid nitrogen and subsequently examined at this temperature. Annealing the sample at 100°C . for 18 hr. and cooling to

23°C. produces material 70–85% crystalline approximately, with a substantial increase in the orthorhombic component and complete disappearance of the triclinic phase.

It was impossible to obtain low crystallinity polymethylene by quenching the molten polymer. Material at least 70% crystalline was formed in contrast to the more amorphous variety prepared *in situ* by the polymerization of diazomethane at low temperatures.

Measurements on the rate of transformation of the triclinic to the orthorhombic form (Fig. 3) were made at -10 and $+5^\circ\text{C}$., giving half-times (for the change) corresponding to 4 hr. and $\frac{2}{3}$ hr., respectively. The ordinate in Figure 3 is similar to that in Figure 2.

Linear Expansion Measurements

At this stage of the investigation, it was thought that the transition temperature was associated with the polymer glass temperature T_g , since no further change was observed between -30°C . and liquid nitrogen temperature. Expansion measurements were made on some of the samples which had been stored at room temperature, by use of polymethylene

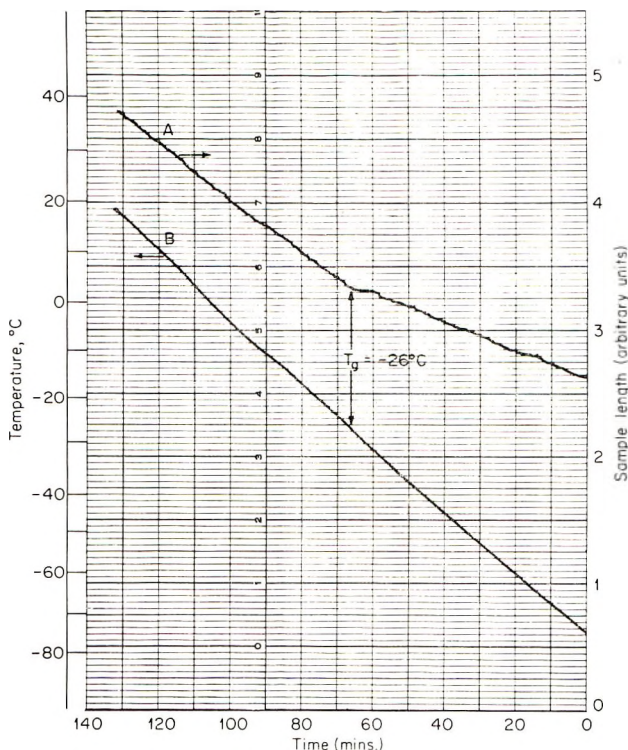


Fig. 4. Change in sample length (recorder output in volts) with time for linear rate of heating (indicated).

plugs $3/16$ in. in diameter fabricated at 5000–10,000 psi. The change in length of the specimen ($1/2$ – $1\frac{1}{2}$ in. usually) was measured at a constant heating rate (ca. 1 – 2°C./min.) and the output recorded on a two-pen recorder. Figure 4 shows the change in sample length and corresponding temperature at a 1°C./min. temperature rise for a polymer of $\bar{M}_v = 1.4 \times 10^5$ which is about 40–50% crystalline. A distinct transition is noted about -26°C. Other more crystalline specimens usually of higher molecular weights, showed less pronounced transitions, sometimes as high as approximately -10°C.

This measurement provides direct evidence for the glass temperature of linear polymethylene. Furthermore, it is not complicated by the triclinic \rightarrow orthorhombic transformation, since the sample was stored many days at room temperature before and after its fabrication prior to measurements; hence it was already in the orthorhombic form. The expansion measurement results indicate that the crystal transition occurs in the region of the glass transition temperature.

Indirectly, it may be generally concluded from crystallization rate studies that T_g lies in the range 0.6–0.7 of the polymer thermodynamic melting point. For polymethylene, this range is approximately -16 to -25°C. , a result which is in agreement with the evidence presented here. Some literature results^{5–8} concur with our T_g 's of -10 to -30°C. depending on the polymer crystallinity in the higher molecular weight range, where T_g should be independent of the molecular weight. The present observations confirm those of Matsuoka and co-workers^{8,9} concerning the strong dependence of the maximum crystallinity of high molecular weight polymethylene on its temperature history; they further indicate that the triclinic form may be obtained in polymerizations producing polymethylene at below -30°C. The present observations on the value of T_g for linear polymethylene confirm the findings of Matsuoka et al. based on their dynamic mechanical experiments.¹⁰

Conclusions

The glass transition temperature of moderately crystalline (~ 40 – 50%) linear polymethylene ($\bar{M}_v = 1.4 \times 10^5$) lies in the range -20 to -30°C.

The polymethylene sample undergoes an observable crystal transition (triclinic to orthorhombic) on warming above about -25°C. ; no significant increase in polymer crystallinity occurs up to and including room temperature.

The polymerization of diazomethane that led to the synthesis of the polymers was supported by the Wright-Patterson Air Force Materials Laboratory, under Contract No. AF 33(657)-7651; the diffraction and linear expansion measurements were supported in part by the Office of Naval Research, under Contract No. Nonr 2693(00). The authors wish to express their appreciation to Dr. T. G Fox for suggesting this study.

References

1. Boyer, R. F., *Rubber Rev.*, **36**, 1303 (1963).
2. Wyman, D. P., and T. G. Fox, Air Force Materials Laboratory Report, TDR-147, April 1964.
3. Deboer, T. J., and H. J. Backer, *Rev. Trav. Chim.*, **73**, 229 (1954).
4. Henry, P. M., *J. Polymer Sci.*, **36**, 3 (1959).
5. Ohlberg, S. M., and S. S. Fenstermaker, *J. Polymer Sci.*, **32**, 514 (1958).
6. Cole, E. A., and D. R. Holmes, *J. Polymer Sci.*, **46**, 245 (1960).
7. Hoffman, J. D., and J. J. Weeks, *J. Chem. Phys.*, **37**, 1723 (1962).
8. Moore, R. S., and S. Matsuoka, *Polymer Division Preprints, Am. Chem. Soc.*, **4**, 711 (1963), and references 1, 2, 3, and 4 contained therein. Paper presented at meeting in New York, September, 1963.
9. Moore, R. S., and S. Matsuoka, *J. Polymer Sci.*, **C5**, 163 (1964).
10. Rogers, C. E., S. Matsuoka, and C. J. Aloisio, *Polymer Division Preprints, Am. Chem. Soc.*, **4**, No. 1, 341 (1963). Paper presented at meeting in Los Angeles, April 1963.

Résumé

On décrit la préparation à basse température de polyméthylène linéaire de haut poids moléculaire. On observe un début de transformation polymorphe (triclinique en orthorhombique) en chauffant ce polymère de faible cristallinité ($\sim 50\%$) jusqu'environ -25°C . On donne également des vitesses relatives de transformation au-dessus de cette température. Une augmentation notable de cristallinité se manifeste en chauffant le polymère à température de chambre à laquelle une certaine phase triclinique persiste encore. Le polyméthylène reçu à 100°C fournit seulement un matériau orthorhombique qui est environ cristallin à 80% . On rapporte une température vitreuse aux environs de -30°C pour le polymère de basse cristallinité.

Zusammenfassung

Die Darstellung von hochmolekularem, linearem Polymethylen bei niedrigen Temperaturen wird beschrieben. Das Einsetzen einer polymorphen Umwandlung (triklin zu orthorhombisch) wird beim Erwärmen dieses niederkristallinen ($\sim 50\%$) Polymeren auf etwa -25°C beobachtet. Relative Umwandlungsgeschwindigkeiten oberhalb dieser Temperatur werden angegeben. Es besteht keine merkliche Kristallinitätszunahme, wie sie beim Erwärmen des Polymeren auf Raumtemperatur eintritt, wo noch etwas trikline Phase vorhanden ist. Tempern des Polyäthylens bei 100°C liefert nur orthorhombisches Material, welches zu etwa 80% kristallin ist. Ein Glasumwandlungstemperatur bei etwa -30°C wird für das niederkristalline Polymere festgestellt.

Received January 22, 1965

Revised July 13, 1965

Prod. No. 4767A

Crystallization in Stretched Polymer Networks.

I. *trans*-Polychloroprene

A. N. GENT, *Institute of Rubber Research,
The University of Akron, Akron, Ohio*

Synopsis

Measurements are described of the rates of crystallization of uncrosslinked *trans*-polychloroprene over a range of temperature and of three crosslinked samples over a wide range of extension and temperature. The large increases in rate with extension are attributed to corresponding increases in the equilibrium melting temperature and hence degree of supercooling. The rise in melting temperature has been measured and is found (1) to account satisfactorily for the observed changes in rate, and (2) to be in good agreement with Flory's treatment of oriented crystallization in stretched networks. The form and magnitude of the changes in tensile stress are also in accord with the formation of oriented crystallites, and seem incompatible with folded-chain crystallization. When reduced to a condition of constant segmental mobility, the rates of crystallization are shown to follow a common dependence upon the degree of supercooling. This relation is compared with the predictions of nucleation theory.

INTRODUCTION

Although the crystallization of polymers from the molten (i.e., completely disordered) state has been studied extensively, comparatively little attention has been paid to the process of crystallization in oriented polymers. Crosslinked materials are convenient for this purpose, since the degree of orientation in the amorphous state can be specified accurately, while small amounts of crosslinking do not seriously affect the crystallization process itself.

Experiments are reported here on the rates of crystallization and the crystal melting temperatures in stretched networks of *trans*-polychloroprene. This material was chosen for experimental convenience, being readily crosslinked and having low rates of crystallization at moderate supercoolings. In a subsequent paper¹ experiments on networks of a similar polymer, *trans*-1,4-polyisoprene, are reported.

The crystallization kinetics of uncrosslinked *trans*-polychloroprene and of crosslinked samples in the unstrained state are described in the following section. The crystallization of crosslinked samples at various extensions and temperatures is described next. In a further section, measurements of the crystal melting temperatures in stretched strips are reported.

CRYSTALLIZATION OF UNSTRAINED *trans*-POLYCHLOROPRENE MATERIALS

Experimental Details

The polychloroprene employed (Neoprene HC, E. I. du Pont de Nemours and Company) contained 93% *trans* linkages. It was received in the form of lumps containing a mass of small pores, less than 1 mm. in diameter. When these were removed by slight milling on a warm mill, the rate of crystallization increased to about twice its former value. The reason for this is not known; it may be due to the effectively finely-divided state of the original material. The results for the milled material have been taken here as representative.

Vulcanizates were prepared, using the mix recipes and vulcanization conditions given in Table I, in the form of sheets about 0.7 mm. thick. To characterize them, the tensile stress σ required to extend test pieces to various extension ratios λ at 95°C., i.e., in the amorphous state, and the volume fraction v_r of the vulcanizate when swollen to equilibrium in benzene at 30°C., were determined. The values of v_r and of the coefficients C_1 and C_2 of the Mooney form of stored energy function,² given by the intercepts and slopes of plots of $\sigma/2(\lambda - \lambda^{-2})$ against λ^{-1} are given in Table II.

The average molecular weights M_c between crosslinks were calculated from the C_1 values assuming simple kinetic theory to apply; they are in-

TABLE I
Mix Recipes and Vulcanization Conditions Employed to Prepare Test Sheets

	Parts by weight		
	A	B	C
Neoprene HC	100	100	100
Extra light calcined magnesia	4	2	4
Zinc oxide	5	5	5
NA 22	—	0.3	0.75
Permalux	0.5	—	—
PBNA	2	—	—
Vulcanization period, min. at 150°C.	30	30	30

TABLE II
Properties of the Vulcanizates

	A	B	C
C_1 , kg./cm. ²	0.47	1.0	1.3
C_2 , kg./cm. ²	1.6	2.1	2.4
v_r	0.15	0.175	0.19
M_c calculated from C_1	42,500	20,000	15,500
μ	0.50	0.48	0.475

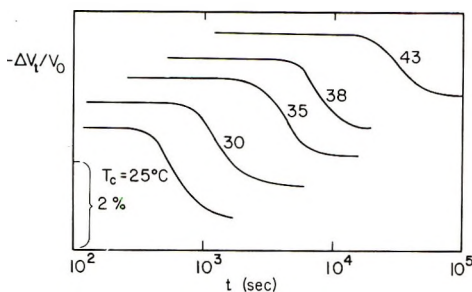


Fig. 1. Crystallization of 93% *trans*-polychloroprene (1).

cluded in Table II. Values of the polymer-solvent interaction parameter μ were then calculated by using the Flory-Huggins relation³ between M_c and v_r . The values obtained are given in Table II also; they are closely similar, averaging 0.485.

The crystallization process was followed dilatometrically⁴ for the uncrosslinked material and for the crosslinked materials in the unstrained state. About 3-g. portions of the materials were sealed into the bulbs of glass dilatometers which were then filled with mercury. Flow of uncrosslinked material in the molten state was prevented by wrapping it in fine stainless steel gauze.⁵ The dilatometer bulbs were about 10 cm. long and 1 cm. in diameter; the stems had an internal diameter of 1 mm. and carried an engraved scale.

After a conditioning period of about 15 min. at a temperature of 95°C., the dilatometers were rapidly transferred to a constant temperature bath. The mercury level in the stem fell rapidly during the first 2 min. as the sample underwent thermal contraction, and then reached a steady level until crystallization ensued, indicated by a further decrease in volume. Some typical experimental relations between the volume contraction and the time at a constant temperature are shown in Figure 1. They show the characteristic features of polymer crystallization, although they are more diffuse than for natural rubber, for example.⁵ The index n in the Avrami relation⁶

$$\Delta V_t = \Delta V_\infty (1 - \exp\{-kt^n\})$$

for phase transformations is correspondingly smaller than the expected values of 4 or 3 for homogeneously or heterogeneously nucleated spherulitic growth, being generally about 2. This is attributed to the irregular structure of the present materials; Gornick and Mandelkern⁷ have shown that the presence of small amounts of noncrystallizing groups causes a marked retardation of the later stages of crystallization.

The rate of crystallization has been characterized by the time $t_{1/2}$ at which one-half of the pseudo-equilibrium volume contraction had occurred, i.e., ignoring the continued slow contraction in volume after the primary crystallization process is over. The observed values have been corrected

(by subtracting 2 min.) to allow for the delay in attaining thermal equilibrium. Values obtained in this way were in good agreement with values obtained using small samples (about 1 mm.³) immersed in a density gradient column, with a much shorter thermal lag.⁸

Rates of Crystallization

The half-times of the primary crystallization process are plotted against the crystallization temperature in Figure 2. The experimental points are omitted from the central relations for clarity.

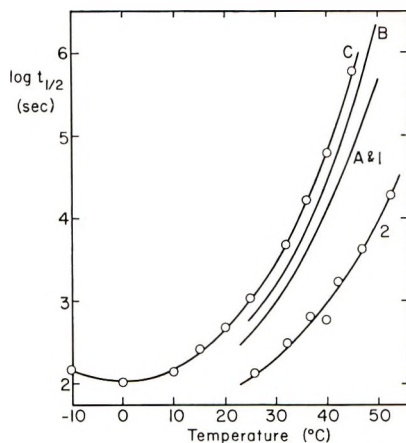


Fig. 2. Experimental relations between the crystallization half-time $t_{1/2}$ and temperature.

At low temperatures crystallization occurred extremely rapidly. For the most highly crosslinked material, C, values of $t_{1/2}$ were determined at temperatures down to -10°C ., revealing a maximum rate at about 0°C . with a half-time of about 100 sec. At higher temperatures, the relations for the uncrosslinked material 1 and the three crosslinked samples are seen to be approximately parallel curves. The relation for vulcanizate A is indistinguishable from that for the uncrosslinked material; the relations for vulcanizates B and C are displaced by about 2.5 and 5°C . to lower temperatures. For comparison, the relation is shown for another polychloroprene (2) containing about 96% *trans* linkages. This is also approximately parallel, displaced by about 10.5°C . with respect to the relation for the uncrosslinked polychloroprene 1. Apparently the low degrees of crosslinking employed here do not greatly affect the rates of crystallization; the maximum effect is equivalent to a decrease in *trans* content of only about 1.5%.

Amounts of Crystallization and Melting Temperatures

The volume contractions at the end of the primary crystallization process, after a time of about $3t_{1/2}$, varied from 1.6 to 2.15%. For the value given

by Maynard and Mochel⁹ for the density of the fully crystalline material (1.35 g./cc.), they correspond to relatively low degrees of crystallinity of about 27% for the 96% *trans*-polychloroprene 2, 23% for material 1, and 20% for the three crosslinked materials prepared from 1.

The melting temperatures were 69.5 and 62°C. for materials 2 and 1, respectively, and about 57°C. for all three crosslinked materials. The differences are roughly in line with the displacements of the rate relations shown in Figure 2 along the temperature axis. However, the present melting temperatures are ill-defined; they depended somewhat upon the crystallization temperature. This was particularly evident for the crosslinked materials, as described later. The above comparison is therefore rather qualitative.

CRYSTALLIZATION IN STRETCHED NETWORKS

Experimental Details

The progress of crystallization in a stretched strip held at constant length was followed by observing the corresponding changes in the retractive force exerted by the sample.¹⁰ The test piece, consisting of a strip about 5 cm. long, 1 cm. wide, and 0.7 mm. thick, was secured between two clamps. The lower one was attached to a rigid frame and the upper one was connected to a force transducer (Statham Instruments Model GI-16-350) secured to the frame. The sample could be subjected to any required degree of extension by adjusting the length of the rigid arm connecting the upper clamp to the transducer.

The sample was stretched in the molten state in a hot bath at 95°C. The frame carrying the sample and transducer was then transferred rapidly to a second bath held at the required crystallization temperature. The baths were filled with silicone oil (Union Carbide L-45, 350 cstokes at 25°C.); preliminary experiments showed that the swelling was less than 3% after one week at 70°C.

Some typical relations between the retractive force f , expressed as a fraction of the initial value f_0 , and the time are shown in Figure 3 for vulcanizate B. A logarithmic time scale has been employed in view of the wide range.

The tensile force decreased substantially as crystallization proceeded. At low extensions the force fell sharply to zero, the sample then becoming bowed. At higher extension ratios, greater than about 3, the force decreased in a more diffuse manner and did not reach zero. These effects are closely similar to those reported previously for vulcanizates of natural rubber¹⁰ and *cis*-1,4-polybutadiene.¹¹ The relative magnitudes of the decrease in force at different extensions are in good agreement with Flory's theoretical treatment¹² of the entropy changes for stretched networks in which oriented crystallites form. The different time functions probably reflect a transition from spherical to uniaxial growth forms as the extension is increased.¹⁰

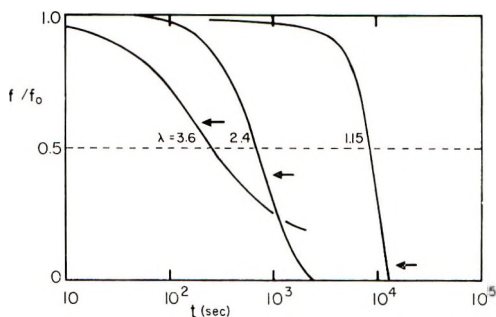


Fig. 3. Experimental relations between the retractive force f , relative to the initial value f_0 , and time t at 40°C . for vulcanizate B at various extension ratios λ .

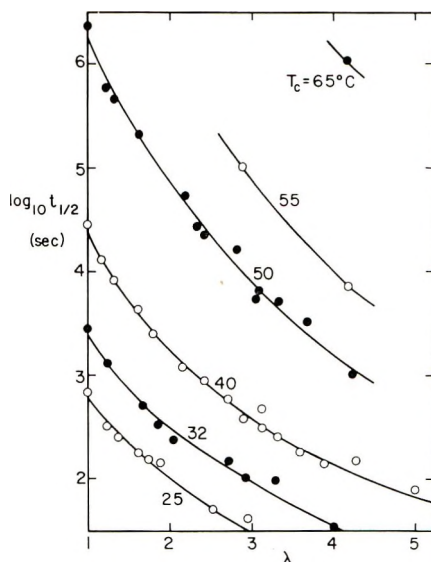


Fig. 4. Relations between the crystallization half-time $t_{1/2}$ and the extension ratio λ for vulcanizate B at various crystallization temperatures T_c .

The rate of crystallization is seen in Figure 3 to be markedly increased by an imposed extension. This effect is considered below.

Rates of Crystallization

Values of the crystallization half-time $t_{1/2}$ were estimated from the stress relaxation relations at various extensions and temperatures. The values chosen for the relations given in Figure 3 are indicated by arrows. At low extensions, when the observed stress changes reflect only the early stages of crystallization, the force decreases sharply, and the probable error in choosing a value for $t_{1/2}$ is small. At large extensions, when the force changes are protracted, the force does not decrease to zero, and a value may be assigned to $t_{1/2}$ with fair precision.

Values of $t_{1/2}$ determined in this way for vulcanizate B are plotted on a logarithmic scale in Figure 4 against the imposed extension ratio λ . Relations are shown for several temperatures in the range 25–65°C., corresponding to a five-decade range of values for $t_{1/2}$. The maximum extension ratio used (5.0) was determined by the breaking extension of the network before crystallization, i.e., in the hot bath. The crystallization half-times shown in Figure 4 at $\lambda = 1$, i.e., in the unstretched state, were determined by interpolation from the dilatometric measurements plotted in Figure 2. They are seen to be in good accord with the values obtained from the stress relaxation measurements at small extensions.

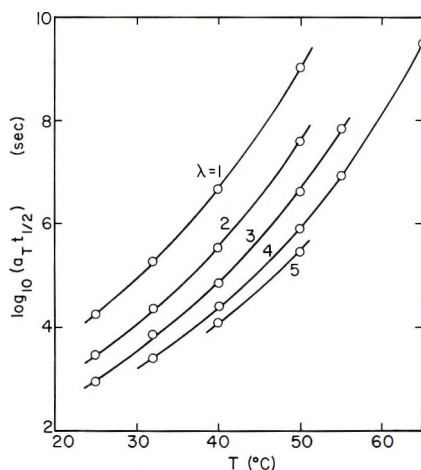


Fig. 5. Relations between the reduced crystallization half-time $a_T t_{1/2}$ and the crystallization temperature T_c for vulcanizate B at various extension ratios.

Over the wide temperature range considered here, substantial changes take place in the segmental mobility. In an attempt to take these changes into account, the half-times $t_{1/2}$ have been multiplied by appropriate reduction factors to refer them to a state of uniform segmental mobility. The reduction factors employed were calculated from the Williams-Landel-Ferry relation¹³

$$\log a_T = 8.86(T - T_s)/(101.6 + T - T_s) \quad (1)$$

so that the uniform mobility is that obtaining at the reference temperature T_s . T_s is generally taken as $T_g + 50^\circ\text{C}$., where T_g is the glass transition temperature.

A value of T_g of $-47 \pm 2^\circ\text{C}$. was determined dilatometrically for vulcanizate C. It is in good agreement with that reported by Yin and Pariser¹⁴ for another polychloroprene (Neoprene W), and has therefore been employed here to calculate values of a_T , although Yin and Pariser also found eq. (1) to apply to their measurements of dynamic mechanical properties only when a higher value for T_g , of -17°C ., was adopted. The

latter seems an unreasonably high value, since the vulcanizates are still quite flexible at that temperature.

The half-times of crystallization for vulcanizate B were read from the relations given in Figure 4 at several integral values of the extension ratio λ . They were then reduced to the uniform mobility obtaining at the reference temperature, $+3^\circ\text{C}$. The reduced values are plotted against the crystallization temperature in Figure 5.

The results are seen to consist of a series of accurately parallel curves, superimposable by horizontal shifts. Similar parallel relations were obtained for vulcanizates A and C when the half-times at various extensions and temperatures were reduced in the same way. The temperature

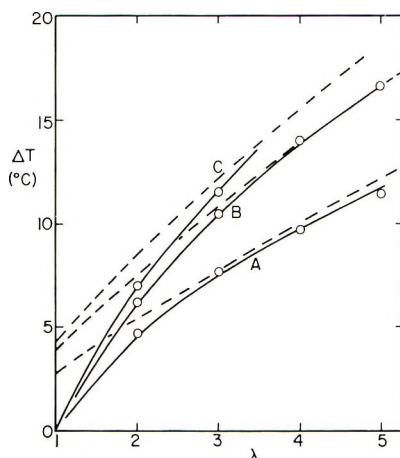


Fig. 6. Temperature shifts ΔT required to superimpose the reduced rate curves at a given extension ratio λ upon the relation for the unstrained material ($\lambda = 1$). The broken curves are calculated from eq. (2).

shifts required to bring the relations for a given extension ratio into coincidence with the relation for the corresponding undeformed material ($\lambda = 1$) are plotted in Figure 6. They are seen to define smooth curves over the whole range of extension, the displacements for a given extension being roughly in line with the degree of crosslinking (Table II).

The rates of crystallization at various extensions thus appear to be related in a simple manner. They depend identically upon temperature when reduced to a condition of constant segmental mobility, and are merely displaced along the temperature scale by various amounts, depending upon the extension and the degree of crosslinking. The displacements presumably reflect changes in the melting temperature with extension. Measurements of the melting temperature in stretched strips are reported in the following section and compared with the observed displacements. The form of the master relation for $t_{1/2}$ as a function of temperature is discussed in the final section.

MELTING TEMPERATURES

Experimental Details

The stress changes which take place when a crystalline test piece is slowly warmed afford a means of studying the process of melting. In particular, the temperature at which the stress regains the value characteristic of the amorphous network may be taken as a measure of the melting temperature for the stretched network. Two typical experimental relations are shown in Figure 7, for strips of vulcanizate B crystallized at 32°C. at extension ratios of 1.68 and 4.20 and then warmed at 0.5°C./min. to the melted state.

At the lower extension melting occurred quite abruptly, and a well-defined melting temperature was obtained, indicated by the vertical arrow on the lower curve. The stress in the melted state did not show the theoretical proportionality to absolute temperature (indicated by the broken

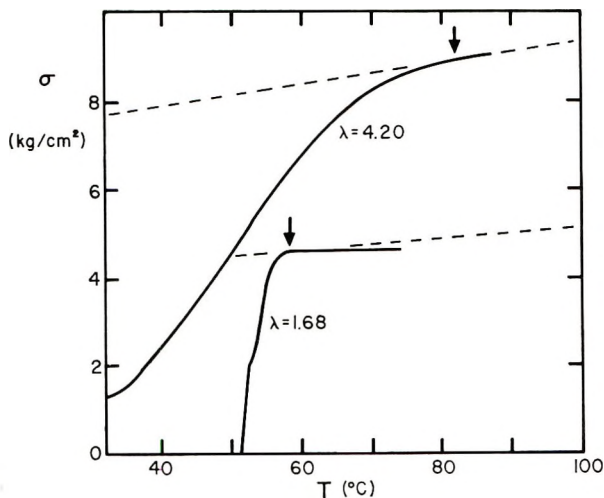


Fig. 7. Stress changes on melting test pieces of vulcanizate B, crystallized at 32°C. at extension ratios of 1.68 and 4.20.

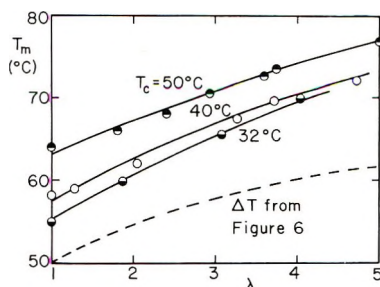


Fig. 8. Relations between the melting temperature T_m for vulcanizate A and the extension ratio λ for various crystallization temperatures T_c .

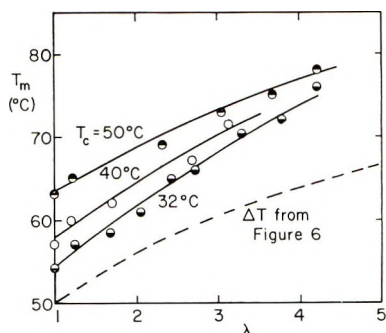


Fig. 9. Relations between the melting temperature T_m for vulcanizate B and the extension ratio λ for various crystallization temperatures T_c .

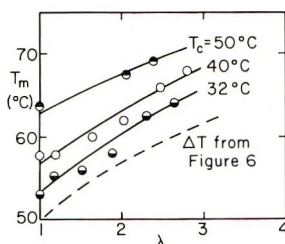


Fig. 10. Relations between the melting temperature T_m for vulcanizate C and the extension ratio λ for various crystallization temperatures T_c .

line) but remained relatively constant, probably due to continued stress relaxation in the lightly vulcanized material. However, this does not seriously affect the assignment of the melting point.

At the larger extension melting was much more diffuse, and it proved difficult to distinguish accurately a temperature at which the stress began to increase in proportion to the absolute temperature, as expected in the wholly amorphous state. The approximate melting temperature (using this as a criterion for melting) is indicated by the arrow on the upper curve in Figure 7.

Even with the limited precision available, it is clear that a substantial rise in melting temperature, of the order of 20°C., has been brought about by the increase in the imposed extension from 1.68 to 4.20. The present technique thus appears to afford a simple means of studying the effect of the degree of extension and the degree of crosslinking on the crystal melting temperature.

Results

The melting temperatures determined in this way are plotted against the imposed extension in Figures 8, 9, and 10 for vulcanizates A, B, and C, respectively. The observed melting temperatures were found to depend upon the crystallization temperature T_c ; relations are therefore shown for three different crystallization temperatures. The values at $\lambda = 1$ were

determined dilatometrically; they are seen to be in good agreement with those determined from the stress changes on melting.

The broken curves in Figures 8, 9, and 10 represent the temperature shifts ΔT required to superimpose the rate curves (Fig. 6). Their vertical positions in Figures 8, 9, and 10 are chosen arbitrarily.

The measured melting temperatures are seen to increase with extension in general agreement with the temperature shifts ΔT . There is some indication that the rise in melting temperature is greater when crystallization took place at low temperatures and also that it generally exceeds the ΔT value at high extensions. However, in view of the uncertainty in determining the melting temperatures the agreement is considered satisfactory.

It thus appears that the large changes in the rate of crystallization brought about by an extension are due mainly to corresponding changes in the melting temperature and hence degree of supercooling.¹⁵ The accelerating effect of a given extension is larger at higher temperatures (Fig. 4). This may now be attributed to the greater dependence of the rate of crystallization upon temperature at high temperatures (Fig. 2), so that a change in the melting temperature has a correspondingly greater effect.

Comparison of Theory with Experiment

Flory has derived a relation for the melting temperature $T_{m\lambda}$ of an oriented crystallite in a stretched network, in the form:¹²

$$T_{m_1}^{-1} - T_{m\lambda}^{-1} = (R/nh) \phi(\lambda) \quad (2)$$

where

$$\phi(\lambda) = (6n/\pi)^{1/2} \lambda - [(\lambda^2/2) + (1/\lambda)]$$

T_{m_1} is the melting temperature for the corresponding unstretched network, R is the gas constant, n is the number of equivalent freely jointed links per network chain, and h is the heat of fusion per mole of links. The product nh is thus the heat of fusion per mole of network chains, given by $h'M_c$ where h' is the heat of fusion per gram.

The right-hand side of eq. (2) has a finite value even at zero extension, $\lambda = 1$. This error arises from the assumptions that the crystallites are perfectly aligned, and that the molecules pass through them in the same sense as their end-to-end vectors. These assumptions are clearly inappropriate for unstretched networks. The values of $T_{m\lambda}$ given by eq. (2) at low extensions will be correspondingly inaccurate.

Values of M_c have been calculated for the present vulcanizates from their elastic behavior (Table II). Corresponding values of n have been obtained assuming the molecular weight of an equivalent random link to be 500, i.e., about 5.5 monomer units. The rise in melting temperature ΔT_m has then been calculated from eq. (2) by using these values for n and a value for h' of 22.7 cal./g., obtained by Maynard and Mochel⁹ from measurements of the melting temperatures of polymer-solvent mixtures. A similar value was obtained for the present materials by differential thermal

analysis, the measured heat of fusion being referred to the crystalline fraction determined from density measurements.

The values of ΔT_m obtained in this way are plotted against the extension ratio λ in Figure 6 as a broken curve for each vulcanizate. The calculated elevations in melting temperature are seen to correspond closely to the measured temperature shifts ΔT . (The temperature shifts have been employed for this quantitative comparison rather than the measured melting temperatures, because the latter are subject to greater uncertainty.) The agreement is satisfactory for all three vulcanizates at extension ratios of 3 and higher. At lower extensions the theoretical relations are less satisfactory, for the reasons given above. Krigbaum and Roe¹⁶ have shown that the crystallite orientation in a similar vulcanizate is virtually complete at extension ratios exceeding 2.5, in good accord with the range in which we find agreement between theory and experiment for vulcanizates having values of M_c ranging from 15,000 to 42,000.

The molecular weight of a random link has been taken as 500, i.e., about 5.5 monomer units, to yield this quantitative agreement. This value seems quite reasonable; it may be compared with the value of about 4.5 monomer units deduced for *cis*-polyisoprene from measurements of the elastic behavior of amorphous networks.¹⁷

Krigbaum and Roe¹⁶ proposed a different relation for the rise in melting temperature with extension, based on the change in free energy of the amorphous network. It differs considerably from that of Flory, predicting a sharper increase in melting temperature with extension at high extensions than at low ones. The present measurements are not of this form, and suggest that their relation is not applicable. Their derivation seems to be in error in assuming that the total strain energy is involved in the free energy of fusion.

DEPENDENCE OF $t_{1/2}$ UPON TEMPERATURE

If the rate-determining step in the crystallization process is the formation of crystal nuclei, the dependence of the half-time $t_{1/2}$ upon temperature takes the form¹⁸

$$\ln t_{1/2} = \text{constant} + f^*/kT_c \quad (3)$$

where k is Boltzmann's constant, T_c is the crystallization temperature, and f^* is the free energy of formation of a critical-size nucleus, given by

$$f^* = 32 \sigma_s^2 \sigma_e / h_v^2 [1 - (T/T_m)]^2 \quad (4)$$

where σ_s , σ_e are the crystal/amorphous interfacial energies for faces parallel and perpendicular to the chain axes, and h_v is the heat of fusion per unit volume. The same form of temperature dependence is retained if growth of the crystals occurs by a subnucleation mechanism requiring a similar (but somewhat smaller) free energy.¹⁹

In Figure 11 the reduced half-times are plotted against the appropriate temperature function given by eqs. (3) and (4), for vulcanizates A, B, and C in the unstretched state. The melting temperatures T_m were taken to be 80, 82, and 84°C., respectively. These values were chosen to give a reasonably linear relation. They are about 20°C. higher than the experimentally measured melting temperatures (Figs. 8, 9, and 10) but the latter are clearly underestimates of the equilibrium melting temperatures. The values employed here do not lead to an accurately linear relation, however, over the wide range of temperature and half-times considered. The results depart significantly from linearity, particularly at low temperatures, indicating that the crystallization does not follow this simple kinetic scheme.

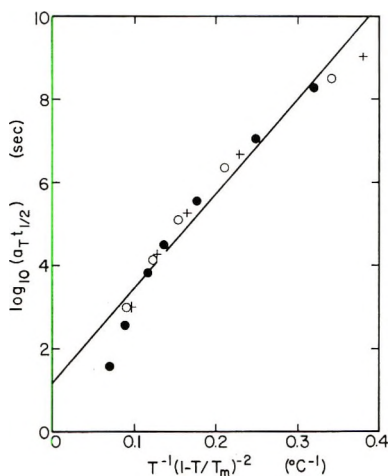


Fig. 11. Reduced half-times $t_{1/2}$ plotted against the temperature function $T^{-1}[1 - (T/T_m)]^{-2}$ for (O) vulcanizate A, (+) vulcanizate B, and vulcanizate C.

A possible cause for this discrepancy is the occurrence of a new crystal form at low temperatures. Differential thermal analysis of the melting of samples crystallized below room temperature revealed a small melting peak at about 25–30°C.

At higher temperatures, where the experimental results are approximately linear in this representation, the slope of the line in Figure 11 corresponds to a value of $\sigma_s^2\sigma_e/h_v^2$ of 2.3×10^{-16} erg. The same value is obtained when σ_s and σ_e are given the reasonable values of 4 and 25 erg/cm.², and h' the value of 22.7 cal./g. employed in the preceding section.

The master relation for the half-time of crystallization, reduced to a standard segmental mobility, is thus in fair accord with theories of nucleation kinetics. At the lowest temperatures crystallization occurs more rapidly than predicted, but this is probably associated with the appearance of a new crystal form.

CONCLUSIONS

The following conclusions are obtained.

(1) Changes in tensile stress afford a simple means of studying the rates of crystallization and the melting temperatures in crosslinked polymers subjected to simple extension.

(2) The form and magnitude of the stress changes in networks of *trans*-polychloroprene are closely similar to those observed for *cis*-1,4-polyisoprene and *cis*-1,4-polybutadiene networks. They are in accord with the formation of oriented crystallites and incompatible with folded chain crystallization at extensions as low as 15%. It seems likely that the present networks do not crystallize by chain folding even in the unstretched state.

(3) The large increases in rate of crystallization with extension are approximately accounted for by corresponding increases in the equilibrium melting temperature. Direct measurements of the melting temperature show similar rises with extension.

(4) The rise in melting temperature is in good agreement with Flory's theoretical treatment of oriented crystallization at extension ratios of 3 and higher (when the crystallite orientation is complete) for three networks having different degrees of crosslinking.

(5) When referred to a constant segmental mobility, namely, that obtaining at $T_g + 50^\circ\text{C}$., the rates of crystallization at various extensions obey a common dependence upon the degree of supercooling. This relation is in fair accord with theories of nucleation kinetics, except at the lowest temperatures where there is some indication of the appearance of a new crystal form.

This work was supported by a research grant from the International Institute of Synthetic Rubber Producers. The experimental assistance of L. Meyer, F. Shepherd, and R. Thames is gratefully acknowledged. The author is also indebted to Dr. P. D. Garn of The University of Akron for measurements of the heat of fusion by differential thermal analysis and for helpful comments.

References

1. Gent, A. N., in preparation.
2. Mullins, L., R. S. Rivlin, and S. M. Gumbrell, *Trans. Faraday Soc.*, **49**, 1495 (1953).
3. Treloar, L. R. G., *The Physics of Rubber Elasticity*, 2nd Ed., Clarendon, Oxford, 1958, p. 135.
4. Bekkedahl, N., and L. A. Wood, *Ind. Eng. Chem.*, **33**, 381 (1941).
5. Gent, A. N., *Trans. Inst. Rubber Ind.*, **30**, 139 (1954).
6. Avrami, M., *J. Chem. Phys.*, **7**, 1103 (1939); *ibid.*, **8**, 212 (1940); *ibid.*, **9**, 177 (1941).
7. Gornik, F., and L. Mandelkern, *J. Appl. Phys.*, **33**, 907 (1962).
8. Boyer, R. F., R. S. Spencer, and R. M. Wiley, *J. Polymer Sci.*, **1**, 249 (1946).
9. Maynard, J. T., and W. E. Mochel, *J. Polymer Sci.*, **13**, 235 (1954).
10. Gent, A. N., *Trans. Faraday Soc.*, **50**, 521 (1954).
11. Crespi, G., U. Flisi, and A. Arcozzi, *Chim. Ind. (Milan)*, **44**, 627 (1962).
12. Flory, P. J., *J. Chem. Phys.*, **15**, 397 (1947).

13. Williams, M. L., R. F. Landel, and J. D. Ferry, *J. Am. Chem. Soc.*, **77**, 3701 (1955).
14. Yin, T. P., and R. Pariser, *J. Appl. Polymer Sci.*, **7**, 667 (1963).
15. Bukhina, M. F., *Vysokomolekul. Soedin.*, **5**, 1725 (1963); *Rubber Chem. Technol.*, **37**, 404 (1964).
16. Krigbaum, W. R., and R. J. Roe, *J. Polymer Sci.*, **A2**, 4391 (1964).
17. Morris, M. C., *J. Appl. Polymer Sci.*, **8**, 545 (1964).
18. Mandelkern, L., *Crystallization of Polymers*, McGraw-Hill, New York, 1964, chap. 8.
19. Mandelkern, L., *Polymer*, **5**, 637 (1964).

Résumé

On décrit la mesure des vitesses de cristallisation du *trans*-polychloroprène non-ponté à plusieurs températures et de trois échantillons pontés dans une large gamme de température et d'extension. Les fortes augmentations de vitesse avec l'extension sont attribuées à des augmentations correspondantes de la température de fusion à l'équilibre et de ce fait du degré de surfusion. Cette augmentation de la température de fusion a été mesurée et (1) s'accorde d'une façon satisfaisante avec les modifications de vitesse observées, (2) est en bon accord avec le traitement de Flory relatif à la cristallisation orientée dans les réseaux étirés. La forme et l'ampleur des changements de la tension d'élongation s'accordent également avec la formation de cristallites orientés, et semblent incompatibles avec une cristallisation en chaînes repliées. Dans des conditions de mobilité segmentaire constante, il s'avère que les vitesses de cristallisation présentent une dépendance normale vis-à-vis du degré de surfusion. Cette relation est comparée aux prédictions de la théorie de la nucléation.

Zusammenfassung

Messungen der Kristallisationsgeschwindigkeit von unvernetztem *trans*-Polychloropren bei mehreren Temperaturen und von drei vernetzten Proben in einem weiten Dehnungs- und Temperaturbereich werden beschrieben. Die grosse Geschwindigkeitszunahme mit der Dehnung wird auf eine entsprechende Zunahme der Gleichgewichtsschmelztemperatur und damit des Unterkühlungsgrades zurückgeführt. Der Anstieg der Schmelztemperatur wurde gemessen und kann (1) die beobachtete Geschwindigkeitsänderung befriedigend erklären und steht (2) in guter Übereinstimmung mit der Behandlung der orientierten Kristallisation in gedehnten Netzwerken nach Flory. Auch Form und Grösse der Änderung der Zugspannung steht in Übereinstimmung mit der Bildung orientierter Kristallite und scheint mit einer Kristallisation in gefalteten Ketten unvereinbar zu sein. Bei Reduktion auf konstante Segmentbeweglichkeit befolgt die Kristallisationsgeschwindigkeit eine einheitliche Abhängigkeit vom Unterkühlungsgrad. Diese Beziehung wird mit den Aussagen der Keimbildungstheorie verglichen.

Received April 15, 1965

Revised May 25, 1965

Prod. No. 4774A

Effect of Some Additives on the Crystalline Transformations of Polybutene-1

I. D. RUBIN, *Texaco Research Center, Beacon, New York*

Synopsis

Differential thermal analysis (DTA) was used to study the effect of α -chloronaphthalene, diphenyl ether, glycerin, and carbon black on the solid-state transformation of form II to I and the high-temperature transition of form III to II of isotactic polybutene-1. α -Chloronaphthalene and diphenyl ether greatly accelerated the transition of II to I while glycerin and carbon black had no appreciable effect on it. The differences in the rates are attributed to variations in the ability of the additives to create defects which would aid in the nucleation and, possibly, growth of the new crystalline phase. The DTA thermogram of structure III crystallites normally shows two peaks. The addition of α -chloronaphthalene and diphenyl ether to structure III crystallites resulted in a DTA thermogram with only one peak. Glycerin and carbon black had no effect on the thermogram. These results are discussed in relation to a possible mechanism for the transformation.

INTRODUCTION

Isotactic polybutene-1 may exist in three distinct crystalline modifications.^{1,2} Cooling of the polymer from the melt results in the formation of the tetragonal modification II, which, on standing at room temperature, slowly transforms into the hexagonal form I. The kinetics of this transition as well as the physical properties of the two polymorphs have been investigated in some detail.^{1,3} It was recently found that structure II was metastable with respect to I at all temperatures below its melting point.⁴ Structure III crystallites, which have been tentatively assigned to the orthorhombic system,⁵ may be obtained most easily by precipitating the polymer from various solvents. In contrast to modifications I and II which have a single DTA (differential thermal analysis) endotherm in the vicinity of their melting points, this modification has two.^{6,7} Under certain conditions, an exothermic peak may be found between the two endotherms.⁷ It was shown that the endotherm appearing at the higher temperature was due to the melting of the tetragonal form; the other endotherm and the exotherm were ascribed to the effects of the transformation of III to II.⁷ Danusso et al. reported recently that on very slow cooling structure III crystallites may be converted directly to those of I.⁸ This reaction proceeds below the melting point of III and involves a solid-solid transformation. On raising the heating rate, however, III is con-

verted to II and not I;⁸ this seems to indicate that stable nuclei of I do not form readily at temperatures close to the melting point.

A fruitful way of examining solid-solid or solid-liquid phase transformations involves the study of the effect of additives on the transformation rates. Boor and Mitchell⁹ and Clampitt and Hughes⁶ reported on the effect of several additives on the rate of transformation of the bulk material from the tetragonal form to the hexagonal one while Holland and Miller indicated that amyl acetate increased the transition rate of single crystals.⁵ We have now extended this work to gain a better understanding of the major factors influencing this transition. The additives used in this study were: α -chloronaphthalene, diphenyl ether, glycerin, and carbon black. These compounds were chosen as representative of three different types of materials. The α -chloronaphthalene and diphenyl ether are solvents for the polymer, the glycerin is a nonsolvent, and the carbon black is an amorphous solid. No crystalline materials were included in the current study, since it has already been established that a number of them accelerate the solid-state transformation of II to I.⁹ In addition, we have also examined the effects of these additives on the high-temperature transition of form III to II using x-rays and DTA.

EXPERIMENTAL

The crystalline polybutene-1 was synthesized in heptane by use of a combination of diethylaluminum chloride and titanium trichloride as the catalyst. It was then extracted with diethyl ether. The DTA and the x-ray runs were made with polymer samples which had been dissolved in boiling toluene, filtered, and precipitated by adding methanol. DTA and x-ray diffraction data³ showed that only structure III crystallites were present in the material. The molecular weight of the polybutene-1, calculated from intrinsic viscosity in decalin at 115°C. by using Stivala's relationship,¹⁰ was found to be 1.65×10^6 . Its ash content was 0.01%.

The polymer-additive blends were prepared by thorough mixing of finely divided polybutene-1 with the desired amount of the additive. To improve the polymer-additive interaction, an alternative procedure was also tried with the α -chloronaphthalene. The polybutene-1 was heated at 60°C. with a large excess of the diluent, filtered, and partially dried at 45–50°C. under vacuum. Since the DTA results on the blends prepared in this manner were similar to those obtained on the samples made by simple mixing of the two components, they are not reported here. The diphenyl ether, m.p. 26–27°C., used in this work was obtained from Eastman Kodak; the reagent grade α -chloronaphthalene was from Fisher Scientific Co., and the C.P. grade glycerin, from J. T. Baker Co. All were used without further purification. The carbon black was a Columbian Carbon Co. product, grade L.C., 100/325 mesh.

The DTA thermograms of the samples were obtained on a differential thermal apparatus, model 12AC, manufactured by the Robert L. Stone Co.

Since this instrument had originally been designed for high-temperature work, it was modified somewhat to increase the accuracy of temperature readings below 400°C. and reduce fluctuations in the heating rate. The thermograms were recorded on a Leeds and Northrup Speedomax G recorder calibrated to give a full scale deflection at 20 μ v. The unit was equipped with Pt-Pt + 10% Rh thermocouples and Inconel specimen cups. α -Alumina was used as the reference material, and the heating rate was 2.5°C./min. The DTA cups were filled by pressing about 0.08 g. of sample tightly into them with the end of a glass rod.

The samples of crystallites of structure II were prepared from those of III by melting the samples in the DTA cups and gradually cooling them back to room temperature over a 2-hr. period. To follow the progress of the transition of II to I, the samples were aged at 24°C. for varying periods of time, and then run on the DTA machine. The fraction of polymer transformed at any given time was obtained by comparing the area of the endotherm associated with the melting of the tetragonal form to the area of this peak immediately after transformation of III to II.

The x-ray diffraction patterns of the powdered polymer samples and blends were obtained on a conventional diffractometer. For the experiments at the elevated temperatures, a heating block was placed directly underneath the sample holder; its temperature was controlled by means of a Variac transformer. A potentiometer with a thermocouple imbedded in the heating block was used to measure the temperature. To study the high temperature transformation of form III to II, the spectra of the samples were recorded repeatedly between 10 and 15° (2θ) while the temperature was being raised at 1.7°C./min. In addition, x-ray spectra were also obtained on the sample containing 10% α -chloronaphthalene while it was heated at 3.2°C./min.

RESULTS AND DISCUSSION

Transition of Form II to Form I

During transformation of crystallites of structure II of polybutene-1 to those of I the DTA peak associated with the melting of the hexagonal form increases with time at the expense of the melting endotherm of the metastable tetragonal structure.^{3,6} The time dependence of the areas under the peaks may be used to estimate the rate of transformation.⁴ It was found now that two of the additives studied, α -chloronaphthalene and diphenyl ether, greatly accelerate the process. Thus, for example, as shown in Table I, after 16 hr. at 24°C. only 5% of a sample of the pure polymer was transformed to the stable modification. In contrast, the sample containing 10% of α -chloronaphthalene was completely changed to the hexagonal polymorph. Similar results were obtained with diphenyl ether. After 1 hr., 10% of the polymer was transformed; after 16 hr., all of it.

Even though the additives drastically accelerated the transformation rate, their effect on the appearance of the thermograms consisted only of

TABLE I
Effect of Additives on Conversion of Polybutene-I from II to I at 24°C.

Additive	Polymer in mixture, wt.-%	Aging time, hr.	Peak location, °C.		Conver- sion, wt.-%
			Form II	Form I	
None	100	1	113	—	0
None	100	16	111	125	5
None	100	51	110	126	55
None	100	64	106	126	71
None	100	8 days	—	126	100
α -Chloronaphthalene	80	1	93	—	<25
α -Chloronaphthalene	80	16	—	121	100
α -Chloronaphthalene	90	1	102	—	0
α -Chloronaphthalene	90	3.5	100	120	47
α -Chloronaphthalene	90	116	—	121	100
Diphenyl ether	90	1	93	—	10
Diphenyl ether	90	16	—	121	100
Glycerin	90	1	111	—	0
Glycerin	90	17	111	123	~5
Glycerin	90	45	110	124	45
Glycerin	90	65	106	125	68
Glycerin	90	99	104	125	77
Glycerin	90	115	101	125	91
Carbon black	90	1	114	—	0
Carbon black	90	16	112	125	14
Carbon black	90	24	109	123	19
Carbon black	90	45	112	126	58
Carbon black	90	17 days	—	123	100

a slight broadening of the peaks accompanied by a simultaneous shift to lower temperatures. This displacement of the endotherms (Table I) was more pronounced in the peaks associated with the melting of the metastable modification.

In contrast to the results obtained when α -chloronaphthalene or diphenyl ether was mixed with the polybutene-1, the addition of 10% carbon black increased the rate only slightly while the addition of a similar amount of glycerin had almost no effect. Neither of these materials affected the appearance of the thermograms.

The large increase in the rate of the solid-state polymorphic transformation of the tetragonal to the hexagonal polybutene-1 on adding α -chloronaphthalene or diphenyl ether is due either to an acceleration in the rate of nucleation of the new phase or to a change in its crystal growth rate. The sigmoidal shape of the transformation curves of the pure polymer and the mixtures with carbon black and glycerin shown in Figure 1 are typical of solid-state reactions characterized by a slow nucleation process. The high initial transformation rate of the polybutene-1- α -chloronaphthalene blend, on the other hand, may be ascribed most reasonably to a fast formation of nuclei of the new phase. This interpretation of the results is in

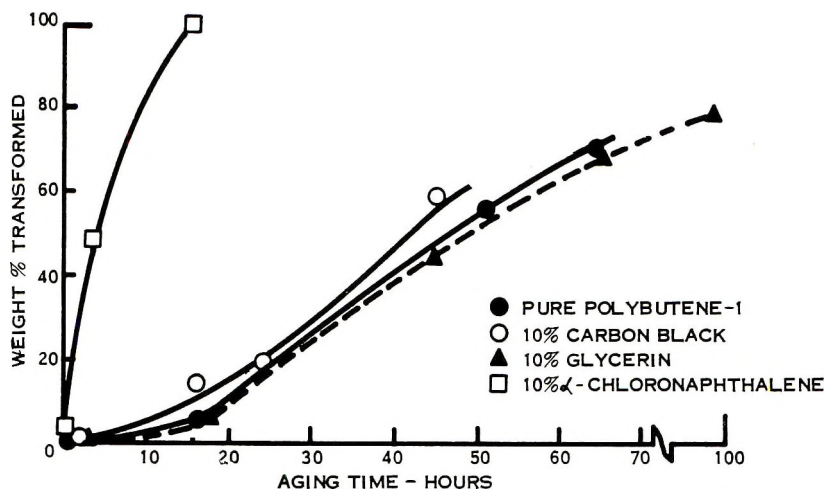


Fig. 1. Effect of carbon black, glycerin, and α -chloronaphthalene on rate of transformation of polybutene-1 from II to I at 24°C.

agreement with data obtained in a previous study. It was found, with a lower molecular weight sample of polybutene-1, that at 20 and 30°C. the reaction proceeded rapidly from the start, while at 45°C. it was characterized by a slow initial rate.⁴ A more rapid nucleation would be expected at the lower temperature.

Since nuclei are formed most readily at specific sites in the crystal lattice generally associated with grain boundaries and lattice defects, the rate of nucleation depends on the number of these sites. The presence of α -chloronaphthalene or diphenyl ether in polybutene-1 during the crystallization of structure II from the melt would be expected to result in smaller crystallites of II and increased grain boundary. This decrease in the perfection of the lattice of II and the resulting increase in the number of possible nucleation sites would thus enhance the nucleation of the stable modification I during the solid-state transformation of II to I. The possibility cannot be ignored, however, that the foreign materials may also contribute to an increase in the rate of growth of the nuclei by loosening the lattice of the tetragonal structure and thereby increasing the mobility of the chain units sufficiently to favor the formation of the hexagonal form. Without a doubt though, the mechanism involved in the increase of the transformation rate observed in this work is more complex than that suggested by Boor and Mitchell,⁹ who found that the reaction could be speeded up by incorporating in the polybutene-1 2-5% of isotactic polypropylene, high-density polyethylene, biphenyl, or stearic acid. They attributed the change in the rate to the presence of a foreign crystalline surface suitable for the development of the nuclei of the new phase. The work reported here shows that a foreign crystalline surface is not a prerequisite for the acceleration of the transition, even though it may be a contributing factor. As discussed previously and as pointed out by a number of investigators¹¹⁻¹³

who have studied predominantly inorganic systems, the significant factor in determining the rates of solid-state polymorphic transformations appears to be the degree of perfection of the lattice and, possibly, the nature and location of the defects. Foreign substances which have no effect on the number or type of the defects and imperfections associated with the formation of the new phase would play no role in changing the rate of polymorphic transformations. Since neither glycerin nor carbon black forms a one-phase system with the polymer melt, it is reasonable to assume that, by and large, these compounds are excluded from the immediate vicinity of the growing crystallites of II during their formation from the melt. They thus exert no appreciable influence on the size of the crystals and their perfection. This interpretation of the transformation rate differences among the polymer samples containing the various additives is reinforced by observations of Clampitt and Hughes,⁶ who reported that the addition of various amounts of aluminum oxide to the polymer did not alter the conversion rate and that thinner polybutene-1 films were converted at a faster rate than thicker ones. Boor and Mitchell⁹ found that, in accord with the postulated mechanism, the initial transformation rate of a sample which had been obtained by quenching the polymer melt at low temperatures was faster than that of a slowly cooled sample.³ Wilski and Grever, however, reported that the half-life of a quenched material was considerably longer than that of a slowly cooled one.¹⁴

High-Temperature Transition of Form III

As was mentioned in the introduction, the DTA thermogram of form III of polybutene-1 has two endothermic peaks in the vicinity of its melting point; in this work they appeared at about 97 and 115°C. Addition of 10% of carbon black had no appreciable effect on the shape of the thermogram or the location of the peaks; this is shown in Figure 2. Similar re-

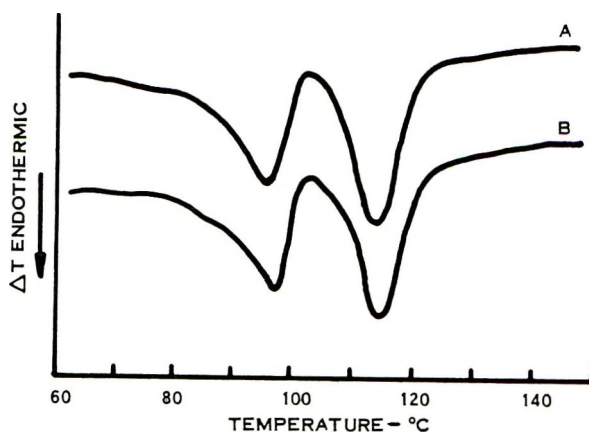


Fig. 2. DTA thermograms of polybutene-1 form III: (A) pure polymer; (B) blend with 10% carbon black.

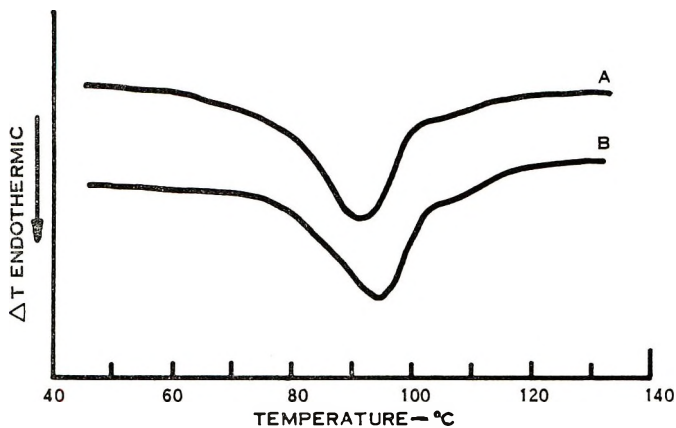


Fig. 3. Effect of solvents on DTA thermogram of polybutene-1 form III: (A) 10% α -chloronaphthalene; (B) 10% diphenyl ether.

sults were observed when the carbon black was replaced by glycerin. In contrast, thermograms of blends with α -chloronaphthalene or diphenyl ether had only one endotherm located at a lower temperature than either of the peaks of the pure polymer. Figure 3 shows typical thermograms of polybutene-1 incorporating, respectively, 10% α -chloronaphthalene and diphenyl ether. The DTA spectra of several of the samples from which the α -chloronaphthalene had been removed either by methanol washing or by evaporation under reduced pressure at 40–50°C. were identical to those of the original crystalline form III in Figure 2. X-ray diffraction data on the original blends yielding a one-peak DTA spectrum revealed that the polymer was in form III.

The disappearance of the melting peaks of form II in the samples incorporating the α -chloronaphthalene and the diphenyl ether could be due to either of two factors. If the tetragonal structure is formed, its melting peak could be depressed sufficiently to coincide with the peak associated with the disappearance of crystals of structure III; the two endotherms would thus be superimposed upon each other. Alternatively, it is conceivable that in the proximity of the polymer melting point, the addition of diluents may inhibit the transformation of III to II. To distinguish between the two possibilities, the samples were heated at a rate comparable to the rate of heating during the DTA measurements and their x-ray patterns were recorded. The results were the same as those of Geacintov et al.⁷ In each case the gradual reduction in height of the structure III peaks was accompanied by the simultaneous formation of the structure II peak, followed by a complete disappearance of all traces of crystallinity. It is therefore apparent that the presence of only one endotherm in the DTA traces is caused by a drastic decrease in the melting point of the crystals of the tetragonal form. The various processes involved in the transformation of III to II and the melting of II have thus been compressed into a narrower temperature interval.

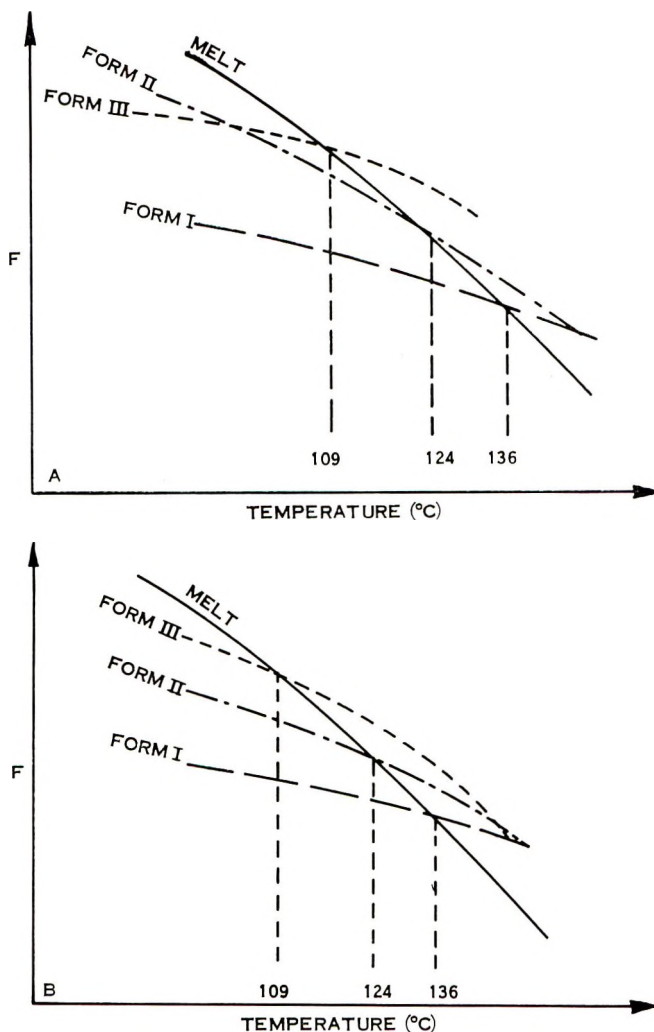


Fig. 4. Possible free energy-temperature relationships for the III to II phase transition of polybutene-1: (A) enantiotropic transformation; (B) monotropic transformation.

This shifting of the structure II peak to a lower value is in interesting contrast to the results of Holden,¹⁵ who studied the transformation in samples which had been annealed near their melting temperature. He observed that the exotherm ascribed to the crystallization of II from the melt and the melting endotherm of II were both delayed (raised to a higher value) by a shift of the lower endotherm to a higher temperature.

Even though the transformation of form III to II has been studied in some detail, the mechanism of the transition is still in doubt. Theoretically, two processes are possible. The conversion could be a direct

solid-solid transformation, or, alternatively, it could proceed through an intermediate molten phase. The peak appearing at the lower temperature could thus represent either a solid-state reaction or a melting process. The exotherm observed occasionally between the two endotherms could, conceivably, be due to additional crystallization from the melt. The formation of a melt was observed by Danusso et al.,⁸ who postulated that the reaction proceeded through an intermediate liquid phase. The various arguments for both types of mechanisms have been discussed at some length by Geacintov et al.⁷ To our knowledge, however, no attempts have been made to date to consider the effects of the relative stabilities of the two polymorphs on the possible validity of either argument.

Figures 4A and 4B represent schematically the two temperature-free energy relationships applicable to the transformation of III to II. At any given temperature the crystalline form with the lower free energy or higher free energy of fusion is the thermodynamically more stable one. Thus, in Figure 4A, representing an enantiotropic type of transition, structure III would be stable at temperatures below the equilibrium temperature while II would be stable in the interval between the equilibrium temperature and the melting point. In Figure 4B, depicting a monotropic type of dimorphism, structure III would be metastable with respect to II at all temperatures. No data are available at present to determine accurately the temperature dependence of the free energies of the two polymorphs; enough information is available, though, to distinguish tentatively between the possibilities represented in the two diagrams. Wilski and Grever¹⁴ determined by means of calorimetry that the heat of melting of the tetragonal form II was 975 cal./mole; they also estimated that the heat of melting of III was similar to that of the hexagonal form (1675 cal./mole). The free energy difference (ΔF) between the liquid and crystalline phases of a substance at a temperature T may be calculated from Hoffman's¹⁶ equation $\Delta F = \Delta H (T_m - T) T/T_m^2$, which takes into account the temperature dependence of the heat of melting (ΔH) and the entropy of melting (ΔS). Since at equilibrium between the two crystalline forms the free energy difference between structures III and II is equal to zero, the equilibrium temperature of the two polymorphs may be obtained from the expression

$$T_{eq} = T_{m2} T_{m3} (\Delta H_2 T_{m3} - \Delta H_3 T_{m2}) / (\Delta H_2 T_{m3}^2 - \Delta H_3 T_{m2}^2)$$

in which the subscripts refer to the two crystalline modifications. Using values of 109 and 124°C. for the melting points of modifications III and II, the equilibrium was established to be at about 91°C. This means that if the heat of melting of form III is reasonable, there should be a temperature region in which II is stable with respect to III. A smaller value for the heat of melting of III would shift the equilibrium to a lower temperature while a slightly higher one would compress the region of thermodynamic stability of the tetragonal structure; a considerably higher value would, on the other hand, lead to the monotropic type of transition pictured in

Figure 4*B*, in which form II would be stable with respect to III at all temperatures. The last alternative, however, appears to be an extremely unlikely one. Danusso and Gianotti's¹⁷ value for the heat of melting of structure III of 1550 ± 150 cal./mole agrees well with Wilski's estimate. Furthermore, structure III crystals are not known to transform to those of II at lower temperatures. One might expect such a transformation if Figure 4*B*, and not 4*A*, were the correct representation of the transition behavior.

During the high-temperature transformation of structure III to II, the incipient nucleation of modification II crystallites could precede the melting of III. Thus, incipient nuclei of II may form at defects in the solid, as suggested previously, even though unfavorable kinetic factors could hinder the completion of the transformation in the crystalline state. Once created, the nuclei could grow by addition of polymer from the molten phase as soon as it forms. A transition behavior of this type might resemble that of heptene-1, in which the metastable lower melting polymorph does not transform to the higher-melting material in the absence of the liquid phase.¹⁸ A transformation proceeding through the liquid phase would be expected to yield poorly formed and low-melting crystals of II in the presence of solvents such as α -chloronaphthalene and diphenyl ether. Materials such as glycerin and carbon black, on the other hand, would not be expected to affect the transition to any large extent. As shown in Table I, the addition of 10% phenyl ether to structure II crystallites of polybutene-1 resulted in a melting point depression of 20°C., while the addition of a similar amount of α -chloronaphthalene resulted in an 11°C. depression. Comparable depressions were obtained in the melting temperature of structure II crystallites formed from III (Figs. 2 and 3). On the other hand, the addition of the two solvents had only a minor effect on the location and appearance of the DTA peak of structure I crystallites formed during the solid-state transformation of II to I (Table I).

The postulated mechanism agrees with Danusso's suggestion that the transformation proceeds through a liquid phase. It also accounts satisfactorily for all of Holden's¹⁴ observations. Formation of more perfect crystals of form III on annealing might reduce the efficiency of nucleation of the new phase and the delayed melting would raise the temperature at which the new form could grow. Similarly, since nucleation from the pure melt is slow at elevated temperatures, it would explain why structure II is formed much more rapidly from III than from the liquid phase. The occasional appearance of a small exotherm following the initial endotherm may represent the tail end of the crystallization of II. The crystallization of the bulk of the material is obviously occurring at the same temperature interval as the melting of III, and the initial endotherm represents the heat difference between the melting of III and most of the formation of II. The rapid crystallization rate of II following the melting of III might preclude the observation of an increase in the amorphous content of the polymer by means of x-rays.⁷

References

1. Danusso, F., and G. Gianotti, *Makromol. Chem.*, **61**, 139 (1963).
2. Zannetti, R., P. Manaresi, and G. C. Buzzoni, *Chim. Ind. (Milan)*, **43**, 735 (1961).
3. Boor, J., Jr., and J. C. Mitchell, *J. Polymer Sci.*, **A1**, 59 (1963).
4. Rubin, I. D., *J. Polymer Sci.*, **B2**, 747 (1964).
5. Holland, V. F., and R. F. Miller, *J. Appl. Phys.*, **35**, 3241 (1964).
6. Clampitt, B. H., and R. H. Hughes, *J. Polymer Sci.*, **C6**, 43 (1964).
7. Geacintov, C., R. S. Schotland, and R. B. Miles, *J. Polymer Sci.*, **C6**, 197 (1964).
8. Danusso, F., G. Gianotti, and G. Polizzotti, *Makromol. Chem.*, **80**, 13 (1964).
9. Boor, J., Jr., and J. C. Mitchell, *J. Polymer Sci.*, **62**, S70 (1962).
10. Stivala, S. S., R. J. Valles, and D. W. Levi, *J. Appl. Polymer Sci.*, **7**, 97 (1963).
11. Hartshorne, N. H., G. S. Walters, and W. O. Williams, *J. Chem. Soc.*, **1935**, 1880.
12. Kotera, Y., and M. Yonemura, *Trans. Faraday Soc.*, **59**, 147 (1963).
13. Koshino, S., T. Oka, and T. Yoshida, *Ann. Rept. Radiation Center Osada Prefect*, **4**, 72 (1963); *Chem. Abstr.*, **61**, 6474h (1964).
14. Wilski, H., and T. Grewer, *J. Polymer Sci.*, **C6**, 33 (1964).
15. Holden, H. W., *J. Polymer Sci.*, **C6**, 209 (1964).
16. Hoffman, J. D., *J. Chem. Phys.*, **29**, 1192 (1958).
17. Danusso, F., and G. Gianotti, *Makromol. Chem.*, **61**, 139 (1963).
18. McCullough, J. P., H. L. Finke, M. E. Gross, J. F. Messerly, and G. Waddington, *J. Phys. Chem.*, **61**, 289 (1957).

Résumé

L'analyse thermique différentielle (DTA) a été employée pour étudier l'influence de l' α -chloronaphtalène, de l'éther phénylique, de la glycérine et du noir de carbone sur la transformation du polybutène-1 isotactique à l'état solide de la forme II à I et sur la transition à haute température de la forme III en II. L' α -chloronaphtalène et l'éther phénylique accélèrent la transition de II en I, tandis que la glycérine et le noir de carbone n'ont presque pas d'effet. On attribue ces différences de vitesse aux variations de l'appétitude des additifs à créer des défauts qui aident à la nucléation et qui peuvent favoriser la croissance d'une nouvelle phase cristalline. Les diagrammes obtenus pour les cristallites de structure III montrent normalement deux maxima. Quand on ajoute aux cristallites de structure III de l' α -chloronaphtalène et de l'éther phénylique le diagramme DTA ne montre plus qu'un maximum. La glycérine et le noir de carbone n'ont pas d'effet sur le thermogramme. Les résultats sont discutés en relation avec un mécanisme possible pour la transformation.

Zusammenfassung

Der Einfluss von α -Chlornaphthalin, Phenyläther, Glycerin und Russ auf die Umwandlung von Form II in I im festen Zustand und auf die Hochtemperaturumwandlung der Form III in II von isotaktischem Polybuten-1 wurde mittels Differentialthermoanalyse (DTA) untersucht. α -Chlornaphthalin und Phenyläther beschleunigten die Umwandlung von II in I stark, während Glycerin und Russ darauf keinen merklichen Einfluss haben. Die Geschwindigkeitsunterschiede werden der verschiedenen Fähigkeit der Zusatzstoffe zur Bildung von Defektstellen zugeschrieben, welche die Keimbildung und möglicherweise auch das Wachstum der neuen kristallinen Phase begünstigen. Das DTA-Thermogramm von Kristalliten der Struktur III zeigt normalerweise zwei Maxima. Der Zusatz von α -Chlornaphthalin und Phenyläther zu Kristalliten mit der Struktur III führt zu einem DTA-Thermogramm mit nur einem Maximum. Glycerin und Russ hatten keinen Einfluss auf das Thermogramm. Die Ergebnisse werden in Beziehung auf einen möglichen Umwandlungsmechanismus diskutiert.

Received March 17, 1965

Revised May 14, 1965

Prod. No. 4772A

Terpolymers of Ethylene and Propylene with *d*-Limonene and β -Pinene

RALPH W. MAGIN, C. S. MARVEL, and
EDWARD F. JOHNSON, *Department of Chemistry,*
University of Arizona, Tucson, Arizona

Synopsis

An experimental program was undertaken to produce a series of ethylene-propylene terpolymers containing either limonene (dipentene) or β -pinene from a variety of Ziegler-Natta type catalysts. All attempts to obtain a satisfactory vulcanizate from the limonene EPT and β -pinene EPT rubbers were unsuccessful.

INTRODUCTION

Ethylene-propylene terpolymers (EPT) have recently enjoyed a great deal of research activity due to their remarkable oxidation and ozone resistance and their desirable elastomeric properties.¹⁻⁴ The practical utilization of these materials has been hindered somewhat by the economic considerations involved in producing them and also the cost of the nonconjugated diene as the third monomer. In order to circumvent the latter problem, limonene and related monoterpenes obtained from citrus oils were chosen as suitable third monomers. Limonene and α - and β -pinenes have been previously homopolymerized by a number of catalysts.⁵⁻⁷ Obviously in the case of EPT rubbers, the Ziegler-Natta catalysts were the catalysts of choice.

Modena, Bates, and Marvel⁵ found that when optically active *d*-limonene was homopolymerized, the resulting polymer was optically inactive. Their work indicated that limonene polymerized into a bicyclic structure (I) as well as the desired structure II. The bicyclic structure was favored over the monocyclic structure by a factor of 1.5-2. In the case of a β -pinene, the expected structure (III) was obtained.

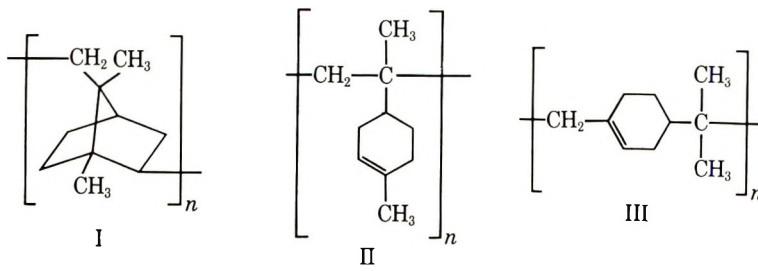


TABLE I

Run no.	Comonomer	Wt. of sample, g.	Catalyst system	Amt. polymer containing 1 mole-equiv. unsaturation, g.	Inherent viscosity on gel-free solution ^a	Propylene units, mole-%	Gel, wt-%
I-49	Dipentene	19.0	Al(<i>i</i> -Bu) ₃ -VOCl ₃ , 1:1	155	1.44	42.5	30.2
I-58	Dipentene	13.0	Al(<i>i</i> -Bu) ₃ -VOCl ₃ , 3:1	2720	1.68	42.8	22.6
I-62	Dipentene	7.2	Al(<i>i</i> -Bu) ₃ -VOCl ₃ , 4:1	574	2.08	46.3	26.8
I-66	Dipentene	22.5	Al(<i>i</i> -Bu) ₃ -TiCl ₄ , 1:1	561	0.957	57.2	12.5
I-69	Dipentene	18.0	Al(<i>i</i> -Bu) ₃ -TiCl ₄ , 3:1	579	0.854	35.2	31.5
I-71	Dipentene	11.1	Al(Et) ₃ -VOCl ₃ , 4:1	364	1.48	42.6	28.2
I-72	Dipentene	6.4	Al(Et) ₃ -VOCl ₃ , 3:1	467	1.38	33.0	30.2
I-73	Dipentene	17.3	Al(Et) ₃ -VOCl ₃ , 2:1	1260	1.39	40.8	19.2
I-74	Dipentene	6.1	Al(Et) ₃ -VOCl ₃ , 1:1	795	1.39	33.0	16.0
I-79	<i>d</i> -Limonene	9.0	Al(Et) ₃ -TiCl ₄ , 2:1	1530	0.837	37.5	37.5
II-23	β -Pinene	16.3	Al(<i>i</i> -Bu) ₃ -VOCl ₃ , 4:1	414	1.70	39.6	18.1
II-24	β -Pinene	17.1	Al(<i>i</i> -Bu) ₃ -VOCl ₃ , 3:1		1.50	45.0	
II-25	β -Pinene	25.4	Al(<i>i</i> -Bu) ₃ -VOCl ₃ , 2:1	4860	1.53	50.0	11.4
II-28	β -Pinene	7.2	Al(<i>i</i> -Bu) ₂ Cl-VOCl ₃ , 4:1	636	1.59	39.3	13.6

^a In benzene at 31°C.

RESULTS AND DISCUSSION

An experimental program was undertaken to evaluate a series of EPT elastomers from a variety of Ziegler-Natta type catalysts. The terpene monomers were introduced into the reaction vessel, containing catalyst and solvent, by vapor entrainment in the ethylene-propylene gas stream. This method was found superior to injecting the terpene into the reaction vessel by means of a hypodermic syringe.

The resulting polymers were purified in the usual manner and freeze-dried from a benzene solution. The purified product was analyzed for unsaturation by the method of Kolthoff, Lee, and Mairs^{8,9} and for methyl group content by infrared analysis.¹⁰ The intrinsic viscosity (0.4% solution in benzene) and gel content were also determined prior to vulcanization. (Gel content was determined by cyclohexane extraction at 23°C. over a 24-hr. period.)¹¹

The polymers sent for vulcanization are reported in Table I. All experimental conditions were kept constant except the types of catalysts employed and the ratio of aluminum alkyl to coordination compound.

The results of vulcanization tests gave highly undercured vulcanizates.* The poor results were attributed to high gel-content and acidic residues in the polymers. Samples I-49, I-58, I-66, I-69, and I-71 were examined by the testing laboratory for gel content, ash content, and spectrographic analysis on the ash residues. The results of these tests are reported in Table II. All attempts to obtain satisfactory vulcanizates on samples I-62, I-72, I-73, I-74, and I-79 were also unsuccessful. Analogous results were obtained with the β -pinene terpolymers, samples II-23, II-24, II-25 and II-28. In all cases, du Pont's Nordel EPT rubber was run as a control. The recipes employed in the vulcanization studies are reported in Table III.

Typical polymerization experiments performed in this study are reported in the experimental section. Where an insufficient amount of polymer was obtained for vulcanization studies, it is so noted. The following catalyst systems were examined: triethylaluminum with vanadium oxytrichloride, titanium tetrachloride, and titanium tetraiodide; triisobutylaluminum with vanadium oxytrichloride, and titanium tetrachloride and diisobutylaluminum chloride with vanadium oxytrichloride and vanadium triacetylacetonate.

It is difficult to explain why structures II and III (from limonene and β -pinene, respectively) which are those incorporated in the terpolymers do not lend themselves readily to vulcanization, even though adequate unsaturation is indicated by titration with perbenzoic acid.

* All vulcanization tests were performed at Battelle Memorial Institute Columbus, Ohio by Mr. Willia, J. Mueller under the supervision of Dr. P. B. Stickney, Chief Polymer Research.

TABLE II. Gel, Ash, and Spectrographic Analyses of Experimental Polymers

	Nordel 1040	I-66	I-71	I-58	I-49	I-69
Gel content, %						
A	—	7.0	10.3	28.5	24.9	47.8
B	—	7.1	19.2	30.2	21.1	43.3
C	—	8.3	3.9	27.3	19.3	43.3
Average	— ^a	7.5	11.1	28.7	21.8	44.8
Ash, %	0.03	0.02	0.08	0.10	0.08	0.06
Spectrographic analysis of ash, % as oxide						
Al	5-20	3-10	5-20	5-20	5-20	5-20
Ba	0.02-0.1	0.02-0.1	0.05-0.2	0.05-0.2	0.02-0.1	0.1-0.5
B	<0.01	0.02-0.1	0.05-0.2	0.02-0.1	0.01-0.05	<0.01
Si	5-20	3-10	5-20	5-20	5-20	5-20
Mn	0.05-0.2	0.1-1.0	0.1-1.0	0.05-0.2	0.05-0.2	0.1-1.0
Fe	1-5	20-40	20-40	20-40	20-40	20-40
Mg	1-5	0.5-2.0	1-5	1-5	1-5	1-5
Sr	0.1-0.5	0.1-0.5	0.1-0.5	0.2-1.0	0.1-0.5	0.1-0.5
Cr	0.3-1.0	0.1-0.5	0.1-0.5	0.02-0.1	0.1-0.5	1-5
Ni	2-10	0.1-1.0	0.1-1.0	0.1-1.0	0.5-2.0	0.1-1.0
Bi	<0.01	1-10	0.01-0.05	0.01-0.05	0.05-0.2	5-20
Ca	2-8	1-5	1-5	3-10	3-10	3-10
Mo	0.01-0.1	0.01-0.1	0.01-0.1	0.01-0.1	0.01-0.1	0.01-0.1
Na	0.5-2	0.1-1.0	0.1-1.0	0.1-1.0	1-5	0.1-1.0
Zn	<0.05	<0.05	<0.05	<0.05	0.1-1.0	<0.05
Ti	0.2-0.6	0.2-0.6	0.1-0.4	0.2-0.6	0.2-0.6	1-3
Ag	<0.05	<0.05	N ^b	N ^b	N ^b	N ^b
Co	<0.05	<0.05	N ^b	<0.05	N ^b	N ^b
Pb	0.01-0.1	0.05-2.0	0.01-0.1	0.01-0.1	0.1-0.5	0.01-0.1
Cu	0.5-2.0	0.1-0.5	0.1-0.5	1-3	2-6	1-3
V	1-5	0.1-0.5	<0.01	<0.01	1-5	0.01-0.1

^a Reported by manufacturer to be gel-free; ^b Not detected.

TABLE III
Vulcanization Recipes

	Samples I-49, I-58, I-66, I-69 and I-71		Samples I-62, I-72, I-73, I-74, I-79, II-23, II-24, II-25 and II-28	
	Unit	Batch	Unit	Batch
Polymer	100	5	100	2
FEF Black	50	2.5	100	2
Circosol 2XH	25	1.25	50	1
Zinc oxide	5	0.25	5	0.1
Stearic acid	1	0.05	1	0.02
Sulfur	1.5	0.075	1.5	0.03
2-Mercaptobenzothiazole (Captax)	0.5	0.025	0.5	0.01
Tetramethylthiuram mono- sulfide (Thionex)	1.5	0.075	1.5	0.03
	183.5	9.225	259.5	5.19

EXPERIMENTAL

Materials

Samples of chemical dipentene and *d*-limonene were furnished by Newport Industries Division of Heyden-Newport Chemical Corporation. The β -pinene was furnished by the Glidden Company. Unless otherwise noted, the monomers were used without further purification. Ethylene and propylene were Matheson C. P. grade and were used directly after passing through two towers of magnesium perchlorate. Heptane, Phillips 99 mole-%, was purified by extraction with sulfuric acid, dried over sodium sulfate, distilled from sodium hydride, and stored over sodium ribbons. Triethylaluminum, triisobutylaluminum, and diisobutylaluminum chloride (Texas Alkyls); vanadium oxytrichloride and vanadium triacetyl acetate (Alfa Inorganics, Inc.); titanium tetrachloride (Matheson, Coleman and Bell) were all used without further purification. Inherent viscosities were determined as a 0.4% benzene solution in a No. 50 Cannon-Fenske viscometer at 31°C.

Preparation of EPT Rubber

General Procedure. A 1-liter reaction flask equipped with efficient stirrer, condenser, and inlet tube was flame-dried under a vigorous stream of prepurified nitrogen. Apiezon grease N was used throughout the system. The solvent was introduced and saturated with an ethylene-propylene gas mixture. The source of third monomer was then connected into the system and the appropriate amounts of catalyst (dissolved in solvent) were introduced into the reaction flask by means of hypodermic syringes.

TABLE IV

Run No.	Catalyst				Component 2				Component 1				Comonomer				Pro-Ethylene				Results																			
	Type		Wt.,		Vol.,		Wt.,		Type		Vol.,		Wt.,		Type		Vol.,		Wt.,			Type		Vol.,		Wt.,		Type		Vol.,		Wt.,		Type		Vol.,		Wt.,		
	ml.	g.	mmole	Type	ml.	g.	mmole	Type	ml.	g.	mmole	Type	ml.	g.	mmole	Type	ml.	g.	mmole	Type		ml.	g.	mmole	Type	ml.	g.	mmole	Type	ml.	g.	mmole	Type	ml.	g.	mmole	Type	min.	ml.	hr.
I-49	Al(<i>i</i> -Bu) ₃	1.00	0.79	3.97	VOCl ₃	0.38	0.69	3.97	Dipentene ^a	10.0	8.45	62.1	1200	700	400	2.4	R.T.	See Table I																						
I-58	Al(<i>i</i> -Bu) ₃	1.57	1.19	6.00	VOCl ₃	0.19	0.35	2.00	Dipentene ^a	4.2	3.55	26.0	668	197	600	2.0	0	See Table I																						
I-62	Al(<i>i</i> -Bu) ₃	1.62	1.27	6.40	VOCl ₃	0.15	0.28	1.60	Dipentene ^a	12.0	10.1	74.5	1000	197	600	2.5	0	See Table I																						
I-66	Al(<i>i</i> -Bu) ₃	1.01	0.79	4.00	TiCl ₄	0.44	0.76	4.60	Dipentene ^a	44.0	34.6	254	1000	197	600	7.0	0	See Table I																						
I-69	Al(<i>i</i> -Bu) ₃	1.51	1.19	6.00	TiCl ₄	0.22	0.38	2.00	Dipentene ^a	13.8	10.8	79.6	1000	197	600	5.0	0	See Table I																						
I-71	Al(Et) ₃	0.88	0.73	6.40	VOCl ₃	0.15	0.28	1.60	Dipentene ^a	14.5	12.3	90.0	1000	197	600	4.25	0	See Table I																						
I-72	Al(Et) ₃	0.82	0.68	6.00	VOCl ₃	0.19	0.35	2.00	Dipentene ^a	26.3	22.2	163	1000	197	600	4.67	0	See Table I																						
I-73	Al(Et) ₃	0.73	0.61	5.33	VOCl ₃	0.25	0.46	2.67	Dipentene ^a	30.0	25.3	186	1000	197	600	5.25	0	See Table I																						
I-74	Al(Et) ₃	0.55	0.46	4.00	VOCl ₃	0.38	0.69	4.00	Dipentene ^a	29.6	25.0	184	1000	197	600	5.0	0	See Table I																						
I-79	Al(Et) ₃	0.73	0.61	5.33	TiCl ₄	0.29	0.51	2.67	<i>d</i> -Limonene	33.0	27.9	205	1000	197	600	4.5	0	See Table I																						
I-80	Al(Et) ₃	0.88	0.73	6.40	TiCl ₄	0.000	0.89	1.60	<i>d</i> -Limonene	33.3	28.0	206	1000	197	600	5.0	0	No polymer obtained																						
I-98	Al(Et) ₃	0.55	0.45	4.00	TiCl ₄	0.000	2.22	4.00	<i>d</i> -Limonene	20.8	17.5	129	1000	197	600	5.25	R.T.	No polymer obtained																						
II-10	Al(<i>i</i> -Bu) ₂ Cl	0.78	0.71	4.00	VTA ^b		1.39	4.00	Dipentene ^a	6.0	5.1	37.3	908	309	600	5.5	0	No polymer obtained																						
II-22	Al(<i>i</i> -Bu) ₂ Cl	1.24	1.13	6.40	VTA ^b		0.56	1.60	Dipentene ^a	24.9	21.0	1.55	908	309	600	5.75	R.T.	No polymer obtained																						
II-23	Al(<i>i</i> -Bu) ₃	1.62	1.27	6.40	VOCl ₃	0.15	0.28	1.60	β -Pinene	8.5	7.3	54	908	309	600	3.0	0	See Table I																						
II-24	Al(<i>i</i> -Bu) ₃	1.50	1.19	6.00	VOCl ₃	0.19	0.35	2.00	β -Pinene	12.0	10.3	76	908	309	600	3.3	0	See Table I																						
II-25	Al(<i>i</i> -Bu) ₃	1.34	1.06	5.33	VOCl ₃	0.25	0.46	2.67	β -Pinene	10.7	9.16	67.5	908	309	600	3.25	0	See Table I																						
II-28	Al(<i>i</i> -Bu) ₂ Cl	1.24	1.13	6.40	VOCl ₃	0.15	0.28	1.60	β -Pinene	10.3	8.95	65	908	309	600	3.25	0	See Table I																						

^a Batch no. BI-0329-07(b.p. 69.0-69.5/°C./20 mm.); ^b V triacetylacetonate; ^c Batch no. BJ-0144-08.

Immediately, the appropriate rates of flow of ethylene and propylene gases were begun and the reaction allowed to run, with vigorous stirring, for the noted period of time and at the stated temperature.

Upon completion of the reaction, 10% hydrochloric acid in methanol (200 ml.), containing a small amount of 2,6-di-*tert*-butyl-*p*-cresol (du Pont Antioxidant No. 29), was introduced, under a nitrogen atmosphere, to destroy the catalyst, and the resulting mixture was thoroughly mixed with excess methanol in a high speed Waring-Blendor. The resulting polymer was collected on a filter and purified by repeated precipitation in methanol from benzene. After five precipitations, the resulting polymer was lyophilized from a benzene solution (approximately 10% in polymer) containing about 0.1% du Pont Antioxidant No. 29. The various physical properties were determined on the dried polymer.

Reaction Parameters. Reaction parameters are listed in Table IV.

Analysis of Unsaturation

Preparation and Standardization of Sodium Thiosulfate Solution. In a dark bottle was placed 13.22 g. (0.09 equiv.) of reagent grade sodium thiosulfate and 900 ml. of freshly boiled distilled water. The resulting solution was allowed to stand at least 24 hr. prior to standardization. The sodium thiosulfate was standardized by titration of the iodine liberated from a solution containing an accurately weighed amount of potassium iodate (0.1–0.15 g., reagent grade, previously dried at $\sim 110^\circ\text{C}$. for 24 hr. and stored in a desiccator), 1 g. of potassium iodide, and 50 ml. of 0.4*M* acetic acid solution to a starch endpoint.

Calculation:

$$\text{Normality} = \frac{(\text{wt. of KIO}_3, \text{ g.}) (6000)}{(\text{m. wt. of KIO}_3) (\text{ml. of Na}_2\text{S}_2\text{O}_3)}$$

Indicator Solution. Approximately 2 ml. of a starch solution, prepared by dissolving 0.5 g. of water-soluble starch in 50 ml. of boiling water and was subsequently filtered and allowed to cool, was used for each titration.

Preparation of Perbenzoic Acid. In a 500-ml. Erlenmeyer flask were placed 5.2 g. (0.22 g.-at. wt.) of sodium and 125 ml. of anhydrous methanol. The resulting solution of sodium methylate was cooled to -15°C . in a salt-ice bath. A precooled solution of 50 g. (0.21 mole) of benzoyl peroxide in 200 ml. of chloroform was added at a moderate rate to the base with vigorous stirring. Upon complete addition of the peroxide, 150 ml. of water containing crushed ice was added to the reaction flask and the contents transferred to a 1-liter separatory funnel containing 350 ml. of water and crushed ice. The sodium perbenzoate was extracted into the aqueous layer and the aqueous layer washed twice with 100-ml. portions of carbon tetrachloride. The perbenzoic acid was liberated by the addition of 225 ml. of cold 1*N* sulfuric acid. The resulting peracid was extracted from the aqueous layer with three 100-ml. portions of benzene. The combined

benzene extracts were washed with two 50-ml. portions of water and dried over sodium sulfate.

Oxidation of Polymer Samples. To a benzene solution containing an accurately weighed amount of polymer (0.15–0.20 g.) was added a 10-ml. aliquot of the freshly prepared perbenzoic acid solution. The sample was then diluted to 100 ml. with benzene and stored in the dark.

Periodically, 25 ml. aliquots were transferred to a 250-ml. iodine flask containing 100 ml. of 0.4*M* acetic acid and 1 g. of potassium iodide. The resulting iodine was titrated to a starch endpoint with the standard sodium thiosulfate solution.

Calculation:

Grams of polymer containing one mole equivalent unsaturation

$$= \frac{(\text{wt. of polymer, g.}) (2000)}{(4) (\text{ml.}_{\text{blank}} - \text{ml.}_{\text{sample}}) (N \text{ of } \text{Na}_2\text{S}_2\text{O}_3)}$$

Determination of Gel Content

An accurately weighed amount of polymer (~0.2 g.) was placed in a 50 ml. ground glass-stoppered Erlenmeyer flask containing a 50-ml. aliquot of reagent benzene. The sample was placed in the dark for 48 hr., care being taken not to disturb the sample during this period. The sample was then decanted through a pair of 100-mesh screens, 0.5 in. apart, into a tared container, and the solvent was removed from the resulting filtrate. The difference in weight between the amount of sample originally taken for analysis and the amount recovered was taken as the insoluble gel portion.

Determination of Methyl Group Content in Polymer

Approximately 30–40 mg. of the polymer was placed between two pieces of aluminum foil (3 × 3 in.) in the center of a spacer consisting of three pieces of heavy aluminum broiling foil containing a 20 mm. diameter hole. The resulting sandwich was placed between two stainless steel blocks preheated in an oven to approximately 200°C. and the sample pressed under 5000 psi pressure for 30 sec. The resulting film was examined on an Infracord Model 137B recording infrared spectrophotometer.

Calculation:

$$\log (A_{8.7}/A_{13.9}) = 0.0286C_3 - 1.3730$$

where $A_{8.7}$ is the absorbance at 8.7 μ , $A_{13.9}$ is the absorbance at 13.99 μ , and C_3 is the mole per cent of C-CH₃ units in the polymer.

We are grateful to Dr. B. Rudner of the Heyden-Newport Chemical Corporation for generous supplies of chemical dipentene and *d*-limonene; to Dr. Carl Bordenca of the Glidden Company for a generous supply of β -pinene. We are indebted to Dr. P. B. Stickney and Mr. William J. Mueller of Battelle Memorial Institute for the vulcanization tests and results and for the gel, ash, and spectrographic analyses reported in Table II.

This is a partial report of work done under contract with the Utilization Research and Development Divisions, Agricultural Research Service, U.S. Department of Agriculture, and authorized by Research and Marketing Act. The contract was supervised by Dr. J. C. Cowan of the Northern Division.

References

1. Natta, G., paper presented at International Synthetic Rubber Symposium, London 1957.
2. Natta G., *Rubber Plastics Age*, **38**, 495 (1957).
3. *Rubber Plastics Age*, **40**, 437 (1959).
4. Wilbur, J. M., Jr., and C. S. Marvel, *J. Polymer Sci.*, **A2**, 4415 (1964).
5. Modena, M., R. B. Bates, and C. S. Marvel, *J. Polymer Sci.*, **A3**, 949 (1965).
6. Roberts, W. J., and A. R. Day, *J. Am. Chem. Soc.*, **72**, 1226 (1960).
7. Marvel, C. S., J. R. Hanley, Jr., and D. T. Longone, *J. Polymer Sci.*, **40**, 551 (1959).
8. Kolthoff, I. M., T. S. Lee, and M. A. Mairs, *J. Polymer Sci.*, **2**, 199 (1947).
9. Braun, G., *Org. Syn.*, **13**, 86.
10. Wei, P., *Anal. Chem.*, **33**, 215 (1961).
11. Black, A. L., *Ind. Eng. Chem.*, **39**, 1339 (1947).

Résumé

On a entrepris un travail expérimental pour préparer une série de terpolymères d'éthylène-propylène contenant du limonène (dipentène) ou du β -pinène, au moyen de divers catalyseurs du type Ziegler-Natta. Tous les essais en vue d'obtenir un produit vulcanisé satisfaisant en partant des caoutchocs de limonène EPT et de β -pinène EPT ont été vains.

Zusammenfassung

Ein Versuchsprogramm zur Herstellung einer Reihe von Äthylen-Propylenterpolymeren mit einem Gehalt an Limonen (Dipenten) oder β -Pinen wurde mit einer Vielfalt von Katalysatoren von Ziegler-Natta-Typ durchgeführt. Versuche zur Gewinnung eines brauchbaren Vulkanisates aus dem Limonen EPT- und β -Pinen EPT-Kautschuk blieben ohne Erfolg.

Received April 26, 1965

Prod. No. 4764A

Phase Separation of Some Acrylonitrile- Butadiene-Styrene Resins

B. D. GESNER, *Bell Telephone Laboratories, Incorporated, Murray Hill,
New Jersey*

Synopsis

One model and two commercial ABS (acrylonitrile-butadiene-styrene) resins have been separated into three polymeric phases: polybutadiene, styrene-acrylonitrile copolymer, and styrene-acrylonitrile copolymer grafted onto polybutadiene. A third commercial ABS resin has been separated into two polymeric phases: styrene-acrylonitrile copolymer and butadiene-acrylonitrile copolymer.

Davenport, Hubbard, and Pettit¹ have arbitrarily classified ABS gum plastics under two different types. Type A is a nitrile rubber-modified styrene-acrylonitrile resin, made by blending the two copolymers. Type B is a graft-modified styrene-acrylonitrile resin, produced by copolymerizing styrene and acrylonitrile in the presence of polybutadiene² or nitrile rubber.³

Manufacturers have been reluctant to divulge information concerning the method of preparation of ABS resins. The phase separation was undertaken to determine the possible processes required for synthesis, to show the relation between physical properties and phase content, and to enhance oxidation studies.

EXPERIMENTAL

Materials

Three commercial ABS resins (I, II, and III) were selected at random for phase separation (Table I).

The following known compounds were prepared for comparison with phases in the different ABS resins. Neutralized disproportionated rosin soap was smeared on a salt plate. Styrene-acrylonitrile copolymer was cast from acetone into a thin film. Butadiene-acrylonitrile copolymer and polybutadiene, coagulated from the latex, were cast from cyclohexane onto separate salt plates. The infrared spectra of these materials were recorded on a Beckman I.R. 8 spectrophotometer at a fast scan.

Phase Separation

Several solvents were tried for extracting the different phases from the ABS resins. The most satisfactory separations were obtained by using xylene, cyclohexane, and acetone in the order indicated in Figure 1 and outlined below for resin I.

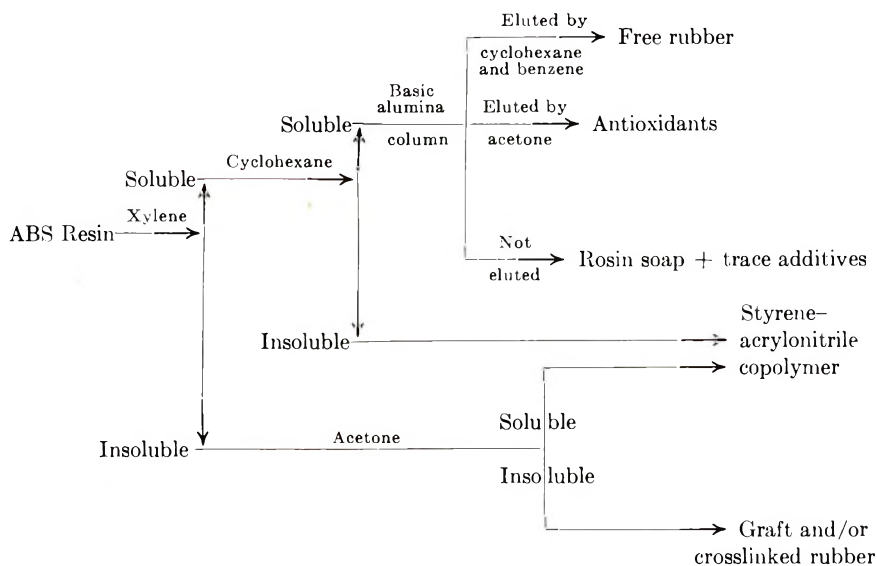


Fig. 1. Flow sheet for the phase separation of ABS resins.

Resin I was stirred in xylene at approximately 100°C. for 24 hr. After this treatment the solid residue was filtered away from the hot xylene solution and saved. The xylene extract was evaporated to dryness in the hood under nitrogen purge. The xylene-soluble residue was stirred in cyclohexane until the tacky material had dissolved. A white precipitate remained undissolved. This material was filtered away from the cyclohexane solution and cast from acetone into a thin film. The infrared spectrum of this material was identical to that of styrene-acrylonitrile copolymer. The clear cyclohexane solution, whose infrared spectrum indicated the presence of rosin and polybutadiene, was evaporated to dryness. The residue was weighed, redissolved in cyclohexane, and passed through a basic alumina column. The cyclohexane- and benzene-eluted materials, upon evaporation of the solvents, gave a material whose infrared spectrum was identical

TABLE I
Physical Properties of the Commercial ABS Resins

Properties	Resin I	Resin II	Resin III
Tensile strength (73°F.), lb./in. ²	6,500	7,000	6,000
Flexural modulus (73°F.), lb./in. ²	310,000	320,000	360,000
Rockwell hardness (R scale)	102	103	105
Impact strength, ft.-lb./in. notch			
73°F.	4.0	3.0	6.0
-40°F.	1.0	1.0	0.6

to that of polybutadiene. The material obtained in the acetone eluant (approximately 0.3% of the total weight of resin and reported in Table III together with rosin soap as additive) was characterized as an alkylated aryl phosphite. The remaining material on the basic alumina column was assumed to be all rosin and its weight was determined by difference.

The xylene-insoluble material was refluxed in acetone for approximately 1 hr. The bulk of the acetone-insoluble fraction was separated from the supernatant liquid by repeated decantation and suction filtration. Two 10-ml. aliquots of the light tan acetone solution were centrifuged at 30,000 rpm for 10 min. The supernatant liquid was removed and evaporated to dryness. The infrared spectrum of this material was identical to that of styrene-acrylonitrile copolymer. The average weight of acetone-insoluble material in the centrifuge tubes was 1.4 mg., corresponding to 0.17 g. in the total solution. This shows that the preliminary decantation and filtration is essentially quantitative in this case. The acetone-insoluble material was pressed into a film at 550 psi and 150°C. The infrared spectrum of this fraction indicated that it was a styrene-butadiene-acrylonitrile terpolymer.

The xylene-insoluble material from resin I was also treated with a 65:35 mixture of dimethylformamide and dimethyl sulfoxide. The soluble material in this solvent pair could also be dissolved in acetone. The infrared spectrum of this material was identical to that of styrene-acrylonitrile copolymer. Resin II was separated into its respective phases by the same technique described above for resin I.

In the cases of resins I and II, which were in the form of pellets, xylene treatment was necessary to digest these materials. Since resin III was already in the form of a fine powder, digestion was not necessary, and the xylene treatment was omitted. Resin III was first refluxed in cyclohexane, and the insoluble residue was stirred in cold acetone. A trace of yellow material and a small amount of a tacky substance were isolated in the cyclohexane extract. The yellow material, which was removed by extraction with cold cyclohexane, was not characterized. The remaining tacky material was smeared on a salt plate. Its infrared spectrum was identical with that of butadiene-acrylonitrile copolymer. The acetone-soluble material was identified as styrene-acrylonitrile copolymer by its infrared spectrum. The infrared spectrum of the acetone-insoluble material was identical with that of butadiene-acrylonitrile copolymer.

A model resin (IV) was prepared, according to the procedure of Daly,² firstly to determine the exact phase composition of a resin prepared by polymerizing the resin comonomers in a rubber latex and secondly to comparatively analyze the phase composition of a known resin-grafted rubber with that of commercial resins.

To a vigorously stirred alkaline solution of sodium persulfate and polybutadiene latex maintained at 60°C. were added a solution of styrene and acrylonitrile and at the same time an alkaline solution of disproportionated rosin soap. After the addition was complete the mixture was stirred at 60°C. for 12 hr. The resulting latex was coagulated with a mixture of formic

TABLE II
Weights of the Solvent-Extracted Phases in Some ABS Resins

ABS resin	Run	Cyclohexane		Acetone	
		Wt. soluble, g.	Wt. insoluble, g.	Wt. insoluble, g.	Wt. insoluble, g.
I	1	1.81	0.62	18.40	8.18
I	2	1.56	0.56	19.40	9.65
II	3	1.88	1.75	17.60	7.60
II	4	1.78	2.40	19.80	7.12
III	5	0.15	0.08 ^a	21.70	8.84
III	6	0.11	0.07 ^a	19.30	8.21
IV	7	2.04	0.02	3.05	4.85

^a Slightly soluble in cyclohexane.

TABLE III
Percentages of Solvent-Extracted Phases

ABS resin	Run	Additives, %	Free rubber, %	Styrene-acrylonitrile copolymer, %	Graft and/or crosslinked rubber, %
I	1	4.5	1.7	65.6	28.2
I	2	3.8	1.2	64.0	31.0
II	3	5.2	1.0	67.4	26.4
II	4	4.5	1.2	71.4	22.9
III	5	0.5	0.3	70.5	28.7
III	6	0.4	0.3	69.7	29.6
IV	7	4.2	16.3	30.7	48.8

TABLE IV
Percentage Composition of the Styrene-Acrylonitrile Phase of the ABS Resins

Phase origin	M_n^a	Acrylonitrile, %	Styrene, %
Resin I	121,400	29.7	70.3
Resin II	113,000	25.9	74.1
Resin III	—	28.4	71.6

^a Method of Shimura et al.⁵

acid, ethanol, and calcium chloride solution. The dried resin (IV) was separated in much the same manner as resins I and II.

Table II summarizes the weights of the phases found in each of the four ABS resins. Table III lists the percentages of each phase found in these ABS resins.

The percentages of acrylonitrile in the styrene-acrylonitrile copolymers listed in Table IV were calculated by using a variation of Scheddel's method.⁴ The graft phases from resins I and II, the whole of resin IV, and the nitrile rubber for resin III were analyzed for nitrogen. From these analyses the percentage acrylonitrile for each was calculated. The percentages of styrene and butadiene, as well, can be calculated, assuming that the

TABLE V
Nitrogen Analyses and Percentage Compositions of the Acetone-Insoluble Phases in the ABS Resins

Phase origin	N, %	Acrylonitrile, %	Butadiene, %	Styrene, %
Resin I	3.47	13.2	55.7	31.1
Resin II	3.06	11.6	55.2	33.2
Resin III	7.95	30.1	69.9	—

TABLE VI
Percentage Compositions of the ABS Resins

ABS resin	Additive, %	Acrylonitrile, %	Butadiene, %	Styrene, %
I	4.1	23.1	18.0	54.8
II	4.8	20.9	14.7	59.6
III	0.5	28.8	20.5	50.2
IV ^a	4.2	13.8	48.3	33.7

^a Calculated from the nitrogen analysis and the amount of butadiene used in its preparation.

ratio of styrene to acrylonitrile in the copolymer is the same as that in the graft. (To achieve compatibility of these two phases, such a circumstance is generally necessary.) These values are listed in Table V. From the percentage phase composition for each ABS resin and the monomeric composition of each phase, the total monomeric composition listed in Table VI was calculated.

DISCUSSION AND CONCLUSIONS

The xylene treatment at 100°C. for 24 hr. might appear harsh; however, when resin I was allowed to stand in acetone at ambient temperature for 30 days and then separated by centrifugation, 30.5% insoluble material (probably graft and free rubber) and 69.5% soluble material (the remaining styrene-acrylonitrile copolymer and additives) were isolated. With the xylene treatment these same values were 31.1 and 68.9%, respectively. The close check of these two procedures seems to indicate that the xylene treatment has not caused any great degree of degradation. More than likely, the alkylated aryl phosphite antioxidant is efficient enough to carry the resin through this step relatively free from oxidation.

Resins I, II, and IV contain random styrene-acrylonitrile copolymer, free polybutadiene rubber, and a gel phase composed of a complex cross-linked and styrene-acrylonitrile copolymer-grafted polybutadiene rubber (resins I and II are analogous to resin IV in the first two components and therefore must be analogous for this last component). Resin III contains random styrene-acrylonitrile copolymer and precrosslinked butadiene-acrylonitrile copolymer. The identity of each phase was made by direct comparison of known infrared spectra with those of the separated phases. The type polymer was determined by solubility behavior. The poly(bu-

tadiene-*co*-acrylonitrile) found in resin III must be considered precross-linked (with, for example divinylbenzene⁶) because the relative intensities of the butadiene infrared bands in this acetone-insoluble material and in the standard nitrile rubber indicates that unsaturation in the separated rubber had not been altered.

The possibility that free polystyrene is present in resins I, II, or IV is excluded, since this homopolymer was not detected in the xylene extracts of these resins. Likewise, no polystyrene was found in the acetone-insoluble fraction of resin III. Free polyacrylonitrile cannot be present in resins I, II, or IV, since the dimethylformamide-dimethyl sulfoxide-soluble materials from these resins were also soluble in acetone. If any free polyacrylonitrile were present in this fraction, it would be acetone-insoluble. Finally, resins I and II were free of nitrile rubber, and resins I, II, and III contained no SBR-type rubber.

Resin III belongs to the type A classification of ABS gum plastics. From the phase composition it is concluded that this material was prepared by blending together precrosslinked nitrile rubber and poly(styrene-*co*-acrylonitrile).⁴ The phase structure of this plastic tends to have an adverse effect on low-temperature impact strength (see Table I). With a glass transition temperature of -41°C ., nitrile rubber can offer little elasticity at low temperatures and under these conditions therefore is ineffective in providing a shock-absorbing character to the plastic.

Resins I and II are type B gum plastics. The presence of free polybutadiene in these resins is incidental and at best shows a deviation from maximum grafting efficiency. They must be prepared by polymerizing styrene and acrylonitrile in a polybutadiene latex.³ It is interesting to find two different resins (as regards source) with such close similarity in gross structure. The rubber content in the graft phase of both resins is nearly identical. The viscosity-average molecular weights of the poly(styrene-*co*-acrylonitrile) phases for both resins are the same within experimental error. The amount of free rubber and additives in both is approximately the same.

Resin II is characterized by a lower graft content and a lower acrylonitrile/styrene ratio than resin I. These two differences are felt in the physical properties of the resins. The tensile and modulus properties (Table I) are higher and the impact properties lower for resin II. This follows properly, since resin II contains the lower amount of graft. (The graft phase is essentially rubber that contains the necessary vehicle to hold it in the resin. The higher the rubber content the greater the impact and the lower the tensile properties will become.) Resin II has better molding characteristics than resin I. This is a direct effect of the styrene/acrylonitrile ratio. The higher the styrene content, the more moldable the material becomes (all other factors being equal). At the same time the chemical resistance should become lower. This may also effect the tensile properties but to a very small degree.

The separation has given an insight into the structures encountered in

ABS resins. An oxidation study of these structures is now under way which hopefully will indicate the areas most vulnerable to attack and methods for stabilizing the same.

The author would like to express his appreciation to F. H. Winslow for supplying key references to articles and patents pertaining to ABS resins, to Mrs. M. Y. Hellman for determining the viscosity-average molecular weights, and to W. L. Hawkins for helpful discussions and suggestions.

References

1. Davenport, N. E., Hubbard, L. W., and Pettit, M. R., *Brit. Plastics*, **32**, 549 (Dec. 1959).
2. Daly, L. E. (to United States Rubber Co.), U.S. Pat. 2,972,593 (Feb. 21, 1961).
3. Chohey, N. R., *Chem. Eng.*, **64**, 154 (1962).
4. Scheddel, R. T., *Anal. Chem.*, **30**, 1303 (1958).
5. Shimura, Y., Mita, I., and Kambe, H., *J. Polymer Sci.*, **B2**, 405 (1964).
6. Daly, L. E. (to United States Rubber Co.), U.S. Pat. 2,924,545 (Feb. 9, 1960).
7. Wiley, R. H., and G. M. Brauer, *J. Polymer Sci.*, **3**, 704 (1948).

Résumé

On a séparé un polymère-modèle et deux résines commerciales ABS en trois phases polymériques: la polybutadiène, le copolymère styrène-acrylonitrile et la copolymère styrène-acrylonitrile greffé sur le polybutadiène. Une troisième résine commerciale ABS a été séparée en deux phases polymériques: le copolymère styrène-acrylonitrile et le copolymère butadiène-acrylonitrile.

Zusammenfassung

Ein Modell- und zwei handelsübliche ABS-Harze wurden in 3 Polymerphasen zerlegt: Polybutadien, Styrolacrylnitrilkopolymeres und Styrolacrylnitrilkopolymeres auf Polybutadien aufgepfropft. Ein drittes handelsübliches ABS-Harz wurde in zwei Polymerphasen zerlegt: Styrol-Acrylnitrilkopolymeres und Butadien-Acrylnitrilkopolymeres.

Received January 29, 1965

Revised April 5, 1965

Prod. No. 4731A

Base-Catalyzed Polymerization of *p*-Styrenesulfonamides. II. *N*-Methyl and *N*-Phenyl Derivatives*

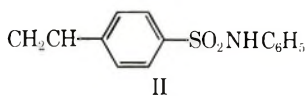
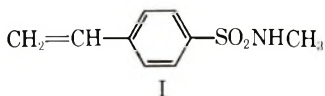
A. KONISHI,† N. YODA,‡ and C. S. MARVEL, *Department of Chemistry,
University of Arizona, Tucson, Arizona*

Synopsis

N-Methyl- and *N*-phenyl-*p*-styrenesulfonamides have been prepared, and they have been polymerized by basic and radical initiators. The polymers prepared by base catalysis contain units resulting from proton-transfer polymerization and units of the vinyl type. The ratio of the two recurring units has been established by determining the —NH— absorption in the infrared. The polymers are completely soluble in strong alkali, which shows that they contain substantial numbers (60–80%) of vinyl-type units, since a proton-transfer unit would not have an acidic sulfonamide group to produce solubility.

Recent work in this laboratory has established that *p*-styrenesulfonamide can be polymerized readily by basic initiators and has shown that this polymer is a copolymer with principally vinyl-type recurring units but probably with some units from proton-transfer polymerization² included. It was believed that investigation of *N*-substituted amides of this class would permit determination of the two types of recurring unit through their infrared spectra, and this has proved to be true.

N-Methyl (I) and *N*-phenyl-*p*-styrenesulfonamides (II) were synthesized



from styrenesulfonyl chloride. The phenyl derivative was also made from β -bromoethylbenzene by chlorosulfonation, conversion of this to the *N*-phenyl-sulfonamide and treatment with alcoholic potassium hydroxide by the general procedure used by Wiley and Ketterer³ to obtain *p*-styrene-

* For the first paper in this series see Yoda and Marvel.¹

† Postdoctoral Research Associate 1963–64, supported by Textile Fibers Department, E. I. du Pont de Nemours and Company. Present address: Kureha Chemical Industry Co., Ltd., Tokyo Laboratory, Shinjuku-ku, Tokyo, Japan.

‡ Postdoctoral Research Associate 1962–63, supported by Textile Fibers Department, E. I. du Pont de Nemours and Company. Present address: Toyo Rayon Company, Ltd., Basic Research Laboratory, Kamakura, Japan.

TABLE I
 Polymerizations of *N*-Methyl-*p*-styrenesulfonamide

Run no.	Monomer, g.	Solvent, ml. ^a	Catalyst, g. ^b	Inhibitor, mg. ^c	Temp., °C.	Time, hr.	Conversion, %	η_{inh}^d
PK-23	12.6	12.6	0.310	1.3	130	19	71.5	0.25
PK-24	12.5	6.3	0.203	1.3	130	19	75.5	0.31
PK-25	14.2	14.2	0.231	1.4	130	19	67.4	0.22
PK-26	23.5	5.9	0.191	2.4	130	19	78.6	0.44
PK-32	3.67	3.67	0.045	3.7	130	24	58.7	0.22
PK-34	3.59	3.59	0.015	3.6	Room	286	0.5	—
PK-35	3.64	3.64	0.015	3.6	130	24	64.9	0.22
PK-40	5.07	5.07 ^e	0.051 ^f	0.51 ^g	80	2	78.0	Insoluble
PK-41	4.79	4.79	0.508	0.48 ^h	80	67	55.5	1.58
PK-48	29.6	29.6	3.00	14.8	80	60	37.2	0.52
PK-50	31.1	31.1	3.16	20.0	80	68	46.0	0.70
PK-61	10.9	54.2 ^h	0.022 ⁱ	None	50	24	7.3	—
PK-65	8.53	8.53	0.173	None	—30	740	0.2	—
PK-66	14.5	14.5	0.243	None	Room	432	0.5	—
PK-67	14.5	14.5	0.243	None	—30	480	0.1	—

^a Dimethylformamide.

^b Lithium *tert*-butoxide.

^c *N*-Phenyl- β -naphthylamine.

^d 0.5% in dimethylformamide solution at 30°C.

^e Benzene.

^f Benzoyl peroxide.

^g Hydroquinone.

^h Ethyl alcohol.

ⁱ Azobisisobutyronitrile.

TABLE II
 Polymerizations of *N*-Phenyl-*p*-styrenesulfonamide

Run no.	Monomer, g.	Solvent, ml. ^a	Catalyst, g. ^b	Inhibitor, mg. ^c	Temp., °C.	Time, hr.	Conversion, %	η_{inh}^d
PK-2	2.00	20.0	None	0.02	130	24	None	—
PK-3	5.00	10.0	0.122 ^e	5.0	130	24	1.5	0.09
PK-4	5.00	10.0	0.087	5.0	130	24	7.3	0.34
PK-6	2.00	4.00	0.023	1.0	Room	144	Trace	—
PK-7	4.00	8.00	0.046	0.04	130	72	22.9	0.50
PK-8	2.00	4.00	None	0.02	130	72	10.0	0.08
PK-10	2.50	5.00	0.029	0.025	100	72	Trace	—
PK-12	5.00	2.50	0.057	0.05	130	72	22.0	0.40
PK-13	5.00	2.50	0.057	0.05	130	72	28.8	0.92
PK-14	5.00	2.50	None	0.05	130	72	81.6	Insoluble
PK-19	10.1	100 ^f	0.050 ^g	None	50	72	None	—
PK-20	12.4	12.4	0.305 ^h	1.2	130	72	14.7	0.12
PK-21	14.8	14.8	0.258	1.5	130	72	21.0	0.18
PK-22	14.5	14.5	0.260	1.4	130	71	13.0	0.07
PK-27	28.6	14.3	0.177	2.9	130	96	17.9	0.32
PK-39	30.4	30.4 ⁱ	0.304 ^h	None	80	138	0.5	—

^a Dimethylformamide.^b Lithium *tert*-butoxide.^c *N*-Phenyl- β -naphthylamine.^d 0.5% dimethylformamide solution at 30°C.^e Potassium *tert*-butoxide.^f Benzene.^g Azobisisobutyronitrile.^h Benzoyl peroxide.

sulfonamide. Both of these substituted sulfonamides proved to be quite unstable toward storage at room temperature in air. They seemed to form peroxides and polymerize spontaneously, and it was very difficult to get the monomers free of polymeric impurities. This had been noted to be true of *N,N*-dimethylsulfonamidostyrene in work reported by Inskeep and Deanin.⁴ This tendency for peroxidation was not noted in the case of the unsubstituted *p*-styrenesulfonamide. The infrared spectra of these monomers due to the sulfonamide portion resembled closely those reported for *p*-toluenesulfonamide and anilide.⁵

Polymerizations were usually carried out in dimethylformamide solution with lithium *tert*-butoxide or potassium *tert*-butoxide as the initiator. Some radical initiated polymerizations were also carried out. The results of the polymerization experiment are summarized in Tables I and II.

The solubility of the polymers in a variety of solvents is indicated in Table III.

TABLE III
Solubility Characteristics of the Polymers

Solvent	<i>N</i> -Methyl- <i>p</i> -styrenesulfonamide	<i>N</i> -Phenyl- <i>p</i> - styrenesulfonamide
Methyl alcohol	Insoluble	Insoluble
<i>n</i> -Hexane	Insoluble	Insoluble
Benzene	Insoluble	Insoluble
Chloroform	Insoluble	Insoluble
Acetone	Partly soluble	Soluble
Glacial acetic acid	Insoluble	Insoluble
Dimethylformamide	Soluble	Soluble
Water	Insoluble	Insoluble
10% HCl aqueous	Insoluble	Insoluble
10% NaOH aqueous	Soluble	Insoluble
5% NaOH aqueous	Partly soluble-soluble	Insoluble
1% NaOH aqueous	Insoluble	Insoluble
10% KOH aqueous	Soluble	Insoluble

Distinctive differences were observed between base-catalyzed and radical-polymerized polymers in their thermal behavior. The polymers obtained by radical polymerization showed a lower melting temperature than the base-catalyzed polymers, which did not melt nor did their color change below 300°C. The polymer has generally good thermal stability; for example, no apparent weight loss of poly-*N*-phenyl-*p*-styrenesulfonamide by heating was observed at 280°C. and 4% loss at 300°C. by thermogravimetric analysis (rate of temperature increase, 3°C./min. in dry air) as shown in Figure 1.

The polymer structures were studied by infrared spectroscopy and their characteristic absorptions were observed at 1160, 1300-1310 (S—O stretching), 1090 (S—N), 1590 (N—H deformation) and 3300 (N—H

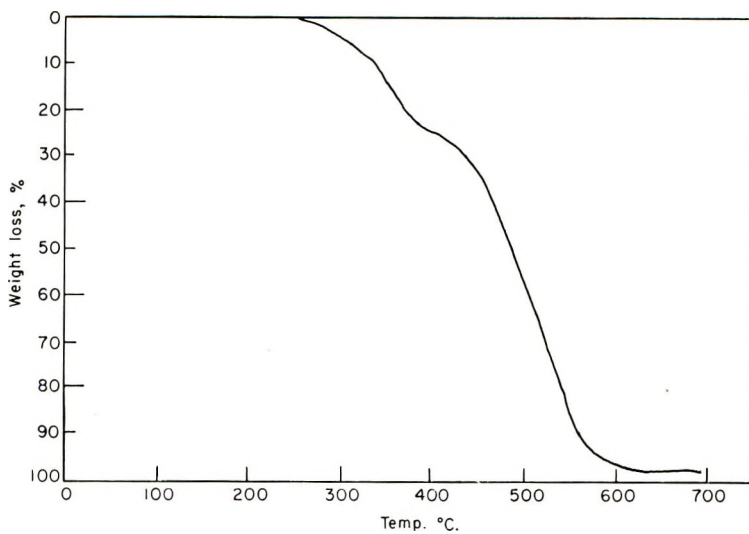


Fig. 1. Thermogravimetric analysis of poly-*N*-phenyl-*p*-styrenesulfonamide.

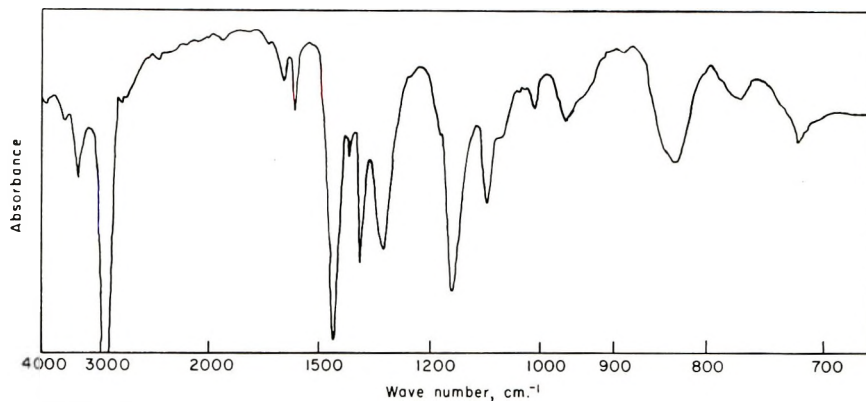


Fig. 2. Infrared spectrum of poly-*N*-methyl-*p*-styrenesulfonamide.

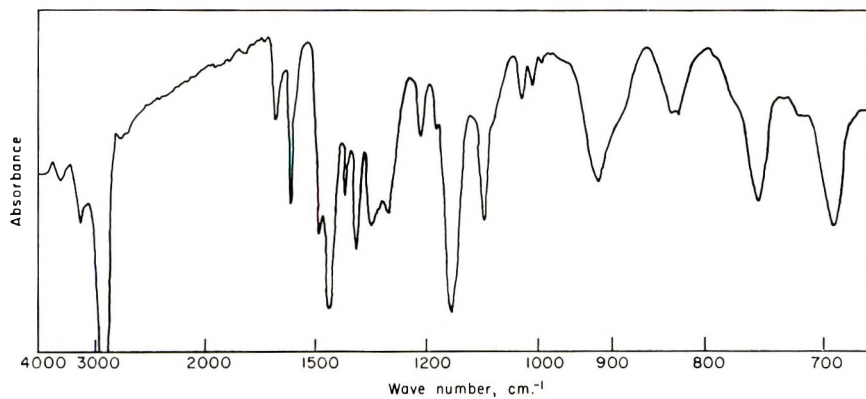


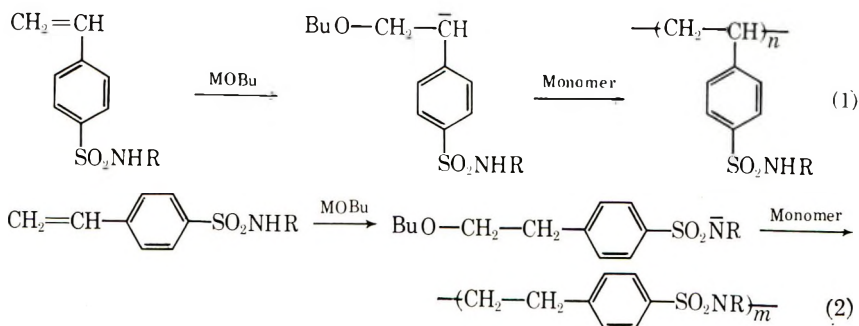
Fig. 3. Infrared spectrum of poly-*N*-phenyl-*p*-styrenesulfonamide.

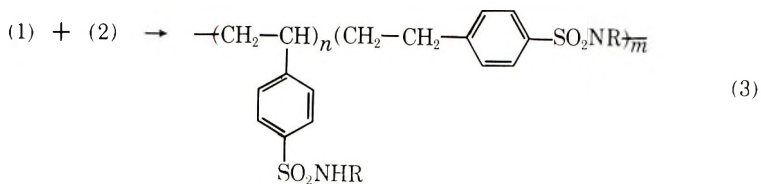
stretching) cm.^{-1} , as shown in Figures 2 and 3. Quantitative estimation of the structures was done on the basis that true proton-transfer polymerization of *N*-monosubstituted *p*-styrenesulfonamide does not produce the polymer which has absorption at $3100\text{--}3200\text{ cm.}^{-1}$ assigned to N-H stretching vibration (in dimethylformamide solution). *N*-Methyl-*p*-toluenesulfonamide, *p*-toluenesulfonanilide, and *N,N*-dimethyl-*p*-toluenesulfonamide were chosen as model compounds of the polyolefin structure (formed through vinyl polymerization) or the polysulfonamide structure (formed through proton-transfer polymerization), respectively. A dimethylformamide solution of the polymers was used for the measurements, and the results obtained are tabulated in Table IV.

TABLE IV
Quantitative Estimation of Polymer Structure

Sample no.	Polysulfonamide structure % proton transfer	Temperature of polymerization, °C.	Monomer used
PK-23	23.7	130	<i>N</i> -Methyl
PK-24	21.3	130	<i>N</i> -Methyl
PK-25	20.0	130	<i>N</i> -Methyl
PK-26	20.8	130	<i>N</i> -Methyl
PK-32	16.3	130	<i>N</i> -Methyl
PK-35	22.0	130	<i>N</i> -Methyl
PK-41	37.4	80	<i>N</i> -Methyl
PK-48	42.4	80	<i>N</i> -Methyl
PK-50	37.7	80	<i>N</i> -Methyl
PK-21	27.7	130	<i>N</i> -Phenyl
PK-22	18.3	130	<i>N</i> -Phenyl
PK-27	28.9	130	<i>N</i> -Phenyl

Although the data are scattered to some extent and the estimated amount of sulfonamide structure seems to be unexpectedly low, it is believed that the base-catalyzed polymerization of these monomers proceeds competitively through both vinyl (1) and proton-transfer polymerization (2), and the proton-transfer reaction is favored at lower temperatures.





In radical polymerization the sulfonamide structure is also formed to some extent, probably via transfer reaction, and such a tendency causes the formation of an insoluble three-dimensional polymer under vigorous conditions as seen in Tables I and II.

EXPERIMENTAL

Preparation of Monomers

***p*-Styrenesulfonyl Chloride.** The compound was prepared from sodium *p*-styrenesulfonate (E. I. du Pont de Nemours and Company) as reported before.¹

***N*-Methyl-*p*-Styrenesulfonamide.** To 93.2 g. of 40% aqueous methylamine solution (Eastman Organic Chemicals) was added dropwise a solution of 101 g. of *p*-styrenesulfonyl chloride in 583 g. of chloroform. The mixture was stirred frequently during the reaction under nitrogen atmosphere. The temperature of the mixture was held below 10°C. by external ice cooling during an interval of 70 min., and the reaction was continued for an additional 22 hr. at room temperature. The product solution was washed with water and sodium chloride solution successively, then neutralized by shaking with 10% hydrochloric acid and finally dried by anhydrous magnesium sulfate overnight. The solvent was removed under reduced pressure. The residual pale brown liquid weighed 71.6 g., or 72.5% of theoretical. The crude product was decolorized by active carbon, and reprecipitated from ethyl alcohol-isopropyl ether in an inert atmosphere to give the pale-yellow solid, m.p. 59–60°C., characteristic infrared absorption at 1160, 1320 (S—O), 1095 (S—N), 1600 (N—H deformation), and 3300 (N—H stretching) cm.⁻¹. The monomer was stored in a chloroform solution made slightly acidic by hydrogen chloride in a refrigerator in an inert atmosphere, and the solvent was removed immediately before the polymerization experiments were carried out.

ANAL. Calcd. for C₉H₁₁O₂NS: C, 54.89%; H, 5.62%; N, 7.10%; S, 16.25%. Found: C, 53.73%; H, 5.64%; N, 7.12%; S, 16.26%.

β -(*p*-Chlorosulfonylphenyl)ethyl Bromide. The material was prepared from β -phenylethyl bromide (Eastman Organic Chemicals) as reported before.⁴

β -(*p*-*N*-Phenylsulfonamidophenyl)ethyl Bromide. To a solution of 32.6 g. of aniline in 326 ml. of benzene was added a solution of 28.4 g. of β -(*p*-chlorosulfonylphenyl)ethyl bromide in 284 ml. of benzene over a period of

30 min. The temperature was held below 25°C. by external cooling. After another 2 hr. at reflux, the benzene solution was cooled, washed with water and 10% hydrochloric acid successively, and dried overnight with anhydrous magnesium sulfate. The solvent was removed under reduced pressure and the residual oil solidified upon standing in a refrigerator. It weighed 29.5 g. (86.8% of the theoretical). Recrystallizations from aqueous ethyl alcohol gave a colorless product melting at 78–79°C.

ANAL. Calcd. for $C_{13}H_{11}O_2NSBr$: C, 49.44%; H, 4.15%; N, 4.12%; S, 9.42%; Br, 23.49%. Found: C, 49.61%; H, 4.21%; N, 4.17%; S, 9.13%; Br, 23.25%.

***N*-Phenyl-*p*-styrenesulfonamide.** A solution of 34.4 g. of potassium hydroxide in 405 ml. of 95% ethyl alcohol was heated to 50°C. and a solution of 139 g. of β -(*p*-*N*-phenylsulfonamidophenyl)ethyl bromide in 369 ml. of 95% ethyl alcohol was added dropwise during an interval of 5 min.; the mixture was stirred frequently and allowed to stand for 15 min. The solution was diluted to one liter with water and neutralized with 10% hydrochloric acid. The brown liquid which separated was extracted by chloroform, and this solution was washed with water and dried overnight with anhydrous magnesium sulfate. The solvent was removed at reduced pressure, and the residual oil became solid upon standing in a refrigerator. It weighed 99.6 g. (93.8% of the theoretical). The crude product was decolorized by active carbon, and reprecipitation from aqueous ethyl alcohol gave the pale-yellow, viscous liquid, m.p. ca. –2 to 0°C., $n_D^{30} = 1.6063$. The monomer showed infrared absorption at 1160, 1335 (S–O), 1095 (S–N), 1610 (N–H deformation), and 3300 cm^{-1} (N–H stretching). An attempt to purify it by distillation or chromatography was unsuccessful. The monomer was also unstable in bulk and was handled as in the case of the *N*-methyl derivative.

ANAL. Calcd. for $C_{14}H_{13}O_2NS$: C, 64.87%; H, 5.05%; N, 5.40%; S, 12.30%. Found: C, 64.69%; H, 5.22%; N, 5.13%; S, 12.20%.

Another preparative method was also employed with the use of *p*-styrenesulfonyl chloride. A solution of 32.0 g. of *p*-styrenesulfonyl chloride in 131 g. of chloroform was reacted with 58.8 g. of aniline in one liter of benzene as in the case of the *N*-methyl derivative. It yielded 37.0 g. of product, and the reprecipitated product was found to be identical with the monomer prepared by the above method.

Polymerizations

In general, all glass-jointed glassware fitted with connecting tubes through Teflon sleeves were used as the polymerization apparatus. The monomer solution and inhibitor were charged and the solvent was removed at reduced pressure and the flask was filled with dry argon. Then, the solvent was charged into the flask; it was cooled to –75°C., evacuated, and then filled with argon. Finally the catalyst was added, and the flask again flushed with argon repeatedly as before. The mixture was shaken to

get good mixing and then allowed to stand. After the polymerization reaction, the contents were diluted with dimethylformamide and poured into a large excess of methyl alcohol. The precipitated polymer was filtered, washed with methyl alcohol successively, and dried *in vacuo* at room temperature. The solvent was dried by calcium hydride and distilled immediately before the polymerization.

Catalysts

The lithium *tert*-butoxide produced by the Lithium Corporation of America, Inc., and potassium *tert*-butoxide prepared by the conventional method were used in these experiments.

Infrared Spectra

The measurements were done by a Perkin-Elmer 137B Infracord. For quantitative estimation of the polymer structure, the spectra of 5–10% of polymer solutions were generally employed and compared with known absorbance of their model compounds with the use of sodium chloride liquid cells (0.095 mm. thickness) by the compensation method. *N*-Methyl-*p*-toluene-sulfonamide, *p*-toluenesulfonanilide, and *N,N*-dimethyl-*p*-toluenesulfonamide (Eastman Organic Chemicals) were used as model compounds, and the solvent was dimethylformamide.

Elemental Analysis

Some typical analytical figures for polymers from *N*-methyl-*p*-styrenesulfonamide ($C_9H_{11}O_2N_5$)_{*n*}, (samples PK-26 and PK-50) and for polymers from *N*-phenyl-*p*-styrenesulfonamide ($C_{14}H_{13}O_2NS$)_{*n*}, (samples PK-7, PK-8, PK-21, and PK-27) are given in Table V.

TABLE V
Elemental Analyses

Sample no.	Calculated				Found			
	C, %	H, %	N, %	S, %	C, %	H, %	N, %	S, %
PK-26	54.89	5.62	7.10	16.25	54.17	5.67	7.50	15.36
PK-50					53.82	5.70	7.07	16.08
PK-7	64.89	5.05	5.40	12.36	64.02	5.26	6.01	11.93
PK-8					63.40	5.39	6.89	11.35
PK-21					64.49	5.10	5.11	12.11
PK-27					64.72	5.40	5.62	12.11

The analysis was carried out by Micro-Tech Laboratories, Inc.

The authors are indebted to Dr. E. L. Wittbecker, Dr. E. B. Jones and Dr. R. L. Thornton of the E. I. du Pont de Nemours and Company for their helpful discussions and the thermogravimetric analyses. This project has been supported from funds supplied by the Textile Fibers Department of E. I. du Pont de Nemours and Company.

References

1. Yoda, N., and C. S. Marvel, *J. Polymer Sci.*, **A3**, 2229 (1965).
2. Breslow, D. S., G. E. Hulse, and A. S. Matlack, *J. Am. Chem. Soc.*, **79**, 3760 (1957).
3. Wiley, R. H., and C. C. Ketterer, *J. Am. Chem. Soc.*, **75**, 4519 (1953).
4. Inskeep, G. E., and R. Deanin, *J. Am. Chem. Soc.*, **69**, 2237 (1947).
5. Baxter, J. N., J. Cymerman-Craig, and J. B. Willis, *J. Chem. Soc.*, **1955**, 669.

Résumé

On a préparé et polymérisé au moyens d'initiateurs radicalaires et basiques des *N*-Méthyl et *N*-phényl *p*-styrène-sulfonamides. Les polymères préparés par catalyse basique contiennent des unités résultant d'un transfert protonique ainsi que des unités du type vinylique. On en a établi le rapport en mesurant l'absorption dans l'infra-rouge de la bande —NH—. Les polymères sont complètement solubles dans les bases fortes; ce qui prouve qu'ils contiennent un nombre important (60–80%) d'unités du type vinyle puisqu'une unité qui a subi le transfert protonique n'aurait plus de groupe sulfonamide pour rendre le polymère soluble.

Zusammenfassung

N-Methyl- und *N*-Phenyl-*p*-styrolsulfonamide wurden dargestellt und mit basischen und radikalischen Startern polymerisiert. Die durch Basenkatalyse dargestellten Polymeren enthalten sowohl Bausteine, die einer Protonenübertragungspolymerisation entsprechen als auch solchen vom Vinyltyp. Das Verhältnis dieser beiden Bausteine wurde durch Bestimmung der —NH—Absorption im Infraroten ermittelt. Die Polymeren sind in starkem Alkali vollständig löslich, was beweist, dass sie eine wesentliche Zahl (60–80%) an Bausteinen von Vinyltyp enthalten, da ein Baustein nach der Protonenübertragungspolymerisation keine Löslichkeit-erzeugende Sulfonamidgruppe besitzen würde.

Received March 30, 1965

Revised April 16, 1965

Prod. No. 4738A

Gas Permeability of Three Isomeric Polyhydroxyethers

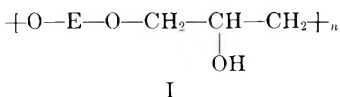
J. A. STENSTROM and W. F. HALE, *Union Carbide Corporation, Plastics Division, Research and Development Department, Bound Brook, New Jersey*

Synopsis

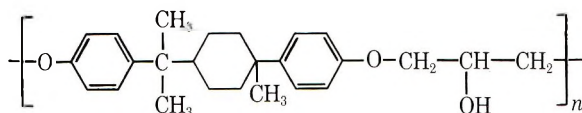
The gas permeation behavior of three isomeric polyhydroxyethers has been studied with the use of hydrogen, helium, oxygen, and carbon dioxide as the test gases. Amorphous polymers were prepared from epichlorohydrin and 1,8-, 2,8-, and 1,2-bis(4-hydroxyphenyl)menthane at equivalent molecular weight levels and therefore differed only in the position of substitution on the menthane unit. The permeabilities of the 1,8-, 2,8-, and 1,2-isomers were in the approximate ratio of 1:2:4 for each gas at 23°C. Also, this ratio was observed to hold from 23 to 80°C. for carbon dioxide. Since the diffusion constants were found to be in the same ratio, the gas solubilities were essentially identical for the three isomeric polymers. Therefore, the permeability data could be related directly to the steric configurations of the polymers and were consistent with the hypothesis that the permeation process is controlled primarily by the degree of chain packing. Activation energy data were interpreted as an indication that the diffusion mechanism is similar for each of the isomers. In addition, the relationship of permeability, density, and glass transition temperature to steric configuration of the isomeric polymers was discussed.

INTRODUCTION

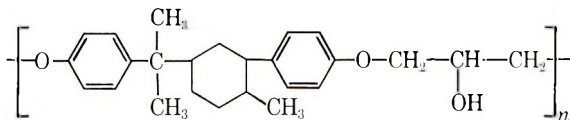
During the study of structure-property relationships for a series of high molecular weight polyhydroxyethers¹ derived from dihydric phenols and epichlorohydrin, the effect of variations in E in structure I on oxygen permeability and moisture vapor transmission was examined. It was observed that relatively minor changes in E



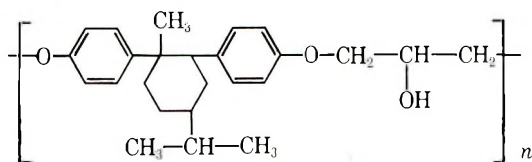
(the dihydric phenol moiety) had a considerable effect on the oxygen permeability of films. Recently, the availability² in these laboratories of three isomeric bis(4-hydroxyphenyl)menthanes provided an opportunity to study in detail the gas permeability characteristics of polymers which differ only in the positions of substitution on the menthane unit. The repeating units for the three polyhydroxyethers, which were prepared from 1,8-bis(4-hydroxyphenyl)menthane, 2,8-bis(4-hydroxyphenyl)menthane, and 1,2-bis(4-hydroxyphenyl)menthane, are shown on the following page, in structures II, III, and IV, respectively.



II



III



IV

Previous investigations of the relation of polymer structure to gas diffusion usually have involved rather important changes in molecular structure. For example, Michaels and Bixler³ have studied natural rubber, hydrogenated polybutadiene, branched and linear polyethylene as a series of analogs of polyethylene with varying crystalline content, and Willmott and Billmeyer⁴ have examined the water vapor diffusion rate for a series of linear aliphatic polyesters with different carbon chain lengths between ester groups. Generally, the physical condition (e.g., degree of crystallinity) and prior history of a polymeric film exerts such an overwhelming influence⁵⁻⁷ on gas diffusion and solubility that the effect of minor structural changes cannot be detected. However, in the present study the polyhydroxyethers were amorphous, and films were easily formed without orientation. Furthermore, the three polymers were readily prepared⁸ at essentially equivalent molecular weights with little or no difference in molecular weight distribution or branching.⁹ The structural similarity of the polymers (similar solubility parameters¹⁰) was expected to result in approximately equivalent gas solubilities and thus permit the direct correlation of steric configuration of the polymer chain, polymer properties, and permeability.

EXPERIMENTAL

Polymer Preparation and Properties

The structures of the dihydric phenols were established by nuclear magnetic resonance spectroscopy,² vapor phase chromatography, infrared spectroscopy, and comparison with known compounds. The known¹¹ reaction of dipentene dihydrochloride with phenol in the presence of aluminum chloride was employed to prepare 1,8-bis(4-hydroxyphenyl)men-

thane (m.p. 165–166.5°C., reported¹¹ 166°C.).* The experimental details of the structure proof² of the 1,2-isomer (m.p. 89–90°C.) and 2,8-isomer (m.p. 99–100°C.) will be reported separately. High molecular weight polyhydroxyethers were prepared in good yield by the direct reaction^{1,8,12} of epichlorohydrin with the diphenols. The properties of the polymers are summarized in Table I.

TABLE I
Polymer Properties

	1,8-Isomer	2,8-Isomer	1,2-Isomer
Reduced viscosity ^a	0.45	0.45	0.46
Tensile modulus, psi ^b	230,000	230,000	240,000
Tensile strength, psi ^b	7,100	9,500	8,100
Elongation at break, % ^b	10–15	10–30	5–15
Tensile impact, ft.-lb./in. ^{3c}	50–100	50–120	70
Carbon, % ^d	77.79	77.22	78.63
Hydrogen, % ^e	8.60	8.52	8.42

^a Tetrahydrofuran, 0.2 g./100 ml., at 25°C.

^b ASTM D882-61T.

^c ASTM D1822-61T.

^d Calculated, 78.91% C.

^e Calculated, 8.48% H.

Gas Permeation Studies

Three-mil films were compression molded at 180–190°C. from powdered polymers which had been dried 16 hours at 60°C. in a vacuum oven. The permeability characteristics of each of the polymers were measured by ASTM D-1434-63 at 23°C. with helium, hydrogen, oxygen and carbon dioxide as gas probes using standard Dow gas permeability cells. Several measurements were made at each set of conditions at various times and with different batches of isomers. It was assumed that Fick's laws of diffusion and Henry's solubility law were obeyed. The diffusion constants were calculated from test data by using the "time-lag" technique first described by Daynes¹³ and perfected by Barrer.¹⁴ Degassed samples supported on 250-mesh bronze screen were used for measurements of the diffusion constants. The permeability was measured from the steady-state, straight-line portion of the pressure versus time curve. The solubility was calculated from the quotient of the permeability and diffusion constant.

Measurements from 23 to 80°C. with carbon dioxide were made with a specially constructed sample holder in a thermostatically controlled oven. The Dow cell was kept at room temperature to act as the pressure sensor and thus the cell calibration was not affected by the test temperature. Only single measurements were made at the high temperatures, as considerable difficulty was experienced with stress-cracking of the samples under sealing pressures at the temperature and time periods required.

* Prepared by F. Apel and L. Conte of these laboratories.

Although the permeability of each gas can be measured with about the same degree of accuracy, the sensitivity and dimensions of the Dow cells are such that the diffusion constants and solubility can be determined with significantly greater accuracy for carbon dioxide than for the other gases. Numerically the data for oxygen solubility of each of the three isomers indicates a difference in solubility. However, the solubilities are so low that the differences probably reflect only the lack of precision in determining the diffusion constants for oxygen. The helium and hydrogen diffusion constants of these isomers were too high to be measured with any reasonable precision with the available equipment.

RESULTS AND DISCUSSION

Permeability Measurements

The room temperature permeability data are shown in Figure 1 and included in Table II. The following observations can be made from Figure 1. Each test gas ranks the isomeric polymers in the same order of increasing permeability, i.e., 1,8 < 2,8 < 1,2. The curves are essentially parallel on the semilogarithmic plot. The permeabilities are, therefore, in the approximately constant ratio of 1:2:4 for each gas for the 1,8-, 2,8-, and 1,2-isomers, respectively. The ratio of the permeabilities between gases is the same as that usually observed with rigid thermo-plastics.^{15a}

TABLE II
Permeability Characteristics of the Polyhydroxyethers at 23°C.

	1,8-Isomer	2,8-Isomer	1,2-Isomer
Permeability P , cc. (STP) mils/100 in. ² -24 hr.-atm.			
He	550	1010	1300
H ₂	365	830	1380
CO ₂	95	180	410
O ₂	20	45	80
Diffusion constant D , cm. ² /sec. $\times 10^{10}$			
CO ₂	15	30	75
O ₂	90	140	220
Solubility S , atm. ⁻¹			
CO ₂	8.5	8.0	7.5
O ₂	0.3	0.4	0.5

The solubility data for carbon dioxide given in Table II indicate that the solubility is about the same in each isomer. Considering that the solubility parameters of the three isomeric polymers are equivalent for all practical purposes, this behavior is intuitively reasonable. The solubility of oxygen follows a similar pattern, although the data are much less precise (see Experimental). Therefore, based on the reasonable assumption that the solubility of each gas is about the same in each of the isomers, either

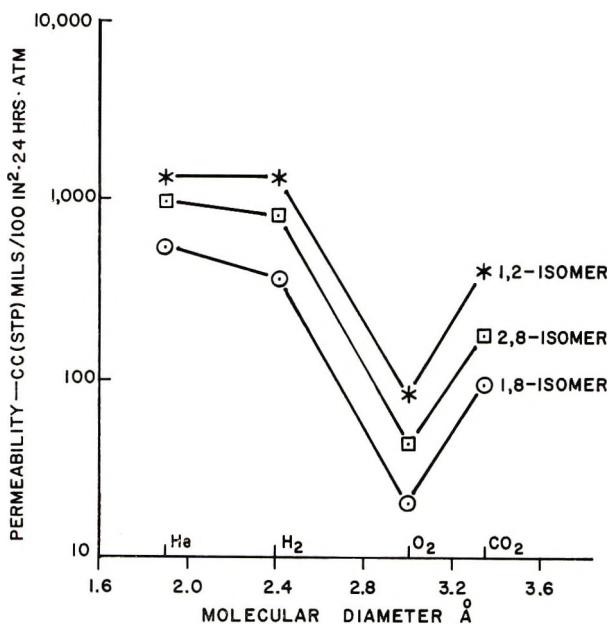


Fig. 1. Permeabilities of polyhydroxyether isomers at 23°C.

the permeability or the diffusion constant can be used as a direct measure of the rate of the diffusion process.

The parallelism recorded in Figure 1 indicates that there is no important change in the mechanism of diffusion with a variation in the size of the gas molecule from 1.9 to 3.3 Å. (He to CO₂) for all three polymers. The observed constant ratio of permeability and diffusion constant of 1:2:4 for the 1,8-, 2,8-, and 1,2-isomers can thus be related directly to the steric configuration of the polymers and the manner in which this will affect chain packing, flexibility and hole formation. A comparison of Dreiding models of the repeat units II, III, and IV, constructed so that the bulkiest groups are oriented equatorially on the cyclohexane ring, indicates that 1,8-isomer yields the most linear polymer chain and is relatively free of bulky side groups. The 1,2-substituted menthane produces a bent stereomodel (the angle is about 39° between chain segments connected through the 1,2 positions) with an isopropylcyclohexyl group forming a large, protruding side group. The 2,8-substituted menthane unit shows intermediate bending of the chain and some protrusion of the cyclohexyl group. Thus, the 1,8-polymer would be expected to have the closest packed chains, followed in order by the 2,8- and 1,2-polymers. Since bulky substituents attached to the main polymer chain would reduce the amount of freedom for intrachain rotation, the 1,8-isomer might be expected to permit the most rotation at room temperature, followed in turn by the 2,8- and 1,2-isomers. The 1,8-polymer should also be the most flexible, via rotation about in-chain bonds, with the other polymers in the same order as above.

These observations are consistent with the hypothesis that the diffusion process with the test gases is controlled by the tightness of chain packing and not by the degree of flexibility or freedom for intrachain rotation.

Activation Energies

Although the room temperature permeabilities and diffusion constants of the three isomers with a given gas are in the ratio 1:2:4, the possibility that a different ratio might be observed at elevated temperatures was briefly investigated with the use of carbon dioxide as the test gas. Carbon dioxide has a relatively low diffusion constant, and this results in a long

TABLE III
Energy Data for Carbon Dioxide Permeation

	1,8-Isomer	2,8-Isomer	1,2-Isomer
E_p , kcal./mole	6.2	4.1	4.7
E_D , kcal./mole	9.5	8.7	9.1
ΔH_s , kcal./mole	-3.2	-4.0	-3.7

time lag which can be measured with greater precision than can be obtained with the other test gases. The permeability, diffusion constant, and solubility data between room temperature and the respective glass transition temperatures of the polymers are well represented by standard Arrhenius-type plots. The permeability-reciprocal temperature curves are shown

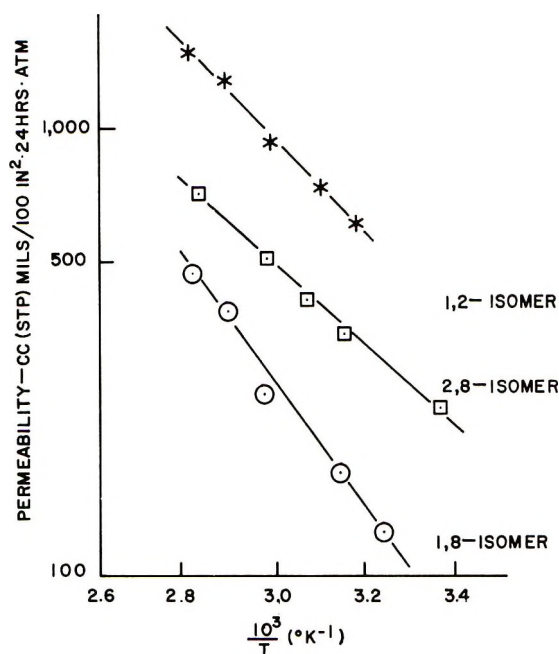


Fig. 2. Temperature dependence of isomer permeabilities.

in Figure 2, and the activation energies for carbon dioxide are listed in Table III. The magnitude of the activation energy for diffusion is the same as has been observed with other amorphous thermoplastics.^{15b} A negative value for ΔH_s is probably due¹⁶ to the heat of condensation of carbon dioxide, and thus the energy for the overall permeation process is less than the energy for diffusion according to eq. (1).

$$E_P = E_D + \Delta H_s \quad (1)$$

Based on the spacing and approximate parallelism of the lines in Figure 2, the 1:2:4 permeability ratio observed at room temperature also holds reasonably well at elevated temperatures. This observation plus the absence of significant differences in the various activation energies is interpreted as an indication that the diffusion mechanism for each isomeric polyhydroxyether is similar. The differences in chain configuration, which have been suggested as being responsible for the observed ratio, apparently are preserved over the temperature range investigated.

Density, Glass Transition Temperature, and Permeability

The relative permeabilities, densities and glass transition temperatures of the isomeric polymers are listed in Table IV. If, as suggested earlier, the differences in tightness of chain packing controls the relative permeability of the three polymers, it might be expected that polymer density would vary in the same manner as permeability. Although the general trend of density values in Table IV is in agreement with this suggestion, the correlation is not completely satisfactory. The expected lower value for the 1,2-isomer relative to the 2,8-isomer is not observed.

TABLE IV
Comparative Properties of the Polyhydroxyethers

	1,8-Isomer	2,8-Isomer	1,2-Isomer
Relative permeability	1	2	4
Density, g./cm. ³ ^a	1.129	1.106	1.106
Glass transition temperature, °C. ^b	135	150	160

^a Average of at least three determinations.

^b Determined by measuring resiliency as a function of temperature.¹

The stereochemical considerations presented previously in an interpretation of the relative permeability data also should influence the value of the glass transition temperature of the polymers. From examination of the Dreiding models and the data in Table IV, it is apparent that the glass transition increases with decreasing chain flexibility and increasing size of side groups on the polymer chain. It is suggested that the corresponding variations in gas diffusion rates and glass transition temperatures are caused, at least in part, by the same stereochemical factors. It should be pointed out that permeabilities were measured from 23 to 80°C., which is still considerably below the major glass transition temperatures given

in Table IV. In addition, several polyhydroxyethers have been found¹ to exhibit a minor or low temperature transition in the neighborhood of -70°C . The high impact strength at room temperature of the subject polymers indicates^{1,17} that minor glass transitions might be detected at low temperatures. No attempt has been made, however, to establish the presence of such minor transitions. A correlation between room temperature diffusion rates and glass transitions above room temperature, similar to that observed here, has been suggested by Boyer.¹⁸

References

1. Reinking, N. H., A. E. Barnabeo, and W. F. Hale, *J. Appl. Polymer Sci.*, **7**, 2135, 2145, 2153 (1963).
2. Beach, W. F., unpublished work.
3. Michaels, A. S., and H. J. Bixler, *J. Polymer Sci.*, **50**, 413 (1961).
4. Willmott, P. W. T., and F. W. Billmeyer, Jr., *Offic. Dig. Federation Soc. Paint Technol.*, **35**, 847 (1963).
5. Roberts, R. W., and K. Kammermeyer, *J. Appl. Polymer Sci.*, **7**, 2175, 2183 (1963).
6. Bixler, H. J., A. S. Michaels, and M. Salame, *J. Polymer Sci.*, **A1**, 895 (1963).
7. Michaels, A. S., H. J. Bixler, and H. L. Fein, *J. Appl. Phys.*, **35**, 3165 (1964).
8. Reinking, N. H., A. E. Barnabeo, and W. F. Hale, in *Polyethers*, Part II, N. G. Gaylord, ed., High Polymers Series, Vol. 13, Interscience, New York, in press.
9. Meyers, G. E., and J. R. Dagon, *J. Polymer Sci.*, **A2**, 2631 (1964).
10. Hildebrand, J. H., and R. L. Scott, *The Solubility of Nonelectrolytes*, 3rd Ed. Reinhold, New York, 1950, Chap. 20.
11. Zinke, A., H. Honel, O. Benndorf, R. Dreuny, and E. Ziegler, *J. Prakt. Chem.*, **156**, 97 (1940).
12. Union Carbide Corporation, Indian Pat. 78,758 (October 6, 1961).
13. Daynes, H. A., *Proc. Roy. Soc. (London)*, **A97**, 286 (1920).
14. Barrer, R. M., *Trans. Faraday Soc.*, **35**, 628 (1939).
15. Rogers, C. E., *Engineering Design for Plastics*, E. Baier, ed., Reinhold, New York, 1964, (a) pp. 682, 683; (b) p. 647.
16. Stannett, V., and H. Yasuda, *Crystalline Olefin Polymers*, Part II, R. A. V. Raff and K. W. Doak, eds., High Polymers Series, Vol. 20, Interscience, New York, 1964, p. 138.
17. Nielsen, L. E., *Mechanical Properties of Polymers*, Reinhold, New York, 1962, p. 180.
18. Boyer, R. F., *Rubber Chem. Technol.*, **36**, 1389, 1390 (1963).

Résumé

Le comportement du point de vue de la perméabilité gazeuse de trois polyhydroxy-éthers isomères a été étudié dans le cas de l'hydrogène, l'hélium, l'oxygène et l'anhydride carbonique comme gaz d'essais. Des polymères amorphes ont été préparés au départ d'épichlorhydrine et de 1,8-, 2,8-, et 1,2-bis(4-hydroxyphényl)menthane à des poids moléculaires équivalents; ils différaient dès lors uniquement par la position des substituants dans le groupe menthane. Les perméabilités des isomères 1,8-, 2,8- et 1,2 étaient dans un rapport de 1:2:4 pour chaque gaz à 23°C . Ce rapport se maintenait de 23 à 80°C pour le CO_2 . Comme les constantes de diffusion étaient dans le même rapport, les solubilités des gaz étaient essentiellement identiques pour les trois polymères isomères. Les résultats de perméabilité peuvent donc être directement reliés aux configurations stériques des polymères et s'accordent avec l'hypothèse que le processus est contrôlé avant tout par le degré d'entassement des chaînes. Les données d'énergie d'activation

indiquaient un mécanisme de diffusion semblable pour chacun des isomères. En outre on a discuté la relation entre la perméabilité, la densité et la température de transition vitreuse et la configuration stérique des polymères isomères.

Zusammenfassung

Das Gaspermeationsverhalten von drei isomeren Polyhydroxyäthern wurde mit Wasserstoff, Helium, Sauerstoff und Kohlendioxyd als Testgas untersucht. Amorphe Polymere wurden aus Epichlorhydrin und 1,8-, 2,8-, sowie 1,2-Bis(4-hydroxyphenyl)menthan mit etwa gleichem Molekulargewicht und daher nur durch die Stellung der Substituenten am Menthanbaustein unterschieden, dargestellt. Die Permeabilität der 1,8-, 2,8- und 1,2-Isomeren stand für jedes Gas bei 23°C etwa im Verhältnis von 1:2:4. Für Kohlendioxyd erwies sich dieses Verhältnis auch von 23 bis 80°C als gültig. Da die Diffusionskonstanten im gleichen Verhältnis standen, war die Gaslöslichkeit für die drei isomeren Polymeren im wesentlichen identisch. Die Permeabilitätsdaten können daher direkt zur räumlichen Konfiguration der Polymeren in Beziehung gesetzt werden und erweisen sich als konsistent mit der Annahme, dass der Permeationsprozess primär durch den Packungsgrad der Ketten bestimmt ist. Die Werte für die Aktivierungsenergie standen ebenfalls mit der Annahme in Übereinstimmung, dass der Diffusionsmechanismus für die Isomeren ähnlich ist. Schliesslich wurde die Beziehung der Permeabilität, der Dichte und der Glasumwandlungstemperatur zur räumlichen Konfiguration der isomeren Polymeren diskutiert.

Received March 30, 1965

Revised May 6, 1965

Prod. No. 4754A

Dilute Solution Properties of High Molecular Weight Poly(isobutyl Methacrylate). II. Light Scattering

RICHARD J. VALLES, *Polymer Research Branch, Picatinny Arsenal, Dover, New Jersey*

Synopsis

A high molecular weight linear sample of poly(isobutyl methacrylate) was fractionated from an acetone-methanol mixture. An adaptation on a Brice-Phoenix photometer made it possible to run light-scattering measurements at angles of 15, 20, and 25°, in addition to the usual angles. The addition of the low angles made the angular extrapolations more accurate. The parameters in the Mark-Houwink equation are reported at several temperatures. The molecular weight range studied was 3×10^6 to 11×10^6 .

INTRODUCTION

Earlier papers from this laboratory have reported the dilute solution properties of a series of the alkyl methacrylates. In this paper we have attempted to obtain the molecular weight and chain dimensions of a high molecular weight methacrylate polymer. To do this successfully, we needed to take measurements at lower angles. In addition to the usual angles, angles of 15, 20, and 25° were measured by use of a Brice-Phoenix light-scattering photometer. These additional low angles made the angular extrapolations very small and have added confidence to the results.

EXPERIMENTAL

Fractionation

The high molecular weight, linear form of poly(isobutyl methacrylate) furnished by Edgewood Arsenal, Maryland, was fractionated using acetone as the solvent and methanol as the nonsolvent. A three-stage fractionation was used, the polymer being successively precipitated from 3, 2, and 0.3% solutions. The fractions were then purified by the frozen-benzene technique.

Viscosity

The viscosity of the polymer was found to be shear-dependent.¹ Corrections for this shear effect were applied by using a five-bulb capillary viscometer.² Data were obtained at zero shear stress. Solutions were prepared, filtered, and diluted in the conventional manner. Flow times for each bulb were measured in duplicate. At least five concentrations were

measured for each fraction, and the intrinsic viscosity was determined in a number of ways.¹

Refractive Index Increment

Refractive index increments were measured with a Brice-Phoenix differential refractometer.³ The refractive index increment, dn/dc for poly-(isobutyl methacrylate) in acetone at 25°C. at wavelengths λ of 5460 and 4360 Å. was 0.117 and 0.122 ml./g., respectively.

Light Scattering

Light-scattering studies were made with a Brice-Phoenix light-scattering photometer. In order to obtain accurate readings at angles of 15, 20, and 25°, it was necessary to keep 500 v. on the photomultiplier tube to insure linearity. This was done by taking the one megohm bleeder resistor in the power supply, and putting it in series with a 150 microammeter. A reading of 60 on the microammeter corresponded to 500 v. on the photomultiplier tube. Then full intensity was obtained by turning up the galvanometer. For low angles, the working standard must be removed for each reading and put back for the zero angle reading. When the galvanometer was at its maximum setting, the photomultiplier was then used in the conventional manner. All solutions were clarified by centrifugation at 52,000*g* for 1 hr. in a Spinco preparative ultracentrifuge. Measurements were made on five concentrations in a series of 14 angles between 15 and 135°. Studies were made at the 5460 and 4360 Å. wavelengths.

RESULTS AND DISCUSSION

Preliminary light-scattering measurements were run in methyl ethyl ketone at 25°C. The results however, were erratic, and reproducible data were difficult if not impossible to obtain. It was suggested⁴ that the solvent acetone be employed. Initial data with this solvent gave poor results, but by reducing the concentration, reproducible results were obtained.

For the most part the Zimm plots⁵ gave relatively straight lines, especially for the lower angles. Fractions F-4B11 and F-2A showed appreciable curvature over the entire range of angles. These are the lowest molecular weight fractions. Runs with fraction F-2A were repeated twice, and the same results were obtained.

Figure 1 is an example of a typical Zimm plot obtained in this manner. As a check on the results the method suggested by Yang⁶ was used. A molecular weight of 5.71×10^6 for fraction F-6B1 was obtained, while the Zimm plot method gave a value of 5.41×10^6 , which is fairly good agreement.

The light-scattering results are listed in Table I. The relationship between the intrinsic viscosity and molecular weight in methyl ethyl ketone at 25°C. is:

$$[\eta]_{\text{MEK}}^{25^\circ\text{C.}} = 8.61 \times 10^{-5} M_w^{0.70} \quad (1)$$

TABLE I
Light-Scattering Results

	Fraction						
	F-3B	F-4B1	F-5B1	F-6B1	Original	F-4B11	F-2A
$M_w \times 10^{-6}$							
$\lambda = 4360 \text{ \AA}$.	10.5	8.33	7.69	5.41	5.00	3.57	2.94
$\lambda = 5460 \text{ \AA}$.	11.1	8.33	7.69	5.41	5.00	3.85	3.13
Average	10.8	8.33	7.69	5.41	5.00	3.70	3.03
R_g							
$\lambda = 4360 \text{ \AA}$.	1703	1667	1228	1069	1168	882	857
$\lambda = 5460 \text{ \AA}$.	1613	1712	1262	1122	1135	1068	1070
Average	1658	1690	1245	1096	1152	975	964
$2.4_2 \times 10^3$							
$\lambda = 4360 \text{ \AA}$.	0.228	0.260	0.267	0.310	0.267	0.202	0.143
$\lambda = 5460 \text{ \AA}$.	0.188	0.229	0.221	0.253	0.167	0.094	0.029

The radius of gyration and the root-mean-square end-to-end distance were calculated from the limiting slope of $(Hc/\tau)_{c=0}$ versus $\sin^2 \theta/2$ from the Zimm plots. The relationship is:

$$R_g = 0.168M_w^{0.57} \tag{2}$$

From a plot of $[\eta]^{2/3}/M^{1/3}$ versus $M/[\eta]$, K was found⁷ to be 8.94×10^{-5} in methyl ethyl ketone at 25°C. This is in good agreement with the value

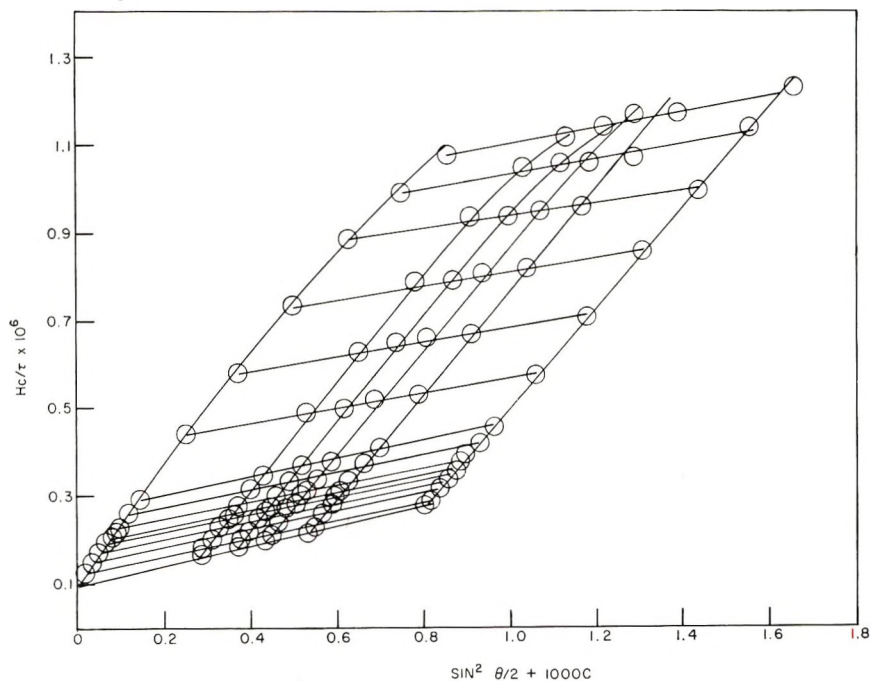


Fig. 1. Hc/τ vs. $\sin^2 \theta/2 + 1000 C$ for fraction F-3B in acetone at 25°C., $\lambda = 4360 \text{ \AA}$.

8.61×10^{-5} shown in eq. (1). Table II gives K and a values in two solvents at several temperatures.

TABLE II
 $[\eta] = KM^a$

Solvent	Temp., °C.	K	a
Acetone	25	0.199×10^{-5}	0.94
MEK	20	5.56×10^{-5}	0.73
MEK	30	7.47×10^{-5}	0.71
MEK	44	2.18×10^{-5}	0.79

The next step will be to run light-scattering and viscosity measurements in a theta solvent by the method described in this paper, and to compare the chain extension of poly(isobutyl methacrylate) thus obtained with the results of other methacrylate studies.⁸⁻¹⁰

The author is indebted to Mrs. C. E. Schramm for assisting in the light-scattering measurements.

References

1. Valles, R. J., and C. E. Schramm, *J. Polymer Sci.*, **A3**, 3664 (1965).
2. Cragg, L. H., and H. van Oene, *Can. J. Chem.*, **39**, 203 (1961).
3. Brice, B. A., and R. Speiser, *J. Opt. Soc. Am.*, **36**, 363 (1946).
4. Debye, P., private communication.
5. Zimm, B. H., *J. Chem. Phys.*, **16**, 1099 (1948).
6. Yang, J. T., *J. Polymer Sci.*, **26**, 305 (1957).
7. Flory, P. J., and T. G. Fox, *J. Am. Chem. Soc.*, **73**, 1904 (1951).
8. Chinai, S. N., and R. A. Guzzi, *J. Polymer Sci.*, **21**, 417 (1956).
9. Didot, F. E., S. N. Chinai, and D. W. Levi, *J. Polymer Sci.*, **43**, 557 (1960).
10. Chinai, S. N., and R. J. Valles, *J. Polymer Sci.*, **39**, 363 (1959).

Résumé

A partir d'un mélange acétone-méthanol on a fractionné un échantillon de polyméthacrylate d'isobutyle linéaire et de poids moléculaire élevé. Une modification au photomètre de Brice-Phoenix a rendu possible les mesures de la diffusion lumineuse aux angles de 15, 20, et 25° en plus des angles habituels. Les mesures effectuées aux petits angles permettent de faire les interpolations angulaires avec plus de précision. On donne pour plusieurs températures les paramètres de l'équation de Mark-Houwink. Le domaine de poids moléculaire étudié est de 3×10^6 à 11×10^6 .

Zusammenfassung

Eine Probe von hochmolekularem, linearem Poly(isobutylmethacrylat) wurde aus einer Aceton-Methanolmischung fraktioniert. Eine Adaptierung eines Brice-Phoenix-photometers ermöglichte die Ausführung von Lichtstreuungsmessungen bei Winkeln von 15, 20, und 25° zusätzlich zu den üblichen Winkeln. Die zusätzliche Messung bei den niedrigen Winkeln erlaubte eine genauere Extrapolation nach den Winkeln. Die Parameter der Mark-Houwink-Gleichung werden für einige Temperaturen mitgeteilt. Der untersuchte Molekulargewichtsbereich lag zwischen $3 \cdot 10^6$ und $11 \cdot 10^6$.

Received March 17, 1965

Revised May 4, 1965

Prod. No. 4758A

Crosslinking of Dialdehyde Starches with Wheat Proteins

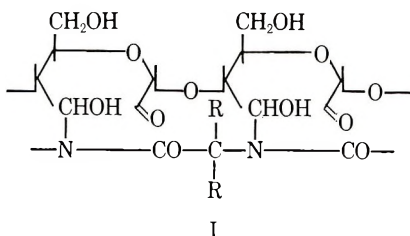
ARUN K. CHATTERJI* and LIONEL K. ARNOLD, *Department of Chemical Engineering, Iowa State University, Ames, Iowa*

Synopsis

A quantitative and degradative study on the gluten-dialdehyde starch reaction product is made, and the possible reaction mechanisms during the degradation reactions are discussed rigorously. The structure of the gluten-DAS reaction product is arrived at by designating a generic protein structure for gluten. This study has produced new evidence regarding crosslinking sites of dialdehyde starches when they react with proteins in general.

Introduction

It was shown by Fein and Filachione¹ that calfskin could be tanned with dialdehyde starch. It was assumed that in this tanning operation the aldehydic groups and peptide linkages reacted in the same fashion as in an addition polymerization process, to give a product which probably had the structure I.



The information regarding this mechanism was very scanty. Sloan et al.² found quite a few years ago that when dialdehyde starch (DAS) was treated with urea, only one mole of urea per repeating unit reacted, leaving one carbonyl group free. These authors did not try to locate which one of the two carbonyl functions was involved in the reaction. On the basis of the earlier work of Jayme et al.,³ showing that, of the two aldehyde groups of periodate-oxidized cellulose, that on C₃ has considerably greater reactivity than the other, they conjectured that one of the carbonyl groups is available for the reaction while the other is left in the hydrated or lactol ring form.

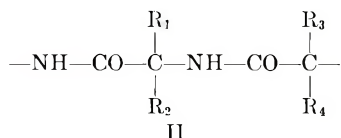
* Present address: Arthur D. Little, Inc., Acorn Park, Cambridge, Massachusetts.

Weakley et al.⁴ reacted dialdehyde starches with casein in aqueous borax dispersions to produce complexes which are irreversibly insoluble in water. Nayudamma et al.⁵ made a study on the combination of DAS with collagens. They investigated the nature of free carbonyl groups by degradation studies of DAS-tanned collagen. They postulated that the free aldehyde groups were those on second carbon atoms of the repeating units of dialdehyde starches.

Experimental

The purpose of our current studies⁶ was to secure more definite information on the nature of the reaction between wheat gluten and DAS. The gluten-DAS reaction product which was studied was made by the following procedure. A 200-ml. portion of a 20% gluten solution in 5% acetic acid solution was reacted with 75 ml. of DAS solution in 5% sodium bisulfite (2 g. DAS/75 ml. solution) at 26°C. for 10 min. with stirring. The hydrophobic product, which settled to the bottom of the beaker, was washed with distilled water three times. The rubbery mass was converted into a fine granular product by treatment in a Waring Blendor with absolute alcohol for 5 min. This product was filtered on a Buchner funnel, air-dried, and bottled.

Gluten, which is an exceedingly complex protein system, can be represented by the general polypeptide structure II.



The structure of DAS is known. Because of the complex structure of the protein, it appeared simpler to find the extent of the crosslinking by determining the residual aldehyde groups of DAS. Degradation experiments were carried out under controlled conditions, and the products of degradation were isolated and identified to determine which of the two aldehyde groups of the glucose residue of DAS is more reactive towards a protein system.

Aldehyde units of DAS and the gluten-dialdehyde starch (G-D) reaction product were first estimated by using two well known methods: the rapid estimation of dialdehyde content of periodate oxystarch through quantitative alkali consumption method of Hofreiter et al.⁷ and the determination of dialdehyde units in periodate-oxidized cornstarches by the borohydride method of Rankin and Mehlretter.⁸ The results are shown in Table I. (The percentages of aldehyde units in G-D products cannot be calculated, as the molecular weights are not known.)

A degradation study, a very useful tool for studying high polymeric reactions, was made with gluten-dialdehyde starch reaction product. When DAS is hydrolyzed under drastic conditions with aqueous acid, glyoxal and

TABLE I
Estimation of Dialdehyde Units

Rapid estimation method				Borohydride reduction method			
Sample	Sample wt., g.	Vol. 0.2660N NaOH, ml.	Dialdehyde units, %	Sample	Sample wt., g.	Diff. in H ₂ vol., ml. ²	Dialdehyde units, %
DAS	0.1572	6.59	93.1	DAS	0.1001	24.8	99.4
DAS	0.1685	6.67	94.0	DAS	0.1010	24.8	98.6
G-D	0.1515	4.01		G-D	0.1004	7.8	
G-D	0.1660	4.07		G-D	0.1001	7.2	
				Gluten	0.1003	0.7	
				Gluten	0.1004	0.5	

D-erythrose are obtained by scission of the acetal bridge linking the first two to the other four carbon atoms of the repeating unit. If the carbonyl group on the second carbon atom remains free in the G-D product, then, on reduction with borohydride and subsequent acid hydrolysis, glycolaldehyde will be obtained. On the other hand, if the aldehyde group on the third carbon atom remains free, erythritol and glyoxal will be obtained from the reaction product under identical conditions.

The method used for degradation was that of Grangaard et al.⁹ In this method, the action of 10% methanolic hydrogen chloride on periodate oxy-starch produces about half the expected amount of glyoxal tetramethyl acetal, which can be isolated by distillation.

The quantitative determination of the glyoxal units present in G-D product before and after reduction with sodium borohydride is used as a means for determining the participation of this unit in the reaction with proteins. Glyoxal can be quantitatively determined by taking advantage of its reaction with 2,4-dinitrophenylhydrazine to form a crystalline derivative of identifiable characteristics.

The estimation of dialdehyde cleavage was carried out in the following way. The sample (0.1–0.2 g.) of the oxystarch (or G-D product) was boiled under reflux for 20 hr. with 25 ml. of methanol containing 2.5 g. of hydrochloric acid. After cooling, the solution was made alkaline with 20 ml. of nearly saturated sodium methylate (made by slow addition of metallic sodium to anhydrous methanol) in methanol, and the volume was adjusted with methanol to 60 ml. The alkaline solution was quantitatively transferred to a 500 ml. distilling flask with exactly 300 ml. of an aqueous solution containing 6.5 g. of sodium chloride and 1 g. of sodium hydroxide. A water condenser was used in the atmospheric pressure distillation and the first, second, and third 100-ml. distillates were collected separately. A 100-ml. portion of water was then added to the still and a fourth 100-ml. portion of distillate collected. A 50-ml. aliquot of each of the four distillates was diluted with an equal volume of 2N hydrochloric acid and hydrolyzed by heating for 75 min. on a steam bath. The hydrolyzates

were examined in the form of the 2,4-dinitrophenylhydrazine derivatives. A 50-ml. portion of a nearly saturated solution of 2,4-dinitrophenylhydrazine (in 2*N* hydrochloric acid) was added to 50 ml. of each hydrolyzed fraction. The precipitates were filtered in a sintered bed crucible, washed with 2*N* HCl, and dried in a vacuum drier at 60°C. for 12 hr. and weighed. The amount of samples used and derivatives obtained by this method are reported in Table II. These results are very significant. These data show that quite a considerable amount of glyoxal is present in the degradation product obtained from the borohydride-reduced G-D product and the magnitude is of the same order as observed in the cases of unreduced G-D product.

TABLE II
Estimation of the Degradation Product Obtained from G-D Product (Both Before and After Reduction with Borohydride)

Wt. of original sample, g.	Wt. of 2,4-dinitrophenylhydrazine derivatives, g.			
	1st fraction	2nd fraction	3rd fraction	4th fraction
	Before Reduction			
0.1591	0.0050	0.0018	0.0014	0.0010
0.1491	0.0056	0.0028	0.0018	0.0008
	After Reduction			
0.1817	0.0056	0.0026	0.0022	0.0008
0.1947	0.0050	0.0026	0.0016	0.0012

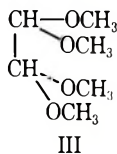
The borohydride reduction was carried out in anhydrous methanol. One-tenth of 1-2 g. of G-D product was suspended in 6 ml. of anhydrous methanol and sodium borohydride (0.012 g. in 1 ml. anhydrous methanol) was added with vigorous stirring. A 25-mg. portion of sodium methylate was then added, and the alkaline reaction mixture was left overnight. An additional amount of sodium borohydride (0.005 g.) was added, and the reaction was allowed to proceed for another 6 hr. A minute crystal of methyl orange was added, and the mixture was neutralized with dilute hydrochloric acid (diluted with anhydrous methanol). Absolute methanol (15 ml.) and 1.5 ml. of concentrated hydrochloric acid were then added, and methanolysis was carried out by refluxing the mixture.

Discussion

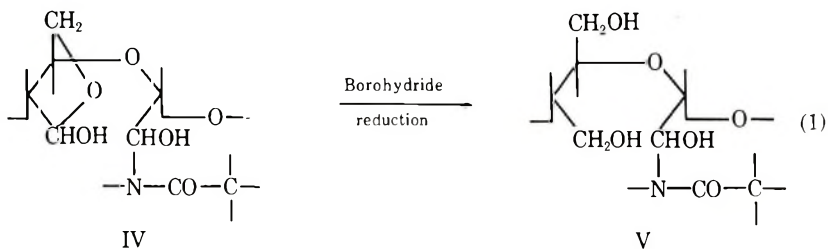
The free aldehyde contents of G-D products are considerably lower than those of DAS. This is so because DAS is the minor component in gluten-DAS product, and some aldehyde groups are crosslinked. Evidence of very low carbonyl content in pure gluten indicates that, in the crosslinked polymer, the DAS chain has quite a number of residual aldehyde groups (Table I). This observation is in accordance with the early work of Sloan et al.,² who reacted dialdehyde starches with urea and observed that one carbonyl group per repeating unit remained free. The important thing to

note is that the reactivity of the aldehyde groups plays a vital role in the reaction of DAS and a protein system. Although the proteins of wheat gluten represent a very complex system, DAS has shown a qualitative identity to its behavior toward urea.

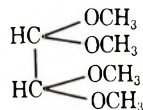
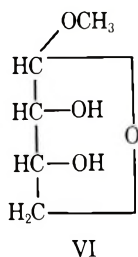
The degradation experiments have answered the obvious question— which carbon atom (C_2 or C_3) of each glucose unit of parent starch is more reactive? The formation of 2,4-dinitrophenylhydrazine derivative (Table II) definitely indicates the presence of tetramethyl acetal of glyoxal (III)



in the methanolysis product from G-D product both before and after borohydride reduction. This can only result from a structure of type IV



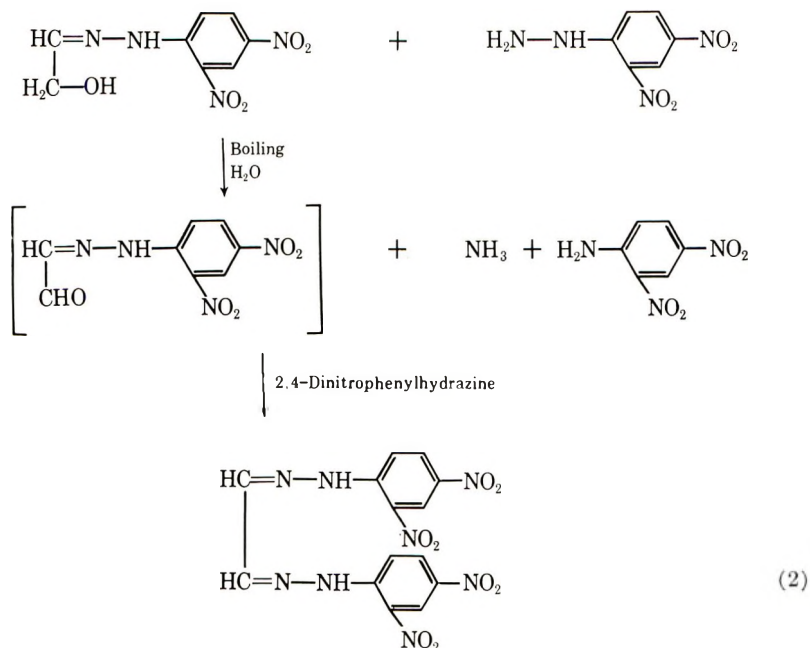
so that, during borohydride reduction, eq. (1), the third carbon atom is reduced and upon subsequent methanolysis, one obtains methylerythroside VI and glyoxal tetramethyl acetal (VII).



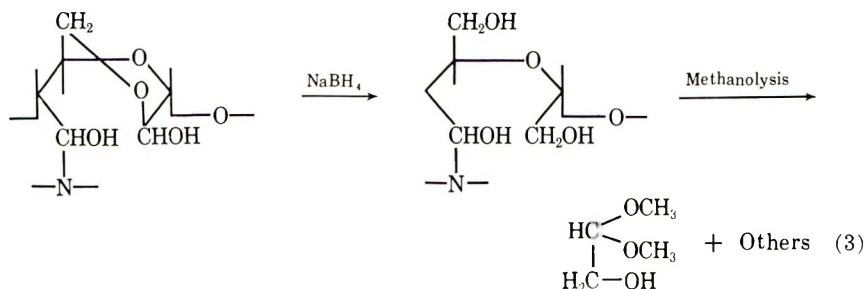
VII

The possibility that 2,4-dinitrophenylhydrazine derivatives are derived from glycolaldehyde is ruled out by the observation of insolubility in water and alcohol.

The final confirmation that 2,4-dinitrophenylhydrazine derivative of glyoxal did not result from the reaction sequence (2)



and that, glycolaldehyde did not come from the sequence (3)

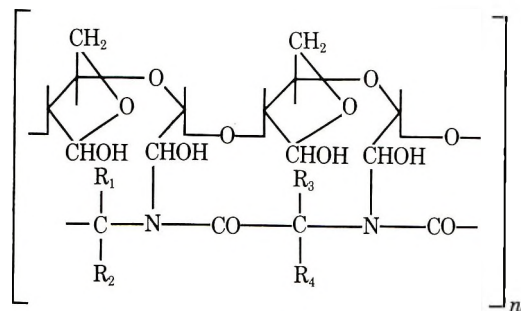


is obtained by carrying out precipitation at room temperature (only glyoxal does it), filtering the osazone of glyoxal, and heating the filtrate when no further precipitation occurred. This was again checked with a blank run using 30% glyoxal solution, about 50% of which was reduced with sodium borohydride (on mole basis).

The results of degradation experiments apparently contradict the findings of Nayudamma et al.,⁵ who were working on the reactions of collagen and DAS. They had estimated the glyoxal, obtained from collagen-treated DAS both before and after borohydride reduction, by using a colorimetric method (Ariyama) with Benedict's uric acid reagent. They found that the color of the reduced sample was of much lower intensity than that of the nonreduced sample. This was attributed to the presence of free carbonyl groups on C₂ in the DAS-tanned collagen.

We believe that our results are more quantitative in nature and hence, more sound than those obtained by using a colorimetric method. This would lead us to accept that the second carbon atom is more reactive than the third and hence the free carbonyl groups in G-D product are mostly on C₃ of every repeating unit in DAS chain.

Thus we may represent the gluten-DAS product by the structural formula VIII.



VIII

This is a partial report of work done in the Iowa Engineering Experiment Station as Project 416-S under contract with the U. S. Department of Agriculture and authorized by the Research and Marketing Act. The contract was supervised by the Northern Regional Research Laboratory of the Agricultural Research Service.

References

1. Fein, M. L., and E. M. Filachione, *Am. Leather Chemists' Assoc. J.*, **52**, 17 (1957).
2. Sloan, J. W., B. T. Hofreiter, R. L. Mellies, and I. A. Wolff, *Ind. Eng. Chem.*, **48**, 1165 (1956).
3. Jayme, G., M. Satre, and S. Maris, *Naturwiss.*, **29**, 768 (1941).
4. Weakley, F. B., C. L. Mehlretter, and C. E. Rist, *Tappi*, **44**, 456 (1961).
5. Nayudamma, Y., K. T. Joseph, and S. M. Bose, *Am. Leather Chemists' Assoc. J.*, **56**, 548 (1961).
6. Chatterji, A. K., Ph.D. Dissertation, Iowa State University of Science and Technology, Ames, Iowa, November 1963.
7. Hofreiter, B. T., B. H. Alexander, and I. A. Wolff, *Anal. Chem.*, **27**, 1930 (1955).
8. Rankin, J. C., and C. L. Mehlretter, *Anal. Chem.*, **28**, 1012 (1956).
9. Grangaard, D. H., E. K. Gladding, and C. B. Purves, *Paper Trade J.*, **115**, 41 (1942).

Résumé

On a effectué une étude quantitative de dégradation du produit de réaction du gluten avec le dialdéhyde de l'amidon et on a discuté d'une façon rigoureuse des mécanismes de réaction possibles ayant lieu pendant la dégradation. On est parvenu à déterminer la structure du produit de réaction gluten-DAS en admettant une structure protéinique pour le gluten. Cette étude constitue une nouvelle preuve de l'existence de sites de pontage des amidons dialdéhydriques lorsqu'ils réagissent avec les protéines en général.

Zusammenfassung

Eine quantitative Untersuchung des Abbaus des Reaktionsprodukts aus Gluten und Dialdehydstärke wird durchgeführt und die möglichen Reaktionsmechanismen für die Abbaureaktionen werden eingehend diskutiert. Die Struktur des Gluten-DAS-Reaktionsprodukts wird durch Aufstellung einer generellen Proteinstruktur für Gluten aufzuklären versucht. Die vorliegende Untersuchung lieferte neue Belege für die Vernetzungsstellen von Dialdehydstärke bei ihrer Reaktion mit Proteinen im allgemeinen.

Received October 28, 1964

Revised May 10, 1965

Prod. No. 4759A

Inorganic Polymers. Part II. The Thermal Bulk Condensation Polymerization of *P*-Phenylphosphonic Diamide

R. A. SHAW and TAKESHI OGAWA, *Department of Chemistry, Birkbeck College, University of London, London, England*

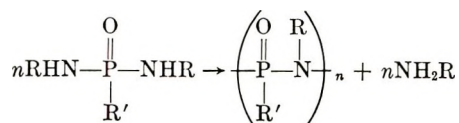
Synopsis

The thermal bulk condensation polymerization of *P*-phenylphosphonic diamide under a variety of conditions is described. Polymerization and degradation processes were observed. The maximum molecular weights attained were about 3000. These polymers, soluble in most organic solvents, are hydrolytically unstable, giving low molecular weight products soluble only in hydroxylic solvents.

INTRODUCTION

It is known that aminophosphazenes, $[\text{NP}(\text{NHR})_2]_3 \text{ or } 4$, ($\text{R} = \text{H}$, alkyl or aryl), undergo thermal condensation polymerizations with simultaneous evolution of ammonia¹ or amines.^{2,3} Because of the large number of functional groups of these monomers, e.g., six in hexaaminocyclotriphosphazatriene,¹ four in tetraaminotetraphenylcyclotetraphosphazatetraene,³ etc., the resultant polymers have highly crosslinked three-dimensional structures and are in general insoluble in solvents which do not decompose them.

Phosphonic diamides, $\text{R}'\text{P}(\text{O})(\text{NHR})_2$, however, possess only two functional groups and undergo analogous condensation reactions. Hence it seemed likely that linear polymers containing a phosphorus-nitrogen backbone would be obtained by the polymerization of such bifunctional compounds:



(where $\text{R} = \text{H}$, alkyl, or aryl, and $\text{R}' = \text{alkyl, alkoxy, aryl, etc.}$)

Coover and co-workers⁴ have reported glassy resins on heating *P*-phenylphosphonic diamide to 200–395°C. under reduced pressure. The reaction was second-order in the temperature range 225–300°C., one mole of ammonia being evolved per mole of monomer, and $+\text{P}(=\text{O})(\text{C}_6\text{H}_5)-\text{NH}+$ was suggested as the structural unit of the product. The materials ob-

tained were partially soluble in dimethylformamide and hot acetone, but insoluble in the common organic solvents. Their molecular weights were found by ebullioscopy in nitrobenzene to be in the range of 350–400.

We have reinvestigated the thermal polymerization of *P*-phenylphosphonic diamide in some detail. The polymers prepared in the temperature range 200–300°C. were soluble (depending on the reaction times, cf. below) in chloroform, 1,2-dichloroethane, carbon tetrachloride, methylene chloride, dimethylformamide, methanol, ethanol, acetone, benzene, etc., and insoluble in water and ethers. The number-average molecular weights of these polymers, determined by vapor pressure osmometry in 1,2-dichloroethane, were found to be 2000–3000.

EXPERIMENTAL

Preparation of *P*-Phenylphosphonic Diamide

P-Phenylphosphonic diamide was prepared by the reaction of dichlorophenylphosphine oxide (supplied by Eastman Kodak Organic Chemicals) with ammonia, by a method similar to the preparation of phosphoric triamide.⁵ A typical preparation is described below.

A 1500-ml. portion of freshly distilled, dry chloroform was placed in a 2-liter, three-necked flask, and cooled to -60 to -70°C ., in an acetone-Dry Ice bath to collect approximately 200 ml. of liquid ammonia. After raising the temperature of the cooling bath to -20°C ., 50 g. of freshly distilled dichlorophenylphosphine oxide, dissolved in 500 ml. of dry chloroform, was added dropwise with vigorous stirring, while ammonia gas was bubbled through the reaction mixture. After several hours the temperature was slowly brought to room temperature, and the reaction mixture left to stand for about 24 hr. The white precipitate obtained was filtered off, washed with chloroform, and dried at room temperature under vacuum. The precipitate was then refluxed for 8–10 hr. with about 150–200 ml. of dry diethylamine in dry chloroform to remove the ammonium chloride formed during the reaction. The yield of crude *P*-phenylphosphonic diamide thus obtained was $>90\%$. Recrystallization from dry methanol (or ethanol) gave colorless, flakelike crystals of the diamide, m.p. 180–185°C. (dec.).

ANAL. Calcd. for $\text{C}_6\text{H}_9\text{N}_2\text{OP}$: C, 46.15%; H, 5.77%; N, 17.95%. Found: C, 46.5%; H, 5.8%; N, 17.8%.

Polymerization Reactions

The polymerizations were carried out (a) in sealed tubes, (b) under oxygen-free, dry nitrogen at atmospheric pressure, and (c) under vacuum. The sealed tubes were of Pyrex glass 10 cm. long with an inner diameter of 1.0 cm., and the monomer was sealed up under vacuum. The polymerizations under nitrogen were carried out in Pyrex glass crucibles of 1 cm. diameter and 2.5 cm. height, on a Stanton thermobalance, Model 1. Thus

the extent of the polymerization reaction could be followed by means of the weight loss recorded. Polymerization temperatures varied from 200 to 300°C. and times from 30 min. to several hours. The nitrogen used as an inert gas was passed through columns containing manganous oxide, silica gel, and phosphorus pentoxide, to remove traces of oxygen and moisture.

For thermogravimetric analysis up to 1000°C. alumina or silica crucibles were used. In contrast to our earlier studies on phosphams^{1,6} no significant differences between the two types of crucibles were observed.

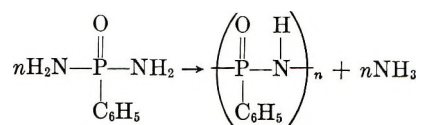
Molecular Weight Measurements

The number-average molecular weights of the polymers obtained were determined at 65°C. with a Mechrolab vapor pressure osmometer Model 301A, in dry 1,2-dichloroethane.

RESULTS AND DISCUSSION

Polymerization Reactions and the Nature of the Polymers Obtained

The results obtained by thermogravimetric analysis (TGA) are shown in Figure 1. It can be seen that there are three distinct steps in the thermal decomposition of the diamide. The weight loss observed ($\sim 11\%$) at the completion of the first step is approximately equivalent to the liberation of one mole of ammonia per mole of diamide (10.9%). Titration of the ammonia evolved in a polymerization reaction at 250°C. was in agreement with the TGA analysis. It seems therefore probable that the first step in the thermal decomposition of the monomer corresponds to the polymerization reaction suggested by Coover and co-workers.⁴



Studies on the second and third steps will be published at a later date together with results obtained from the TGA of other phosphorus-nitrogen polymers.

The polymers obtained in the temperature range 200–300°C. under a nitrogen atmosphere or under vacuum were colorless, transparent, extremely viscous materials, which on cooling solidified to hard glassy resins. The resins thus obtained were thermoplastic and soluble in most organic solvents except in light petroleum, ethers, and water. It seems therefore likely that the polymers consist predominantly of unbranched chains or large cycles. Earlier investigators⁴ suggested, to account for the low molecular weights (300–400) observed, that the materials obtained in the temperature range 200–270°C., consisted mainly of cyclic dimers

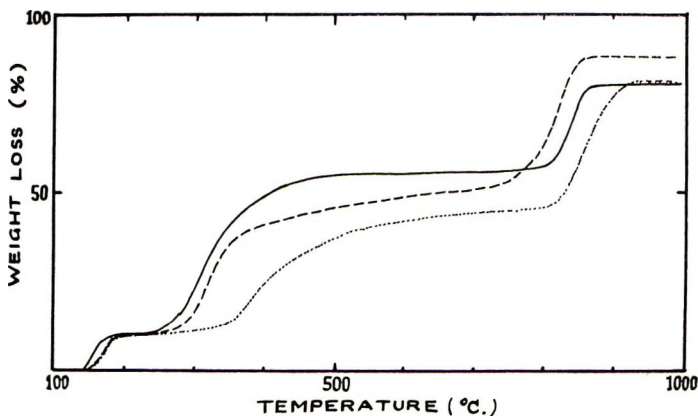
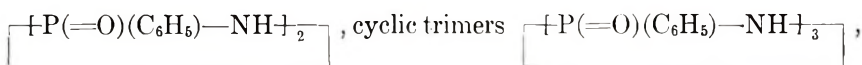


Fig. 1. TGA curves of *P*-phenylphosphonic diamide: (—) in flat silica crucible, heating rate 1000°C./7 days; (--) in cylindrical alumina crucible, heating rate 1000°C./7 days; (···) in cylindrical alumina crucible, heating rate 1000°C./24 hr.



or mixtures of these with linear polymers. In the present work no evidence for the formation of cyclic dimers or trimers was obtained.

The polymers obtained in the present work were soluble in the usual organic solvents mentioned above. Initially clear solutions of the polymers in chloroform or dichloroethane, however, became cloudy on standing, and precipitates appeared, if the solvents were insufficiently dried, or the polymers ground to a fine powder in the laboratory atmosphere. When a lump of the polymer was dissolved without prior grinding in rigorously dried solvents the solutions remained clear, and no precipitates appeared. The precipitates formed were insoluble in the same and other nonpolar solvents, but were soluble in methanol and ethanol. These findings show the polymer to be highly hygroscopic and readily hydrolyzed by water. Hydrolysis would account also for the observations by earlier workers,⁴ who believed these polymers to be insoluble in the usual organic solvents.

Attempts to fractionate the polymer by precipitation with light petroleum from chloroform solution gave fractions varying from viscous resins to fine powders, but their molecular weights measured in chloroform containing 5% methanol (required to dissolve the chloroform insoluble precipitates) were all in the region of 600–800. The resultant solutions vigorously corroded the aluminum block of the osmometer. When small quantities of water or ammonia were added to the clear chloroform solutions of the polymer, white precipitates, soluble in methanol or water, appeared at once.

These results show that polymers obtained from *P*-phenylphosphonic diamide are extremely sensitive to hydrolysis, ammonolysis, and probably also to reactions with other compounds containing active hydrogen atoms. The reaction with ammonia shows the polymerization reaction to be a reversible one.

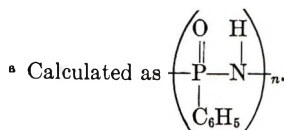
To minimize hydrolysis, molecular weight determinations, described in the following section, were carried out in rigorously dried 1,2-dichloroethane (distilled from barium oxide) in which lumps of polymers were dissolved without prior grinding.

Relationship between the Number-Average Molecular Weights and the Polymerization Conditions

When polymerizations are carried out in sealed tubes the ammonia evolved cannot escape, and can therefore react reversibly with the polymer. The products thus obtained were hard white solids, large portions of which were insoluble in 1,2-dichloroethane, but soluble in methanol. The percentage of the soluble fraction did not change significantly with polymerization times >2 hr., and it appears that an equilibrium is established between the 1,2-dichloroethane-soluble polymer and the insoluble product. The number-average molecular weights of the soluble polymers showed random variations within the range of 650–1300 (Table I).

TABLE I
Number-Average Molecular Weight of the 1,2-Dichloroethane-Soluble Fractions of Polymers Obtained in Sealed Tubes at 235°C.

Sample no.	Polymerization time, hr.	Soluble fraction, %	Number-average molecular weight	Degree of polymerization n^a
1	1/2	17	980	7.0
2	1	18	650	4.7
3	2	32	1150	8.2
4	4	26	1000	7.2
5	8	26	870	6.2
6	10	27	1210	8.7
7	25	33	1310	9.3



The 1,2-dichloroethane-insoluble fraction probably consists of short-chain oligomers with terminal NH_2 groups, the monomer being insoluble in 1,2-dichloroethane, chloroform, etc., but soluble in alcohols and water. When these insoluble oligomers were heated at 240°C. under a nitrogen atmosphere, ammonia gas was evolved, and colorless resins, soluble in 1,2-dichloroethane, were obtained. It is obvious that the ratio of the number of amino groups to the size of the oligomer or polymer molecules will be an important factor in determining their solubilities in chlorinated hydrocarbons. The same will apply to hydrolysis product. (cf. earlier discussion).

TABLE II
Number-Average Molecular Weights of Polymers Obtained under Vacuum

Sample no. ^a	Polymerization temp., °C.	Polymerization time, min.	Solubility in 1,2-dichloroethane, %	Number-average molecular weight	Degree of polymerization n
8	235	50	100	2050	14.7
9	"	70	100	2180	15.5
10	"	80	100	2300	16.5
11	"	100	100	2430	17.5
12	245	30	100	2380	17.1
13	260	150	100	2000	14.3
14	"	900	11	1750	12.5

^a All polymerizations carried out with same batch of monomer.

The molecular weights of the 1,2-dichloroethane-soluble polymer obtained in sealed tube experiments were much lower than those obtained either under a nitrogen atmosphere or under vacuum (Tables II and III). This points again to the reversibility of the polymerization reaction of *P*-phenylphosphonic diamide, and to obtain polymers with higher molecular

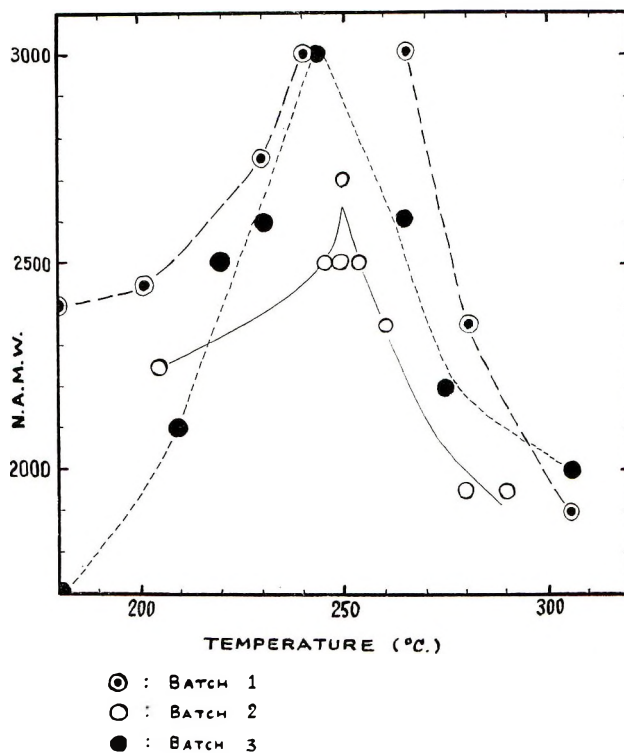
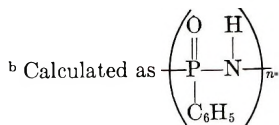


Fig. 2. Relationship between the number-average molecular weight and the polymerization temperature: (⊙) batch 1; (○) batch 2; (●) batch 3.

TABLE III
Number-Average Molecular Weights of Polymers Obtained at Various Temperatures under a Nitrogen Atmosphere

Sample no. ^a	Polymerization temp., °C.	Number-average molecular weight	Degree of polymerization n^b
1-1	180	2400	17.3
1-2	205	2450	17.6
1-3	230	2740	19.7
1-4	240	3000	21.6
1-5	265	3000	21.6
1-6	280	2350	16.9
1-7	305	2200	15.8
2-1	205	2250	16.2
2-2	246	2500	18.0
2-3	250	2500	18.0
2-4	250	2700	19.4
2-5	255	2500	18.0
2-6	260	2350	16.9
2-7	280	1950	14.0
2-8	290	1950	14.0
3-1 ^c	180	1700	12.2
3-2 ^c	208	2100	15.1
3-3	220	2500	18.0
3-4	230	2600	18.7
3-5	243	3000	21.6
3-6	265	2600	18.7
3-7	275	2200	15.8
3-8	305	2000	14.4

^a Samples 1-1 to 1-7 from same batch of monomer, 2-1 to 2-8 from another, etc.



^c Polymerization times for samples 3-1 and 3-2 were 2 and 1 hr. respectively; for all other samples 30 min.

weights the polymerization must be carried out under conditions favoring the removal of the liberated ammonia.

To determine whether diffusion effects of the ammonia gas influence the molecular weight of the polymer, polymerizations were carried out at 250°C. under a nitrogen atmosphere with amounts of monomer varying from 0.05 to 0.5 g. No significant differences in the molecular weights of the polymers obtained were observed.

The results shown in Table III are plotted in Figure 2. It can be seen that near 250°C. a maximum occurs in the number-average molecular weights of the polymer. The monomer melts with decomposition at 180–185°C. During this fusion process polymerization commences, leading to dimers, trimers, etc. Some of these may have higher melting points

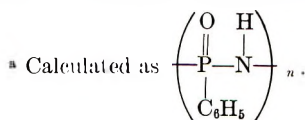
than the monomer. These oligomers will contribute to making the reaction system highly viscous, hindering diffusion of monomer to the growing polymer chain or oligomer-oligomer interactions. On the other hand, thermal processes will continue to start new oligomers tending to give low molecular weight products. As the polymerization temperature is increased, the reaction system becomes more mobile and favors somewhat higher molecular weights. At higher temperatures still, degradation processes become important and compete with the polymerization reactions. The balance of these two effects gives maximum molecular weights near 250°C. Initial degradation processes are accompanied by little or no further ammonia evolution, and the products remain completely soluble in 1,2-dichloroethane. At temperatures near 280°C. ammonia evolution becomes again noticeable, molecular weights decrease further, but this time accompanied by increasing amounts of the polymer becoming insoluble. These insoluble fractions are equally insoluble in hydroxylic solvents, showing that they do not contain significant quantities of monomer or short-chain oligomers, and thus differ significantly from the products obtained in sealed-tube polymerizations.

Polymerizations carried out under nitrogen at 230 and 250°C. with varying reaction times show a similar trend at each temperature (Table IV). There is a rapid build-up to maximum molecular weights which decrease again with extended reaction times, pointing again to a balance of polymer building and degradation processes.

Further elimination of ammonia observed at temperatures >280°C. is probably indicative of crosslinking of chains and/or macrocycles. As this proceeds the polymer becomes less soluble in 1,2-dichloroethane, and this

TABLE IV
Relationship between the Number-Average Molecular Weights of Polymers and the Polymerization Time at Constant Temperatures

Temp., °C.	Time, hr.	Number-average molecular weight	Degree of polymerization n^a
230	1/2	2600	18.7
"	1 1/4	2450	17.6
"	2	2550	18.3
"	4	2200	15.8
"	16	1400	10.1
250	1/3	2100	15.1
"	1/2	2800	20.1
"	1	2200	15.8
"	2	2100	15.1
"	3	2100	15.1
"	13	1600	11.5



insoluble fraction, e.g., the bulk of sample 14 in Table II, is now insoluble in any solvent including hydroxylic ones.

The purity of the monomer is another factor influencing the molecular weight. Likely impurities are hydrolysis and/or methanolysis products. Figure 2 shows three different curves. Their features are similar, indicating the same optimum polymerization temperature in each case. The molecular weights of polymers obtained at this optimum temperature from different batches of monomer are shown in Table V. Although no quantitative analyses of the hydroxyl or methoxyl groups (likely terminating groups) were made, it seems that the molecular weight is significantly

TABLE V
Relationship between the Number-Average Molecular Weight of the Polymers and the Purity of the Monomer^a

Monomer batch		Number-average molecular weight
1	Freshly prepared, 1st crop from recrystallization	3000
1	2nd crop from recrystallization	2500
1	3rd crop from crystallization	2200
2	Freshly prepared, 1st crop from recrystallization	2400
2	2nd crop from crystallization	2100
3	monomer kept for 1 year	3000

^a Polymerization at 250°C. for 30 min. under an N₂ atmosphere.

affected by the purity of the monomer. When about 2% of phenylphosphonic acid, or its ammonium salt, was added to the monomer prior to polymerization, the resultant polymers had molecular weights lower by 10 and 15%, respectively, than those obtained in the absence of these additives.

Possible Structures of the Polymers

The results of elementary analyses of the polymers are shown in Table VI, together with values calculated for cyclic and linear structures. Differences are not large, but favor, if anything, the cyclic structures, although linear structures with a limited amount of crosslinking cannot be excluded. The infrared spectra were too indistinct to throw light on this problem.

Condensation polymerization, as measured by weight loss on a thermobalance, at temperatures <230°C. for 1/2 hr., was 90–95%, while at temperatures >250°C. for 1/2 hr. it was almost 100%. If the polymerization time was prolonged for several hours, 100% conversion could also be attained at lower temperatures. The molecular weight, however did not increase with conversion beyond 95%. For example, if the polymer obtained at 200°C. was subsequently heated at 250°C. for a further 1/2 hr., no

CONCLUSIONS

with carbon compounds, this is by no means the case in phosphorus-nitrogen chemistry.⁷⁻⁹ The initially formed polymers degrade at higher temperatures and/or prolonged reaction times to lower molecular weight, still soluble species, probably smaller ring structures. Further degradation accompanied by ammonia evolution and loss of solubility is probably due to crosslinking.

The thermal bulk condensation polymerization of *P*-phenylphosphonic diamide leads to soluble polymers. As the reaction is reversible removal of the condensation product, ammonia, is essential. The maximum molecular weights obtained were about 3000. The optimum polymerization temperature was found to be near 250°C. Higher temperatures or prolonged reaction times lead to degradation giving initially, soluble products of lower molecular weights, and eventually insoluble materials. Macrocyclic structures (or linear polymers with a limited degree of crosslinking) degrading to lower cyclic compounds, and finally to cross-linked polymers are compatible with, but not proven by, the experimental evidence. Experiments to determine whether the thermal degradation of the polymer is connected with the presence of nitrogen-hydrogen bonds in the P—NH—P bridges are in progress. The polymer is hydrolytically unstable, yielding low molecular weight materials soluble only in hydroxylic solvents.

The authors are indebted to the Agricultural Research Service of the U. S. Department of Agriculture for generous financial support (under P.L. 480).

References

1. Shaw, R. A., and M. C. Miller, *J. Chem. Soc.*, **1964**, 3233.
2. Bode, H., and H. Clausen, *Z. Anorg. Chem.*, **258**, 99 (1949).
3. Shaw, R. A., and T. Ogawa, unpublished results.
4. Coover, Jr., H. N., R. L. McConnell, R. Land, and N. H. Shearer, Jr., *Ind. Eng. Chem.*, **52**, 412 (1960).
5. Klement, R., *Inorganic Syntheses*, Vol. VI, E. G. Rochow, ed., McGraw-Hill, New York, 1960, p. 108.
6. Shaw, R. A., and T. Ogawa, *J. Polymer Sci.*, in press.
7. Patat, F., and P. Derst, *Angew. Chem.*, **71**, 105 (1959).
8. Shaw, R. A., *J. Polymer Sci.*, **8**, 1603 (1960).
9. Shaw, R. A., B. W. Fitzsimmons, and B. C. Smith, *Chem. Rev.*, **62**, 247 (1962).

Résumé

On décrit la polymérisation par condensation thermique en masse du diamide *p*-phénylphosphonique dans diverses conditions. On observe de processus de polymérisation et de dégradation. Les poids moléculaires maxima atteints sont d'environ 3000. Ces polymères solubles dans la plupart des solvants organiques, sont hydrolytiquement instables et donnent des produits de bas poids moléculaires, solubles seulement dans les solvants hydroxyliques.

Zusammenfassung

Die thermische Kondensationspolymerisation von *p*-Phenylphosphondiamid in Substanz unter verschiedenen Bedingungen wird beschrieben. Es wurden Polymerisations- und Abbauprozesse beobachtet. Das höchste erreichte Molekulargewicht betrug etwa 3000. Die in den meisten organischen Lösungsmitteln löslichen Polymeren sind hydrolytisch unbeständig und liefern niedermolekulare nur in hydroxylhaltigen Lösungsmitteln lösliche Produkte.

Received March 2, 1965

Prod. No. 4734A

Anionic Polymerization of ω -Lactam. Part II. Polymerization of ϵ -Caprolactam by Alkali Metal and Imino Chlorides

TAKAYA YASUMOTO, *Plastics Laboratory, Toyo Rayon Co., Ltd.,
Tokodori, Showaku, Nagoya, Japan*

Synopsis

It has been found that imino chlorides may be used as cocatalysts for the alkaline polymerization of ϵ -caprolactam. Addition of an imino chloride shortens the induction period before polymerization, and the polymerization proceeds rapidly at a low temperature below the melting point of the polymer. A mechanism is proposed for the anionic polymerization of ϵ -caprolactam with alkali metal and an imino chloride. It involves the formation of a reactive *N*-imidoyl lactam and chain propagation by the stepwise addition of anionic lactams at the end of a molecule. The conditions for the polymerization have been carefully investigated. As the concentration of imino chloride increases, the conversion and relative viscosity increase slightly, but ϵ -caprolactam is unpolymerizable when equimolar quantities of imino chloride and alkali metal are present, or when there is a higher concentration of imino chloride than of alkali metal.

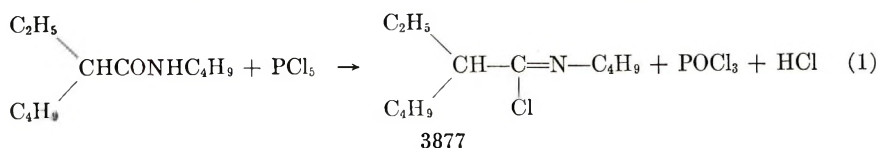
INTRODUCTION

It has been shown that the alkaline polymerization of ω -lactams can be accelerated by the addition of certain compounds¹⁻¹⁰ as cocatalyst. In our previous paper¹² we showed that ketenimines are effective as cocatalysts for the alkaline polymerization of ϵ -caprolactam. The polymerization proceeds rapidly at low temperature below the melting point of the polymer. Furthermore, imino chlorides were found to be useful cocatalysts to activate the alkaline polymerization of ϵ -caprolactam. The present paper reports, on the conditions of polymerization of ϵ -caprolactam with alkali metal and imino chlorides, and the results of this study are discussed.

EXPERIMENTAL

Synthesis of Imino Chlorides

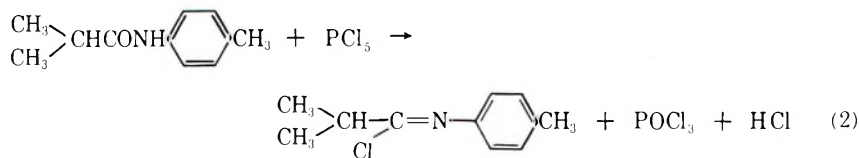
Preparation of *N*-(*n*-Butyl)- α -ethylcaproimino Chloride. The imino chloride was obtained by the reaction between *N*-(*n*-butyl)- α -ethylcaproamide and phosphorus pentachloride as shown in eq. (1):



The reaction mixture consisting of 149 g. (0.75 mole) of *N*-(*n*-butyl)- α -ethylcaproamide and 313 g. (1.50 mole) of phosphorus pentachloride in 1.2 liters of dry benzene was heated under reflux for 3 hr. The imino chloride was isolated by vacuum distillation from the reaction mixture; b.p. 69–70°C./0.5 mm.; yield 85.6% (140 g.); n_D^{25} 1.4490.

ANAL. Calcd. for $C_{12}H_{24}NCl$ (M.W. 317.5): C, 66.21%; H, 11.03%; N, 6.44%; Cl, 16.32%. Found: C, 66.21%; H, 11.24%; N, 6.26%; Cl, 15.87%.

Preparation of *N*-(*p*-Tolyl)isobutyrimino Chloride. This imino chloride, as shown in eq. (2), was prepared by a procedure similar to that described above. The imino chloride was isolated by vacuum distillation from a reaction mixture consisting of 133 g. (0.75 mole) of *N*-(*p*-tolyl)isobutyramide and 313 g. (1.50 mole) of phosphorus pentachloride in 1.2 liters of dry benzene after a 3-hr. reflux period: b.p. 85–88°C./1.0 mm.; yield 87.8% (129 g.); n_D^{25} 1.5296.



ANAL. Calcd. for $C_{11}H_{14}NCl$ (M.W. 195.5): C, 67.52%; H, 7.16%; N, 7.16%; Cl, 18.16%. Found: C, 67.23%; H, 7.37%; N, 7.10%; Cl, 17.78%.

Polymerization of ϵ -Caprolactam

In order to eliminate the effect of moisture the monomer should be absolutely dry. Thus once-distilled ϵ -caprolactam was kept over P_2O_5 in a desiccator and distilled again under vacuum just before polymerization. In each polymerization, potassium metal was used as catalyst, and the effects of imino chlorides were investigated.

ϵ -Caprolactam, molten at 90°C., was poured into an ampule equipped with a nitrogen inlet tube, and the desired amount of potassium metal was added to the lactam under an inert atmosphere. After the catalyst was completely dissolved, the calculated amount of an imino chloride was added and mixed uniformly. The bulk polymerization of the mixture took place even at low temperature (180°C.), i.e., below the melting point of the polymer. The block polymer formed was shaved thinly. About 5 g. of the weighed sample was extracted with hot water for 10 hr. and dried, and then the conversion to polymer was calculated. After the measurement of conversion, 0.250 g. of the dried sample was dissolved in 25.0 ml. of 98% concentrated H_2SO_4 , and the relative viscosity (η_{rel}) of the solution was measured by an Ostwald viscometer at $25 \pm 0.05^\circ C$.

RESULTS

Effects of Imino Chlorides on the Alkaline Polymerization of ϵ -Caprolactam

In the bulk polymerization of ϵ -caprolactam with 2.0 mole-% of potassium metal at 180°C., the effects of *N*-(*n*-butyl)- α -ethylcaproimino chloride (BCIC) and *N*-(*p*-tolyl)isobutyrimino chloride (TBIC) are shown in Table I. It is obvious from these data that the polymerization of ϵ -caprolactam is accelerated by addition of an imino chloride. It was necessary to carry on heating for over 10 hr. to reach 90% conversion in the polymerization with potassium metal only, but by addition of an imino chloride the polymerization reached 90% conversion after 30–60 min. heating. Thus imino chlorides as cocatalyst for the alkaline polymerization of ϵ -caprolactam can shorten the induction period before polymerization and make the polymerization proceed more rapidly. It was also found that, with addition of an imino chloride, rapid polymerization would take place at a low temperature i.e., below the melting point of the polyamide. According to Table I, the effect of *N*-(*p*-tolyl)isobutyrimino chloride was slightly greater than that of *N*-(*n*-butyl)- α -ethylcaproimino chloride.

TABLE I
Effects of Imino Chlorides on the Alkaline Polymerization of ϵ -Caprolactam^a

Expt. no.	Imino chloride concentration, mole-%	Time, min.	Conversion, %	Relative viscosity, η_{rel}
101	0	360	79.3	—
102		480	85.0	—
103		720	89.1	—
104		1020	92.2	2.52
105		1500	95.2	2.48
106	BCIC, 1.0	60	73.1	—
107		120	89.8	—
108		240	95.0	—
109		480	95.1	2.77
110		720	96.8	2.75
111	TBIC, 1.0	30	93.8	—
112		60	94.6	—
113		120	95.5	—
114		240	96.7	2.81

^a Catalyst: K, 2.0 mole-%; polymerization temperature: 180°C.

Effects of Potassium Metal and Imino Chloride Concentrations on Conversion and Relative Viscosity

When conversion and relative viscosity were studied at various concentrations of potassium metal and *N*-(*n*-butyl)- α -ethylcaproimino chloride, the experimental results shown in Table II were obtained. All polymeri-

zations were carried out at 180°C. for 10 hr. Both conversion and relative viscosity decreased with increasing concentration of potassium metal. On the other hand, both conversion and relative viscosity increased slightly with increasing concentration of the imino chloride. In uses of other cocatalysts^{12,14} for the alkaline polymerization of lactams, it has been observed that both conversion and relative viscosity decreased with increasing concentration of cocatalyst. The peculiar effect of imino chloride concentration is probably due to a decrease of the practical concentration of catalyst, due to its being consumed by reaction with the chlorine of the imino chloride. As shown in Table II, it was found that ϵ -caprolactam was unpolymerizable when equimolar quantities of imino chloride and catalyst were added or when imino chloride concentration was greater than catalyst concentration. These results are attributed to the complete consumption of catalyst by imino chloride. A precipitate of potassium chloride formed from the potassium salt of ϵ -caprolactam and imino chloride was observed in the polymerization system. Consequently, in the polymerization the imino chloride concentration should be less than the catalyst concentration.

TABLE II
Effects of Potassium Metal and *N*-(*n*-Butyl)- α -ethylcaproimino Chloride
Concentration on Conversion and Relative Viscosity^a

Expt. no.	Potassium metal concentration, mole-%	Imino chloride concentration, mole-%	Conversion, %	Relative viscosity η_{rel}
121	1.0	1.0	Nonpolymerizable	
122	2.0	1.0	96.8	2.75
123	3.0	1.0	93.4	2.58
124	4.0	1.0	92.2	2.28
125	5.0	1.0	91.1	2.09
126	6.0	1.0	88.8	1.82
127	7.0	1.0	88.1	1.75
128	2.0	0.5	92.3	2.67
129	2.0	1.5	96.9	2.79
130	2.0	2.0	Nonpolymerizable	
131	2.0	2.5	Nonpolymerizable	

^a Polymerization at 180°C. for 10 hr.

Effect of Polymerization Temperature

Table III shows the effect of polymerization temperature on conversion and relative viscosity in the polymerization with a constant concentration of 2.0 mole-% of potassium metal and 1.0 mole-% of *N*-(*n*-butyl)- α -ethylcaproimino chloride. The higher the polymerization temperature was, the more rapidly the polymerization proceeded. The polymerization at 230°C. went to completion almost instantaneously. However, conversion and relative viscosity decreased with increasing polymerization temperature.

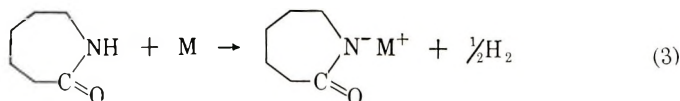
TABLE III
Effect of Polymerization Temperature on Conversion and Relative Viscosity^a

Expt. no.	Temperature, °C.	Time, min.	Conversion, %	Relative viscosity, η_{rel}
106	180	60	73.1	—
107		120	89.8	—
108		240	95.0	—
109		480	95.1	2.77
110		720	96.8	2.75
151	200	20	76.3	—
152		40	90.0	—
153		90	90.5	—
154		180	90.4	—
155		360	91.5	2.56
156	230	10	89.6	—
157		30	89.5	—
158		60	89.4	—
159		180	88.9	2.31

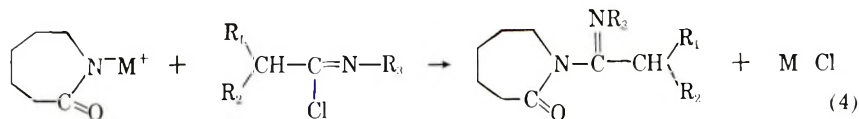
^a Catalyst: K, 2.0 mole-%; co-catalyst: *N*-(*n*-butyl)- α -ethylcaproimino chloride, 1.0 mole-%.

DISCUSSION

The reaction mechanisms are discussed as follows. Alkali metals are reacted with ϵ -caprolactam, giving alkali salts of ϵ -caprolactam as shown in eq. (3):

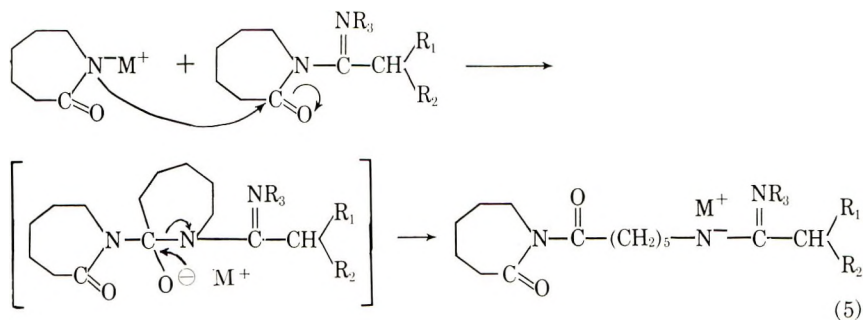


where M denotes an alkali metal. These salts act as catalysts for the anionic polymerization of ϵ -caprolactam.¹⁵ It is presumed that imino chloride reacts with the salt of ϵ -caprolactam to give *N*-imidoyl lactam as shown in eq. (4). A precipitate of alkali metal chloride was observed in the polymerization system. The action of imino chlorides which shortened the induction period before polymerization and made the polymerization proceed rapidly, are probably due to the formation of *N*-imidoyl lactam as in eq. (4):



where R_1, R_2 and R_3 are hydrocarbon radicals such as alkyl and allyl. *N*-Imidoyl lactams are as reactive as *N*-acyl lactams, and these lactam rings are expected to open very easily. As shown in eq. (5), it is supposed that the carbonyl group of *N*-imidoyl lactam is attacked by a lactam anion,

followed by ring opening of the *N*-imidoyl lactam and formation of a new *N*-acyl lactam. Furthermore, it is considered that the *N*-acyl lactam formed is also attacked by a lactam anion, followed by ring opening of the *N*-acyl lactam and addition of a new anionic lactam, and thus the propagation to a polymer proceeds continuously by stepwise addition of anionic lactams.¹⁴⁻¹⁹



A metal cation adding to a polymer transfers to a lactam and a proton is then transferred from lactam to polymer, and thus a new iminium salt of lactam is formed.

The author takes this opportunity to thank Mr. T. Sakamoto and Mr. S. Wakano for permission to publish this report.

References

- Mottus, E. H., R. M. Hedrick, and J. M. Butler, U. S. Pat. 3,017,391 (1962); J. M. Butler, R. M. Hedrick, and E. H. Mottus, U. S. Pat. 3,017,392 (1962); Imperial Chemical Industries, Brit. Pat. 908,220 (1962).
- Wichterle, O., Brit. Pat. 904,229 (1962).
- Barnes, C. E., W. O. Ney, Jr., and W. R. Nummy, U. S. Pat. 2,809,958 (1957); Arnold Hoffman & Co., Brit. Pats. 749,332 and 754,944 (1956); Badische Anilin-u. Soda Fabrik, Brit. Pat. 868,808 (1961).
- Black, W. B., and H. G. Clark, U. S. Pat. 2,912,415 (1959).
- Lautenschlager, H., H. Friederich, W. Schmidt, and K. Dachs, U. S. Pat. 2,907,755 (1959).
- Butler, J. M., R. M. Hedrick, and E. H. Mottus, U. S. Pat. 3,028,369 (1962).
- Schnell, H., and G. Fritz, U. S. Pat. 3,015,652 (1962); H. Schnell, and J. Nentwig, U. S. Pat. 3,061,592 (1962).
- Bayer, Brit. Pat. 945,218 (1963).
- Imperial Chemical Industries, Brit. Pats. 924,453 (1963); 931,013 (1963); 931,393 (1963); 931,394 (1963).
- Mottus, E. H., and R. M. Hedrick, U. S. Pat. 3,086,962 (1963); Monsanto Chemical Co., Brit. Pat. 921,047 (1963); Badische Anilin u. Soda Fabrik, Brit. Pat. 921,278 (1963); Imperial Chemical Industries, Brit. Pat. 944,307 (1963).
- du Pont, Brit. Pat. 955,917 (1964).
- Yasumoto, T., *J. Polymer Sci.*, in press.
- Stevens, C. L., and J. C. French, *J. Am. Chem. Soc.*, **75**, 657 (1953); *ibid.*, **76**, 4398 (1954).
- Yoda, N., and A. Miyake, *J. Polymer Sci.*, **43**, 117 (1960).
- Wichterle, O., J. Sebenda, and J. Kralicek, *Fortsch. Hochpolymer-Forsch.*, **2**, 578 (1961).

16. Heikens, D., *Makromol. Chem.*, **18**, 62 (1956).
17. Kurland, R. J., and E. B. Wilson, Jr., *J. Chem. Phys.*, **27**, 585 (1957).
18. Murahashi, S., H. Yuki, and H. Sekiguchi, *Ann. Repts. Inst. Fiber Chem. Osaka Univ.*, **10**, 88, 93 (1957).
19. Hall, H. K., Jr., *J. Am. Chem. Soc.*, **80**, 6404 (1958).

Résumé

On a trouvé que les chlorhydrates d'imine peuvent être utilisés comme catalyseur de la polymérisation alcaline des ϵ -caprolactames. Par addition d'un chlorhydrate d'imine, il est possible de réduire la période d'induction précédant la polymérisation qui se déroulera rapidement à une température moindre, inférieure au point de fusion du polymère. On propose un mécanisme pour la polymérisation anionique des ϵ -caprolactames par les métaux alcalins et un chlorhydrate d'imine; il comporte la formation d'une *N*-imidoyl-lactame réactive et une propagation de chaîne par une addition par étape des lactames anioniques à la fin de la molécule qui polymérise. Pour une concentration en chlorhydrate d'imine croissante, le rendement et la viscosité relative augmentent légèrement mais pour des quantités équimoléculaires ou supérieures en chlorhydrate d'imine par rapport au métal alcalin, l' ϵ -caprolactame reste non polymérisé.

Zusammenfassung

Iminochloride erwiesen sich als brauchbare Katalysatoren für die alkalische Polymerisation von ϵ -Kapolaktam. Durch Zusatz eines Iminochlorids kann die Induktionsperiode vor der Polymerisation abgekürzt werden und die Polymerisation verläuft rasch bei niedriger Temperatur unterhalb des Schmelzpunktes des Polymeren. Ein Mechanismus für die anionische Polymerisation von ϵ -Koprolaktam mit Alkalimetall und einem Iminochlorid unter Bildung eines reaktionsfähigen *N*-Imidoyllaktams und Kettenwachstum durch schrittweise Addition von anionischen Laktamen an ein Molekülende wird vorgeschlagen. Die Polymerisationsbedingungen wurden sorgfältig untersucht. Bei steigender Iminochloridkonzentration nehmen Umsatz und relative Viskosität etwas zu, bei äquimolaren Mengen von Iminochlorid und Alkalimetall oder einer höheren Konzentration an Iminochlorid als derjenigen an Alkalimetall konnte jedoch ϵ -Kapolaktam nicht polymerisiert werden.

Received March 19, 1965

Revised April 22, 1965

Prod. No. 4745A

Interactions in Binary Polymer Systems

G. R. WILLIAMSON and B. WRIGHT, *Shell Chemical Company Limited, Carrington Plastics Laboratory, Carrington, Urmston, Manchester, England*

Synopsis

Dilute solution viscosity measurements have been made on eleven ternary polymer systems (two polymers, one solvent). Calculation of the polymer-polymer interaction coefficient between unlike polymer molecules by the Krigbaum and Wall treatment is not generally applicable. The empirical relationship derived by Catsiff and Hewitt has been used, and the interaction between polymers in these systems has been qualitatively interpreted on this basis.

Introduction

In recent years a number of blends of different polymers have become commercially important. In many of these products the existence of chemically grafted units is of major importance in providing adhesion between the two polymer types, e.g. high-impact polystyrenes. Interesting products can be formed from two polymers without requiring the formation of a chemical graft, but where weaker secondary forces such as the hydrogen bond, play a dominant part.

There are many examples of ternary systems (two polymers, one solvent) in which the interaction between the different polymers is so strong that a polymer adduct can be isolated and which has properties quite different from either parent polymer. A famous example was the so-called pH muscle system described by Kuhn.^{1,2} A product was obtained containing 70-50% poly(vinyl alcohol) (PVA) and 30-50% poly(acrylic acid) (PAA) from an aqueous solution containing equal quantities of PVA and PAA. The product isolated was no longer water soluble. Strips of this material when immersed in water could be made to dilate at high pH, and contract at low pH, simulating muscle action.

An interaction product formed between PAA and high molecular weight poly(ethylene oxide) (PEO, Union Carbide Polyox) has been fully described.^{3,4} The interaction product is insoluble in water and its properties are different from either parent polymer.

Nylon has also been shown to complex with PAA, and afterwards the excess PAA can be dissolved away, leaving a three-dimensional web of nylon, spot welded with PAA.⁵ A suggested commercial application was to use the interaction product as a warp size to prevent machine shutdown in nylon spinning caused by fuzz balls formed from loose ends and fibrillation of the fiber.

We have examined a number of other mixed polymer (ternary) systems. In some systems, mixing solutions of different polymers produced an immediate precipitate—a behavior similar to the examples described. Several mixed polymer systems examined in solution, did not develop a precipitate or a turbidity, and it was of interest to show whether polymer interaction occurred in these cases.

Information regarding polymer-solvent interactions can be obtained from solution viscosity measurements, and it seemed likely that similar measurements on mixed polymer solutions could show the presence of interactions between the different polymers.

Experimental

We measured the reduced specific viscosity of single and mixed polymer systems over a range of concentrations up to 0.01 g./ml. at 25°C., using an Ubbelohde type viscometer.

Most of the polymers used were commercial samples, and no attempt was made during this investigation to characterize the materials. Poly(acrylic acid) and poly(methacrylic acid) were made in the laboratory by bulk polymerization with benzoyl peroxide as catalyst.

Results and Discussion

In order to analyze the viscosity behavior of binary polymer systems for interactions it is necessary to have an equation which predicts the behavior of an ideal system. For this purpose we have considered the following two expressions.

Krigbaum and Wall⁶ developed the following equation for ideal mixed polymer solutions:

$$\eta_{sp,m} = [\eta_1]c_1 + [\eta_2]c_2 + b_{11}c_1^2 + b_{22}c_2^2 + 2\sqrt{b_{11}b_{22}}c_1c_2 \quad (1)$$

where $\eta_{sp,m}$ is the specific viscosity of the mixed polymer solution; $[\eta_1]$ and $[\eta_2]$ are intrinsic viscosity of polymer components 1 and 2, respectively; c_1 and c_2 are concentrations of components 1 and 2, respectively, in the mixed polymer solution; and b_{11} and b_{22} are specific interaction coefficients of components 1 and 2 in single polymer solutions.

Catsiff and Hewett,⁷ on the other hand, developed a completely empirical equation

$$\eta_{sp,m} = [c_1(\eta_{sp,1})_c + c_2(\eta_{sp,2})_c]/c \quad (2)$$

where $\eta_{sp,m}$ is the specific viscosity of the mixed polymer solution; $(\eta_{sp,1})_c$ and $(\eta_{sp,2})_c$ are specific viscosities of polymer components 1 and 2, respectively, at a concentration of $c = c_1 + c_2$; and c_1 and c_2 are concentration of components 1 and 2, respectively.

Although this relationship does not have any theoretical justification as a definition of ideal behavior, using (2) Catsiff and Hewett showed that $\eta_{sp,m}$ could be quantitatively predicted for mixed polymer solutions of a methac-

rylate copolymer containing lauryl, stearyl, or methyl methacrylate and a small quantity of 2-methyl-5-vinylpyridine, and polyisobutylene in mineral oil. Now, in the case of polymers whose solutions behavior is described by the familiar Huggins equation,⁸

$$\eta_{sp}/c = [\eta] + k[\eta]^2c \quad (3)$$

and if we put $k[\eta]^2 = b$, a term which arises from polymer interactions at finite concentrations, eq. (2) may be expanded into the form

$$\eta_{sp,m} = [\eta_1]c_1 + [\eta_2]c_2 + b_{11}c_1^2 + b_{22}c_2^2 + (b_{11} + b_{22})c_1c_2 \quad (4)$$

Equation (4) is identical to eq. (1) except for the coefficient of the c_1c_2 term. This is the polymer-polymer interaction term in which we are especially interested.

For mathematical convenience, Krigbaum and Wall defined the inter-specific interaction coefficient for ideal behavior of mixed polymer solutions as

$$b_{12} = \sqrt{b_{11}b_{22}} \quad (5)$$

For eq. (4) the coefficient now becomes

$$b_{12} = (b_{11} + b_{22})/2 \quad (6)$$

The definition of the ideal b_{12} according to eq. (5) suffers from a serious difficulty. Occasionally b_{11} or b_{22} may be negative (as for example in the case of poly(methacrylic acid) in water) in which case b_{12} is imaginary. Clearly, the definition is useless in such circumstances. We are then forced to use eq. (6) as the definition of ideal behavior throughout our work, despite its empirical basis.

An alternative definition of ideal solution behavior may be obtained by considering the intrinsic viscosity of the mixed polymer solution. Here, it makes no difference whether we base our definition on the equations of Krigbaum and Wall or of Catsiff and Hewett. Both equations lead to:

$$(\eta_{sp,m}/c)_{c \rightarrow 0} = [\eta_1](c_1/c)_{c \rightarrow 0} + [\eta_2](c_2/c)_{c \rightarrow 0} \quad (7)$$

Thus, the intrinsic viscosity of a mixture of two polymers is the weight average of the intrinsic viscosities of the two polymers taken separately. In our examination of mixed polymer solutions we have used eq. (6) and (7) as criteria of ideal behavior. Table I shows the observed and calculated [from eq. (2)] values of $(\eta_{sp,m}/c)_{c \rightarrow 0}$ and b_{12} for eleven mixed polymer systems. According to the magnitude of the deviations from ideal behavior, these systems can be divided into four classes (see Table I).

Class a. Systems in class a show near ideal behavior. Thus, for example, Figure 1 shows how the viscosity of a mixture of styrene-acrylonitrile copolymer and poly(methyl methacrylate) in methyl ethyl ketone depends on concentration. Interaction in these cases is judged to be very slight.

TABLE I
Observed and Calculated Intrinsic Viscosities of Mixing $(\eta_{sp,m}/c)_{c \rightarrow 0}$ and the Polymer-Polymer Interaction Coefficient b_{12} for Several Mixed Polymer Systems at 25°C. and concentration range 0-0.01 g./ml.

Polymer system ^a	$(\eta_{sp,m}/c)_{c \rightarrow 0}$		b_{12}	
	Observed	Calculated from eq. (2)	Observed	Calculated from eq. (2)
Class a				
SANC + PMMA in MEK	0.52	0.47	0.02	0.10
SANC + PEVE in MEK	0.40	0.36	0.03	0.09
PEVE + PMMA in dioxane	0.19	0.17	0.05	0.03
PVA + PEI in water	0.50	0.40	0.08	0.32
PVP + PEVE in dioxane	0.27	0.33	0.11	0.11
Class b				
PAA + PVA in water	>2.0	0.53	Curve of negative slope	Curve of positive slope
PMAA + PVA in water	0.27	0.58	0.02	0.24
Class c				
PEO + PEI in water	1.20	0.52	0.32	1.23
PEO + PVA in water	1.50	0.78	Curve of positive slope	1.58
Class d				
PVP + SANC in dioxane	≈0.9	0.66	0.17 ^b	0.17
PVP + PMMA in dioxane	≈1.1	0.48	-0.02 ^b	0.07

^a Abbreviations: SANC = styrene-acrylonitrile copolymer; PMMA = poly(methyl methacrylate); PEVE = poly(vinyl ethyl ether); PVA = poly(vinyl alcohol); PEI = poly(ethylene imine); PVP = poly-2-vinylpyridine; PAA = poly(acrylic acid); PMAA = poly(methacrylic acid); PEO = poly(ethylene oxide). ^b Concentration 0.005-0.01 g./ml.

Class b. The polymer systems in class b show large deviations from ideality, as is seen from Figure 2, for example, which describes the behavior of poly(acrylic acid) and poly(vinyl alcohol) in water. These systems usually become turbid at concentrations higher than 0.02 g./ml. They are judged to interact strongly.

Class c. Mixed polymer systems in class c show smaller deviations from ideal behavior than class b systems, as shown for example in Figure 3 for the poly(ethylene oxide)/poly(ethylene imine)/water system. Interaction is considered to be small in these systems.

Class d. Finally, the remaining two systems placed in class d show ideal behavior at concentrations above 0.005 g./ml., but deviate strongly at lower concentrations, as shown in Figure 4. The apparently ideal behavior at higher concentrations may, we feel, be fortuitous.

In all cases where the systems were apparently non-ideal the value of $(\eta_{sp,m}/c)_{c \rightarrow 0}$ was higher than the ideal value, with the exception of the poly(methacrylic acid)/poly(vinyl alcohol)/water system which gave a lower value. It appears, therefore, that reduced specific viscosity measurement may give some qualitative information about interaction between polymers,

in that large deviations from ideal behavior (as defined by Catsiff and Hewett) may be interpreted as signs of polymer interaction. Quantitative explanations for the deviations observed, such as very low or negative

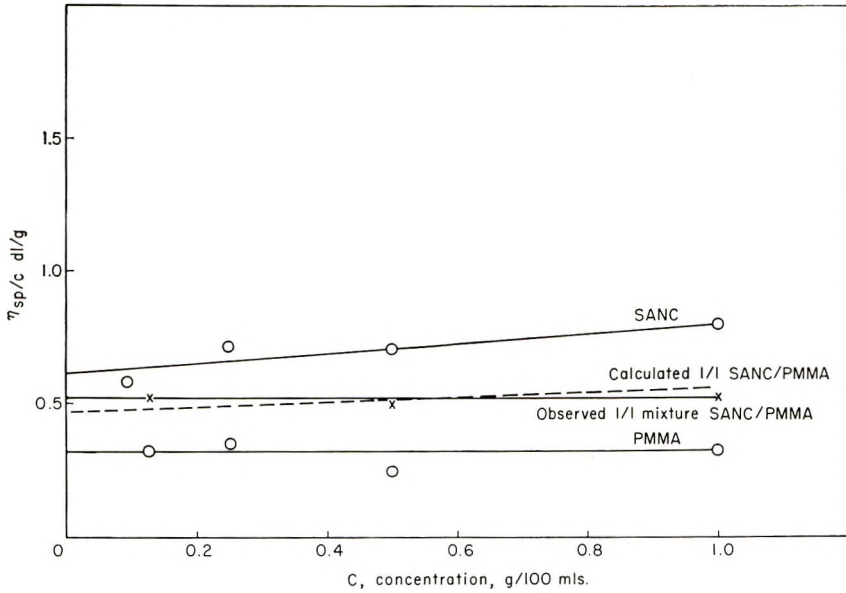


Fig. 1. Reduced specific viscosities of styrene-acrylonitrile copolymer (SANC), poly(methyl methacrylate) (PMMA), and SANC/PMMA mixture in methyl ethyl ketone (25°C.).

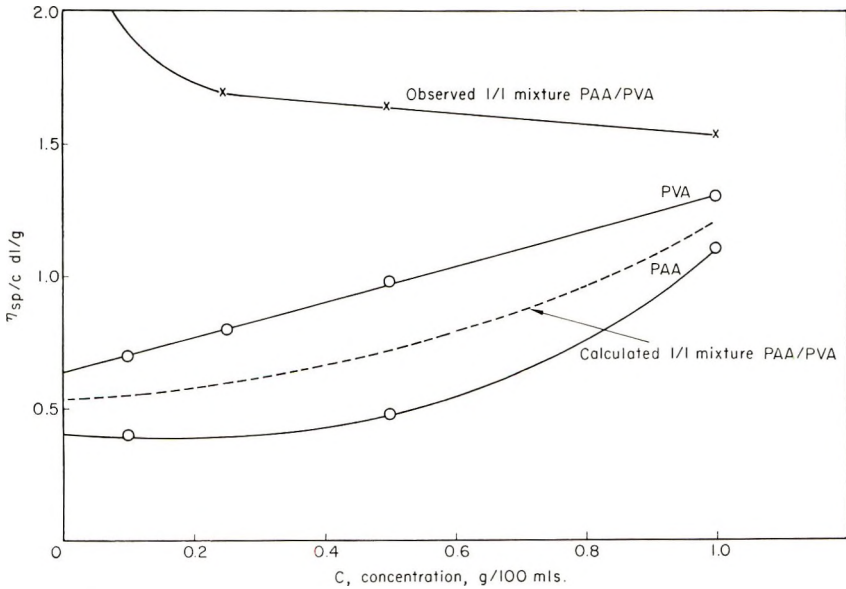


Fig. 2. Reduced specific viscosities of poly(acrylic acid) (PAA), poly(vinyl alcohol) (PVA), and PAA/PVA mixture in water (25°C.).

values of b_{12} (which is probably associated with polyelectrolyte behavior), and the nonideal value of $(\eta_{sp,m}/c)_{c \rightarrow 0}$ would require a much fuller and more detailed examination.

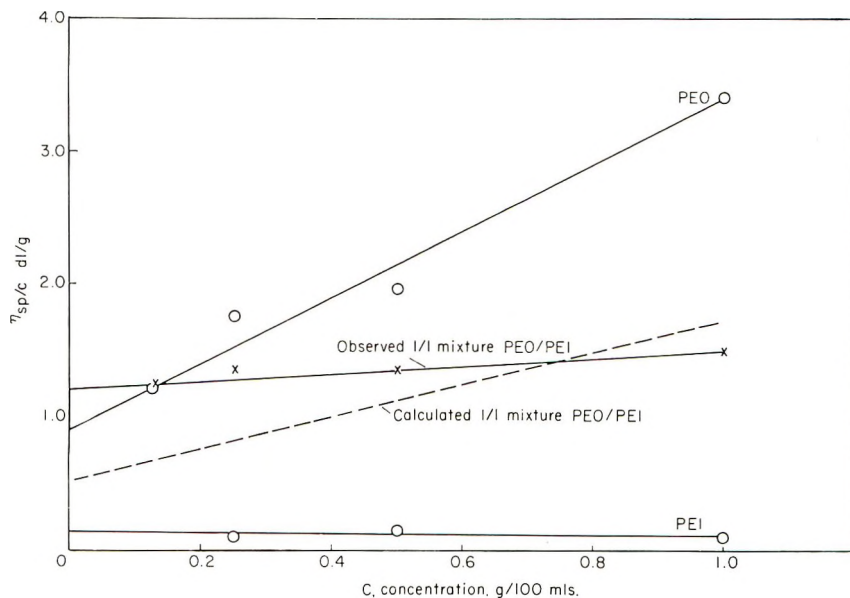


Fig. 3. Reduced specific viscosities of poly(ethylene oxide) (PEO), poly(ethylene imine) (PEI), and PEO/PEI mixture in water (25°C.).

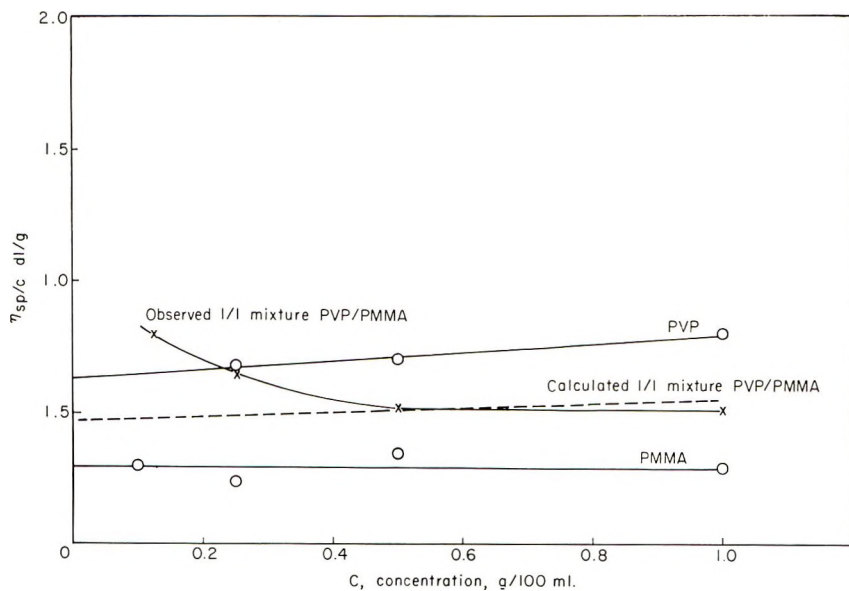


Fig. 4. Reduced specific viscosities of poly-2-vinylpyridine (PVP), poly(methyl methacrylate) (PMMA), and PVP/PMMA mixture in dioxane (25°C.).

Conclusions

The equation of Catsiff and Hewett provides a useful reference base for determining interactions between polymers in solution. The behavior of ternary systems (two polymers, one solvent) when compared with the predictions of this equation, may be conveniently divided into four classes: class a systems show near ideal behavior; class b systems show large deviations from ideal behavior, and interactions are judged to be strong; class c systems show smaller deviations than those in class b, and interactions are considered to be small; class d systems show ideal behavior at concentrations greater than 0.005 g./ml. and show deviations from ideality below this concentration.

The authors wish to thank Shell Chemical Company Limited for permission to publish and Mrs. M. Murphy for viscosity determinations.

References

1. Kuhn, W., B. Hargitay, A. Katchalsky, and H. Eisenberg, *Nature*, **165**, 514 (1950).
2. Wassermann, A., *Size and Shape Changes of Contractile Polymers*, Pergamon Press, London, 1960, p. 42.
3. Smith, K. L., A. E. Winslow, and D. E. Petersen, *Ind. Eng. Chem.*, **51**, 1361 (1959).
4. Bailey, F. E., R. D. Lundberg, and R. W. Callard, *J. Polymer Sci.*, **A2**, 845 (1964).
5. Davidson, R. L., and M. Sittig, *Water-Soluble Resins*, Reinhold, New York, 1962, p. 143.
6. Krigbaum, W. R., and F. T. Wall, *J. Polymer Sci.*, **5**, 505 (1950).
7. Catsiff, E. H., and W. A. Hewett, *J. Appl. Polymer Sci.*, **6**, 962, S30 (1962).
8. Huggins, M. L., *J. Am. Chem. Soc.*, **64**, 2716 (1942).

Résumé

On a effectué des mesures de viscosité en solution diluée sur onze systèmes polymériques ternaires (deux polymères, un solvant). On ne peut pas appliquer d'une façon générale le calcul du coefficient d'interaction polymère-polymère entre les molécules de polymères au moyen du traitement de Krigbaum et Wall. On a employé la relation empirique déduite par Catsiff et Hewitt et sur cette base, on a interprété qualitativement l'interaction entre les polymères dans ces systèmes.

Zusammenfassung

An 11 ternären Polymersystemen (zwei Polymere, ein Lösungsmittel) wurde die Viskosität in verdünnter Lösung gemessen. Die Berechnung des Polymer-Polymerwechselwirkungskoeffizienten zwischen ungleichen Polymermolekülen nach der Methode von Krigbaum und Wall ist nicht allgemein anwendbar. Die von Catsiff und Hewitt abgeleitete empirische Beziehung wurde benützt und auf dieser Grundlage die Wechselwirkung zwischen Polymeren in diesen Systemen qualitativ interpretiert.

Received January 28, 1965

Revised May 20, 1965

Prod. No. 4760A

Determination of Degree of Crosslinking in Natural Rubber Vulcanizates. Part VII. Crosslinking Efficiencies of Di-*tert*-butyl and Dicumyl Peroxides in the Vulcanization of Natural Rubber and Their Dependence on the Type of Natural Rubber

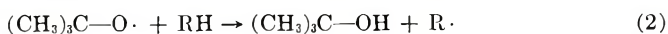
G. M. BRISTOW, C. G. MOORE, and R. M. RUSSELL,
The Natural Rubber Producers' Research Association,
Welwyn Garden City, Herts., England

Synopsis

The efficiency with which di-*tert*-butyl peroxide and dicumyl peroxide vulcanize (crosslink) natural rubber depends on the type of natural rubber. Crosslinking efficiencies of the peroxides are increased by acetone extraction of the rubber and by increasing the concentration of peroxide but in no case studied was either peroxide 100% efficient. These findings indicate that the natural rubber samples contain non rubber compounds which compete with the rubber hydrocarbon for reaction with the peroxide. The implications of these findings are: (1) that the values of chemical crosslinks determined by Moore and Watson from the yields of *tert*-butyl alcohol and methane formed when an unextracted deproteinized pale crêpe is crosslinked with di-*tert*-butyl peroxide may be overestimated; and, thus, (2) the calibration of Mullins which relates the number of chemical crosslinks in a natural rubber-peroxide vulcanizate to the number of physically manifested crosslinks may require revision.

I. INTRODUCTION

On the basis of the chemistry of interaction of di-*tert*-butyl peroxide with monoolefins and low molecular weight polyisoprenes,¹ Moore and Watson² proposed the reaction sequence (1)–(6) for the vulcanization of natural rubber with di-*tert*-butyl peroxide at 110–140°C. *in vacuo*:



where RH is natural rubber hydrocarbon (*cis*-1,4-polyisoprene), H is an α -methylene or α -methyl hydrogen atom, and, therefore, R \cdot is a polyisoprenyl radical.

The chemistry of vulcanization of natural rubber with dicumyl peroxide, $C_6H_5C(CH_3)_2-O-O-C(CH_3)_2C_6H_5$, will be similar to that described above for vulcanization with di-*tert*-butyl peroxide.

The combination of polyisoprenyl radicals according to eq. (6) constitutes the crosslinking of the natural rubber hydrocarbon. If it is assumed that this is the sole fate of the polyisoprenyl radicals, then the number of chemical crosslinks produced in the rubber network is equal to $1/2$ (number of molecules of *tert*-butyl alcohol + methane) formed and can be determined, therefore, from the yields of *tert*-butyl alcohol and methane produced in the vulcanization process. Evidence for the validity of the above assumption was obtained from the model olefin experiments cited above^{1,2} and was subsequently confirmed by Parks and Lorenz,³ who showed that the diisoprenyl radicals ($C_{10}H_{17}\cdot$) derived from the reaction of 2,6-dimethyl octa-2,6-diene ($C_{10}H_{18}$) with dicumyl peroxide underwent quantitative dimerization.

A possible complication considered by Moore and Scanlan⁴ was permanent unimolecular scission of the polyisoprenyl radicals ($R\cdot$) derived from natural rubber. This would lead to a loss in chemical crosslinks and thus to an overestimate of the number of crosslinks as deduced from the amounts of *tert*-butyl alcohol and methane formed. However, recent reliable estimates based on sol-gel analysis of dicumyl peroxide-natural rubber vulcanizates indicate that permanent scission of polyisoprenyl radicals is insignificant.^{5,6}

On the basis of the above evidence, confidence has been placed in the estimates of chemical crosslinks based on the yields of *tert*-butyl alcohol and methane formed when an unextracted deproteinized pale crêpe natural rubber sample is vulcanized with di-*tert*-butyl peroxide *in vacuo*.² The values of chemical crosslinks in the vulcanizates were related to the equilibrium swelling values of the vulcanizates in *n*-decane² and to their stress-strain properties^{7,8} and thus a calibration was established between the number of chemical crosslinks and the number of physically manifested crosslinks in natural rubber-peroxide vulcanizates.⁸

The present paper reports data which show that the efficiency with which di-*tert*-butyl peroxide or dicumyl peroxide crosslink natural rubber depends on: (1) the type of natural rubber used; (2) whether the rubber is unextracted or acetone-extracted before vulcanization; and (3) the concentration of peroxide. In particular, it is shown that the actual sample of unextracted deproteinized pale crêpe used by Moore and Watson² is less efficiently crosslinked than the other types of natural rubber used here. The reasons for and implications of these findings are considered, and it is concluded that some revision is probably required of the estimates of chemical crosslinks as made by Moore and Watson² and thus of the calibration of Mullins⁸ relating chemical and physical crosslinks. It is further concluded that the equating of chemical crosslinks formed to the amount of dicumyl peroxide decomposed during the press vulcanization of natural rubber^{9,10} is not universally valid for all types of natural rubber.

II. EXPERIMENTAL METHODS AND MATERIALS

Materials

Di-*tert*-butyl peroxide (Laporte Chemical Co. Ltd.) was purified by distillation as described by Moore and Watson.² Gas-liquid chromatographic analysis showed the product to be >99.5% pure, and infrared spectrometric analysis indicated the absence of carbonyl and hydroxyl groups. Dicumyl peroxide was purified by recrystallization of the commercial product (Hercules Powder Co.) from ethanol. The product melted at 39.5°C. and was shown by infrared spectrometric analysis to be devoid of carbonyl and hydroxyl groups.

Four types of natural rubber were used: (1) yellow circle grade RSS1 (N, 0.40%); (2) No. IX pale crêpe (sample A: N, 0.35%; Sample B: N, 0.35%); (3) "A highly purified rubber" (United States Rubber Co.) (N, 0.03%); and (4) deproteinized pale crêpe (N, 0.09%) from the batch used by Moore and Watson.² Some measure of purification of these rubbers was effected by hot acetone extraction for 24 hr. in the dark under oxygen-free nitrogen, followed by drying the extracted rubber to constant weight *in vacuo*. In no case did this treatment decrease the nitrogen content of the rubber.

Sol and gel fractions of some of the above rubbers were obtained by swelling the acetone-extracted unmastered rubbers in cyclohexane for 48 hr. at room temperature in the dark in the absence of air. The gel fraction was obtained by drying to constant weight *in vacuo* that portion of the swollen rubber which was retained on filtration of the swollen rubber through a lens tissue; the sol fraction was recovered from the filtrate by freeze drying.

For purposes of comparison a synthetic high *cis*-1,4-polyisoprene was used; this was sample of Natsyn 200 (Goodyear Tire and Rubber Co.) which was shown by infrared spectrometry to be devoid of $\text{CH}_2=\text{CHR}$ groups and to contain 2% $\text{CH}_2=\text{CRR}'$ groups. Samples of the Natsyn 200 were extracted by the same procedure as was used for natural rubber.

Vulcanization Procedure

In order to permit accurate determinations of the crosslinking efficiencies of the peroxides to be made, the vulcanization procedure must allow the quantitative and homogeneous incorporation of the peroxides in the rubber followed by vulcanization under completely anaerobic conditions with 100% retention of the peroxides in the rubber. The extent to which these requirements can be fulfilled depends upon the nature of the peroxide used. Further, it is desirable that the time and temperature of vulcanization should be such as to lead to complete decomposition of the peroxide; this avoids the necessity of estimating the amount of peroxide decomposed either by direct determination of unreacted peroxide or indirectly from kinetic data of rates of peroxide decomposition.

Vulcanization with Di-*tert*-butyl Peroxide. The procedure adopted was that previously used by Moore and Weston,² in which the vulcanization reaction is effected *in vacuo*. This permits quantitative introduction of the peroxide into the reaction vessel and anaerobic vulcanization, but does not permit complete retention of the volatile peroxide in the rubber. However, by vulcanizing equal weights and sizes of the different types of rubber simultaneously in the same vessel an estimate of relative crosslinking efficiencies for the several rubbers is possible, although the absolute crosslinking efficiencies are not significant.

Masticated samples of the rubbers were obtained by several passes through the tight nip of a laboratory mill at ca. 45°C. Viscosity data for the rubbers were obtained at this stage. Flat, bubble-free sheets were then obtained by molding the masticated rubber for one minute in aluminum mold frames between sheets of cellophane in a press at 110°C.

Accurately weighed pieces of identical weight (1 g.) and size of each type of rubber were cut from the molded sheets and placed together in a 25-ml. flask which was then evacuated overnight at $<10^{-5}$ mm. Hg pressure. By using the procedure of Moore and Watson,² a known weight of di-*tert*-butyl peroxide was distilled *in vacuo* onto the rubber samples in the flask which was then sealed at a pressure of $<10^{-5}$ mm. Hg. The rubber was allowed to imbibe the peroxide for at least 16 hr. at room temperature, and then vulcanization was effected by heating the samples for 70 hr. at 140°C. in a silicone oil bath. Published data^{2,11} indicate that these conditions lead to $>99.9\%$ decomposition of the peroxide.

Vulcanization with Dicumyl Peroxide. The most convenient way found for incorporating dicumyl peroxide into the rubber was by mill mixing. The rubber was slightly masticated on a laboratory mill at ca. 45°C., and a known weight of peroxide was then incorporated into the weighed rubber samples either by direct addition of the solid peroxide or as a rubber-peroxide masterbatch. The compounded rubber was then rolled up and passed endwise several times through the tight nip of the mill to ensure complete dispersion of the peroxide. Viscosity data for the rubber component of the mixes were obtained at this stage, corrections being applied for the amounts of peroxide present. Vulcanization was effected by heating the rubber mixes in 2-mm.-thick mold frames between sheets of cellophane for 2 hr. at 150°C. in a steam-heated press. Published data¹⁰ indicate that the peroxide is $>99.9\%$ decomposed under these conditions, and this was confirmed by the constancy of the equilibrium swelling values in *n*-decane of vulcanizates prepared by heating mixes at 150°C. for 105–185 min.

The possibility exists that the above vulcanization conditions are not completely anaerobic and thus that some oxidative degradation of the rubber chains occurs during the vulcanization process. Evidence that such oxidative degradation is not significant is: firstly, that only small viscosity changes are produced when typical masticated rubbers are subjected to the press vulcanization conditions in the absence of dicumyl peroxide (Table I), although if the observed viscosity changes are due to

atmospheric oxygen then somewhat greater changes might be anticipated when dicumyl peroxide is present; secondly, that the deliberate inclusion of air during the vulcanization process by only partially filling the mold produces vulcanizates which exhibit only slight surface degradation; and finally and most compellingly, that the application of sol-gel analysis to natural rubber-dicumyl peroxide vulcanizates prepared under press conditions indicates insignificant amounts of main-chain scission.^{5,6}

TABLE I
Effect on the Viscosity of Natural Rubber of Press Heating of Rubber for 2 Hr. at 150°C.

Natural rubber type	[η] _{toluene} at 25°C., dl./g.			
	Unextracted rubber		Extracted rubber	
	Control	Heated	Control	Heated
RSS1	2.32	2.64	2.72	2.86
Pale crêpe	2.67	2.53	1.90	2.26 ^a
Highly purified rubber	3.04	3.33	2.95	2.92

^a Some gel produced on heating.

Attempts were made to devise alternative methods to those described above to ensure quantitative incorporation of the peroxide in the rubber and to achieve anaerobic vulcanization. These proved to be impractical. Thus, the peroxide was added to the rubber by solvent imbibition from petroleum ether (b.p. 30–40°C.), followed by removal of the solvent *in vacuo*. However, despite the relatively high volatility of the solvent it could not be removed completely without some loss of peroxide from the rubber. Conducting the vulcanization process *in vacuo* as with the di-*tert*-butyl peroxide-natural rubber system also led to loss of peroxide as judged by the lower crosslinking efficiency observed with this method as compared with the mill mixing and press vulcanization procedure.

Determination of Number-Average Molecular Weights (\bar{M}_n) of Rubbers Prior to Vulcanization

The limiting viscosity numbers [η] of the rubbers were determined in toluene at 25°C. by use of Ubbelohde suspended level viscometers. [η] values in toluene were converted into [η] values in benzene (in deciliters per gram) by means of the relationship:

$$[\eta]_{\text{toluene}} = 1.076 [\eta]_{\text{benzene}} - 0.15 \quad (7)$$

and from these, values of \bar{M}_n were derived by using the relationship:¹²

$$[\eta]_{\text{benzene}} = 2.29 \times 10^{-7} \bar{M}_n^{1.33} \quad (8)$$

Natsyn 200 was assumed to conform to eqs. (7) and (8) which were derived for cold-masticated natural rubber.

Determination of Degree of Chemical Crosslinking ($^{1/2}M_{c, \text{chem}}^{-1}$) of Vulcanizate Networks and Crosslinking Efficiencies of the Peroxides

The vulcanizates were allowed to swell to equilibrium in a considerable excess of *n*-decane at 25°C. in the dark and the swollen weights measured after 48 hr. After removal of most of the *n*-decane by deswelling in acetone, final drying to constant weight was carried out *in vacuo* in the dark at 70°C. Equilibrium values of v_r , the volume fraction of rubber network in the swollen vulcanizate network, were calculated from the swollen and deswollen weights of the vulcanizate networks and use of the values of 0.910 and 0.725 g./ml. for the densities of the rubber network and *n*-decane, respectively, at 25°C. The empirical relationship reported by Mullins⁸ for natural rubber vulcanizate networks produced by vulcanization with di-*tert*-butyl peroxide or dicumyl peroxide was used to derive values of the elastic constant C_1 from the v_r values, and then values of $^{1/2}M_{c, \text{chem}}^{-1}$ (gram-moles of chemical crosslinks per gram of rubber network) were derived from the equation:⁸

$$C_1 = (^{1/2}\rho RT M_{c, \text{chem}}^{-1} + 0.78 \times 10^6)(1 - 2.3 M_{c, \text{chem}} \bar{M}_n^{-1}) \quad \text{dynes/cm.}^2 \quad (9)$$

where ρ is the network density, R the gas constant, T the absolute temperature, \bar{M}_n the number-average molecular weight of the rubber prior to vulcanization, and $M_{c, \text{chem}}$ the number-average molecular weight of the chain segments between crosslinks in the network.

The crosslinking efficiency of the peroxides, expressed as a percentage, is defined as:

$$(^{1/2}M_{c, \text{chem}}^{-1} / [\text{Peroxide}]_{\text{decomposed}}) \times 100$$

III. RESULTS

Table II records the crosslinking efficiencies of di-*tert*-butyl peroxide in the vulcanization of various types of natural rubber and a synthetic *cis*-1,4-polyisoprene (Natsyn 200) *in vacuo* at 140°C. The absolute crosslinking efficiencies are of limited significance, since some of the peroxide will have decomposed in the gas phase and will therefore not be available for crosslinking purposes; however, relative crosslinking efficiencies can be derived therefrom taking the unextracted deproteinized pale crêpe as used by Moore and Watson² as leading to a peroxide efficiency of 100%. The data show: (1) that the unextracted deproteinized pale crêpe is crosslinked less efficiently than the other types of natural rubber and Natsyn 200; (2) removal of nonrubber material from the rubbers by acetone extraction leads to a marked increase in the crosslinking efficiency of the peroxide, but the extent of the increase depends on the type of rubber; and (3) increase in the peroxide concentration increases the efficiency of the crosslinking process in all cases.

TABLE II
 Crosslinking Efficiency of Di-*tert*-butyl Peroxide in the Vulcanization of Natural Rubber and Natsyn 200 (70 Hr. at 140°C. *in vacuo*)

Expt. no.	Peroxide concentration, g.-mole/g. rubber $\times 10^5$	Rubber type	[η] toluene (25°C.), dl./g.	$\bar{M}_n \times 10^{-5}$	v_r (<i>n</i> -decane, 25°C.)	$1/2 M_c$, chem. $\times 10^5$, g.-mole chemical crosslinks/g. rubber network	Crosslinking efficiency of peroxide, %	Relative crosslinking efficiency of peroxide, %
1	8.20	Unextracted RSSI	3.50	2.51	0.2916	4.57	55	108
		" pale crêpe (Sample B)	4.01	2.81	0.2863	4.34	52	102
		" Natsyn 200 deproteinized	2.84	2.11	0.3006	5.22	63	124
2	4.66	" pale crêpe	2.71	2.03	0.2798	4.19	51	100
		Extracted RSSI	4.16	2.88	0.2675	3.24	70	140
		" pale crêpe (Sample B)	3.80	2.60	0.2663	3.39	73	146
		" Natsyn 200 deproteinized	2.97	2.20	0.2615	3.22	69	138
		" pale crêpe	2.90	2.15	0.2473	2.65	57	114
		Unextracted deproteinized	2.71	2.03	0.2365	2.32	50	100
3	8.22	Extracted RSSI	4.16	2.88	0.3371	7.18	87	124
		" pale crêpe (Sample B)	3.80	2.60	0.3374	7.26	88	126
		" Natsyn 200 deproteinized	2.97	2.20	0.3322	7.11	87	124
		" pale crêpe	2.90	2.15	0.3214	6.45	79	113
		Unextracted deproteinized	2.71	2.03	0.3085	5.73	70	100

TABLE III
 Crosslinking Efficiency of Dicumyl Peroxide in the Press Vulcanization of Natural Rubber (2 Hr. at 150°C.)

Rubber type	Peroxide concentration, g.-mole/g. rubber $\times 10^5$	$[\eta]$ toluene (25°C.), dl./g.	$\bar{M}_n \times 10^{-5}$	v_r (<i>n</i> -decane, 25°C.)	$\frac{1}{2}M_c$, chem. $\times 10^5$, g.-mole chemical crosslinks/g. rubber network	Crosslinking efficiency of peroxide, %
Unextracted RSSI	5.56	2.17	1.76	0.2688	3.82	69
	7.41	1.91	1.60	0.2980	5.19	70
Extracted RSSI	11.11	1.95	1.63	0.3438	8.21	74
	3.70	2.02	1.67	0.2487	3.02	82
	6.30	1.99	1.65	0.2952	5.26	84
	7.41	1.95	1.63	0.3166	6.50	88
Unextracted pale crêpe (Sample A)	11.11	2.08	1.71	0.3744	10.57	95
	3.70	3.22	2.37	0.2211	1.68	45
Unextracted pale crêpe (Sample B)	7.41	3.03	2.25	0.2760	3.76	51
	7.41	1.91	1.60	0.2858	4.80	65
Extracted pale crêpe (Sample A)	11.11	1.95	1.63	0.3345	7.63	69
	1.83	3.87	2.71	0.1984	1.13	62
	3.70	4.00	2.78	0.2574	2.75	74
Unextracted deproteinized pale crêpe	5.55	3.36	2.44	0.2852	4.16	75
	7.41	3.84	2.69	0.3211	6.25	84
	7.41	1.91	1.60	0.2858	4.80	65
	11.11	2.08	1.71	0.3332	7.48	67

TABLE IV
Relationship Between Nitrogen Content of Natural Rubber and the Crosslinking Efficiency of Dicumyl Peroxide in the Press Vulcanization of Natural Rubber (2 Hr. at 150°C.)

Rubber Type	Nitrogen in rubber, %	Peroxide Concentration, g.-mole/g. rubber) $\times 10^6$	$[\eta]_{\text{toluene}}$ (25°C.), dl./g.	$\bar{M}_n \times 10^{-6}$	ν_r (<i>n</i> -decane, 25°C.)	$\frac{1}{2}M_{c,\text{chem.}}^{-1}$ $\times 10^6$, g.-mole chemical cross- links/g. rubber network	Crosslinking efficiency of peroxide, %
RSSI							
Extracted	0.41	3.70	3.17	2.33	0.2604	3.04	82
Sol fraction	0.27	7.41	3.68	2.61	0.3260	6.40	86
Gel fraction	0.48	3.70	2.97	2.32	0.2542	2.82	76
		7.41	3.23	2.37	0.3153	5.97	81
		3.70	3.44	2.48	0.2596	2.93	79
		7.41	3.79	2.67	0.3241	6.50	88
Pale crêpe (Sample A)							
Extracted	0.35	3.70	2.83	2.14	0.2381	2.27	61
Sol fraction	0.01	7.41	2.87	2.17	0.3125	5.85	79
Gel fraction	0.52	3.70	2.73	2.09	0.2381	2.30	62
		7.41	2.86	2.16	0.2934	4.69	63
		3.70	3.15	2.32	0.2442	2.40	65
		7.41	2.80	2.12	0.3136	5.94	80
Highly purified rubber							
Unextracted	0.03	3.70	3.90	2.73	0.2463	2.33	63
Extracted	0.03	7.41	3.62	2.58	0.3063	5.33	72
Sol fraction	<0.01	3.70	4.16	2.86	0.2601	2.84	77
Gel fraction	0.03	7.41	3.67	2.60	0.3219	6.36	86
		3.70	3.60	2.57	0.2419	2.22	60
		7.41	4.45	3.01	0.2573	2.67	72
		3.70	4.74	3.16	0.3186	6.03	81

These features are also observed for the press vulcanization of several types of natural rubber with dicumyl peroxide at 150°C. (Tables III and IV).⁹ The crosslinking efficiency values given in Tables III and IV are more significant than those of Table II, since in the press vulcanization with dicumyl peroxide there will be no loss of peroxide due to gas-phase decomposition. Despite this, the crosslinking efficiencies of dicumyl peroxide are below 100%, sometimes appreciably below this value, and they only approach 100% in the vulcanization of acetone-extracted RSS1 at high peroxide concentrations.

IV. DISCUSSION

The above results suggest that with both di-*tert*-butyl peroxide and dicumyl peroxide the derived *tert*-butoxy, cumyloxy, and methyl radicals react not only with hydrogen atoms of the rubber hydrocarbon but also with nonrubber constituents present in the rubber. Only a portion of these reactive nonrubbers appears to be readily extractable with hot acetone, and the relative amount depends on the type of rubber. For the synthetic polyisoprene, antioxidants added during manufacture and not readily removed by subsequent acetone extraction will play a similar competitive rôle to the nonrubbers present in natural rubber. The nature of the nonrubbers in natural rubber which scavenge some of the peroxide and thus lead to crosslinking efficiencies below 100% is not known. However, the data of Table IV indicate that they cannot be solely nitrogenous compounds, since there is no correlation between the crosslinking efficiencies of the peroxide and the nitrogen content of the rubber sample. The amount of reactive nonrubbers in a rubber sample must be very small ($\ll 5\%$) relative to the rubber hydrocarbon present, and thus the fact that the peroxide crosslinking efficiencies observed are appreciably below 100% indicates that nonrubbers react much more rapidly with the free radicals derived from the peroxide than does the rubber hydrocarbon. A consequence of this is that, since there will be only a limited amount of nonrubbers available, then crosslinking efficiencies should increase with increasing peroxide concentration as is observed experimentally.

If, as would seem almost inevitable, the *tert*-butoxy and methyl radicals react with the nonrubbers in the same way as they react with rubber hydrocarbon to produce *tert*-butyl alcohol and methane, then the estimates of chemical crosslinks made by Moore and Watson² will be overestimates, since they are based on the assumption that each chemical crosslink formed in the deproteinized pale crêpe used by them is to be equated with $\frac{1}{2}$ -[mols.-*tert*-BuOH + CH₄] formed. A consequence of the above is that the values of the crosslinking efficiencies of di-*tert*-butyl peroxide and dicumyl peroxide for the other rubber samples used here (Tables II, III, and IV) will also be overestimates. The present results also cast doubt on the validity of determinations of chemical crosslinks in natural rubber samples which have been based on an assumed 100% crosslinking efficiency of dicumyl peroxide in the press vulcanization of natural rubber.^{9,10}

It is concluded from the present work that a revision of the estimates of chemical crosslinks by Moore and Watson² and thus of the calibration [eq. (9)] of Mullins⁸ relating physical crosslinks to chemical crosslinks in natural rubber vulcanizates is called for. This will necessitate the use of a rigorously pure *cis*-1,4-polyisoprene, so that the rubber hydrocarbon can be guaranteed to be the sole source of the *tert*-butyl alcohol, cumyl alcohol, and methane formed on vulcanization of the rubber with di-*tert*-butyl peroxide or dicumyl peroxide.

We thank Mr. G. M. C. Higgins for the spectroscopic data in this work which forms part of the research program of The Natural Rubber Producers' Research Association.

References

1. Farmer, E. H., and C. G. Moore, *J. Chem. Soc.*, **1951**, 131, 142.
2. Moore, C. G., and W. F. Watson, *J. Polymer Sci.*, **19**, 237 (1956).
3. Parks, C. R., and O. Lorenz, *J. Polymer Sci.*, **50**, 287 (1961).
4. Moore, C. G., and J. Scanlan, *J. Polymer Sci.*, **43**, 23 (1960).
5. Scott, K. W., *J. Polymer Sci.*, **58**, 517 (1962).
6. Bristow, G. M., *J. Appl. Polymer Sci.*, **7**, 1023 (1963).
7. Mullins, L., *J. Polymer Sci.*, **19**, 225 (1956).
8. Mullins, L., *J. Appl. Polymer Sci.*, **2**, 1 (1959).
9. Lorenz, O., and C. R. Parks, *J. Polymer Sci.*, **50**, 299 (1961).
10. Thomas, D. K., *J. Appl. Polymer Sci.*, **6**, 613 (1962).
11. Raley, J. H., F. F. Rust, and W. E. Vaughan, *J. Am. Chem. Soc.*, **70**, 88, 1336 (1948).
12. Mullins, L., and W. F. Watson, *J. Appl. Polymer Sci.*, **1**, 245 (1959).

Résumé

L'efficacité avec laquelle le peroxyde de ditertiobutyle et le peroxyde de dicumyle vulcanisent le caoutchouc naturel dépend du type de caoutchouc naturel. L'efficacité de pontage des peroxydes augmentent par extraction du caoutchouc à l'acétone et par augmentation de la concentration en peroxyde, mais dans aucun des cas étudiés, l'efficacité n'atteint 100%. Les résultats indiquent que les échantillons de caoutchouc naturel contiennent des composés non-caoutchouteux qui entrent en compétition avec les hydrocarbures caoutchouteux pour la réaction avec le peroxyde. De ces indications il découle d'une (1) que l'on a surestimé les valeurs des pontages chimiques déterminées par Moore et Watson, au départ des quantités d'alcool *tert*-butylique et de méthane formées lorsqu'un crêpe non extrait et déprotéinisé a été ponté par le peroxyde de di-*tert*-butyle et (2) que d'autre part il faut revoir le calibrage de Mullins qui relie le nombre de pontages chimiques dans un caoutchouc naturel vulcanisé au peroxyde, au nombre de pontages qui se manifestent par voie physique.

Zusammenfassung

Die Vulkanisations (Vernetzungs-)ausbeute von Di-*tert*-butylperoxyd und Dicumylperoxyd bei Naturkautschuk hängt vom Typ des Naturkautschuks ab. Die Vernetzungsausbeute der Peroxyde wird durch Acetonextraktion des Kautschuks und durch Erhöhung der Peroxydkonzentration vergrößert, in keinem der untersuchten Fälle besass jedoch eines der Peroxyde eine Ausbeute von 100%. Diese Befunde zeigen, dass Naturkautschukproben nicht kautschukatige Verbindungen enthalten, welche mit dem Kautschukkohlenwasserstoff in der Peroxydreaktion konkurrieren. Man muss daraus schliessen, (1) dass der von Moore und Watson aus der *tert*-Butylalkohol- und Methan- ausbeute bei der Vernetzung von nichtextrahiertem, von Eiweiss befreitem hellem Crêpe

mit Di-*tert*-butylperoxyd bestimmte Wert der chemischen Vernetzung ein zu hoher sein kann; und daher (2) die Kalibrierung von Mullins, welche die Zahl der chemischen Vernetzungstellen in einem Naturkautschuk-Peroxydvulkanisat zur Anzahl der physikalisch wirksamen Vernetzungsstellen in Beziehung setzt, eine Revision erfordern könnte.

Received February 8, 1965

Prod. No. 4766A

Aromatic Poly(phenylene)4-phenyl-1,2,4-triazoles*

J. R. HOLSTEN and M. R. LILYQUIST,
*Exploratory Research Department, Chemstrand Research Center, Inc.,
Durham, North Carolina*

Synopsis

High molecular weight poly(*m,p*-phenylene)4-phenyl-1,2,4-triazole has been prepared by the cyclocondensation reaction of aniline with high molecular weight poly(*m,p*-phenylene) hydrazide in polyphosphoric acid (PPA). It is proposed that the cyclocondensation reaction proceeds through the attack of "free" aniline on either or both of two intermediate substrate polymers (a polyhydrazide phosphate and/or a protonated polyoxadiazole) to provide the desired polytriazole composition. The nature of the intermediate substrate polymer is determined primarily by the reaction temperature. Known model compounds containing the 4-phenyl-1,2,4-triazole ring were prepared from model hydrazide compounds under cyclocondensation reaction conditions to demonstrate the validity of this synthesis approach to the polytriazoles. Thermally stable fibers and films having maximum zero strength temperatures of 465 and 490°C., respectively, have been prepared from formic acid solutions of poly(*m,p*-phenylene)4-phenyl-1,2,4-triazole. Thermogravimetric and differential thermal analyses of this polymer showed that the polymer was stable in nitrogen up to 512°C.

INTRODUCTION

The investigation of thermally stable, linear polymer systems has received increased emphasis during the past several years, due largely to demands for heat resistant synthetics as laminates, films, and fibrous materials. Abshire and Marvel¹ prepared several low molecular weight poly(phenylene)4-phenyl-1,2,4-triazoles and showed them to have a high degree of thermal stability. This paper describes our research leading to the synthesis of high molecular weight poly-3,5-(*m,p*-phenylene)4-phenyl-1,2,4-triazole suitable for formation into films and fibers.

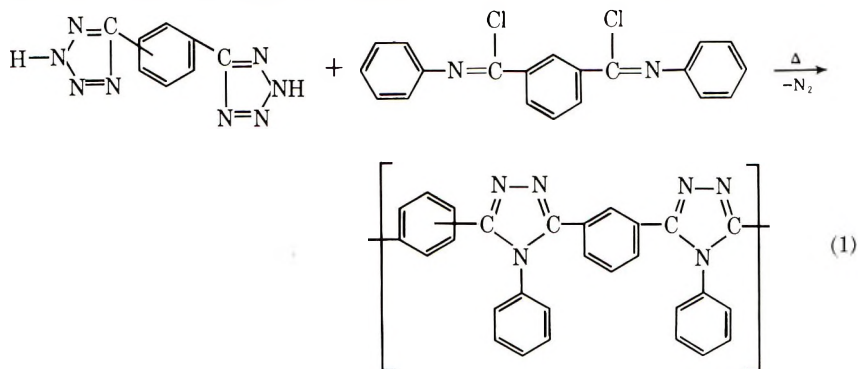
DISCUSSION

Synthesis Routes to Poly-1,2,4-triazoles

Numerous synthesis routes to the 1,2,4-triazoles have been reported in the literature;² however, relatively little work has been reported on polymers containing the 1,2,4-triazole unit in the structural backbone. Bates, Fisher and Wheatly³ described the preparation of a variety of poly-4-

* Presented in part at the Symposium on Novel Polymer Structures at the 145th Meeting of the American Chemical Society, New York, N. Y., September 1963.

aminotriazoles from the fusion of diacid hydrazides in the presence of excess hydrazine. Weidinger and Kranz⁴ reported the preparation of poly(*p*-phenylene)4-H-1,2,4-triazole from the mass condensation of terephthalohydrazide and terephthalonitrile. Similarly, cyanocarboxylic acid hydrazides⁵ have been condensed to afford 4-H-1,2,4-triazole polymers. Abshire and Marvel¹ demonstrated the feasibility of preparing poly(phenylene)4-phenyl-1,2,4-triazoles by the reaction of either *m*- or *p*-phenylene bis-tetrazole with *N,N'*-diphenylisophthalamidoyl chloride eq. (1)

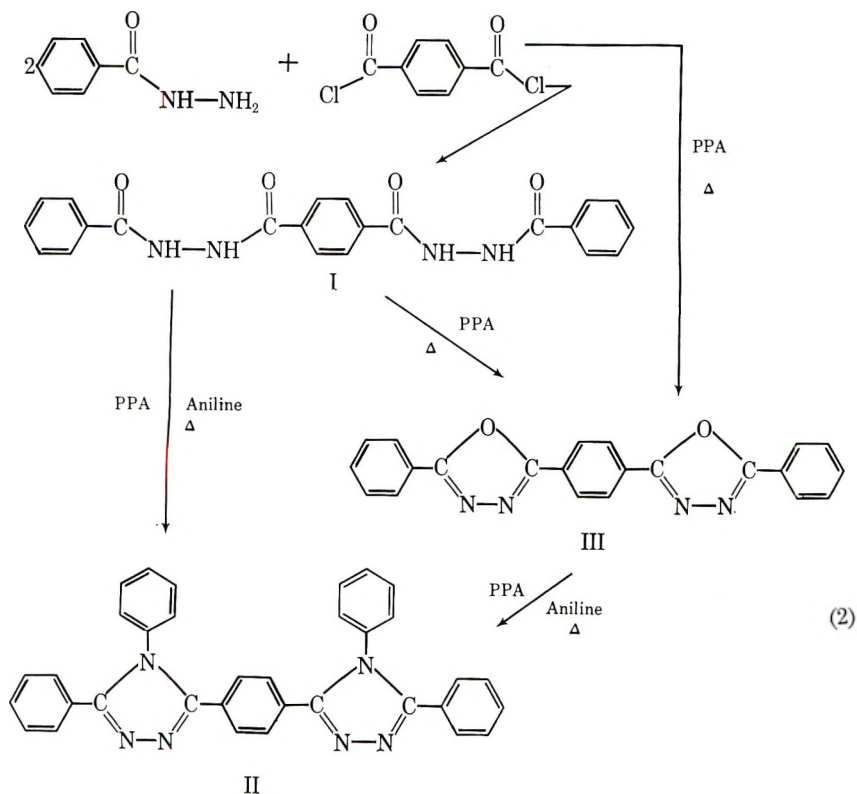


Although these 4-phenyl-1,2,4-triazole polymers were characterized by good thermal stability, the molecular weights attained were too low to exhibit fiber or film forming properties. Further study of this reaction route in our laboratories failed to achieve polymers of film-forming molecular weights. The molecular weight build-up was seriously hampered by the extreme moisture sensitivity of the diimidoyl chlorides and the lack of a satisfactory polymerization solvent. These same factors prevented the attainment of high molecular weight 4-phenyltriazole compositions by the solution polymerization of aromatic diimidoyl chlorides with isophthalohydrazide. Therefore, other synthesis routes to the aromatic poly 4-phenyltriazoles were sought.

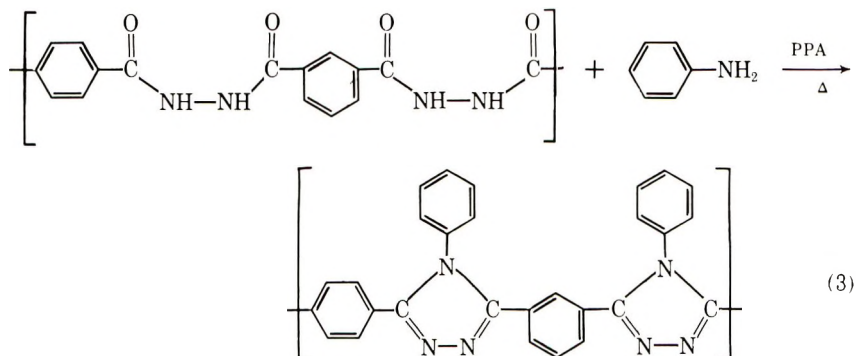
Model Compounds and Reactions

In the quest for a new synthesis route to the poly 1,2,4-triazoles the most promising route appeared to be that involving the cyclocondensation reaction of *sym*-diacylhydrazines with amines. Busch⁶ reported the preparation of 3,4,5-triphenyl-1,2,4-triazole by heating *sym*-dibenzoylhydrazine with aniline and phosphoric anhydride at 250°C. By using excess polyphosphoric acid (PPA; 82–84% P₂O₅) as the dehydrating agent and reaction medium, with a stoichiometric excess of aniline over the dibenzoylhydrazine, the triphenyltriazole was obtained in high yield at a reaction temperature of only 200°C.

Evidence for the triazole structure was obtained from synthesis studies of known model compounds and by comparative infrared spectra. A schematic diagram of the reactions of the model compounds is shown in eqs. (2).

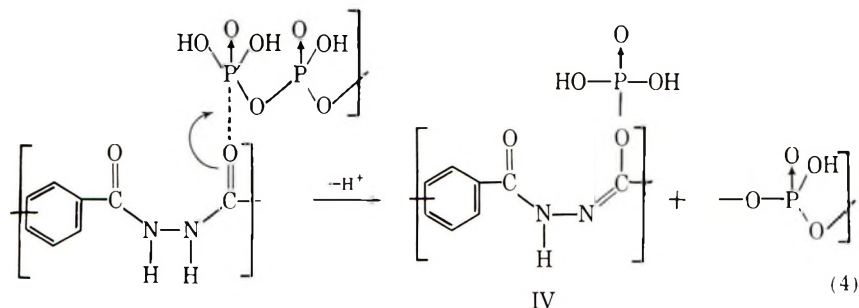


The hydrazide model compound (I), prepared from benzohydrazide and terephthaloyl chloride, was converted to the corresponding model triazole compound (II) by the cyclocondensation reaction with aniline in PPA. This model triazole compound was identical to a known sample which had been prepared previously by the reaction of *p*-phenylene bistetrazole with *N*-phenylbenzimidoyl chloride as described by Huisgen and co-workers.⁷ It was found that in the absence of aniline, hot PPA readily caused the cyclodehydration of the hydrazide structure (I) to give the model oxadiazole compound (III). The infrared spectrum and melting point of the oxadiazole prepared by this cyclodehydration process were identical to those of the known compound prepared by reacting terephthaloyl chloride and 5-phenyltetrazole according to another general procedure described by Huisgen and co-workers.⁸ Compound III was also formed directly by reacting benzohydrazide and terephthaloyl chloride in PPA. To gain further information about the cyclocondensation reaction, the model oxadiazole compound (III) was heated at 240°C. in a mixture of aniline and PPA. The only product isolated was the corresponding model triazole compound (II). The cyclocondensation reaction was then successfully applied to the preparation of poly-3,5-(*m*-,*p*-phenylene)4-phenyl-1,2,4-triazole from the corresponding polymeric symmetrical hydrazine derivative, poly(*m*-,*p*-phenylene)hydrazide [eq. (3)].



Cyclocondensation Reaction Mechanism

From an extensive study of the cyclocondensation reaction, it is postulated that the reaction proceeds by two routes, depending primarily on the reaction temperatures involved. Both routes have a common initial adduct (IV) formed between the polyhydrazide and the PPA.



At temperatures below 200°C., the reaction proceeds primarily through the attack of free aniline at the carbon atom of the newly formed carbon-phosphate linkage. The phosphate moiety is thereby displaced from the carbon atom with concomitant loss of a proton from the newly formed aniline adduct, followed by internal cyclodehydration to give the triazole ring. At higher reaction temperatures, the remaining carbonyl oxygen atom of IV loops around and displaces the phosphate grouping to give a protonated oxadiazole ring. Free aniline then attacks one of the carbon atoms of the protonated oxadiazole ring to break the carbon-oxygen bond. This intermediate then undergoes cyclodehydration with loss of a proton to form the triazole ring.

Evidence that the cyclocondensation reaction proceeded by two routes was provided by a reaction in which the polyhydrazide was added to the aniline-PPA reaction medium at 225°C., stirred at this temperature for 15 min., and the resulting mixture then cooled to 203°C. The mixture was stirred at 203–204°C. for 24 hr. Under these latter conditions, a polyhydrazide added to an aniline-PPA reaction medium at 203–204°C. was normally converted entirely to the polytriazole composition. However,

the product isolated was shown by its solubility characteristics and infrared spectrum to be almost completely poly(phenylene) oxadiazole. From these results it was concluded that cyclocondensation reactions carried out entirely at 203–204°C. did not proceed primarily through the oxadiazole intermediate. A cyclocondensation reaction carried out entirely at 225°C., required 18 hr. to convert the added polyhydrazide completely to the polytriazole composition. Presumably, all cyclocondensation reactions run at 225°C. and higher proceed primarily through the oxadiazole intermediate.

The presence of free aniline in an acidic medium such as PPA was supported by the analogous conclusions of Meiboom and co-workers⁹ and by an actual NMR study of the aniline-PPA system. Meiboom et al. had concluded from their study of proton exchange rates involving substituted ammonium ions in an acidic medium that the formation of free base was the rate-determining step in the exchange sequence. A study of the NMR spectra of the aniline-PPA system over the temperature range of 158–223°C. showed only a single rapid exchange peak, the half-width of which varied inversely with temperature. These data indicated that the aniline-PPA salt was dissociating to give the free acid and free aniline in increasing concentrations as the temperature was raised. Dissociation of the PPA-base salt to give the free base was shown to be important in the cyclocondensation reaction by the failure of the stronger bases, ammonia and 4-aminopyridine, to afford the corresponding 4-substituted polytriazoles when substituted for aniline in the cyclocondensation reaction. Presumably, the salts formed between the stronger bases and the PPA did not dissociate under cyclocondensation reaction conditions to afford a significant concentration of free base. Polyoxadiazole was the only product isolated from these reactions.

Cyclocondensation Reaction Variables

The poly(*m*-,*p*-phenylene)hydrazide samples used in the study of the cyclocondensation reaction were prepared by the procedure of Frazer and Wallenberger.¹⁰ Polyhydrazide samples having inherent viscosities up to 3.4 (0.5% in DMSO) were prepared by adding solid terephthaloyl chloride portionwise to a solution of isophthalohydrazide in hexamethylphosphoramide at 5°C. Polyhydrazides having inherent viscosities in the range of 2.0–2.5 were prepared in *N*-methyl-2-pyrrolidone containing 3 wt.-% of dissolved lithium chloride. In all polyhydrazide preparations it was mandatory that the intermediates and solvent be scrupulously pure and dry if high molecular weight polymer was to be obtained.

Since the cyclocondensation reaction involves a reaction on the preformed poly(phenylene)hydrazide backbone, it seems reasonable to assume that a direct relationship should exist between the molecular weights of the precursor polyhydrazides and the resultant polytriazoles. However, demonstration of this relationship was hampered by variable polymer chain degradation which occurred as a result of side reactions during the

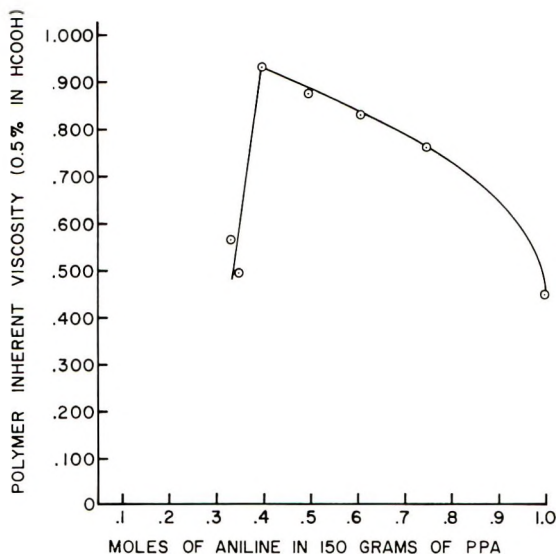
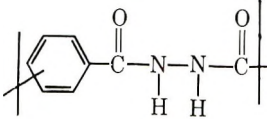
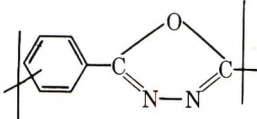
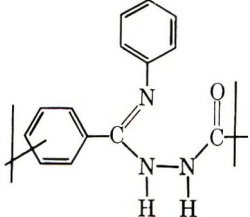
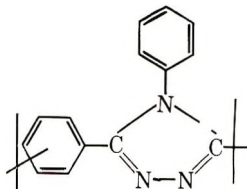


Fig. 1. Effect of aniline to PPA ratio on polytriazole molecular weight.

cyclocondensation reaction. These side reactions are believed to be primarily of two types, transamidative and hydrolytic, as shown by the following experiments. Isophthalanilide was obtained in nearly quantitative yield by heating poly(*m*-,*p*-phenylene)hydrazide and excess aniline in the presence of aniline hydrochloride, and *N,N'*-dibenzoylhydrazine was converted to benzanilide in good yield by heating with 85% phosphoric acid and aniline at 250°C. under 90 psig nitrogen. It therefore seems reasonable to assume that some transamidative chain cleavage occurs under cyclocondensation reaction conditions. Extensive hydrolytic polymer chain degradation and cyclodehydration occurred when a poly(phenylene)hydrazide was added to PPA in the absence of aniline. This same degradation undoubtedly occurs to some extent in the presence of aniline in the cyclocondensation reaction medium.

Studies of the cyclocondensation reaction conditions and the composition of the reaction medium, coupled with appropriate modifications, have resulted in a significant decrease in the extent of the chain cleaving side reactions. A study of the reaction medium composition revealed that some function in the PPA (probably free acid) was reacting with the precursor polymer to degrade it, but aniline reacted with this function in stoichiometric amounts to prevent or decrease its degradative action on the polymer. The experimentally determined optimum stoichiometric ratio of aniline to PPA was 0.4 mole of aniline to every 150 g. of PPA. The refractive indices of the PPA samples indicated that the P_2O_5 content of the PPA was essentially 84%.¹¹ The dramatic effect of the aniline-PPA ratio on the molecular weight of the resultant polymer is portrayed by Figure 1, in which the inherent viscosities of the resultant polytriazoles are

TABLE I
 Elemental Analyses of Precursor and Product Polymers

Polymer Structure	C, %	H, %	N, %	O, %	Ash, %
Theory					
	59.26	3.73	17.28	19.74	—
	66.66	2.80	19.44	11.10	—
	70.87	4.67	17.71	6.74	—
	76.69	4.14	19.17	—	—
Washed product	74.71	4.34	18.21	1.85	0.38

plotted against the number of moles of aniline used with 150 g. of PPA. An explanation for the stoichiometric relationship shown to exist between the aniline and PPA would be somewhat speculative because of the nebulous composition of PPA. However the aniline is believed to react with the PPA in an acid-base type salt-formation reaction. When insufficient aniline was present (less than 0.4 mole/150 g. PPA), the free acid functions, supposedly, brought about the relatively rapid solution and hydrolytic degradation of the precursor polymer. When an excess of aniline was present, solution of the precursor polymer was very slow, and transamidative chain degradation was probably largely responsible for the gradual drop-off in product molecular weight.

The cyclocondensation reaction was considered to be complete when all of the precursor polymer had been dissolved in the reaction medium. The rate at which the precursor polymer dissolved was affected primarily by two factors: reaction medium composition and reaction temperature. Those factors which tended to decrease the effective primary acid concentration in the PPA also decreased the rate of solution. The aniline-PPA

ratio affected the free acid concentration and thus the solution rate. Lower reaction temperatures also decreased the solution rate by slowing the aniline-PPA salt dissociation rate. Reaction mixtures heated at 260°C. were in solution after 3 hr., while those carried out at 204°C. required 24 hr. to effect solution of the precursor polymer; a 70-hr. period was required at 185°C., 96 hr. at 180°C., and 140 hr. was needed to effect complete solution at 175°C.

In general, the products obtained at the lower temperatures were of higher molecular weight (20,000-29,000), lighter in color, and contained negligible formic acid insoluble precursor polymer residues. The use of low reaction temperatures diminished the rate of the polymer chain degrading side reaction more than it did that of the reactions leading to the desired product. However, elemental analyses of a polytriazole sample prepared at 175°C. (Table I) showed that complete precursor polymer conversion did not occur at the lower reaction temperatures. Comparison of the theoretical carbon, hydrogen, nitrogen, and oxygen contents of the proposed precursor forms to that of the polytriazole (Table I) indicated that the principal impurity in the triazole polymer was probably the open chain aniline-polyhydrazide adduct.

Thermal and Formic Acid Stability

The thermal stability of the more uniform poly(phenylene)triazole composition was demonstrated by thermogravimetric (Fig. 2) and differential thermal analyses (Fig. 3). Both analyses showed a decomposition temperature of 512°C. under nitrogen. Rapid weight loss occurred from 515 to 575°C. with only very gradual weight loss up to 900°C. At 900°C.

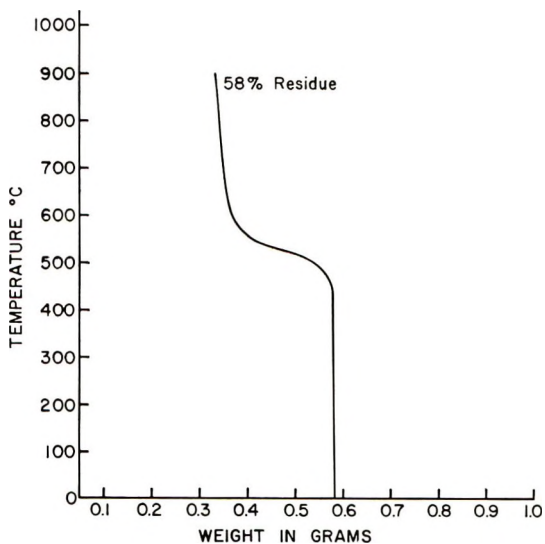


Fig. 2. TGA plot of poly(*m*-,*p*-phenylene)4-phenyl-1,2,4-triazole in nitrogen.

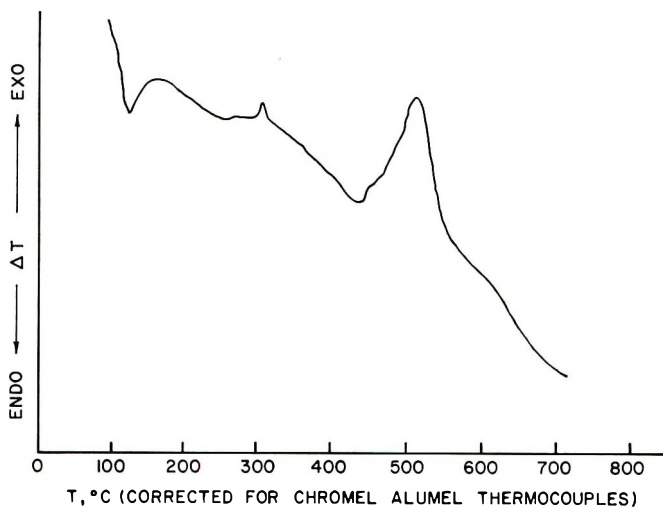


Fig. 3. DTA thermogram of poly(*m-,p*-phenylene)4-phenyl-1,2,4-triazole.

there remained a carbonized residue which corresponded to 58% of the initial polymer sample weight.

Formic acid was found to be an excellent solvent for the poly(*m-,p*-phenylene)4-phenyl-1,2,4-triazole composition. Solutions containing as much as 35% by weight of polymer were obtained. The polytriazole composition was shown to be stable in formic acid solution by failure of the solution viscosity of the polymer in formic acid to decrease after having been heated under reflux for 24 hr. Formic acid was therefore used as the polymer solvent for viscosity determinations and dope preparations.

Molecular Weights

The number-average molecular weights (\bar{M}_n) of several poly(*m-,p*-phenylene)4-phenyl-1,2,4-triazole samples were determined by membrane osmometry, a 90% phenol, 9.9% water, and 0.1% sodium chloride mixture being used as the solvent. The polymer solutions for these measurements were freed of visible particles by careful filtration through fritted glass filters. The \bar{M}_n values of these samples ranged from 13,670 to 26,750.

TABLE II
Molecular Weight and Viscosity Data

\bar{M}_n	$[\eta]^a$, dl./g.	η_{inh} (0.5% in 90% formic acid)
13,670	1.79	1.310
18,700	2.05	1.455
20,840	2.20	1.549
21,760	2.32	1.607
26,750	2.56	1.838

^a Extrapolated from four viscosity measurements.

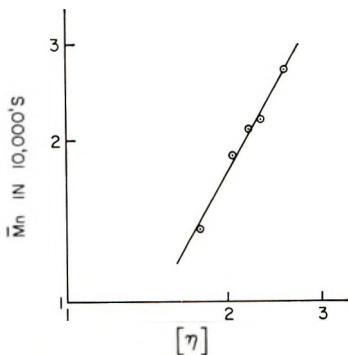


Fig. 4. Plot of intrinsic viscosities vs. M_n of poly(*m,p*-phenylene)4-phenyl-1,2,4-triazole samples.

The corresponding intrinsic and inherent viscosity values for these samples are listed in Table II.

These values exhibit a straight-line relationship with each other when the number-average molecular weight is plotted against the intrinsic viscosity on a log-log scale (Fig. 4) and against the inherent viscosity on a normal, nonlogarithmic scale.

Formation of Fibers and Films

Poly(*m,p*-phenylene)4-phenyl-1,2,4-triazole ($\bar{M}_n = 29,750$) was wet-spun from a 20% solids dope in formic acid to give, after hot drawing, fiber having a tenacity of 2.52 g./den. and zero-strength temperature of 465°C. The relatively low strength of these fibers has been attributed in part to the absence of strong interchain bonding forces. It is believed that polymers having molecular weights in the range of 40,000–50,000 will be necessary to attain high fiber tensile properties with the poly(phenylene)4-phenyltriazole system.

Clear, strong flexible film was cast from a 10% solution of poly(*m,p*-phenylene)4-phenyltriazole ($\bar{M}_n = 27,000$) in formic acid. This film was dimensionally stable in boiling water, and when stretched to twice its initial length at 320°C., it had a zero-strength temperature of 490°C.

Evaluation of these fibers and film will be described in a later paper.

EXPERIMENTAL

Preparation of Polyhydrazide

Materials. Terephthaloyl chloride was obtained from Hooker Chemical Co. and purified by vacuum fractional distillation from anhydrous potassium carbonate followed by recrystallization of the main distillate fraction from anhydrous isoctane under dry nitrogen. Isophthalohydrazide was obtained from Olin Mathieson Chemical Company. The product was recrystallized from water with a decolorizing carbon treatment and dried to a moisture level of 0.04% or below. Commercial samples of hexamethyl-

phosphoramidate (Eastman Chemical Products, Inc.) and *N*-methyl-2-pyrrolidone (General Aniline and Film Corp.) were fractionally distilled from calcium hydride under reduced pressure such that the boiling ranges fell below 100°C. The distillate was considered satisfactory for use when the moisture level was less than 0.02%. Anhydrous lithium chloride was obtained by pulverizing the commercial product (B & A reagent grade, General Chemical) under toluene and azeotropically removing the moisture. The residue was filtered under dry nitrogen and residual toluene removed under vacuum.

Polymerization. Isophthalohydrazide, 97.0 g. (0.5 mole), was dissolved at 50°C. under dry nitrogen in 1250 ml. of hexamethylphosphoramide. The solvent was introduced dropwise from a dropping funnel into the reaction vessel through a 16 × 1 in. column packed with freshly regenerated 4A, 1/16 in. pellet molecular sieves. The solution was cooled to 3–5°C. and 101.5 g. (0.5 mole) of terephthaloyl chloride added in five nearly equal portions over a 2-hr. period with stirring. The cooling bath was removed from around the reaction vessel 2 hr. after the final acid chloride portion had been added. Stirring was continued without cooling for an additional 2-hr. period to give a clear, viscous, colorless solution. The polymer was precipitated and chopped repeatedly in deionized water with the use of a 1-gal. Waring Blendor until the final washings no longer gave a positive chloride ion test with silver nitrate solution. The dried polymer was ground in a Wiley mill to pass a 30-mesh screen in order to facilitate its subsequent solution in the cyclocondensation reaction. Polyhydrazides prepared in this manner had inherent viscosities ranging from 2.5 to 3.2 (0.5% in DMSO). If desired, the yellow iminolic form of the polyhydrazide can be obtained by coagulating the polymer dope in a saturated sodium bicarbonate solution.

By substituting *N*-methyl-2-pyrrolidone containing 3% dissolved lithium chloride for the hexamethylphosphoramide in the above procedure, polyhydrazide samples having inherent viscosities in the range of 1.8 to 2.4 were obtained.

Preparation of Poly(*m*-,*p*-phenylene)4-phenyl-1,2,4-triazole

Materials. Aniline was fractionally distilled under reduced pressure, and the water-white distillate stored under dry nitrogen in sealed amber-colored bottles in the refrigerator. Polyphosphoric acid (PPA) was used as received from Matheson, Coleman and Bell. The refractive indices of the samples examined were 1.4720–1.4730, which corresponds to a P₂O₅ content of 83.5–84.0%.¹¹

Cyclocondensation Reaction. A 3000-g. portion of PPA was heated to 150°C. and stirred under dry nitrogen. Aniline, 751 g. (8.1 mole), was added dropwise with stirring at such a rate that the temperature of the reaction mixture did not exceed 190°C. The temperature of the resulting solution was adjusted to 175°C. and 97.2 g. of poly(*m*-,*p*-phenylene) hydrazide (η_{inh} 3.085) then added. The mixture was stirred and heated at 174–176°C. for 140 hr., during which time the polyhydrazide dissolved

to form a homogeneous solution. The clear, light orange, fairly viscous solution was poured hot into deionized water in two operating 1-gal. Waring Blenders. Sodium hydroxide pellets were added cautiously to the resulting hot slurries until the agglomeration points were reached. The mixtures were filtered and the combined residue reslurried in a Waring Blender, first in 5% sodium hydroxide solution and then twice in deionized water. The residue was then extracted continuously with hot ethanol in Soxhlet extractors until the extract effluent solutions were colorless. The combined residue was then dried in a vacuum oven at 80–120°C.

The residual formic acid-insoluble precursor polymer present in this product was nil. This was determined by dissolving 0.2000 g. of the product in 20 ml. of boiling 98–100% formic acid in a centrifuge tube. This solution was cooled and centrifuged. The supernatant solution was decanted and 10 ml. of fresh formic acid added. This mixture was heated to the boil and then filtered through a tared coarse-grade fritted glass filter. The transfer to the filter was aided by additional formic acid wash. The residue was dried on the filter and weighed. The percentage formic acid insoluble content in the polytriazole product was then calculated.

The poly(*m*-,*p*-phenylene)4-phenyl-1,2,4-triazole obtained from the above described reaction had a number-average molecular weight of about 28,000. Polytriazoles having number-average molecular weights of about 21,500 and 26,000 were obtained by the above procedure run at 180–182°C. for 96 hr. from polyhydrazide samples having inherent viscosities of 2.39 and 2.94, respectively.

Zero-Strength Temperature Test

A stress load of 20 psi was placed upon the fiber or film specimen to be tested and the weighed specimen suspended from an electronic balance into a glass tube. A nitrogen atmosphere was maintained within the tube. The tube was heated at a constant rate by a Hoskin's furnace controlled by a temperature-time programmer. The electronic balance and thermocouples from within the heated tube were wired into an *X*,*Y*-type recorder. The *X*-*Y* plot of the specimen weight as a function of temperature was terminated when the test specimen ruptured. The temperature at which rupture occurred was termed the zero-strength temperature.

We are indebted to Professor W. H. Urry of the University of Chicago for suggesting the reaction mechanisms for the cyclocondensation reaction.

This research was supported by the United States Air Force, Research and Technology Division.

References

1. Abshire, C. J., and C. S. Marvel, *Makromol. Chem.*, **44-46**, 388 (1961).
2. Potts, K. T., *Chem. Revs.*, **61**, 87 (1961).
3. Bates, H., J. W. Fisher, and E. W. Wheatly, U. S. Pats. 2,512,599; 2,512,600; 2,512,601; 2,512,624; 2,512,625; 2,512,626; 2,512,627; 2,512,628; 2,512,629; 2,512,630 (1950); assigned to Celanese Corporation of America.

4. Weidinger, H., and J. Kranz, *Chem. Ber.*, **96**, 1064 (1963).
5. Badische Anilin-, u. Soda-Fabrik, Belg. Pat. 628,618 (February 2, 1963).
6. Busch, M., *J. Prakt. Chem.* [2], **89**, 552 (1914).
7. Huisgen, R., J. Sauer, and M. Seidel, *Chem. Ind. (London)*, **1958**, 1114; *Chem. Ber.*, **93**, 2885 (1960).
8. Sauer, J., R. Huisgen, and H. J. Sturm, *Tetrahedron*, **11**, 241 (1960).
9. Grunwald, E., A. Loewenstein, and S. Meiboom, *J. Chem. Phys.*, **27**, 630 (1957).
10. Frazer, A. H., and F. T. Wallenberger, *J. Polymer Sci.*, **A2**, 1147 (1964).
11. Downing, R. G., and D. E. Pearson, *J. Am. Chem. Soc.*, **83**, 1718 (1961).

Résumé

On a préparé du poly(*m*-,*p*-phénylène)4-phényl-1,2,4-triazole de haut poids moléculaire par la réaction de cyclocondensation de l'aniline avec le poly(*m*-,*p*-phénylène)hydrazide de haut poids moléculaire dans de l'acide polyphosphorique (PPA). On suggère que la réaction de cyclocondensation a lieu par l'attaque de l'aniline "libre" sur chacun ou sur les deux polymères intermédiaires (un phosphate de polyhydrazide et/ou un polyoxadiazole protoné) pour obtenir la composition désirée de polytriazole. La nature du polymère intermédiaire est déterminée principalement par la température de réaction. Des composés modèles connus contenant le noyau du 4-phényl-1,2,4-triazole ont été préparés à partir de composés du modèle hydrazide, dans des conditions de réaction de la cyclocondensation pour démontrer que la validité de cette synthèse se rapproche des polytriazoles. Des fibres et films, thermorésistants présentant respectivement des températures maximum de 465 à 490°C à partir desquelles ils perdent leur résistance mécanique, ont été préparés à partir de solutions, dans de l'acide formique, de poly(*m*-,*p*-phénylène)4-phényl-1,2,4-triazole. Des analyses thermogravimétrique et thermique différentielle effectuées sur ce polymère ont montré qu'il était stable dans de l'azote jusqu'à 512°C.

Zusammenfassung

Hochmolekulares Poly(*m*-,*p*-phenylen)4-phenyl-1,2,4-triazol wurde durch die Zykl Kondensierungsreaktion von Anilin mit hochmolekularem Poly(*m*-,*p*-phenylen)hydrazid in Polyphosphorsäure (PPA) dargestellt. Es wird angenommen, dass die Zykl kondensierungsreaktion über einen Angriff von "freiem" Anilin auf entweder eines oder beide der intermediären Substratpolymeren (ein Polyhydrazidphosphat und/oder ein protoniertes Polyoxydiazol) unter Bildung der gewünschten Polytriazolzusammensetzung verläuft. Die Natur des intermediären Substratpolymeren wird primär durch die Reaktionstemperatur bestimmt. Bekannte Modellverbindungen mit dem 4-Phenyl-1,2,4-triazolring wurden aus Modellhydrazidverbindungen unter den Bedingungen der Zykl kondensationsreaktion dargestellt, um die Gangbarkeit dieses Syntheseweges zu dem Polytriazolen zu zeigen. Thermisch stabile Fasern und Filme mit Festigkeitsverlust bei Maximaltemperaturen von 465 bzw. 490°C. wurden aus Ameisensäurelösungen von Poly(*m*-,*p*-phenylen)4-phenyl-1,2,4-triazol dargestellt. Thermogravimetrische und Differentialthermoanalyse dieses Polymeren zeigte, dass es in Stickstoff bis zu 512°C beständig war.

Received March 17, 1965

Revised May 26, 1965

Prod. No. 4768A

NMR Study of Vinyl Chloride-Vinylidene Chloride Copolymer

J. L. McCLANAHAN* and S. A. PREVITERA,† *W. R. Grace and Co., Washington Research Center, Clarksville, Maryland*

Synopsis

A study of the proton magnetic resonance spectra of poly(vinyl chloride) (PVC), poly(vinylidene chloride) (PVDC), and vinyl chloride-vinylidene chloride (VC-VDC) copolymer has resulted in a clearer understanding of the copolymer NMR spectra. Comparison of the homopolymer spectra with the copolymer spectra, including information obtained from decoupling experiments, indicated that the chain structure of the eight copolymers studied were of two different types. The simplest type copolymer chain contained head-to-tail VDC sequences, head-to-head or tail-to-tail VDC sequences, and VC-VDC sequences. The second type copolymer contained all of the sequences of type I copolymers and, in addition, contained VC sequences. The average length of these VC sequences was less than four VC units. The composition of seven of the copolymers was determined by chlorine analysis and by an NMR method of analysis which was based on the above conclusions. The agreement between the results of the two methods of analysis was quite good.

INTRODUCTION

A number of papers have reported NMR studies of poly(vinyl chloride) (PVC),¹⁻⁶ poly(vinylidene chloride) (PVDC),³ and VC-VDC copolymers.^{3,7} None of these papers, however, thoroughly described the NMR spectra of VC-VDC copolymers. We have, consequently, studied the H¹ NMR spectra of 10% chlorobenzene solutions of these polymers at 160°C. Hexamethyldisiloxane ($\tau = 9.94$) was used as internal reference, and the spectra were calibrated by the sideband technique. Chemical shifts are reported as τ values. The NMR instrument used in this study was a Varian DP-60 NMR spectrometer. Decoupling experiments were performed by using the Varian V-3521 integrator as described by Johnson.⁸

NMR SPECTRUM OF PVC

The NMR spectrum of PVC (Fig. 1) consisted of a high field multiplet centered at $\tau = 7.91$ and a low field multiplet centered at $\tau = 5.59$. These absorptions were assigned to methylene and methyne protons, respectively.

* Present address: The University of Mississippi, University, Mississippi.

† Present address: W. R. Grace and Co., Overseas Chemical Division, Passirano di Rho, Italy.



Fig. 1. NMR spectrum of PVC.

Theoretically their ratio should be 2:1; experimentally this ratio varied between 2:0.9 and 2:0.95.

The interpretation of the NMR spectrum of PVC has been controversial. Johnsen¹ and Bovey and Tiers² have described the high field multiplet as overlapping triplets with the high field triplet assigned to methylene protons of syndiotactic sequences and the low field triplet assigned to methylene protons of isotactic sequences. Tincher⁴ and Doskocilova⁵ have performed a more general analysis which does not assume the magnetic equivalence of the methylene protons of an isotactic unit. Both methods have been used to calculate the isotactic-syndiotactic content of PVC. No evidence was cited for the existence of monomer units that had polymerized head-to-head or tail-to-tail.

NMR SPECTRUM OF PVDC

The NMR spectrum of PVDC (Fig. 2) consisted of a relatively sharp singlet centered at $\tau = 6.14$. This indicates that only one type of proton was present and that the PVDC chain resulted from one type polymerization, presumably head-to-tail.

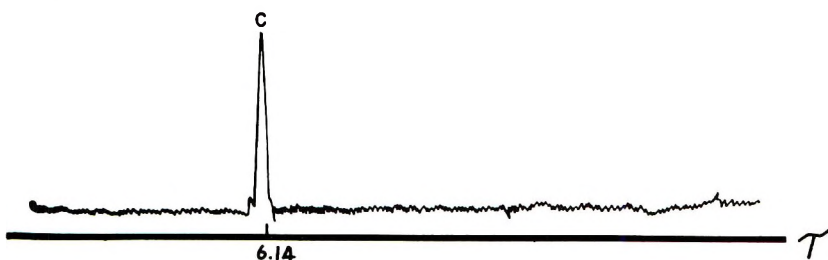


Fig. 2. NMR spectrum of PVDC.

NMR SPECTRUM OF VC-VDC COPOLYMER

The NMR spectra of eight VC-VDC copolymers were examined. The spectra of these copolymers were basically of two different types, and this seemed to be determined by the composition of the copolymer rather than by the method of copolymer preparation or the source of the copolymer (for example, see Table I).

TABLE I
Type Spectrum, Method of Manufacture, Source, and Composition for Typical Copolymers Studied

Copolymer	Type spectrum	Method of manufacture	Source	VC, wt.-%
I (Saran UP25)	I	Suspension	Dow Chemical Co.	23.3
II (IXAN WV725)	I	Emulsion	Solvay Chemical Co.	23.7
VI (Saran CI12)	II	Suspension	Kureha Kasei Co.	11.2

The spectrum shown in Figure 3 represents the simplest type (type I) and consists of: (1) a doublet (*B*), $J \sim 6.0$ cycle/sec., centered at $\tau = 6.84$, (2) a singlet (*C'*) at $\tau = 6.27$, (3) a singlet (*C*) at $\tau = 6.14$, and (4) a multiplet (*E*) centered at $\tau = 5.05$.

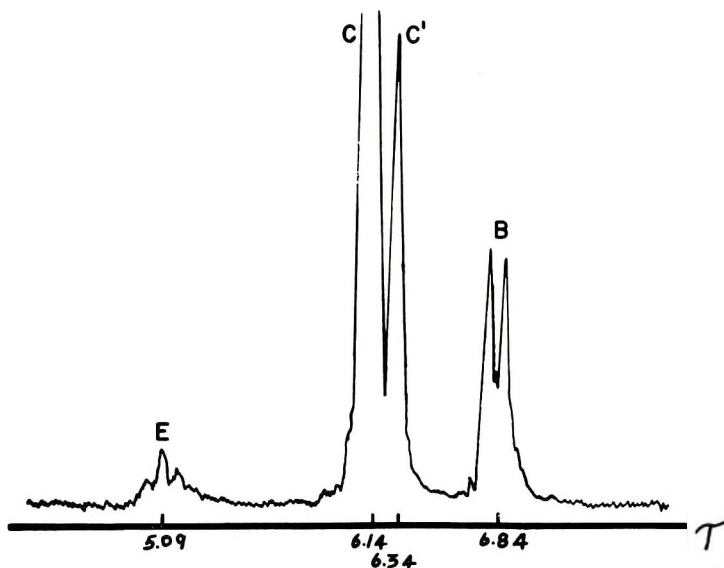


Fig. 3. NMR spectrum of type I copolymer.

Absorption *B* was not observed in the PVC or PVDC spectra, but was observed in the spectra of all copolymers studied. The chemical shift of this absorption was intermediate between the chemical shifts of the methylene protons of the homopolymers. This indicates that *B* should be assigned to methylene protons of the boundary structure. Evidence from decoupling experiments and intensity measurements supports this assignment.

Absorption *C* was observed in the spectrum of PVDC and was also observed in the spectra of all copolymers studied. This absorption was, therefore, assigned to VDC segments in the copolymer chain. Again the segments are presumed to result from head-to-tail polymerization of VDC units.

Peak C' appeared in all of the copolymer spectra but was not observed in either homopolymer spectrum. The sharpness of the peak is strong evidence that it must be assigned to methylene protons from VDC units, since there was no observed proton-proton spin coupling. The chemical shift is also consistent with such an argument. Since absorption C was assigned to VDC units that polymerized head-to-tail, this absorption must be assigned to VDC units that polymerized head-to-head or tail-to-tail (see Discussion).

Absorption E was observed only in the copolymer spectra. When E was irradiated as B was recorded, B collapsed to a singlet. Also, the relative intensities of B and E were 4 and 1, respectively. These data are strong evidence that absorptions B and E must be assigned to $-\text{CH}_2-$ and $-\text{CHCl}-$ protons of the boundary structure, i.e., $\text{R}-\text{CCl}_2-\text{CH}_2-\text{CHCl}-\text{CH}_2-\text{CCl}_2-\text{R}$. It should be noted that the methylene protons of this sequence are very similar and it is not surprising that the NMR spectrum cannot distinguish between methylenes from VC and VDC units.

The second type spectrum (type II) may be illustrated by Figure 4. All

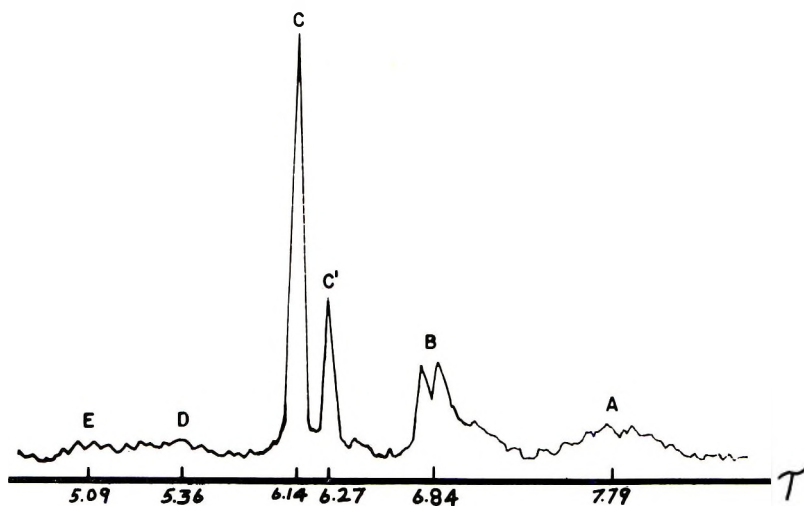


Fig. 4. NMR spectrum of type II copolymer.

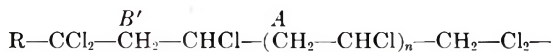
of the absorptions observed in Figure 3 are present in this spectrum. In addition, three other absorptions are observed: (1) a broad absorption (A) centered near $\tau = 7.79$, (2) a broad absorption (B') centered near $\tau = 7$, and (3) a broad absorption (D) centered near $\tau = 5.36$.

Although absorption A of the copolymer has a chemical shift to slightly lower field than the high field absorption of PVC, this absorption must be assigned to methylene protons of VC segments in the copolymer chain. The shift to lower field could result from short VC segments in close proximity to VDC units.

The chemical shift of D is also to lower field than the low field absorption of PVC. This shift could also result from long range deshielding effects not present in PVC. This absorption is assigned to tertiary protons of VC

segments. Four of the copolymer spectra showed absorptions *A* and *D*, and four did not. The disappearance of *A* and *D* in all cases substantiates the above assignments.

Absorption *B'* is assigned to methylene protons of the boundary structure



The appearance of *B'* simultaneously with *A* and *D*, and the closeness of *B'* to *B*, supports this assignment.

Chemical shifts for all polymer samples studied are given in Table II.

TABLE II
Chemical Shift Data (τ) for All Polymers Studied

Polymer	τ					
	<i>A</i>	<i>B</i>	<i>C</i>	<i>C'</i>	<i>D</i>	<i>E</i>
PVC-I	7.93	—	—	—	5.51	—
PVC-II	7.93	—	—	—	5.59	—
PVDC	—	—	6.14	—	—	—
Copolymer I	7.81	6.84	6.12	6.28	5.41	5.04
Copolymer II	7.76	6.82	6.10	6.25	5.41	5.09
Copolymer III	7.79	6.85	6.12	6.30	—	5.05
Copolymer IV	7.76	6.90	6.14	6.30	—	5.04
Copolymer V	—	6.88	6.18	6.29	—	5.07
Copolymer VI	—	6.85	6.14	6.29	—	—
Copolymer VII	—	6.84	6.12	6.28	—	—
Copolymer VIII	—	6.84	6.14	6.27	—	5.05

QUANTITATIVE ANALYSIS OF VC-VDC COPOLYMER BY NMR

Based on the above assignments the methylene absorptions may be assigned as follows:

$$\text{VC (CH}_2\text{)} = A + \frac{1}{2}B + B'$$

$$\text{VDC (CH}_2\text{)} = C + C' + \frac{1}{2}B$$

and one can readily determine the monomer content if the above assignments are correct. Since the methylene proton ratio of the VC and VDC units is 1:1

$$\begin{aligned} N_{\text{VC}} &= \frac{A + \frac{1}{2}B + B'}{A + \frac{1}{2}B + B' + C + C' + \frac{1}{2}B} \\ &= \frac{2A + B + 2B'}{2(A + B + B' + C + C')} \end{aligned}$$

where N_{VC} = mole fraction VC.

Also

$$\text{Wt. VC} = N_{\text{VC}} \times \text{molecular wt.}_{\text{VC}} = 62.5N_{\text{VC}}$$

$$\text{Wt. VDC} = N_{\text{VDC}} \times \text{molecular wt. VDC} = 97.0N_{\text{VDC}} = 97.0(1 - N_{\text{VC}})$$

Therefore

$$\begin{aligned} \text{Wt.-% VC} &= \frac{\text{Wt. VC}}{\text{Wt. VC} + \text{Wt. VDC}} \times 10^2 \\ &= \frac{1.81N_{\text{VC}}}{2.81 - N_{\text{VC}}} \times 10^2 \end{aligned}$$

The results of these calculations are recorded in Table III. The composition as determined by chlorine analysis is also recorded.

TABLE III

Copolymer	VC, wt.-%	
	By chlorine analysis	By NMR analysis
I	23.3	23.4
II	23.7	23.3
III	22.0	21.4
IV	21.6	19.3
V	12.0	9.8
VI	11.2	8.0
VII	—	8.0
VIII	8.0	7.0

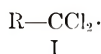
The agreement is quite good; however, it is interesting to note that the error is always in the same direction, i.e., the NMR results are always lower.

DISCUSSION

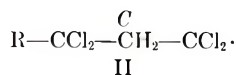
On the basis of these results we visualize the polymer chain as follows.

Polymer Chains That Are Represented by Type I Spectra

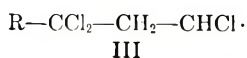
Since the VDC content of these polymers is quite high, 89 wt.-%, we consider the propagating chain⁹ as



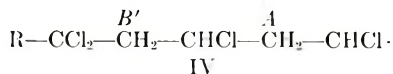
Considering only head-to-tail addition of monomer units the next step is



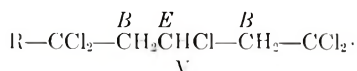
or



The methylene protons of the newly added monomer unit of II are assigned to peak *C*. Assignment of the protons of III cannot be made until the next monomer unit is added.

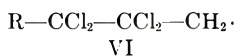


or

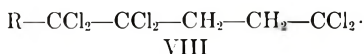


Since peaks *A* and *B'* do not appear in type I spectra, VC units do not enter the chain in sequence as shown in IV.

The simple approach described above accounts for all of the absorptions of type I spectra except *C'*. Okuda⁷ assigned this absorption to methylene protons of VDC units that polymerized head-to-head. This assignment seems reasonable, though it is difficult to understand why VDC units would polymerize head-to-head in the copolymer

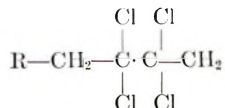


and not do so in PVDC. Head-to-head addition would be followed by either tail-to-head or tail-to-tail addition, yielding VII or VIII, respectively.

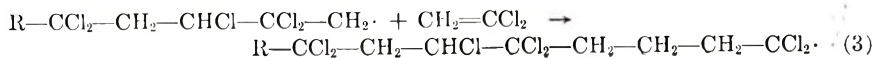
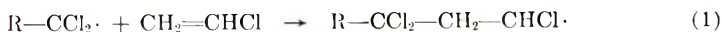


Wilson⁹ has shown that in PVDF head-to-head addition is always followed by tail-to-tail addition. It would not be surprising if the same were true in PVDC, and in any event it seems that VIII would at least be competitive with VII. These arguments dilute this assignment of *C'*, since VIII introduces two new types of VDC methylene groups and there is NMR evidence for only one new type.

If, however, one assigns *C'* to methylene protons that result from tail-to-tail addition of VDC units there seems to be a somewhat more logical explanation for observing *C'* only in copolymer spectra. First, the absence of head-to-head addition in PVDC



is attributed to steric hindrance. Now consider a chain segment which results from the propagation steps of eqs. (1)-(3).



In the product of eq. (2) steric effects are not as pronounced, and head-to-head addition might occur. Now tail-to-tail addition of a VDC unit results in the formation of methylene protons which may be assigned to C' . The ratio of $C:C'$ decreases as the VC concentration increases (see Table IV), and this indicates that VC is in some way involved. In any event, the assignment of C' to methylene protons from VDC is demanded by the absence of spin-spin splitting and the results reported in Table III.

TABLE IV
Composition and $C:C'$ Ratio for All Copolymers Studied

Copolymer	VC, wt.-% (determined by NMR)	Ratio $C:C'$
I	23.4	1.43:1
II	23.3	2:1
III	21.4	1.8:1
IV	19.3	2:1
V	9.8	3.8:1
VI	8.0	4.1:1
VII	8.0	3.3:1
VIII	7.0	3.8:1

Polymers That Are Represented by Type II Spectra

As noted earlier, the spectra of these polymers have absorptions A , B' , and D which are not present in type I copolymer spectra. These absorptions result when two or more VC units enter the polymer chain in sequence. The methylene protons of the first VC unit that enters the chain are represented by B' . The methylene protons of the VDC unit that terminates the VC sequence are also assigned to B' . Absorptions A and D are assigned to all other methylene and tertiary protons, respectively, of the VC sequence. Comparison of A , B , and B' indicates that the average VC sequence does not contain more than four VC units.

The authors wish to thank Dr. R. W. McKinney and Dr. A. D. Ketley for helpful discussions. We also acknowledge the assistance of Dr. F. Cavallaro in performing the chlorine analyses and Mr. J. R. Bell in carrying out the experimental NMR measurements.

References

1. Johnsen, U., *J. Polymer Sci.*, **54**, S6 (1961).
2. Bovey, F. A. and G. V. D. Tiers, *Chem. Ind. (London)*, **1962**, 1826.
3. Chujo, R., S. Satoh, T. Ozeki, and E. Nagai, *J. Polymer Sci.*, **61**, 171 (1962).
4. Tincher, W. C., *J. Polymer Sci.*, **62**, S148 (1962).
5. Daskocilova, D., *J. Polymer Sci.*, **B2**, 421 (1964).
6. Bovey, F. A., E. W. Anderson, D. C. Douglass, and J. A. Manson, *J. Chem. Phys.*, **39**, 1199 (1963).
7. Okuda, K., *J. Polymer Sci.*, **A2**, 1749 (1964).
8. Johnson, L. F., Varian Associates Publication Number 87-100-082, 5 (1962).

9. Alfrey, T., J. Bohrer, and H. Mark, *Copolymerization*, Interscience, New York, 1952.
10. Wilson, C. W., *J. Polymer Sci.*, **A1**, 1305 (1963).

Résumé

L'étude des spectres de résonance magnétique protonique du chlorure de polyvinyle (PVC), du chlorure de polyvinylidène (PVDC) et d'un copolymère du chlorure de vinyle (VC)-chlorure de vinylidène (VC-DC) a permis de comprendre plus clairement le spectre RMN du copolymère. La comparaison du spectre de l'homopolymère avec celui du copolymère, y compris les informations obtenues par la technique du décompoupage, ont montré que la structure caténaire des hauts copolymères examinés relèvent de deux types différents. Le type le plus simple de chaîne copolymérique contenait des séquences de VDC tête-à-queue, des séquences de VDC et VC-VDC tête-à-tête ou queue-à-queue. Le second type de copolymère contenait toutes les séquences du type I de copolymères et, additionnellement, des séquences VC. La longueur moyenne de ces séquences VC était plus courte que 4 unités VC. La composition centésimale de sept des copolymères a été déterminée par analyse du chlore et par une méthode analytique de RMN qui se basait sur les conclusions décrites ci-dessus. L'accord entre les résultats obtenus par ces deux méthodes d'analyse était satisfaisant.

Zusammenfassung

Eine Untersuchung der protonmagnetischen Resonanzspektren von Polyvinylchlorid (PVC), Polyvinylidinchlorid (PVDC) und des Vinylchlorid-Vinylidinchlorid (VC-DC)-Kopolymeren führte zu einem besseren Verständnis der Kopolymer-NMR-Spektren. Ein Vergleich der Homopolymerspektren mit den Kopolymerspektren zeigt zusammen mit der aus Entkopplungsversuchen erhaltenen Information, dass die Kettenstruktur der acht untersuchten Kopolymeren zwei verschiedenen Typen angehörte. Der einfachste Typ der Kopolymerkette enthielt Kopf-zu-Kopf-VDC-Sequenzen, Kopf-zu-Kopf-oder Schwanz-zu Schwanz-VDC-Sequenzen und VC-VDC-Sequenzen. Das Kopolymere vom Zweiten Typ enthielt sämtliche Sequenzen des Kopolymeren vom Typ I und zusätzlich noch VC-Sequenzen. Die Mittlere Länge dieser VC-Sequenzen betrug weniger als vier VC-Einheiten. Die prozentuelle Zusammensetzung von sieben dieser Kopolymeren wurde durch Chloranalyse sowie durch eine NMR-Analysenmethode bestimmt, welche auf obigen Schlussfolgerungen beruhte. Die Übereinstimmung zwischen den Ergebnissen der beiden Analysenmethoden war recht gut.

Received February 25, 1965

Revised April 21, 1965

Prod. No. 4743A

Thermochemistry of Polymerization Part III. Thermochemical Aspects of Propagation of Polymerization

HIDEO SAWADA, *Central Research Laboratory, Dainippon Celluloid Company, Tsurugaoka, Oi, Irumagun, Saitama, Japan*

Synopsis

A statistical thermodynamic method of treating propagation of polymerization is developed. The effect of temperature on the sequence distribution of syndiotactic and isotactic units in free-radical polymerization is discussed. This theory applies to the problem of probabilities of various possible modes of addition, namely head-to-head and head-to-tail addition, 1-2 and 1-4 addition, and formation of *cis* and *trans* configurations.

Introduction

In the previous paper¹ the simplest case of the problem of equilibrium copolymerization was solved; the results obtained there, however, are limited in application to copolymer of two monomer units. As several workers have shown,²⁻⁵ the development of the stereochemical relations between successive monomer units in a vinyl polymer may be treated as a problem in copolymerization.

On the other hand, it is known that at some elevated temperature certain vinyl polymers decompose by stepwise loss of monomer units in a reaction which is essentially the reverse of polymerization.⁶ Therefore, it is expected that if a polymer were treated at some elevated temperature, depolymerization-polymerization would determine the sequence distribution of syndiotactic and isotactic units in the polymer.

In this paper we have developed a general theory of sequence distribution of syndiotactic and isotactic units which is analogous to that of two monomer units.

Theoretical

Huggins⁷ originally suggested, in 1944, that a decrease in reaction temperature should increase the stereospecificity of a free-radical propagation. It is now becoming well established that low-temperature propagation by a free radical yields predominantly syndiotactic placements.⁸⁻¹⁰ These indications have received theoretical support by several workers.^{3,9-11} They expressed the ratio of syndiotactic to isotactic units in the polymer in

terms of the difference between the free energies of activation from a purely kinetic point of view.

However, it is known that at high temperatures certain vinyl polymers tend to undergo depolymerization reactions. Hence, we can assume that equilibrium polymerization–depolymerization will be achieved at some elevated temperature and will determine the sequence distribution of syndiotactic and isotactic units. It is of interest to consider this equilibrium from a purely statistical thermodynamic point of view.

In a radical polymerization the placement of the end unit is not decided until the next unit has been added. However, this does not affect the statistical argument. We shall designate the probability of a syndiotactic placement as f_{syn} . (Here, f_{syn} is essentially the same as Coleman's β .³) The interaction energies of dl and dd pairs are denoted by H_{dl} and H_{dd} , respectively. The energy H_{dl} is approximately the heat of polymerization per mole of syndiotactic placement and similarly for H_{dd} . We shall employ the convention of Lewis and Randall,¹² according to which any gain in a quantity on the part of a system is considered to be positive and any loss negative. Since heat is evolved during the polymerization, the molar heat of polymerization is given by

$$\Delta H = - [H_{dl}f_{\text{syn}} + H_{dd}(1 - f_{\text{syn}})] \quad (1)$$

Next we shall calculate the entropy change ΔS . The homopolymer can be considered as a copolymer of the d - and l - derivatives of the same monomer. Orr¹³ computed the number of ways of arranging the monomer units in the polymer molecule. From this number the entropy of stereoregularity per mole is

$$\Delta S_{\text{st}} = - R[f_{\text{syn}}\ln f_{\text{syn}} + (1 - f_{\text{syn}})\ln(1 - f_{\text{syn}})] \quad (2)$$

where R is the gas constant. Thus, the total entropy change per mole involved in polymerization reaction can be written as

$$\Delta S = - [S_{dl}f_{\text{syn}} + S_{dd}(1 - f_{\text{syn}})] - R[f_{\text{syn}}\ln f_{\text{syn}} + (1 - f_{\text{syn}})\ln(1 - f_{\text{syn}})] \quad (3)$$

where S_{dl} and S_{dd} denote the entropy change per mole of the respective placements.

We consider the polymerization reaction as occurring at some constant temperature T , and may write for the change in free energy for this reaction

$$\Delta F = \Delta H - T\Delta S \quad (4)$$

Substituting eqs. (1) and (3) into eq. (4), we have

$$\Delta F = - [H_{dl}f_{\text{syn}} + H_{dd}(1 - f_{\text{syn}})] + T[S_{dl}f_{\text{syn}} + S_{dd}(1 - f_{\text{syn}})] - TR[f_{\text{syn}}\ln f_{\text{syn}} + (1 - f_{\text{syn}})\ln(1 - f_{\text{syn}})] \quad (5)$$

Equilibrium polymerization–depolymerization will ultimately lead to an equilibrium distribution of syndiotactic and isotactic units along the chains.

This equilibrium sequence distribution is determined as a function of temperature by the requirement that the change in free energy ΔF be a minimum with respect to the change in f_{syn} . Thus, we find at $\partial\Delta F/\partial f_{\text{syn}} = 0$

$$f_{\text{syn}} = 1/[1 + \exp\{(H_{dd} - H_{dt})/RT - (S_{dd} - S_{dt})/R\}] \quad (6)$$

In Figure 1 we have plotted f_{syn} as a function of T for the case where $H_{dd} < H_{dt}$ and $S_{dd} = S_{dt}$. Regardless of the sign of the $(H_{dd} - H_{dt})$ terms,

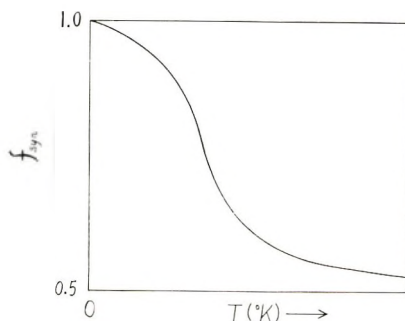


Fig. 1. Temperature dependence of f_{syn} for case where $H_{dt} > H_{dd}$ and $S_{dt} = S_{dd}$.

f_{syn} will always be $1/(1 + \exp\{S_{dt} - S_{dd}\}/R\}$ at sufficiently large values of T , since $f_{\text{syn}} \rightarrow 1/(1 + \exp\{S_{dt} - S_{dd}\}/R)$ as $T \rightarrow \infty$. If $S_{dd} = S_{dt}$, the polymer will be atactic at sufficiently elevated temperatures, since $f_{\text{syn}} \rightarrow 1/2$ as $T \rightarrow \infty$. When $H_{dt} = H_{dd}$ and $S_{dd} = S_{dt}$, at any temperature f_{syn} is equal to $1/2$, and hence perfectly atactic polymer is produced. When $H_{dd} > H_{dt}$, at low temperatures f_{syn} is very close to zero, and hence isotactic propagation becomes increasingly dominant as the polymerization temperature is decreased. When $H_{dd} < H_{dt}$, at low temperatures f_{syn} is very close to unity, and hence the probability of forming long syndiotactic sequences can be increased by lowering the temperatures.

Substitution of eq. (6) into eq. (1) gives

$$\Delta H = - \left[\frac{H_{dt} - H_{dd}}{1 + \exp\{(H_{dd} - H_{dt})/RT - (S_{dd} - S_{dt})/R\}} + H_{dd} \right] \quad (7)$$

If $(H_{dd} - H_{dt})$ is positive, at low temperatures, ΔH will approach $-H_{dd}$, yielding isotactic polymers. If $(H_{dd} - H_{dt})$ is negative, at low temperatures, ΔH will approach $-H_{dt}$, yielding syndiotactic polymers. Regardless of the sign of $(H_{dd} - H_{dt})$ terms, at high temperatures, ΔH will approach $-(H_{dd} + H_{dt})/2$ when $S_{dd} = S_{dt}$. Thus, the atactic polymers will be produced.

The lower energy levels for the syndiotactic configuration as compared to the isotactic configuration are shown by Fordham⁴ for stereoregular polymers from free-radical propagation. This case corresponds to a case for which $H_{dd} < H_{dt}$. Hence, syndiotactic propagation in free-radical polymerization is enhanced over isotactic propagation by decreasing polymerization temperature.

The difference in the changes of free energy accompanying syndiotactic and isotactic propagation is

$$\Delta F_{dl} - \Delta F_{dd} = - (H_{dl} - H_{dd}) + T(S_{dl} - S_{dd})$$

Syndiotactic propagation in free-radical polymerization is more exothermic than isotactic propagation. If $(S_{dl} - S_{dd}) > 0$, there must be a temperature at which $(\Delta F_{dl} - \Delta F_{dd})$ is zero. This temperature is given by

$$T_0 = (H_{dl} - H_{dd}) / (S_{dl} - S_{dd}) \quad (8)$$

At this temperature the polymer is atactic. It appears below this temperature the product of the syndiotactic propagation is more stable thermodynamically than the product of the isotactic propagation; above this temperature, the product of the latter propagation is the more stable. Such a situation is shown in Figure 2.

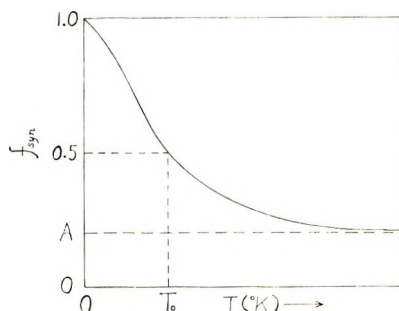


Fig. 2. Temperature dependence of f_{syn} for case where $H_{dl} > H_{dd}$ and $S_{dl} > S_{dd}$. $A = 1/[1 + \exp\{(S_{dl} - S_{dd})/R\}]$.

The opposite situation, for which $(S_{dl} - S_{dd})$ is negative, is shown in Figure 3. From eq. (8) we see that $(S_{dl} - S_{dd})$ must be positive in order for T_0 to be positive, since in this case $(H_{dl} - H_{dd})$ is positive. If $(S_{dl} -$

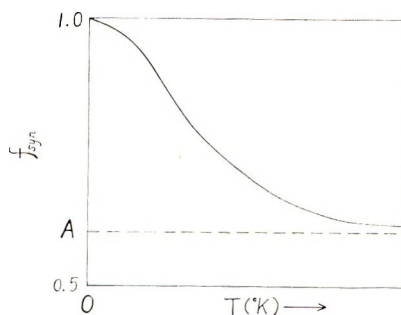


Fig. 3. Temperature dependence of f_{syn} for case where $H_{dl} > H_{dd}$ and $S_{dl} < S_{dd}$. $A = 1/[1 + \exp\{(S_{dl} - S_{dd})/R\}]$.

S_{dd} is negative but $(H_{dl} - H_{dd})$ is positive, $(\Delta F_{dl} - \Delta F_{dd})$ will always be negative even at sufficiently large values of T , and hence the product of the syndiotactic propagation is always thermodynamically stable.

At the ceiling temperature T_c , the system is in thermodynamic equilibrium and ΔF is zero.¹⁴ Writing $\Delta F = 0 = \Delta H - T_c \Delta S$, we have

$$\frac{T_c S_{dl} - H_{dl} - T_c R \ln [1 + \exp \{ (H_{dd} - H_{dl}) / RT_c - (S_{dd} - S_{dl}) / R \}]}{1 + \exp \{ (H_{dd} - H_{dl}) / RT_c - (S_{dd} - S_{dl}) / R \}} + \frac{T_c S_{dd} - H_{dd} - T_c R \ln [1 + \exp \{ (H_{dl} - H_{dd}) / RT_c - (S_{dl} - S_{dd}) / R \}]}{1 + \exp \{ (H_{dl} - H_{dd}) / RT_c - (S_{dl} - S_{dd}) / R \}} = 0 \quad (9)$$

Equation (9) does not lend itself readily to the calculation of T_c . However, eq. (9) is solved for T_c when $H_{dd} = H_{dl}$ and $S_{dd} = S_{dl}$. The ceiling temperature for this case is

$$T_c = \frac{H_{dd} + H_{dl}}{S_{dd} + S_{dl} - 2R \ln 2} = \frac{H_{dd}}{S_{dd} - R \ln 2}$$

This is the ceiling temperature for atactic polymers.

An alternative approach to the problem is based on quasi-chemical approximation.^{15,16} On this assumption two dd pairs combine to form two dl pairs according to the "reaction":



We have by analogy with chemical equilibrium

$$N_{dl}^2 / N_{dd}^2 = \exp \{ -\Delta F / kT \} \quad (10)$$

where ΔF is the change of free energy accompanying this reaction, N_{dd} and N_{dl} are the number of dd pairs and dl pairs, respectively, and k is the Boltzmann constant.

The change of free energy accompanying this reaction is

$$-\Delta F = 2(H'_{dl} - H'_{dd}) - 2T(S'_{dl} - S'_{dd}) \quad (11)$$

where $(H'_{dl} - H'_{dd})$ and $(S'_{dl} - S'_{dd})$ refer to the enthalpy and entropy change per link. Substituting eq. (11) into eq. (10) gives

$$\begin{aligned} N_{dl} / N_{dd} &= \exp \{ (H'_{dl} - H'_{dd}) / kT - (S'_{dl} - S'_{dd}) / k \} \\ &= \exp \{ (H_{dl} - H_{dd}) / RT - (S_{dl} - S_{dd}) / R \} \end{aligned} \quad (12)$$

The probability of a syndiotactic placement f_{syn} is given by

$$f_{\text{syn}} = N_{dl} / (N_{dl} + N_{dd}) \quad (13)$$

From eqs. (12) and (13) we find

$$f_{\text{syn}} = \frac{1}{1 + \exp \{ (H_{dd} - H_{dl}) / RT - (S_{dd} - S_{dl}) / R \}} \quad (14)$$

Equation (14) is identical to eq. (6).

The considerations presented here apply also to the problem of probabilities of the various possible modes of addition, namely head-to-head and

head-to-tail addition, 1, 2 and 1, 4 addition, and formation of *cis* and *trans* configurations.

The author wishes to thank Dainippon Celluloid Company for permission to publish this work.

References

1. Sawada, H., *J. Polymer Sci.*, **A3**, 2483 (1965).
2. Bovey, F. A., and G. V. D. Tiers, *J. Polymer Sci.*, **44**, 173 (1960).
3. Coleman, B. D., *J. Polymer Sci.*, **31**, 156 (1958).
4. Fordham, J. W. L., *J. Polymer Sci.*, **39**, 321 (1959).
5. Miller, R. L., and L. E. Nielsen, *J. Polymer Sci.*, **46**, 303 (1960).
6. Tobolsky, A. V., and A. Eisenberg, *J. Am. Chem. Soc.*, **82**, 289 (1960).
7. Huggins, M. L., *J. Am. Chem. Soc.*, **66**, 1991 (1944).
8. Fox, T. G., B. S. Garrett, W. E. Goode, S. Gratch, J. F. Kincaid, A. Spell, and J. D. Stroupe, *J. Am. Chem. Soc.*, **80**, 1768 (1958).
9. Fox, T. G., W. E. Goode, S. Gratch, G. M. Huggett, J. F. Kincaid, A. Spell, and J. D. Stroupe, *J. Polymer Sci.*, **31**, 173 (1958).
10. Fordham, J. W. L., P. H. Burleigh, and C. L. Sturm, *J. Polymer Sci.*, **41**, 73 (1959).
11. Hughes, R. E., paper presented at 133rd Meeting, American Chemical Society, San Francisco, Calif., April 1958; *Abstracts of Papers*, p. 10R.
12. Lewis, G. N., and M. Randall, *Thermodynamics and the Free Energy of Chemical Substances*, McGraw-Hill, New York, 1923, p. 97.
13. Orr, R. J., *Polymer*, **2**, 74 (1961).
14. Dainton, F. S., and K. G. Ivin, *Quart. Rev.*, **12**, 61 (1958).
15. Fowler, R. H., and E. A. Guggenheim, *Statistical Thermodynamics*, 3rd Ed., Cambridge Univ. Press, London, 1952, p. 576.
16. Eyring, H., D. Henderson, B. J. Stover, and E. M. Eyring, *Statistical Mechanics and Dynamics*, Wiley, New York, 1964, p. 304.

Résumé

On développe dans cet article une méthode thermodynamique statistique s'appliquant à l'étape de propagation de la polymérisation. On discute de l'influence de la température sur la distribution séquentielle d'unités syndiotactiques et isotactiques en polymérisation radicalaire. Cette théorie s'applique au problème des divers modes possibles de probabilités d'addition, à savoir l'addition tête-à-tête et tête-à-queue, l'addition 1,2 et 1,4 ainsi que la formation de configuration *cis* et *trans*.

Zusammenfassung

Eine statistische thermodynamische Methode zur Behandlung der Wachstumsreaktion bei der Polymerisation wird entwickelt. Der Einfluss der Temperatur auf die Sequenzverteilung syndiotaktischer und isotaktischer Einheiten bei der radikalischen Polymerisation wird diskutiert. Die Theorie kann auf das Problem der Wahrscheinlichkeit der verschiedenen Möglichkeiten beim Additionsschritt, nämlich Kopf zu Kopf- und Schwanz zu Schwanz-Addition, 1,2- und 1,4-Addition sowie Bildung von *cis*- und *trans*-Konfigurationen angewendet werden.

Received April 26, 1965
Prod. No. 4761A

Fracture Properties of Carboxylic Rubbers

J. C. HALPIN, *Air Force Materials Laboratory, Wright-Patterson AFB, Ohio*
and University of Dayton Research Institute, Dayton, Ohio,
 and F. BUECHE,* *University of Dayton, Dayton, Ohio*

Synopsis

Rupture properties of sulfur and zinc oxide vulcanizates of a carboxylic rubber have been experimentally determined. When the logarithm of the strength at break is plotted against the logarithm of the strain at break, failure envelopes are obtained for the two vulcanizates which diverge at long times or high temperatures. As a consequence of this experimental fact it is apparent that, while there exists a failure envelope which uniquely describes a given viscoelastic system, there is no general shape of the failure envelope representative of all the rupture properties of an elastomer through all degrees of vulcanization. It is shown that the molecular fracture theory of Bueche and Halpin provides a quantitative basis for the analysis of the strength properties of elastomers through a wide range of vulcanizate quality, provided the specific character of the network structure is taken into account. It is suggested that the so-called "unique" strength properties of metal oxide vulcanizates are in reality a natural reflection of a sparse network crosslinkage concentration.

INTRODUCTION

Current concepts^{1,2} regarding the strength properties of elastomers envision the rupture process to be one dominated by the slow propagation of tears or cracks within a deformed viscoelastic solid. Upon application of an external load or deformation, a critical tear or crack is initiated at a microscopic flaw and begins to increase in size with time. The crack grows slowly at first (starts at the time of load application) and then accelerates to a very rapid propagation rate as the stress at the crack tip increases with increasing crack dimensions. The growth mechanism of the tear or crack is visualized as an ideally simple process in which an aggregate of molecular chains, constituting the perimeter of the tear tip, stretch viscoelastically under the influence of a high stress concentration until their maximum extensibility is reached and they rupture. In this fashion the tear or crack propagates through the solid resulting in sample rupture or fracture.

A recent theoretical approach^{1,2} which emphasizes the above concepts has achieved substantial success in the development of a viscoelastic crack propagation model enabling a prediction of the ultimate properties. The theory states that the stress at break, σ_b , is inversely proportional to the "generalized" creep compliance, $\Gamma(t)$:

$$\sigma_b = K/\Gamma(t_b/q) \quad (1)$$

* On leave to the Peace Corps, Middle East Technical University, Ankara, Turkey.

where t_b is the total time taken to rupture the sample, q is a constant which relates the time scale of the molecular deformation at the tear root to t_b . K is a slowly varying parameter related to the critical rupture conditions at the crack tip. A general nonlinear function of the strain at break is shown to be proportional to the ratio of the "generalized" compliance of the macroscopic bulk polymer, $\Gamma(t_b)$, to the compliance of the molecular elements undergoing dynamic deformation, $\Gamma(t_b/q)$, at the crack root. In particular

$$\phi(\alpha_b) = K [\Gamma(t_b)/\Gamma(t_b/q)] \quad (2)$$

where $\phi(\alpha)$ is a nonlinear strain function characteristic of the specific network structure of the vulcanizate. The "generalized" creep function $\Gamma(t)$ is defined as

$$\Gamma(t) \equiv \phi[\alpha(t)]/\sigma \quad (3)$$

Implicit in this expression, for a general creep function, is the assumption that the viscoelastic nonlinearity observed in amorphous rubbers is a reflection of the nonlinear stress-strain response of the material and is not indicative of a fundamental variation in the physics of segmental motion with deformation. In fact, it is found that as an excellent approximation, the time dependence of the compliance can be factored out of the strain dependence over a considerable portion of the reduced time scale.³

An analysis of the theoretical model² clearly shows that the relaxation process associated with the molecular movement of the chains at the crack tip, not the absolute rate of bond rupture, is the factor controlling the strength of the materials. This point is amply supported by experimental evidence.^{1,2,4,7} Furthermore, the existence of a universal WLF equation, capable of reducing the time-temperature dependence of the ultimate properties, indicates that the precise nature of the chemical bonding along the polymer backbone (assuming an amorphous polymer) does not strongly influence the macroscopic strength properties, we are assuming a comparison at comparable values of $T - T_g$. The primary differences between elastomeric materials, at comparable values of $T - T_g$, are to be found in the dependence of the macroscopic viscoelastic response upon the specific network structure incurred during the vulcanization process. In our case, the appropriate viscoelastic function is the "generalized" creep curve $\Gamma(t)$. The purpose of this communication will be to show how the ultimate properties and the failure envelope depend upon the character of the generalized creep response $\Gamma(t)$.

To accomplish this task, a carboxylic rubber, vulcanized in two different ways, one with sulfur (SCR) and the other with zinc oxide (ZCR), was examined. The sulfur cure yields a typical network structure which approaches the physical model envisioned by the kinetic theory at high degrees of vulcanization. In contrast, several workers have noted that the introduction of metal oxides into elastomers containing carboxylic groups

yielded vulcanizates with enhanced strength properties⁸⁻¹¹ at ambient conditions. The source of these enhanced properties is thought to lie in the susceptibility of the crosslinkages to rupture and reform under stress. It is envisioned that this process of crosslinkage slip provides a mechanism which prevents individual network chains from becoming overstressed and thereby permits the deformed network as a whole to bear a higher stress. The proponents of this view find some support for this thesis in the increased extensibility and strong relaxation processes, at long times, inherent in this vulcanizate;⁹⁻¹¹ however, a high rate-dependent stress and increased extensibility may also be indicative of a low crosslinkage density.¹²⁻¹⁴ The concept of strong relaxation process refers to the long-time stress decay observed in some network structures at times and temperatures where it is to be expected that a network chain can become fully extended in a fraction of a second.¹³ In any event, it will be shown that the ZCR cure yields an unusual failure envelope, which is a direct consequence of relaxational processes impressed upon the elastomer by the specific network topology and structure incurred during the vulcanization process.

EXPERIMENTAL

The failure properties of a carboxylic butadiene/acrylonitrile terpolymer, Hycar 1072, were determined over a 100°C. range by using an Instron testing machine fitted with a special telescoping thermostatted cabinet. The temperature in the vicinity of the specimen undergoing a test was controlled $\pm 0.5^\circ\text{C}$. Crosshead speeds of 20.0, 2.0, and 0.2 in./min. were employed at each temperature.

Tensile tests were made on dumbbell-type specimens which were stamped from vulcanized sheets (0.08 in. thick) with a die. The dumbbell specimens having a gage length of 0.94 cm. and a width of 0.159 cm. were tested in the usual manner. Only samples which broke sharply in the test region were considered good breaks. The computed tensile strength was based upon the original cross-sectional area. The elongation at break was obtained by the direct observation of bench marks on the gage section of the sample. Stress-strain curves were determined by using ring-type specimens and techniques described earlier.^{1,2}

The techniques used in the creep experiments have been described in detail elsewhere.⁴ After the application of a fixed load on the end of the sample the elongation was observed as a function of time with a cathetometer. The sample temperature was maintained constant to within $\pm 0.2^\circ\text{C}$. The time-temperature equivalence was used to obtain the tensile creep behavior of the vulcanizates over many decades in time. Creep data were obtained at several temperatures between -60 and $+60^\circ\text{C}$. with a maximum elongation ratio of 2.2 for both vulcanizates.

Vulcanizates of the carboxylic butadiene-acrylonitrile terpolymer were prepared by Dr. K. Scott of the Goodyear Tire and Rubber Company by using the recipe given in Table I.

TABLE I
Compound Recipes for the Carboxylic Terpolymer. Vulcanizates Were Prepared in a
Mold under Pressure for the Time and Temperature Given

	Metal carboxyl	Sulfur
Polymer (Hycar 1072)	100	100
Zinc oxide	5.0	—
Sulfur	—	4
Diphenylguanidine	—	1.75
Time/temperature	30 min., 305°F.	5 min., 300°F.

RESULTS

When the data for the two rubbers are plotted in the form of $\log(\sigma_b T_0/T)$ versus $\log t_b$, where t_b is the time to break, the curves for various temperatures are found to exhibit a natural order in the same fashion as other viscoelastic measurement. The resulting curves can then be superimposed by shifting along the $\log t_b$ axis until all the data points fall along a single continuous curve, the shift distance required to effect superposition being denoted by $\log a_t$. By using the values of $\log a_t$ obtained for each vulcanizate the elongation at break was also superimposed. The master curves obtained in this fashion for the SCR and ZCR vulcanizates are shown in Figures 1 and 2. It is apparent that the ultimate stress and strain curves of the SCR vulcanizate follow the same general pattern as found for other well vulcanized gum rubbers. An examination of the data for the ZCR network shows the normal loss in strength with increasing temperature; however, the elongation at break increases rapidly with increasing temperature. (The recovery for the specimen broken at 100°C. with $\alpha_b \sim 13$ was 96%.)

An alternate procedure for comparing the ultimate properties is to plot the logarithm of the strain at break against the logarithm of the reduced stress at break to obtain the "failure envelopes" (Fig. 3). The difference in the network responses is immediately obvious due to the dramatic divergence of the failure envelopes with increasing temperature. On examining this figure one should note that both envelopes are coincident at decreased temperatures in the vicinity of the envelopes' normal maximum. As will be shown in succeeding sections the dramatic difference between these failure envelopes is the normal manifestation of differences in the dynamic network properties. As a direct consequence one must conclude that there is no general or unique shape for the failure envelopes which will represent large variations in network topology or structure.

To establish the point that the time-temperature dependencies of the two vulcanizations are viscoelastically similar in nature, the following analysis can be performed. Let us adopt the view that the temperature dependence of the ultimate properties is similar in form to the Arrhenius equation. One may then write

$$a_t \simeq \exp \left\{ -E/RT + E/RT_0 \right\} \quad (4)$$

or

$$\ln a_t \simeq -E/RT + E/RT_0 \quad (4')$$

where E is the apparent activation energy for the temperature dependence of the rate determining processes. Hence, a plot of $\log a_t$ against $1/T$ should give rise to a straight line of slope $(-E/R)$ as is shown in Figure 4.

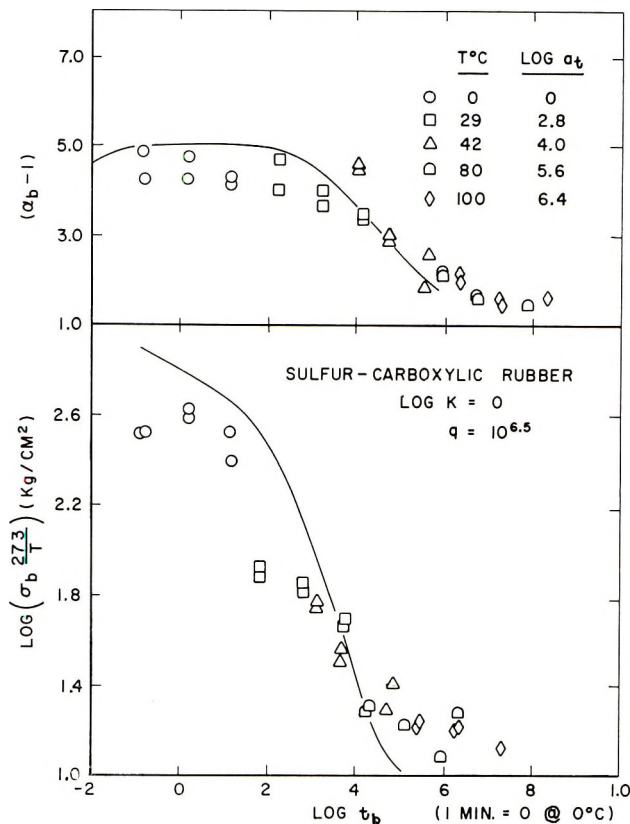


Fig. 1. Reduced experimental plot and theoretical prediction of the time to break of the tensile strength and ultimate elongation for a sulfur-cured carboxylic rubber.

The shift factors were those determined in the construction of Figures 1 and 2. As can be seen the two vulcanizates yield identical results, suggesting an apparent activation energy of 26.2 kcal./mole. This value, for the activation energy, is in the range characteristic of normal viscoelastic processes for network chains in rubbers.

Creep Response

The dynamic response of the two different network structures, which give rise to the geometric differences of the failure curves in Figure 3, can be characterized by their creep response (Fig. 5). The creep response for the SCR rubber is indicative of a tight, permanent, three-dimensional network

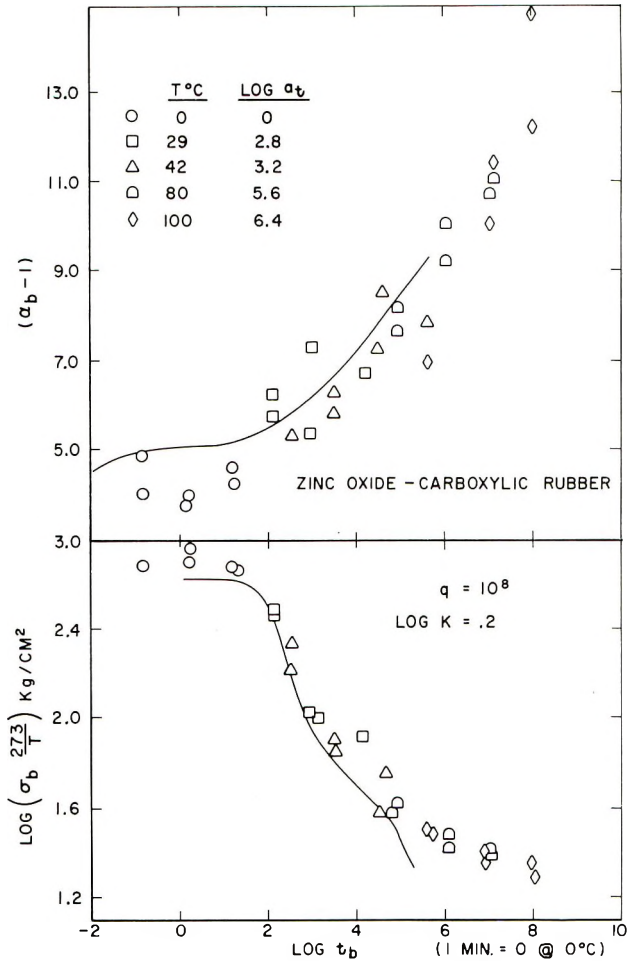


Fig. 2. Reduced experimental plot and theoretical prediction of the time to break of the tensile strength and ultimate elongation for a zinc oxide-cured carboxylic rubber.

which responds quickly under load and then remains at nearly constant elongation for long times thereafter. This typical creep response is directly associated with the ordinary rupture properties for the SCR system and for well vulcanized elastomers in general. In contrast to the SCR rubber, the zinc oxide cure exhibits a response characteristic of the situation in which the primary molecules have not been tied into a stable network. As a result, the rubber never reaches an equilibrium extension under the applied load, instead it continues to elongate indefinitely. The unusual shape of the failure envelope for the ZCR vulcanizate is a direct consequence of the geometry of the creep curve. This will be shown in the next section.

It is important to note that no permanent set was observed for either vulcanizate after deformation under constant load at 60°C. Repeated deformations of the ZCR rubber at 25 and 98°C. did show evidence of a

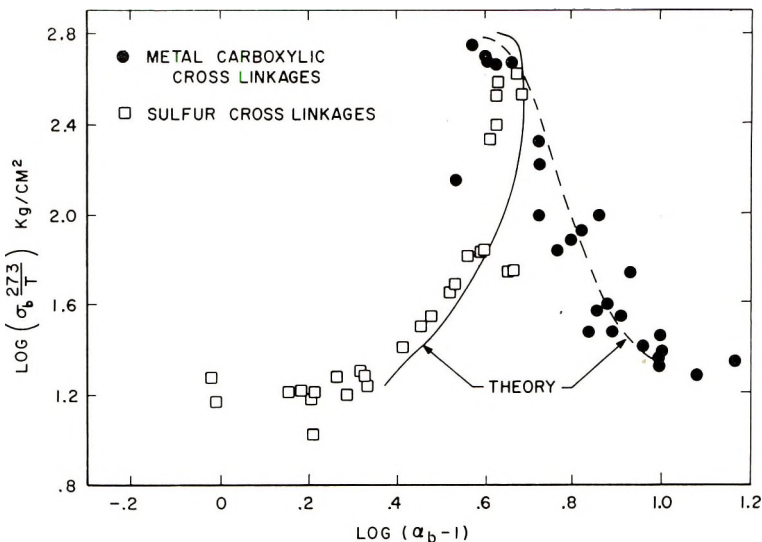


Fig. 3. Comparison of failure envelopes for a carboxylic rubber as a function of the vulcanization quality. The solid curves are the theoretical predictions.

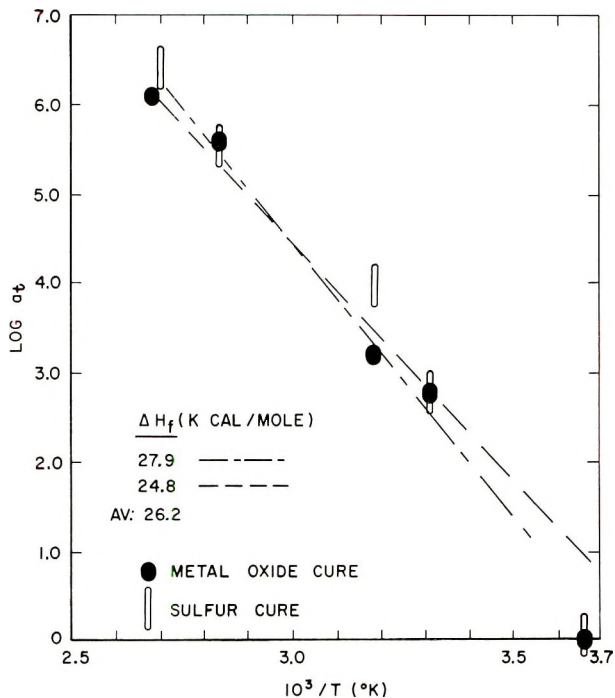


Fig. 4. Arrhenius plot of the WLF shift parameters used to estimate the effect of the vulcanization system upon the apparent activation energy.

small “Mullin’s softening” effect. However, the modulus change due to network breakdown was overshadowed by the pronounced time and tem-

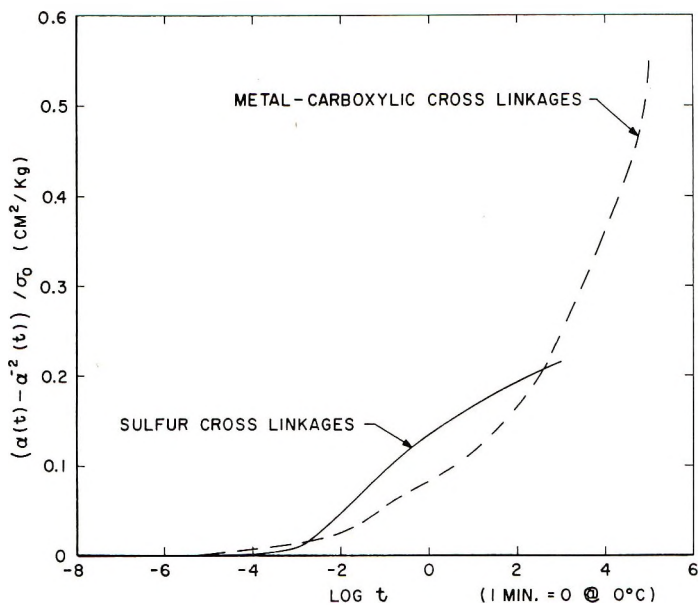


Fig. 5. Comparison of the creep curves for the sulfur cure and zinc oxide cure of a carboxylic rubber.

perature dependence of the modulus for the ZCR vulcanizate compared to the SCR vulcanizate. There was no evidence which suggested that the ruptured crosslinks reformed.

Comparison Between Theory and Experiment

In the development of the failure theory it was tacitly assumed that the stress-strain relationship could be taken as

$$\sigma = [\Gamma(t)]^{-1}\phi(\alpha) \quad (5)$$

where $\Gamma(t)$ is the generalized tensile compliance and $\phi(\alpha)$ is the equilibrium strain expression for a real vulcanized elastomer. While the actual form of the stress-strain relationship is not important to the derivation of the theory, as long as the time dependence can be factored³ into $\Gamma(t)$, the quantitative comparison between theory and experiment will depend upon a judicious choice for $\phi(\alpha)$.

In an effort to provide a reasonable but approximate treatment, the authors have adopted the following procedure for fitting the theory and the data.

The nonlinear strain function is written in the form

$$\phi(\alpha) \simeq (\alpha - \alpha^{-2})\rho(\alpha) \quad (6)$$

where the first term on the right-hand side is the usual kinetic theory term for small deformations. The term $\rho(\alpha)$ represents a correction to the kinetic theory in order that the deviations¹⁴ at moderate elongations, symbolized by a finite value of C_2 in the Mooney-Rivlin treatment, and the

effects of finite extensibility¹⁴ can be taken into account. An estimate of $\rho(\alpha)$ is obtained from a standard Mooney-Rivlin plot of the stress-strain response of the vulcanizate at temperatures removed from the glass temperature. $\rho(\alpha)$ is defined as:

$$\rho(\alpha) \equiv (1/2C_1)[\sigma/(\alpha - \alpha^{-2})] \quad (7)$$

$2C_1$ is obtained from the Mooney-Rivlin plot of the stress-strain data, as are the values of $\sigma/(\alpha - \alpha^{-2})$ for each value of α . If the reader examines one of the Mooney-Rivlin plots in Figure 6 it should be apparent that $\phi(\alpha)$ will provide a strain expression analogous to the kinetic theory relationship developed by Treloar,¹⁵ if the slope (C_2 in the Mooney-Rivlin relationship) at modest values of α is zero. At small deformations, $\rho(\alpha)$ will be unity and $\phi(\alpha)$ will reduce to the Hookean strain.

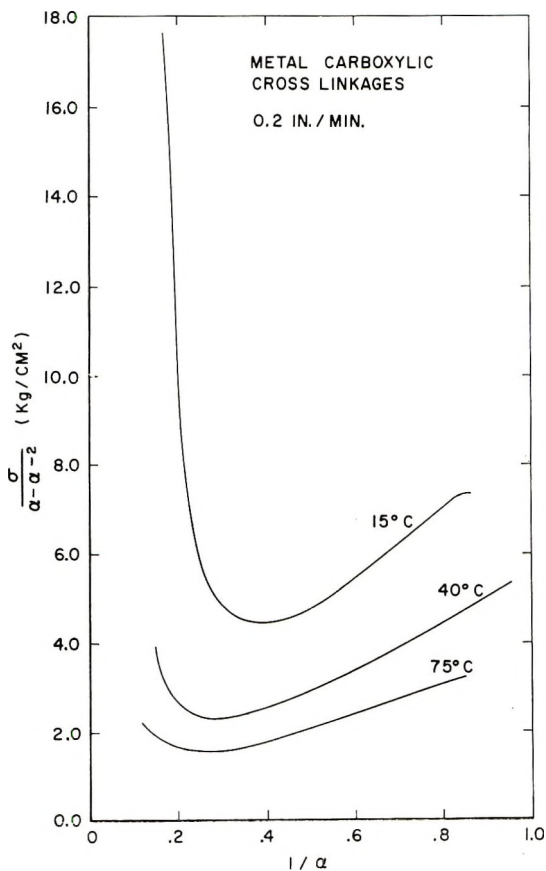


Fig. 6. Mooney-Rivlin plots at different temperatures for the zinc-cured carboxylic rubber.

For real network structures the creep response can be represented to a good approximation by

$$\Gamma(t) \equiv \{ [\alpha(t) - \alpha^{-2}(t)] / \sigma \} \rho[\alpha(t)] \quad (8)$$

where eq. (7) is evaluated from the Mooney-Rivlin plot for each value of $\alpha(t)$. The nonlinear strain function will be independent of both time and temperature over a considerable portion of the reduced time scale provided the primary molecules, during vulcanization, have been tied into a stable network exhibiting a plateau in the response at long times.

For the sulfur-vulcanized carboxylic rubber the network structure is sufficiently "tight," thus fulfilling the requirement for the straight-forward application of this approach. The generalized creep function was computed, according to eqs. (7) and (8), utilizing a stress-strain curve obtained at 40°C. and low stress creep data illustrated in Figure 5. Adopting the procedures developed in previous communication,^{2,4} a value of $q = 10^6$ ⁵ was found to give a curve of $-\log \Gamma(t)$ lying parallel to $\log \sigma_1$ of Figure 1. The value of $\log K$ needed to shift the $-\log \Gamma(t)$ along the stress axis was found to be zero. A curve of $\log [\phi(\alpha)]$ versus α was then computed in accordance with eq. (6). By utilizing the $\log [\phi(\alpha)]$ plot, the values of q and K obtained here, and performing the computation indicated by eq. (2), a theoretical curve of α_b versus $\log t$ is obtained. The results, shown in Figure 1, are indicative of good agreement between theory and experiment. Furthermore, the failure envelope can also be predicted by utilizing the same values of q and K determined from the time to break curves. The predicted envelope is illustrated in Figure 3. The substantial agreement between the theoretical prediction and the experimental data substantiates the integrity of K , q , and $\phi(\alpha)$ for a well vulcanized elastomer.

The physical situation, regarding the carboxylic-zinc oxide cure, is complicated by the inability of the polyvalent metal ions to tie the primary molecules into a stable network structure which exhibits a plateau in the response at long times. This difficulty can be appreciated when one recognizes that the lack of a steady-state elastic compliance necessarily invalidates the concept of a unique equilibrium value of M_c which characterizes the network structure. Instead, this response implies the concept of an apparent M_c which is time- and temperature-dependent through the range of experimental observation. A strong time-temperature dependence of M_c necessarily requires a time-temperature dependence of the "upturn" in the stress-strain curve, as the magnitude of the maximum extensibility is directly related,¹⁵ in principle at least, to the magnitude of M_c . One should also expect that the overall shape, the change in magnitude of C_2 , of the stress-strain curve will also be a function of time and temperature. The expected sensitivity of the stress-strain response to rate of deformation and temperature is borne out by the Mooney-Rivlin plots in Figure 6. Note the increasing value of α at the point of the upward inflection (maximum extensibility) and the change in slopes (the C_2 values). As a consequence, the persistence of marked creep or, conversely, rapid stress relaxation, at long times, necessarily negates the existence of a unique steady-state expression for $\phi(\alpha)$ which will characterize the network response over a wide range of testing variables. However, an approximate

treatment of this behavior can be executed by utilizing an appropriate stress-strain curve in the temperature range of immediate interest for the computation of $\phi(\alpha)$. For the ZCR rubber the generalized creep function $\Gamma(t)$ was estimated from creep data and a 40°C. stress-strain plot. By using this $\Gamma(t)$ curve and the fitting procedure outlined earlier a fit was obtained with the experimental strength data as shown in Figure 2. The value of q was found to be 10^8 with $\log K$ equaling 0.2.

In order to predict the elongation at break, eq. (6) and the stress-strain curves at 15, 40, and 70°C. were used to compute plots of $\log [\phi(\alpha)]$ versus α for each temperature (see Fig. 7). (In examining the figure one

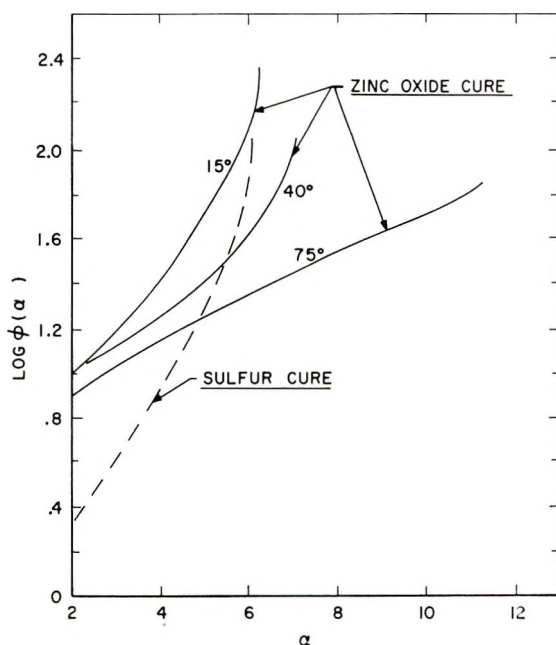


Fig. 7. Plot of the logarithm of the general strain functions for the sulfur- and zinc oxide-cured carboxylic rubber against the relative elongation.

should note the $\phi(\alpha)$ function for the SCR vulcanizate and the fact that it is insensitive to an increase in temperature or time scale.) Next the ratio $\log [\Gamma(t)/\Gamma(t/10^8)]$ was computed from the general creep curve for several different values of the time to break. By using eq. (2), the value of $\log K$ determined above and the $\log [\phi(\alpha)]$ curves an estimate of the elongation at break was made. In performing this operation the value of α was obtained from the $\phi(\alpha)$ curve in the temperature range appropriate to the magnitude of the time to break. (This operation is made possible through the use of the time-temperature superposition technique.) The striking results are shown in Figure 2. To be consistent one should now go back and recompute the theoretical σ_b curve in a similar fashion. This would improve the fit at long times. However, the data indicate a diver-

gence from any estimate of the strength we could make. The reason for this discrepancy is not apparent at this time.

In Figure 3 a comparison between the theoretical and experimental failure envelopes is made. As one can readily see, the theory is capable of representing the failure properties of viscoelastic bodies possessing a wide diversity in properties.

DISCUSSION

From the above treatment it appears that the strength observed in amorphous rubbers is intimately linked to the magnitude of K and the behavior of the creep curves. The values of K obtained here are of the same order of magnitude. It is difficult to assess the physical significance of the difference in the values of K due to the approximate nature of the nonlinear viscoelastic treatment. If K does not vary greatly with variations in the vulcanization system, then differences in the strength properties must be related to differences in the creep response (or any other dynamic response) of the two vulcanizates. The problem of gaining some understanding of the different rupture properties is then reduced to ascertaining the reasons for the differences in the creep curves shown in Figure 5.

As mentioned earlier, the SCR creep curve is typical of well-vulcanized synthetic elastomers and is, in principle, explicable from accepted network theory of viscoelastic response.¹⁶ By this statement we wish to imply that the SCR creep response roughly approximates the response we expect for a perfect tetrahedral network. The question is then, what causes the mechanical degeneracy which is exhibited by the response of the ZCR vulcanizate? One point of view⁸⁻¹¹ suggests that the marked creep and rapid stress relaxation in the region of time scale normally associated with the plateau region is due to a chemical relaxation process involving an exchange reaction between the electrovalent crosslinks on different chains. The proponents^{9,11} of this view suggest that the cleavage and reformation of the electrovalent crosslinkages should result in higher strength properties by the dissipating excessive local over stresses incurred during extension due to the random length distribution of network chains. Accordingly, the shorter chains are subjected to abnormally high stress and rupture at relatively low sample elongations. If, however, the crosslinks can slip under the localized high-stress concentrations, the local stress will be dissipated by spreading the load over neighboring chains. The proponents¹¹ then argue that chain ruptures would introduce "molecular flaws" into the network, thereby enhancing local-stress inhomogeneity and leading progressively to catastrophic rupture, while wholesale crosslink interchange would allow for a uniform sharing of the force through the network and thereby permitting the deformed network as a whole to bear a higher stress.

These arguments, based upon a chemical relaxation mechanism, require that when the rubber network is maintained in a deformed condition, the breaking or slip of a crosslink causes the disappearance of the strained

network chains associated with that crosslink. The subsequent reforming of the crosslinks produces an equal number of network chains, but these are in a molecularly unstrained configuration, even though the rubber network as a whole is under strain. On removal of the deformation the sample should retract due to the influence of the remaining original network structure, but this restoring force will be resisted by the new network structure. In other words, the released sample will return to a length at which the opposing forces of these two networks just balance each other. This chemical-relaxation mechanism implies that the strained ZCR vulcanizate would eventually become completely relaxed and that its permanent set would be large. Our experimental results show that the large deformation observed at long times and high temperatures both in creep and rupture experiments is recoverable. Similar results have been reported by Cooper,⁹ Dogadkin et al.,¹¹ Cunneen, Moore, and Shephard,¹⁷ and Zakharov¹⁰ for both creep and stress relaxation. In the efforts cited no evidence was found which indicates any change in network density after large sustained deformations. Both Cunneen et al.¹⁷ and Zakharov¹⁰ present stress-relaxation data showing very rapid relaxation with respect to the equivalent sulfur vulcanizate with the relaxation ceasing at roughly one-half the value observed for the equivalent sulfur vulcanizate. This indicates that the number of crosslinks remaining is significantly less than that found in ordinary vulcanized rubber. Both authors suggest that the divalent metal crosslinks are relatively permanent and are responsible for the high elastic recovery of these vulcanizates. Zakharov¹⁰ proposes that the sparse network of chemical crosslinks may be explained by the improbability of realizing a high frequency of network chains from the low frequency of distribution of carboxylic groups along the primary molecular chains.

If chemical relaxation (crosslinkage interchange) was the significant rate-contributing or -controlling agency then one should see a difference in the apparent activation energies for ZCR versus the SCR vulcanizate. The data in Figure 4 indicate that the activation energies are identical and of the proper order of magnitude for normal physical viscoelastic processes for network chains in rubber. As a consequence, we do not find any evidence to support the contention that the deformational and strength properties of carboxylic rubbers are uniquely dependent upon the nature of the crosslink within the network.

At this point it is pertinent to note that Zakharov was able to show that the initial stress, after a rapid stretch of a metal oxide vulcanizate of carboxylic rubber, is higher in each case than for the comparable sulfur vulcanizate. The carboxylic rubbers show a considerable drop in stress in time while the sulfur vulcanizate reaches equilibrium rather quickly. At long times, the carboxylic rubbers, compared to SCR, exhibit more than twice the drop in stress. These observations are virtually identical to situations found in lightly crosslinked vulcanizates in general. By this we mean that if one examines a vulcanizate near the maximum in the

strength versus degree of crosslinking curve and compares it with a more tightly crosslinked rubber, results similar to those reported by Zakharov are obtained.¹³ The differences in the creep curves of Figure 5 are identical to the differences observed in the response of lightly versus highly crosslinked gum elastomers.¹⁴ Furthermore, if one examines the strength as a function of the degree of crosslink density at a suitably chosen $T - T_g$ (40–50°C.) and strain rate, it is possible to obtain a ratio of strength at the maximum to the strength at high crosslink density of approximately $3-3^{1/2}$. Thus it is possible to take any gum elastomer with any suitable curing system and obtain the same relative strength properties as are quoted in literature⁸ for the carboxylic rubbers. It is our belief that the peculiar properties of carboxylic vulcanizates are due, for the major part, to anomalies in the physical relaxation processes of sparsely crosslinked networks and are not uniquely dependent upon the chemical nature of the crosslinkages.

Reflecting upon these circumstances one must conclude that the master curves utilized here in the treatment of the ultimate properties reflect the detailed viscoelastic character of the vulcanizate undergoing rupture in a manner analogous to the way the deformation properties of a body are reflected in the creep response. In direct analogy with the creep response, a near equilibrium strength is only realized at exceedingly long times and high temperature and then only for networks possessing a sufficient three-dimensional topology. Correlations relating strength properties to kinetic theory parameters are, therefore, necessarily limited in validity to those vulcanizates which have realized some minimum state of "three-dimensionality" in the network structure.

CONCLUSION

The molecular fracture theory of Bueche and Halpin provides a quantitative basis for the analysis of the strength properties of elastomers through a wide range of vulcanization provided the specific molecular character of the network structure is taken into account. It is shown that the failure curves represent, in a direct manner, the complete viscoelastic character of the elastoviscous solid undergoing rupture. As a consequence, any attempt to correlate the rupture properties of rubbers over a wide range of vulcanization with parameters obtained from the equilibrium kinetic theory will be frustrated if the changing dynamical character of the network response is not taken into account. This point is supported by the experimental fact that there is no unique shape of the failure envelope representative of the rupture properties of an elastomer through all degrees of vulcanization.

The experimental results obtained here, with regard to the quality of metal oxide vulcanization of carboxylic rubber, suggests that the so-called "unique" physical properties of this vulcanizate are in reality natural reflections of a sparse network crosslinkage concentration. The strength

advantage exhibited by the SCR vulcanizate over a typical SBR rubber is merely the reflection of the difference in crosslinkage density and a higher glass transition temperature for the carboxylic elastomer.

The portion of this work carried out at the University of Dayton Research Institute was supported by the Nonmetallic Materials Division, Air Force Materials Laboratory, Research and Technology Division, under Contract AF 33(657)-10688. The portion of this work carried out in the Physics Department at the University of Dayton was supported by a grant from the Goodyear Tire and Rubber Company as a part of Goodyear's program in support of fundamental research on synthetic rubber.

References

1. Bueche, F., and J. C. Halpin, *J. Appl. Phys.*, **35**, 36 (1964).
2. Halpin, J. C., *J. Appl. Phys.*, **35**, 3133 (1964).
3. Halpin, J. C., *J. Polymer Sci.*, **B2**, 959 (1964).
4. Halpin, J. C., and F. Bueche, *J. Appl. Phys.*, **35**, 3142 (1964).
5. Bueche, F., *J. Appl. Phys.*, **24**, 738 (1955); **28**, 784 (1957).
6. Smith, T. L., *J. Polymer Sci.*, **32**, 99 (1958); *J. Appl. Phys.*, **35**, 27 (1964); *J. Polymer Sci.*, **A1**, 3597 (1963).
7. Smith, T. L., and P. J. Stedry, *J. Appl. Phys.*, **31**, 1892 (1960).
8. Brown, H. P., *Rubber Chem. Technol.*, **30**, 1347 (1957).
9. Cooper, W., *J. Polymer Sci.*, **28**, 195 (1958).
10. Zakharov, N. D., *Rubber Chem. Technol.*, **36**, 569 (1963).
11. Dogadkin, B. A., Z. N. Tarasova, and I. I. Gol'berg, *Proc. Rubber Technol. Conf. 4th (London)*, **1962**, 65.
12. Bueche, F., *J. Appl. Polymer Sci.*, **1**, 240 (1959).
13. Bueche, F., and T. J. Dudek, *Rubber Chem. Technol.*, **36**, 1 (1963).
14. Dudek, T. J., and F. Bueche, *J. Polymer Sci.*, **A2**, 812 (1963); F. Bueche, *J. Polymer Sci.*, **25**, 305 (1957).
15. Treloar, L. R. G., *The Physics of Rubber Elasticity*, Clarendon Press, Oxford, 1958; L. R. G. Treloar, in *Die Physik der Hochpolymeren*, H. A. Stuart, Ed., Springer-Verlag, Berlin, 1956, Chap. 5.
16. Bueche, F., *Physical Properties of Polymers*, Interscience, New York, 1962, Chap. 16.
17. Cunneen, J. I., C. G. Moore, and B. R. Shephard, *J. Appl. Polymer Sci.*, **3**, 11 (1960).

Résumé

On détermine la résistance à la rupture d'un caoutchouc carboxylé vulcanisé par le soufre et l'oxyde de zinc. Lorsqu'on porte en graphique logarithmique la force de rupture, en fonction de la déformation à la rupture, on obtient des enveloppes de rupture qui divergent aux temps longs ou aux températures élevées. On peut en conclure qu'il existe bien des enveloppes de rupture qui décrivent de manière non ambiguë un certain système viscoélastique mais que l'enveloppe de rupture représentant le comportement d'un élastomère à tous les taux de vulcanisation n'existe pas. On montre que la théorie moléculaire de la rupture de Bueche et Halpin fournit une base quantitative pour analyser la résistance à la rupture des élastomères dans un large domaine de vulcanisation à condition que le caractère propre du réseau soit pris en considération. Ceci suggère que les propriétés "uniques" des vulcanisats d'oxyde métallique sont en réalité le reflet naturel d'un réseau à taux de partage limité.

Zusammenfassung

Die Brucheigenschaften von Schwefel- und Zinkoxydvulkanisaten eines Karboxylkautschuks wurden experimentell bestimmt. Beim Auftragen des Logarithmus der Bruchfestigkeit gegen den Logarithmus der Bruchspannung werden für die beiden Vulkanisate Bruchenvolpen erhalten, welche sich bei langer Dauer oder hoher Temperatur unterscheiden. Als Folge dieses experimentellen Befundes muss man annehmen, dass, während zur Beschreibung eines gegebenen viskoelastischen Systems allein eine Bruchenvolpe besteht, keine allgemeine, für alle Brucheigenschaften eines Elastomeren bei allen Vulkanisationsgraden repräsentative Gestalt der Bruchenvolpe besteht. Die molekulare Bruchtheorie von Bueche und Halpin liefert eine quantitative Grundlage für die Analyse der Festigkeitseigenschaften von Elastomeren über einen weiten Vulkanisationsbereich, vorausgesetzt, dass der spezifische Charakter der Netzwerkstruktur berücksichtigt wird. Es wird angenommen, dass die sogenannten "einzigartigen" Festigkeitseigenschaften von Metalloxydvulkanisaten in Wirklichkeit die natürliche Folge einer geringen Vernetzungsstellenkonzentration sind.

Received July 6, 1964

Revised March 22, 1965

Prod. No. 4736A

Study of Hydrogen Bonding in Poly(vinyl Alcohol) by a Nuclear Magnetic Resonance Method

RAMDAS P. GUPTA, *The Royal Institute of Technology, Division of Physical Chemistry, Stockholm, Sweden*, and ROY C. LAIBLE, *U. S. Army, Natick Laboratories, Natick, Massachusetts*

Synopsis

The effect of water fixation in poly(vinyl alcohol) yarn has been studied by the NMR method. Water content in the PVA specimen was varied by exposing the specimen to different relative humidity conditions. The NMR wide line spectra have been registered for samples of PVA (a) dried at 80°C. for 24 hr., (b) conditioned to 40% relative humidity, and (c) conditioned to 80% relative humidity. Wide line spectra for the dry specimen of PVA have a broad band only, but the 40% relative humidity conditioned sample has a broad band and a narrow band, and at the same time the sample conditioned to 80% relative humidity has a broad band and two narrow bands. Variation of intensity as a function of water content has been studied. Variation of wide and narrow band intensity shows that at low relative humidity water enters the amorphous and crystalline regions and is held there by the formation of hydrogen bonds. Hydroxyl groups may replace hydrogen atoms at random on a carbon chain without destroying crystallinity. In the amorphous regions water molecules are held relatively free and are accommodated in voids. This would then account for the second peak in the narrow band of the spectrum seen at higher water contents.

Introduction

The polymer, poly(vinyl alcohol), has been the subject of many investigations because of its theoretical and practical interest.¹ Poly(vinyl alcohol) does not have a unique chain structure because the OH groups are randomly distributed up and down with respect to the plane of the zigzag backbone, and one would consider the chain as a copolymer of isotactic and syndiotactic copolymer.² Nuclear magnetic resonance studies have included poly(vinyl alcohol) in D₂O,³ stretched poly(vinyl alcohol),⁴ the influence of irradiation,^{5,6} and the effect of heat treatments.⁷ In this present work the effect of water fixation on the NMR line shape of highly oriented poly(vinyl alcohol) yarn has been studied. This was accomplished by varying the water content in PVA by the use of different relative humidity conditions.

Experimental

The specimen of poly(vinyl alcohol) used in this experiment was in the form of a high tenacity multifilament yarn obtained from Kurashiki Rayon

company. The yarn had an estimated crystallinity of greater than 65% based upon density measurements and a high birefringence in the range of 0.039. The sample was tightly packed in a glass tube for NMR experiment. The specimen was conditioned to the desired relative humidity maintained in a desiccator. After about two weeks exposure, when the specimen had attained a constant weight, the NMR line shape was determined. In this way, the NMR line shape was recorded at various relative humidity conditions, i.e., at varying water contents of PVA.

A Varian model NMR instrument suitable for wide line work was used at 14.8 Mcycles radio frequency for the study of proton nuclei in the specimen of PVA. The spectrometer settings of radiofrequency field, modulation field, amplification, etc. were kept constant for all measurements, so that the derivative line shape would be comparable. The same quantity of dry specimen of PVA was exposed to different relative humidity conditions, and thus weight, volume, and surface of the dry specimen of PVA was the same in all cases. Therefore, it is possible to compare the areas under the narrow bands.

The area under the absorption band is proportional to the band intensity and is determined, in this case, by calculating the first moment of the experimentally obtained derivative line shape. Their first moments of the narrow and wide bands have been computed separately, and these are equal to the areas under the absorption band for narrow and wide bands, respectively. The first moment has been taken as a measure of intensity in arbitrary units. The radiofrequency field was maintained below the saturation limit.

Results and Discussion

Figures 1-3 show the derivative NMR line shapes of PVA specimen after three conditioning treatments.

Figure 1 shows the derivative line shape of a PVA specimen dried at 80°C. for 24 hr. This line shape has a broad band and a very small narrow band. The narrow band shows that, even after this heating, a small quantity of water is left in the lattice of PVA. This indicates that some water mole-

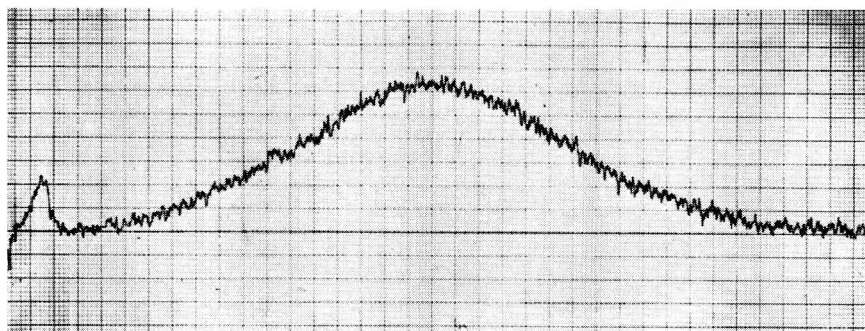


Fig. 1. NMR derivative line shape of dry PVA. Only the first half of the band is shown.

cules are tightly bound to the lattice and are difficult to remove. The wide band intensity is contributed to by the protons in CH_2 , CH , and OH groups of the PVA sample.

Figure 2 is the derivative line shape of the same sample at 40% R.H. In this case, the wide band and narrow band intensity have both increased

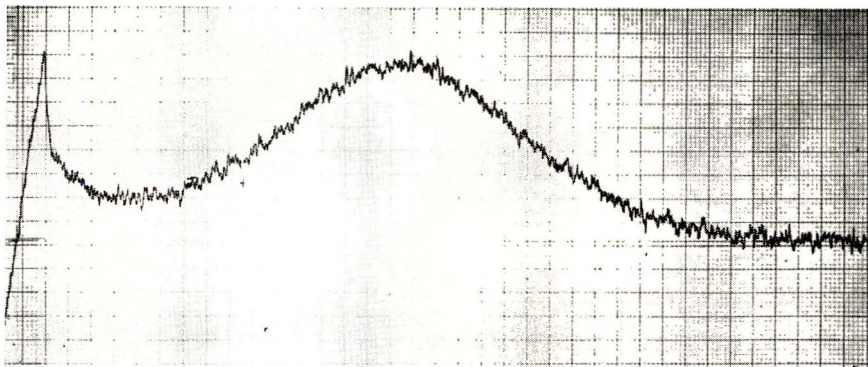


Fig. 2. NMR derivative line shape of PVA conditioned to 40% R.H.

compared to the previous line shape, showing that water fixation has taken place in crystalline as well as amorphous regions of the specimen. There is a further increase in the narrow and wide band intensities of the spectrum of the same sample conditioned at 80% R.H., as shown in Figure 3.

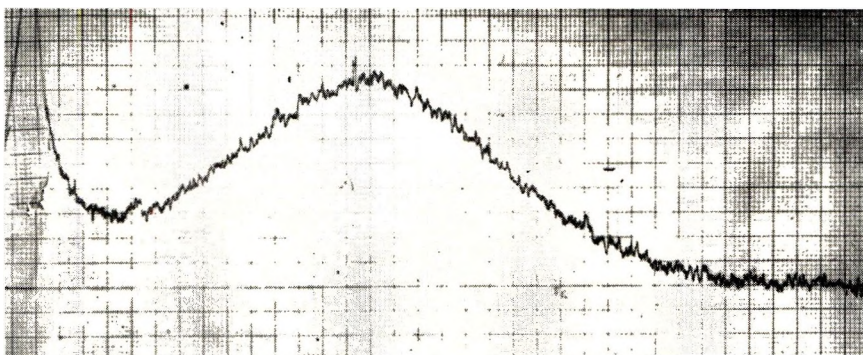


Fig. 3. NMR derivative line shape of PVA at 80% R.H.

The narrow line has only one peak for the sample conditioned at 40% R.H. and for the sample dried at 80°C. On the other hand, the sample conditioned at 80% R.H. exhibits two peaks, as shown in Figure 4.

The sharper peak in the narrow band is probably due to free water held in the sample. The broader peak of the narrow band is due to water held in the amorphous regions of the specimen by the formation of hydrogen bonds.

Figure 5 shows the variation of spectral intensity of the NMR line as a function of water content of the specimen. The wide band, the narrow

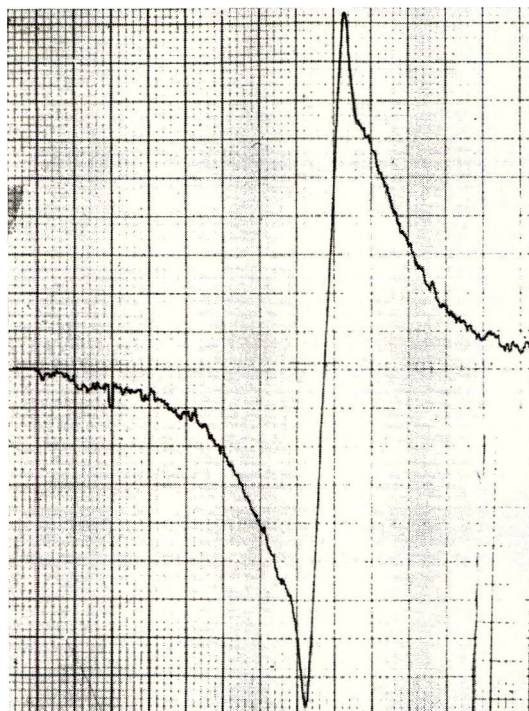


Fig. 4. NMR line shape of PVA at 80% R.H. Only the narrow band as a whole is shown here.

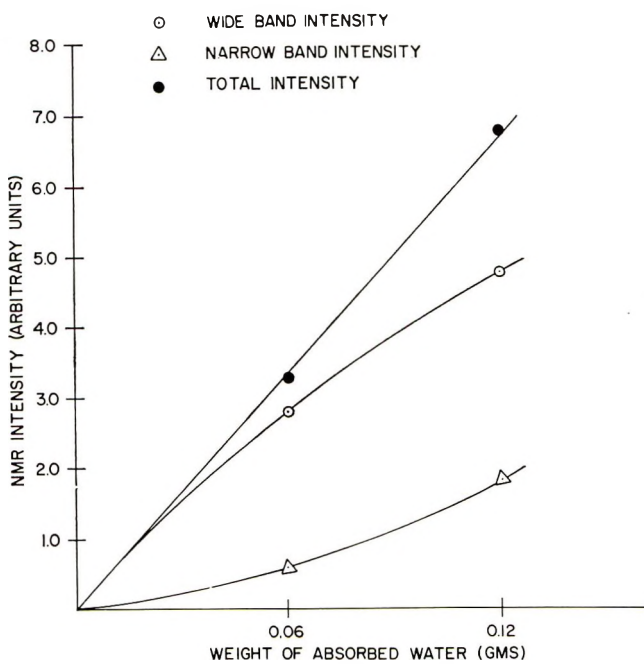


Fig. 5. Variation of NMR intensity with increase in water content of PVA.

band, and the total line intensities have been plotted separately in this figure. The error estimated in the calculation of intensity is about 2%; therefore, one can get only a rough idea of intensity variation from this figure. The total intensity is nearly proportional to the amount of water added to the specimen. Variation of wide and narrow band intensity shows that at low relative humidity water enters the amorphous and crystalline regions and is held there by the formation of hydrogen bonds. The hydrogen bonds formed, in both the amorphous and crystalline regions, are shown as interchain hydrogen bonds in Figure 6, based on x-ray evidence of Bunn.^{8,9} It should also be pointed out that hydroxyl groups may replace hydrogen atoms at random on a carbon chain without destroying crystallinity; therefore, not all of the intermolecular hydrogen bonds shown in Figure 6 would be formed. In these cases (mismatch) and in defect regions

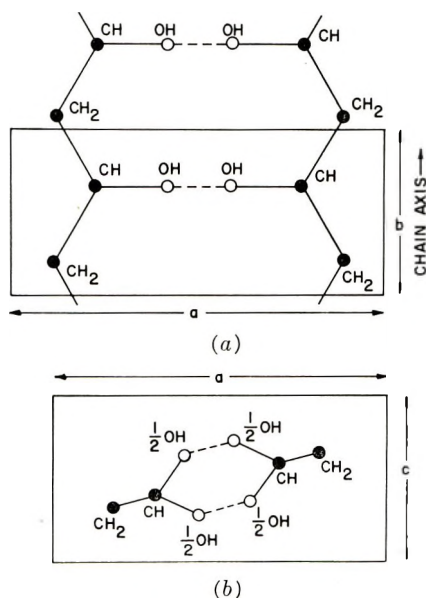


Fig. 6. Hydrogen bonds in poly(vinyl alcohol): (a) lateral section of molecule; (b) cross section of molecule. The broken lines indicate the hydrogen bonds.

where the distance between OH units is large, which leads to weak bonding, water molecules could replace the much stronger hydrogen bond. Cases where water molecules are held free, probably in the amorphous regions of the specimen, would require voids to accommodate them. This would then account for the second peak in the narrow band of the spectrum seen at higher relative humidities.

Conclusions

From the change in NMR intensity with water content, it appears that the hydrogen bonding is altered in the crystalline as well as in the amorphous regions. At lower humidity, both types of regions appear to be

equally available. At higher humidity conditions, some of the water molecules appear to be free, indicating some sort of void structure in the amorphous regions.

Résumé

L'effet de la fixation d'eau dans des fibres d'alcool polyvinylique a été étudié par la méthode de la RMN. La teneur en eau des échantillons était variée en exposant les spécimens à des conditions d'humidité relative différentes. Les spectres de RMN en large raie ont été enregistrés sur des échantillons de PVA (*a*) séchés à 80°C. durant 24 heures (*b*) soumis à 40% d'humidité relative (*c*) soumis à 80% d'humidité relative. Le spectre en raie large du PVA sec révèle uniquement une bande large, mais l'échantillon à 40% conditionné à 40% d'humidité relative montre une raie large et une raie étroite; l'échantillon conditionné à 80% d'humidité relative donne une raie large et deux raies étroites. Les variations de l'intensité en fonction de la teneur en eau ont été étudiées. La variation de la largeur et de l'intensité des raies montre qu'une faible quantité d'eau d'humidité relative pénètre les régions cristallines et amorphes et y est retenue par la formation de liens hydrogène. Des groupements hydroxyles peuvent statistiquement remplacer des atomes d'hydrogènes sur la chaîne carbonée sans en détruire la cristallinité. Dans les régions amorphes les molécules d'eau sont relativement libres dans des lacunes. Ceci s'accorderait donc avec l'apparition du second pic étroit observé dans le spectre à teneur élevée en eau.

Zusammenfassung

Der Einfluss der Wasserfixierung auf Polyvinylalkoholgarne wurde nach der NMR-Methode untersucht. Der Wassergehalt der PVA-Proben wurde durch Einwirkung verschiedener relativer Feuchtigkeit auf die Proben variiert. Die NMR-Breitlinienspektren wurden für (*a*) bei 80°C. durch 24 Stunden getrocknete, (*b*) bei 40% relativer Feuchtigkeit und (*c*) bei 80% relativer Feuchtigkeit konditionierte PVA-Proben aufgezeichnet. Das Breitlinienspektrum der trockenen PVA-Probe besitzt nur eine breite Bande, die bei 40% r.F. konditionierte Probe besitzt eine breite und eine enge Bande und die bei 80% r.F. konditionierte Probe eine breite und zwei enge Banden. Die Abhängigkeit der Intensität vom Wassergehalt wurde untersucht. Die Abhängigkeit der Intensität der breiten und der engen Bande zeigt, dass bei niedriger relativer Feuchtigkeit Wasser in die amorphen und kristallinen Bereiche eindringt und dort durch die Bildung von Wasserstoffbindungen festgehalten wird. Hydroxylgruppen können die Wasserstoffatome an einer Kohlenstoffkette statistisch ohne Zerstörung der Kristallinität ersetzen. In den amorphen Bereichen befinden sich verhältnismässig freie, in Leerstellen untergebrachte Wassermoleküle. Sie könnten für das zweite, in der engen Bande des Spektrums bei höherem Wassergehalt beobachtete Maximum verantwortlich sein.

References

1. Kurosaku, S., and T. Furumaya, *Repts. Progs. Phys. Japan*, **1958**, 157.
2. Ke, B., *Newer Methods in Polymer Characterization*, Polymer Reviews, Vol. VI, Interscience, New York, 1964, p. 77.
3. Danno, A., and N. Hayakawa, *Bull. Chem. Soc. Japan*, **35**, 1748 (1962).
4. Yamogata, K., and S. Hirota, *Oyo Butsuri*, **30**, 261 (1961).
5. Fujiwara, S., *J. Polymer Sci.*, **44**, 93 (1960).
6. Fujiwara, S., *J. Polymer Sci.*, **51**, 515 (1961).
7. Nahara, S., *Kobunshi Kagaku*, **15**, 105 (1958).
8. Bunn, C. W., *Nature*, **161**, 929 (1948).
9. Billmeyer, F., *Textbook of Polymer Chemistry*, Interscience, New York, 1962.

Received February 9, 1965

Revised April 1, 1965

Prod. No. 4730A

Kinetics of Reaction of Ferricyanide with Mercaptan Solubilized in Polystyrene Latex

E. J. MEEHAN, I. M. KOLTHOFF, and M. S. TSAO, *School of Chemistry, University of Minnesota, Minneapolis, Minnesota*

Synopsis

The rate of reaction of ferricyanide with *n*-octyl mercaptan solubilized in polystyrene latex has been measured. The mercaptan was dissolved completely in the latex polymer particles before the addition of ferricyanide. The latices were prepared with potassium myristate, sodium tetradecyl sulfate, and dodecylammonium chloride, as surfactants. In each latex the reaction was first-order to ferricyanide, mercaptan, and hydroxyl ion. The rates in myristate and tetradecyl sulfate latices were approximately equal, but smaller by about five orders of magnitude (extrapolated to the same pH) than the rate in the dodecylammonium chloride latex. The reaction apparently occurs on the surface of the polymer particles and thus is favored in the latex with positively charged particles on the surface of which the ferricyanide is adsorbed as counterion.

The reaction of *n*-octyl mercaptan with ferricyanide has been studied in homogeneous acetone-water medium.¹ The kinetics are somewhat involved, but in the pH range 7-11 the reaction was found to be first-order to mercaptan and to ferricyanide, and the rate constant was proportional to $[\text{OH}^-]$. In acid medium (pH 2.8-5.5) no simple kinetic law was observed.

In the present paper a preliminary study is described of the rate of oxidation by ferricyanide of mercaptan which is solubilized in polystyrene latex. The work was discontinued a few years ago, but is reported in the hope that it may stimulate further research.

Latices were prepared with potassium myristate, sodium tetradecyl sulfate (NaTDS), and dodecylammonium chloride (DDA·HCl) as emulsifiers. The first two yield negatively charged polymer particles, and the rates were examined in the pH range between about 8 and 10. With DDA·HCl the latex is positively charged. The rate of reaction was studied in the pH range 3.5 to 5.5.

EXPERIMENTAL

Chemicals

The sources of mercaptan and other chemicals were as described before.² The mercaptan was vacuum-distilled. The sulfur content determined

by amperometric titration with silver nitrate³ was 98% of the theoretical value. Potassium myristate was prepared from myristic acid (Eastman), recrystallized from ethanol, and dried under vacuum. DDA·HCl was prepared from dodecylamine (Armour), precipitated from cold ethanol by addition of ether, washed with ether, and dried under vacuum. NaTDS was an experimental sample from Procter and Gamble.

Latices

Latices were prepared with the recipe (parts by weight); styrene 100, water 180, soap or detergent 5 (⁵/₄ in one experiment as noted), and potassium persulfate 0.3 or 0.05. Polymerization was carried out for 10–12 days at 50°C.; the conversion was practically 100%, and all the persulfate had reacted. The latices were steam-distilled. Spectrophotometric measurement (290 m μ) showed that the concentration of residual monomer was less than 0.1%.

Procedure

The latex was diluted with air-free water and weighed into a bottle closed with a perforated metal cap containing a self-sealing Buna-N gasket. After addition of buffer or other reagent, air was replaced by nitrogen and a known amount of mercaptan was added by syringe. The bottle was shaken at 35 rpm for 15–20 hr. to dissolve the mercaptan. Such a shaking period is more than long enough to dissolve *n*-octyl mercaptan completely in latex polymer particles.² The mercaptan content was determined at the end of the shaking period. An air-free solution of potassium ferricyanide was injected, and the mixture was rotated at 35 rpm, 25°C. At suitable intervals a 2–3 g. sample of latex was ejected under nitrogen into a few milliliters of vigorously stirred coagulant. The myristate and DDA·HCl latices were coagulated with 6*N* nitric or sulfuric acid, and the NaTDS latex was coagulated with saturated barium nitrate solution. All the unreacted mercaptan remained in the coagulum, and no measurable reaction with ferricyanide occurred within 2 hr. when the latter reagent was added after coagulation. The coagulum was filtered, quickly rinsed with ethanol to remove adsorbed water, and dissolved in 50 ml. of warm benzene. No measurable amount of mercaptan was extracted by rinsing with ethanol. The polymer in benzene solution was coagulated by slow addition to an equal volume of vigorously stirred ethanol, and mercaptan was determined in the supernatant liquid by amperometric titration with silver nitrate.³ Ferricyanide was determined spectrophotometrically in the combined filtrate and washings after aqueous coagulation (Beckman DU, 420 m μ , 1 or 10 cm. cell). When ferricyanide was added to mercaptan-free latex, less than 1% disappeared in 24 hr. In a few instances ferrocyanide was determined in the combined filtrate and washings by titration with ceric ammonium sulfate with the use of ferroin as indicator. The sum of ferricyanide and ferrocyanide always was equal to the original ferricyanide. Experiments with systems containing approximately equimolar mercaptan and ferricyanide showed that the molar reaction ratio was 1:1, as expected.

In experiments with myristate, DDA·HCl and NaTDS latices the polymer concentrations were about 0.14, 0.14, and 0.12 g./g. latex, respectively. In most of the kinetic experiments the concentrations of mercaptan and ferricyanide were about 0.04 and 0.001 mmole/g. latex, respectively. The pH was adjusted by various additions (sodium carbonate, sodium acetate, etc.) depending upon the latex. The oxidation to disulfide liberates H^+ . It was not always possible to add enough buffer to keep pH constant for the whole reaction because of the danger of coagulation of the latex. Whenever a buffer of inadequate capacity was used, the decrease of pH caused a pronounced slowing down of the reaction.

RESULTS AND DISCUSSION

The reaction order with respect to ferricyanide was unity, as shown by the fact that plots of $\log [Feic]$ versus time, with excess of mercaptan, were linear within experimental error to 90% reaction in all systems in which the pH was constant. Also, the variation of the pseudo first-order rate constant when $[RSH]$ was varied eightfold showed that the reaction was first-order to mercaptan. Figure 1 shows the dependence of the overall second-order rate constant upon pH in the three latices. k_{2L} is defined at a given pH by the relation

$$-d[Fe(CN)_6^{3-}]/dt = k_{2L} [Fe(CN)_6^{3-}] [RSH] \quad (1)$$

and is expressed as liter/mole-sec. The numbers in Figure 1 apply to a polymer content of 0.13 ± 0.01 g. per latex, the polymer being prepared with 5 parts of emulsifier. Since the density of the latex is close to 1 g./ml., the reactant concentrations, measured as mmole/g. latex, correspond fairly closely to mole/liter. (The distribution is not uniform, however, because the system is heterogeneous.)

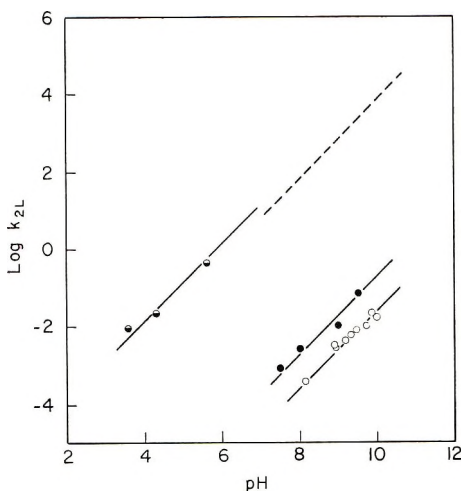


Fig. 1. Dependence of second-order rate constant upon pH: (O) K myristate latex; (●) NaTDS latex; (● with dot) DDA·HCl latex; (--) hypothetical k_{2w} .

The straight lines of Figure 1 have 45° slopes, so in each latex the rate constant was directly proportional to $[\text{OH}^-]$. The rate constants in myristate and NaTDS latices were of the same order, but smaller by about five orders of magnitude, at the same pH, than the rate constant in DDA·HCl latex.

The addition of potassium nitrate, ferrocyanide, or myristate to the myristate latex had no measurable effect upon the rate except insofar as the addition changed the pH of the latex. Also, the rate in the myristate latex was approximately doubled when the weight of polymer per gram latex was doubled; when the latex made with 5 parts of myristate was replaced with one prepared with $5/4$ parts of myristate, but containing the same weight of polymer per gram latex, the value of k_{2L} was reduced about 15%.

The fact that the rate was doubled when the concentration of polymer was doubled does not permit any conclusion about the relation of rate either to number or total area of polymer particles, since both were doubled. The effect upon the rate of using polymer prepared with less soap indicates that the rate may be proportional to the area, rather than to the number. This conclusion is reached as follows. If both latices (i.e., those prepared with 5 and with $5/4$ parts of myristate) followed Smith-Ewart Case II kinetics,⁴ the number of polymer particles should vary as $[\text{soap}]^{2/3}$ and the total area for equal weights of polymer therefore should vary as $[\text{soap}]^{1/3}$. Accordingly, a decrease in soap from 5 to $5/4$ parts causes a decrease in number of particles and in total area of particles from 100 to 43 and 76%, respectively. Considering that the simple calculation does not take into account the heterogeneous distributions of sizes, the agreement between the observed 15% reduction in rate and the predicted 24% reduction indicates that the rate may be proportional to area. It would be desirable to combine rate determinations with accurate particle size determinations to settle the question.

In homogeneous medium (60% by volume acetone–water) the reaction is first-order to ferricyanide, mercaptan, and hydroxyl ion, above pH (in the medium) ca. 7.¹ There are pronounced specific cation effects in acetone–water which have not been found in latex, possibly because the surface of the particles is the locus of the reaction. The total cation (K^+ , Na^+ , or $\text{C}_{12}\text{H}_{25}\text{NH}_3^+$) concentration in the latices of Figure 1 was around 0.037*M*. At such concentration the second-order rate constant in acetone–water, at pH above 7, is given by eq. (2):

$$\log k_{2A-w} = -9.9 + \text{pH} \quad (2)$$

where pH is measured in the medium and k is in liter/mole-sec. An estimate of the rate in hypothetical homogeneous aqueous medium may be made from eq. (2). The dependence upon pH undoubtedly arises from a rate-determining reaction between $\text{Fe}(\text{CN})_6^{3-}$ and RS^- , with rate constant k_s ; hence in solvent S the rate should be given by eq. (3):

$$-d[\text{Fe}(\text{CN})_6^{3-}]/dt = k_s[\text{Fe}(\text{CN})_6^{3-}][\text{RS}^-] \quad (3)$$

If the pH is not high enough to cause appreciable ionization of RSH (as in the present experiments) eq. (3) becomes:

$$-d[\text{Fe}(\text{CN})_6^{3-}]/dt = k_s K_{\text{RSH}} [\text{Fe}(\text{CN})_6^{3-}] [\text{RSH}] [\text{H}^+]^{-1} \quad (4)$$

where K_{RSH} is the acid dissociation constant. Comparative pH values of various buffers in water and in acetone-water¹ show that $\text{p}K_a$ for several uncharged acids is 1.5 ± 0.1 unit larger in the mixed solvent than in water; also, $\text{p}K_w$ is 1.4 unit larger than in water. Hence it is probable that $\text{p}K_{\text{RSH}}$ is 1.4 unit larger in 60% acetone-water than in water.

The value of k_s is different in the two solvents, primarily because of the difference in dielectric constants, equal to 80 in water, 45 in the acetone-water mixture used. Assuming an equilibrium distance in the critical complex of 3 Å, it may be calculated³ that for reactants with charges of -3 and -1 the rate constant in water should be about 250 times the rate in acetone-water, i.e., $\Delta \log k_s = 2.4$.

Correcting for the changes in k_s and K_{RSH} , the rate constant in homogeneous aqueous medium should be given approximately by eq. (5):

$$\log k_{2w} = -6.1 + \text{pH} \quad (5)$$

which is drawn as the broken line in Figure 1.

It is seen that in the negatively charged myristate and NaTDS latices k_{2L} is five orders of magnitude smaller than the predicted value in homogeneous aqueous medium. The main reason must be that the reaction occurs on the surface of the polymer particles where the negative charge of the surface repels the ferricyanide ions. An additional factor may be that the negative charge of the surface causes a marked decrease of the dissociation constant of the mercaptan on the surface. For example, it has been found that $\text{p}K_a$ of *p*-nitrophenol is 0.8 units larger in solutions of sodium dodecyl sulfate (in which the detergent micelles are negatively charged) than in water.⁶

It is striking that the value of k_{2L} in the DDA·HCl latex agrees so closely with the predicted value of k_{2w} ; this agreement undoubtedly is partly fortuitous. The value of the dielectric constant at the surface of the particles is unknown. Also, the value of K_{RSH} on the positively charged surface should be larger than it is in water, thus increasing the value of k_{2L} . Both these factors are probably relatively small compared to the fact that the surface attracts the ferricyanide ions, and a fraction of these must be present as counterions, which tends to increase the rate greatly. On the other hand, the fact that the reaction can occur only upon the surface rather than in the whole volume of the latex, must reduce the rate. The approximate agreement of k_{2L} in the DDA·HCl latex with the extrapolated value of k_{2w} suggests these factors may cancel.

Finally, it is of interest that the reaction appears to be first order to mercaptan, ferricyanide, and hydroxyl ion over the whole pH range investigated in the different latices (Fig. 1). In acetone-water, proportionality of rate to $[\text{OH}^-]$ was observed only above pH 7 in the medium, which is equivalent to pH 5.6 in water. In acetone-water the kinetics at low pH differed markedly from the kinetics observed above pH 7. The reaction was not first order to ferricyanide; there was an increase in rate of

the order of 20-fold after 20–30% of the ferricyanide had reacted. Also, the reaction rate was practically the same at pH 2.9 and 5.5, whereas above pH 7 such a change in pH changes the rate about 400-fold. Further, the initial rate even at pH 5.5 was larger by about 25-fold than would correspond to extrapolation of the rate observed at pH above 7, i.e., by extrapolation of eq. (2). The latter two facts may indicate that a direct reaction of ferricyanide with RSH may occur, which becomes important only at low pH. None of these abnormalities were observed in the acid latex.

The conclusion therefore is justified that the negatively charged surfactant accelerates the rate of reaction in latex of solubilized mercaptan with ferricyanide.

This work was carried out under a grant from the National Science Foundation.

References

1. Kolthoff, I. M., E. J. Meehan, M. S. Tsao, and Q. W. Choi, *J. Phys. Chem.*, **66**, 1233 (1962).
2. Meehan, E. J., I. M. Kolthoff, and P. R. Simha, *J. Polymer Sci.*, **16**, 471 (1955).
3. Kolthoff, I. M., and W. E. Harris, *Ind. Eng. Chem., Anal. Ed.*, **18**, 61 (1946).
4. Smith, W. V., and R. H. Ewart, *J. Chem. Phys.*, **16**, 592 (1946).
5. Frost, A. A., and R. G. Pearson, *Kinetics and Mechanism*, Wiley, New York, 1961, p. 145.
6. Harries, D. G., W. Bishop, and F. M. Richards, *J. Phys. Chem.*, **68**, 1842 (1964).

Résumé

On a mesuré la vitesse de la réaction du ferricyanure avec le *n*-octyl-mercaptan, solubilisé dans un latex de polystyrène. Le mercaptan était complètement dissous dans les particules polymériques du latex avant l'addition du ferricyanure. Les réseaux ont été préparés avec du myristate de potassium, du tétradécyl-sulfate de sodium, et du chlorure de dodécyl-ammonium comme agents tensio-actifs. Dans chaque latex la réaction était du premier ordre par rapport au ferricyanure, au mercaptan et à l'ion hydroxyle. Les vitesses dans les réseaux de myristate et de sulfate de tétradécyle étaient presque égales, tandis qu'elles étaient plus petites de cinq ordres de grandeur (extrapolées au même pH) que la vitesse dans le latex au chlorure de dodécyl-ammonium. La réaction se fait apparemment sur la surface des particules polymériques et est donc favorisée dans le latex qui contient des particules chargées positivement et sur la surface desquelles le ferricyanure est absorbé comme ion de signe contraire.

Zusammenfassung

Die Geschwindigkeit der Reaktion von Ferricyanid mit in Polystyrollatex solubilisiertem *n*-Oktylmercaptan wurde gemessen. Das Merkaptan wurde in den Latexpolymerpartikeln vor dem Zusatz von Ferricyanid vollständig gelöst. Die Latices wurden mit Kaliummyristat, Natriumtetradecylsulfat und Dodecylammoniumchlorid als Emulgatoren hergestellt. In jedem Latex war die Reaktion von erster Ordnung in Bezug auf Ferricyanid, Merkaptan und Hydroxylion. Die Geschwindigkeiten in Myristat und Tetradecylsulfatlatices waren etwa gleich, jedoch um etwa fünf Größenordnungen (extrapoliert auf das gleiche pH) kleiner als die Geschwindigkeiten im Dodecylammoniumchloridlatex. Die Reaktion verläuft offenbar an der Oberfläche der Polymerpartikeln und wird daher in dem Latex mit positiv geladenen Teilchen begünstigt, an dessen Oberfläche das Ferricyanid als Gegenion adsorbiert wird.

Received March 23, 1965
Prod. No. 4746A

Dilute Solution Properties of Polyoctene-1. Analysis by the Kurata-Stockmayer Method

JACK B. KINSINGER and LARRY E. BALLARD, *Department of Chemistry, Michigan State University, East Lansing, Michigan*

Synopsis

Dilute solution properties of polyoctene-1 have been measured by light scattering, osmometry, and viscometry and Mark-Houwink expressions determined in two thermodynamically good solvents and one solvent at the Flory (θ) temperature. The data have been interrelated and analyzed by the Kurata-Stockmayer technique and are shown to have good correspondence with the theory in some cases and moderately poor in others. However, the data are not sufficiently precise to permit all aspects of the adequacy of such a two-parameter theory to be judged.

The dilute solution properties of high polymers have claimed the attention of researchers during the past three decades and the body of scientific literature describing this aspect of polymer science is now considerable. It is fortunate that an excellent review has appeared recently which condenses and analyzes the available data thoroughly.¹ It is unfortunate, however, that so few data have been published for the *n*-alkyl series of the poly- α -olefins, since this homologous series represents one of the structurally least complicated organic polymers, and differences in properties resulting predominantly from steric hindrances among the pendant groups might be more easily correlated than from similar series of more polar polymers.² Finally, it is of interest to analyze the data according to some recent propositions concerning a method to obtain the unperturbed dimensions of polymer chains from intrinsic viscosity data in thermodynamically good solvents.¹

EXPERIMENTAL

The sample of polyoctene-1 was generously provided by Union Carbide Chemicals Company and was prepared with a Ziegler-type catalyst. When received, the sample was a yellow, tacky, rubbery material.

Purification and Fractionation

Before prepurification of the bulk polymer, one fractionation was performed by the standard technique of solvent-nonsolvent pair (cyclohexane-acetone, respectively) precipitation at constant temperature

(30°C.) in very dilute solution. Each precipitated fraction was redissolved in cyclohexane, filtered, then finally recovered by freeze-drying. These fractions, however, remained somewhat discolored. It was discovered later that a white precipitate formed if the bulk polymer was dissolved in *n*-nonane, and when the residue was filtered or centrifuged free of the solution, clear, water-white polymer could be recovered. The white residue failed to ignite, and it produced a sharp crystalline pattern indicative of inorganic residue.

Purification of a second portion of the bulk polymer by dissolution in *n*-nonane followed by centrifugation and reprecipitation was undertaken, and the resulting clear polymer was separated by fractional precipitation into eleven fractions. The fractionation data for the second sample are shown in Table I.

It can be seen that fractions 1A and 2A do not fall within the usual order of decreasing $[\eta]$ with increasing fraction number. This we feel was due to heterogeneity (perhaps branched species and/or separation by tacticity) in the bulk sample. No further measurements were taken with these two fractions.

TABLE I
Intrinsic Viscosity of Polyoctene-1 Fractions

Fraction	Intrinsic viscosity		Wt.-% of fraction
	Solvent	$[\eta]$, dl./g	
1A	Cyclohexane, 30°C.	6.37	7.50
2A		6.72	1.54
3A		9.30	3.45
4A		9.64	3.33
5A		8.60	8.10
6A		5.41	18.92
7A		4.19	12.50
8A		2.90	11.19
9A		1.75	15.47
10A		1.00	8.93
11A		0.30	8.33
2'	Bromobenzene, 25°C.	6.64	
7'		2.61	
7A		1.95	
8A		1.51	
9A		1.00	
10A		0.44	
2'		3.41	
7A	Phenetole, 50.4°C. (Θ solvent)	0.86	
9A		0.51	
2'		1.26	
7'		0.65	

Viscosity

Viscosity measurements were made with a Cannon-Fenske-Ubbelohde type dilution viscometer at constant temperature. It is noted the intrinsic

viscosities in cyclohexane at 30°C. are rather large; however, shear corrections were not made. Estimation of shear corrections from the data of Fox and Flory indicates for these solutions that such corrections should be negligible.³ For viscosity measurements taken at the Flory temperatures, the usual precautions to prevent incipient precipitation were undertaken. The viscosity data also appear in Table I.

Osmometry

The number-average molecular weight for two fractions were determined at 30°C. in cyclohexane with a Pinner-Stabin type osmometer. The membranes were made of denitrated gel-cellophane grade 450 and were treated with a 5% solution of NaOH for 24 hr. to render them more permeable to solvent. They were conditioned to the solvent, cyclohexane, by the method of Yanko.⁴ The time constant for the membrane used was 567 min. Since the molecular weight of most of the fractions was extremely high, it was possible to obtain reliable number-average molecular weights for only two fractions (Table II).

Light Scattering

The weight-average molecular weight of six fractions was determined with a Brice-Phoenix light-scattering photometer. All measurements were taken in a Wittnauer cylindrical cell with the unpolarized green line of mercury (5416 Å.). Solutions of polyoctene-1 in bromobenzene were filtered through ultra-fine sintered glass before use, and one pass was sufficient to render them free of dust. Additional concentrations were prepared by diluting the system while it remained in the scattering cell. The specific refractive increment (dn/dc) was determined with a Brice-Phoenix differential refractometer that had been calibrated previously with both aqueous sucrose and aqueous KCl solutions. The value of (dn/dc) in bromobenzene at 30°C. was -0.105 . Analysis of the data was made through both Zimm plots and the Debye dissymmetry technique, the former giving the more reliable and internally consistent results.

Phase Equilibria

Phase diagrams in the liquid-liquid region of separation were constructed from the data taken from four fractions over a volume fraction of polymer (v_2) range of 0.005-0.05 in phenyl ethyl ether. The precipitation temperature was established by viewing the solution while the temperature was lowered slowly. The solutions had a temperature range over which turbidity changed, but the precipitation temperature T_p was judged by eye to be that temperature where the maximum change in turbidity occurred. The value of T_p fluctuated over a temperature region with repeated measurements, but the range was usually within $\pm 0.2^\circ\text{C}$. Solutions of different concentration were obtained by a successive dilution technique. The Flory temperature (θ) was obtained by plotting $1/T_c$ against

TABLE II
Light-Scattering and Osmotic Pressure Data

Fraction	$\bar{M}_w \times 10^{-6}$ ^a	$\bar{M}_n \times 10^{-6}$	$(A_2)_{07}$ cm. ³ -mole/g. ² $\times 10^4$ (bromobenzene, 25°C.) ^b	$(A_2)_{07}$ cm. ³ -mole/g. ² $\times 10^4$ (cyclohexane, 30°C.)	$(\bar{L}_z^2)^{1/2}$, Å.	$\Phi_{0w} \times 10^{-21}$	$(A_2)_w \bar{M}_w / [\eta]$ (bromobenzene, 25°C.)	$(A_2)_n \bar{M}_n / [\eta]$ (cyclohexane, 30°C.)
5A	4.0	—	1.62	—	2150 ^b	1.83	180	—
6A	2.5	—	1.98	—	1600	1.97	190	—
7A	1.68	—	2.15	—	1200	1.87	190	—
8A	1.25	—	2.22	—	980	2.27	180	—
9A	0.61	0.54	2.95	3.89	675	2.25	180	120
10A	0.25	0.24	3.12	4.58	382	2.25	178	115

^a Data from Zimm plots only.

$(1/X^{1/2} + 1/2X)$ and extrapolating the linear curve to infinite molecular weight, where X is related to the degree of polymerization as defined by Flory.⁵ The thermodynamic parameters, as calculated from eq. (1), appear in Table III.

$$1/T_c = 1/\theta[1 + 1/\Psi_1(1/X^{1/2} + 1/2X)] \quad (1)$$

TABLE III
Thermodynamic Parameters from Upper Critical Solution Measurements

Solvent	θ , °C.	Ψ_1	$\Delta\bar{H}_1/v_2^2$, cal./mole	$(\Delta\bar{S}_1/v_2^2)$, cal./mole-deg.
Phenyl ether	50.4	0.813	788	1.66

ANALYSIS OF DATA

In their review, Kurata and Stockmayer¹ carefully analyzed published data to test their theory and based their judgment, in part, on some rather stringent requirements for the second virial coefficient A_2 . We prefer to take a similar attitude with our data.

We have determined the A_2 values for six fractions by light-scattering measurements in the moderately good solvent bromobenzene at 30°C. and by osmometry for two fractions in cyclohexane (an exceptionally good solvent) at 30°C. It has been stated that the generally accepted maximum value for $A_2M/[\eta]$ in a good solvent should be about 150. This quantity, calculated from our data, appears in the last two columns of Table II. The two values calculated from the osmotic pressure data meet this requirement, but the values obtained from light-scattering measurements are slightly over 160 due, in part, to the different molecular weight averages. Kurata and Stockmayer, on a theoretical basis, reject the idea that values much above 160 can be considered as acceptable measurements; however, the compound errors inherent in measuring A_2 , M , and $[\eta]$ undoubtedly make the experimental limits 160 ± 20 . While our data are not all within the imposed upper limit, we feel they are sufficiently good to justify further use of the theory and are in line with much of the published data.

The second restriction in A_2 requires that over a short molecular weight range, the coefficient γ in the empirical expression:

$$A_2 = \text{constant } M^{-\gamma}$$

should be ≤ 0.15 . Our data are plotted in Figure 1 as $\log A_2$ against $\log \bar{M}_w$, and the least-squares fit gives a value for γ of 0.22 ± 0.02 . Here, the value again exceeds the upper limit imposed by the theoretical restriction, but literature values of this magnitude and higher are very common.

We do not propose, therefore, that the data collected here are of such high precision as to present a rigorous test of the Kurata-Stockmayer method. We accept what experimental data we have gathered under reasonably favorable conditions with very standard equipment and ask

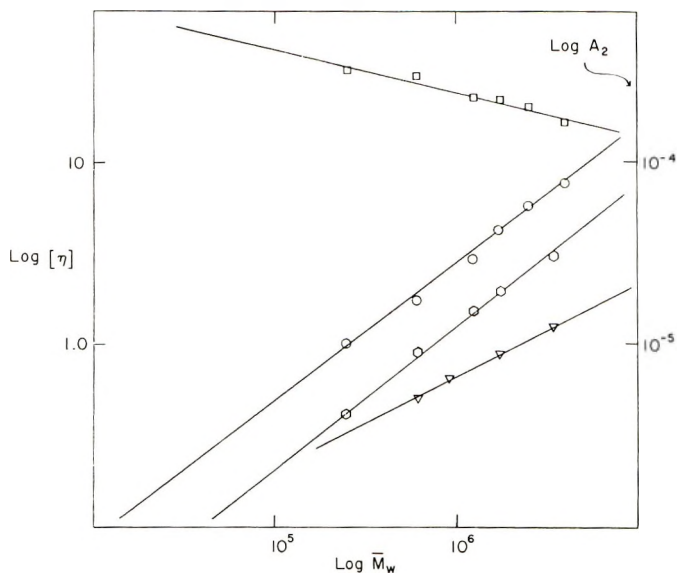


Fig. 1. Plots of $\log [\eta]$ vs. $\log \bar{M}_w$: (○) cyclohexane, 30°C.; (○) bromobenzene, 30°C.; (▽) phenetole, 50.4°C.; (□) (right-hand coordinates) $\log A$, vs. $\log \bar{M}_w$ bromobenzene, 25°C.

how well can such data agree with the expectations of the theory. While more precise data are available in the literature, Kurata and Stockmayer apparently did not analyze any single set by the methods attempted here.

Mark-Houwink Constants

From the light-scattering and viscosity data in Tables I and II, we find by the method of least squares the following weight-average molecular weight-intrinsic viscosity relationships for polyoctene-1 in the solvents and at the temperatures indicated.

Cyclohexane, 30°C.:

$$[\eta] = 5.75 \times 10^{-5} \bar{M}_w^{0.78}$$

Bromobenzene 25°C.:

$$[\eta] = 2.90 \times 10^{-5} \bar{M}_w^{0.78}$$

Phenetole, 50.4°C.:

$$[\eta] = 6.55 \times 10^{-4} \bar{M}_w^{0.50}$$

The data are displayed in Figure 1.

Unperturbed Coil Dimensions

We can now evaluate the unperturbed dimensions by three techniques from the data at hand: (1) from intrinsic viscosity measurements at the Flory temperature (θ), by using the well-established techniques of Flory and

his co-workers; (2) from the perturbed mean-square, end-to-end dimensions as determined by light scattering with the aid of the Kurata-Stockmayer theory; (3) by intrinsic viscosity measurements in good solvents using the Kurata-Stockmayer (K-S) technique. It is important that when the K-S method is used, the detailed calculation of all parameters and values for the physical constants be duplicated as Kurata and Stockmayer have done; otherwise, the data are not internally self-consistent.

Method 1. The viscosity-weight-average molecular weight data taken at the Flory temperature are shown in Figure 1. The slope of the line has been drawn to 0.5 to fit the limiting relation:

$$[\eta] = KM^{0.50} \quad (2)$$

Straightforward calculations give a value of $K = 6.5 \times 10^{-4}$ at 50.4°C . in phenyl ethyl ether. From K , the unperturbed dimensions can be calculated, but first corrections due to molecular weight heterogeneity must be applied. According to the Fox-Flory relationship:

$$K = (\Phi)_0 [\bar{L}_0^2/M]^{3/2} \quad (3)$$

where $(\Phi)_0$ is the hydrodynamic constant, \bar{L}_0^2 is an "average" unperturbed mean-square, end-to-end dimension, and M is an "average" molecular weight. If \bar{M}_w is used, the $(\Phi)_0$ must be corrected for molecular weight heterogeneity. Thus, $(\Phi)_{0w} = g_w(\Phi)_0$, where $(\Phi)_0$, according to K-S, is the Kirkwood-Riseman⁶ theoretical value of 2.87×10^{21} , $g_w = \Gamma(h + 1.5) / (h + 1)^{1/2} \Gamma(h + 1)$, and $\bar{M}_w/\bar{M}_n = (h + 1)/h$, these latter expressions

TABLE IV
Unperturbed Dimensions and Related Parameters

Method	Solvent		$K \times 10^4$	$[(\bar{L}_w^2)_0/\bar{M}_w]^{1/2} \times 10^{11}$	$T, ^\circ\text{C}$.	Remarks
1	Phenetole		6.5	625 ± 30	50.4	Fox-Flory method
2	Bromobenzene	<i>a</i>	4.2	535 ± 50	25.0	Light scattering only (iteration)
		<i>b</i>	5.1	575 ± 50	30.0	$g(\alpha_\eta)$ from viscosities
3	Bromobenzene	<i>a</i>	5.0	570 ± 50	25.0	Iteration
		<i>b</i>	5.75	600 ± 60	25.0	$g(\alpha_\eta)$ from viscosities
	Cyclohexane	<i>a</i>	10.0	710 ± 60	30.0	Iteration
		<i>b</i>	10.6	730 ± 70	30.0	$g(\alpha_\eta)$ from viscosities
	Phenetole	<i>a</i>	6.6	637 ± 20	50.4	K-S equation

arising from the use of the Schultz molecular weight distribution function.⁷ We have only two measured values of \bar{M}_w/\bar{M}_n , which are 1.12 and 1.05. Since these are unusually small for the fractionation procedure adopted, we preferred to use a more realistic value of $\bar{M}_w/\bar{M}_n = 1.25$ which gives $h = 4$, $g_w = 0.94$, $(\Phi)_{0w} = 0.94 (\Phi)_0$.

The resulting value of $[(\bar{L}_w^2)_0/\bar{M}_w]^{1/2}$ is shown in Table IV.

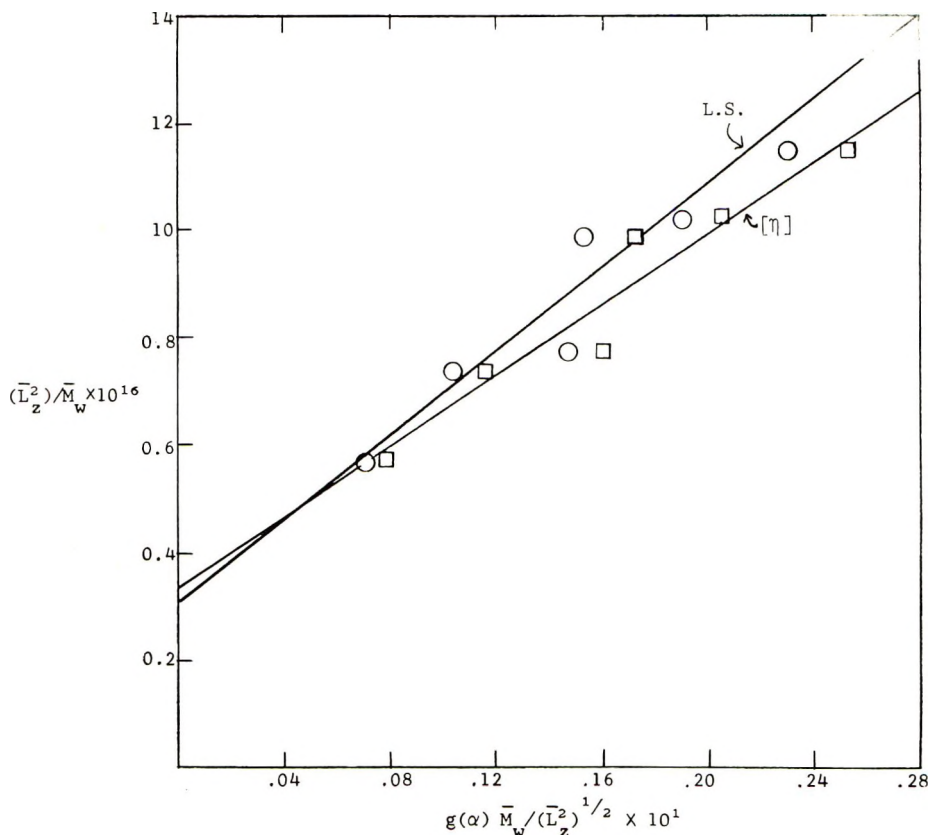


Fig. 2. Plots of \bar{L}_z^2/\bar{M}_w vs. $g(\alpha)\bar{M}_w/(\bar{L}_z^2)^{1/2}$ for polyoctene-1 in bromobenzene, 25°C.: (O) $g(\alpha)$ by iteration, $(\bar{L}_z^2)^{1/2}$ from Zimm plots; (\square) $g(\alpha_\eta)$ from ratio of $[\eta]$ in bromobenzene and $[\eta]_\theta$ in phenetole.

Method 2. According to Kurata and Stockmayer, the relationship between the mean-square (Z -average) perturbed end-to-end dimensions and the thermodynamic expansion factor, α , is:

$$\bar{L}_z^2/\bar{M}_w = A^2 + 42.1 \times 10^{-2}B[g(\alpha) \cdot \bar{M}_w/(\bar{L}_z^2)^{1/2}] \quad (4)$$

where

$$A^2 = (\bar{L}_z^2)_0/\bar{M}_w \quad (5)$$

$$g(\alpha) = 8\alpha^3/(3\alpha^2 + 1)^{3/2} \quad (6)$$

and B is a constant which is characteristic of the statistical elements in the perturbed chain.* Thus, to obtain A^2 , measured values of \bar{L}_z^2/\bar{M}_w are

* A in eq. (5) is not to be confused with A_2 , the second virial coefficient. We prefer to maintain the K-S nomenclature throughout.

plotted against $\bar{M}_w/(\bar{L}_z^2)^{1/2}$ to obtain an approximate A^2 at the intercept and from which $g(\alpha)$ can be calculated according to eqs. (3), (6), and (7).

$$\bar{L}_z^2/(\bar{L}_z^2)_0 = \alpha^2 \quad (7)$$

Variations in A^2 by successively employing this iterative calculation are minimized after a few trials, and a fixed value of A^2 is obtained. The plots according to eq. (4) are shown in Figure 2. Because of inherent scatter in the data, the best lines were obtained by the method of least squares. The best value of the intercept = 0.332×10^{-16} . Hence,

$$[(\bar{L}_z^2)_0/\bar{M}_w]^{1/2} = 582 \times 10^{-11}$$

but since

$$[(\bar{L}_z^2)_0/\bar{M}_w]^{1/2} = [(h + 2/h + 1)(\bar{L}_w^2)_0/\bar{M}_w]^{1/2}$$

it follows that

$$[(\bar{L}_w^2)_0/\bar{M}_w]^{1/2} = 535 \times 10^{-11}$$

According to K-S, it is also possible from these data to calculate the expansion factor directly from the ratio of the intrinsic viscosity in bromobenzene to that in the theta solvent, phenyl ethyl ether. In calculating the expansion factor this way, we accept the K-S assumption that the $g(\alpha)$ function for the equilibrium measurements by light scattering is identical to that for the dynamic viscosity measurement, $g(\alpha_\eta)$, except that they differ only by a multiplicative constant which affects only the slope of the plot and not the intercept. In this case, we mix light-scattering measurements (that is, \bar{L}_z^2 and \bar{M}_w) and obtain $g(\alpha_\eta)$ directly from viscosity studies, since $[\eta]/[\eta]_\theta = \alpha_\eta^3$. These data are also plotted in Figure 2 according to eq. (4) where they can be compared with the iterative light-scattering data. The chain dimensions are also listed in Table IV. Although the fluctuations in the data are relatively large, it is gratifying that the final dimensions, as obtained by method 2, are so close.

Method 3. This calculation relies purely on viscosity data and the Kurata-Stockmayer theory in the following form:

$$[\eta]^{2/3}/M^{1/3} = K^{2/3} + 0.363(\Phi)_0 B [g(\alpha_\eta)M^{2/3}/[\eta]^{1/3}] \quad (8)$$

We have viscosity measurements in three solvents: cyclohexane, bromobenzene, and phenyl ethyl ether. Applying eq. (8) first to the theta solvent data, we find the slope of the line zero as predicted by theory. The intercept and the end-to-end dimensions, as calculated therefrom, are shown in Table IV, and their agreement with the values obtained from method (1) are excellent, as they should be in this limiting case.

With the two thermodynamically good solvents, the data are less satisfactory with respect to obtaining reliable unperturbed end-to-end dimensions. We have used the raw experimental data; i.e., the measured \bar{M}_w from light-scattering data rather than \bar{M}_w values taken from the smooth curves of Figure 1 at the viscosity noted. As can be seen in Figure 3,

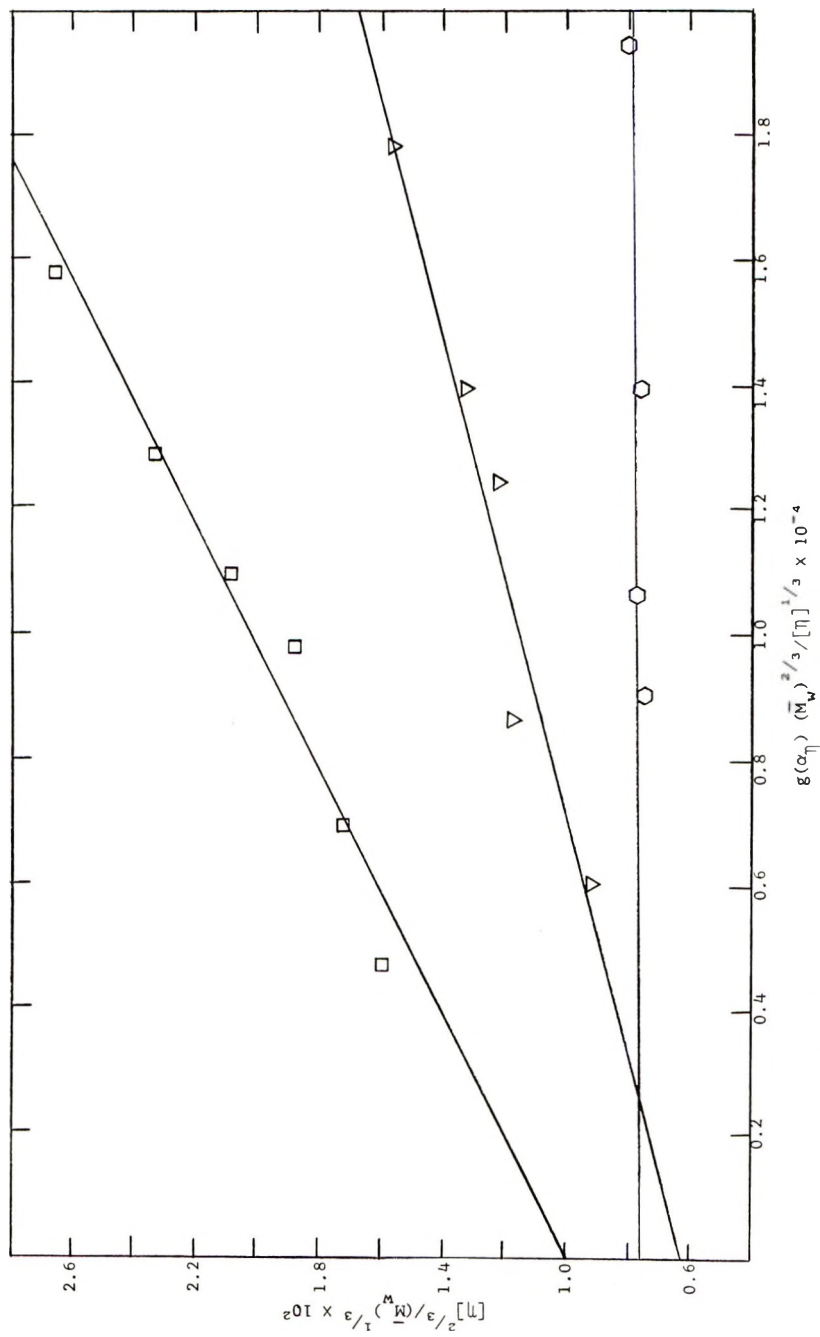


Fig. 3. Plots of $[\eta]^{2/3}/(\bar{M}_w)^{1/3}$ vs. $[\bar{M}_w]^{2/3}/[\eta]^{1/3}$, $g(\alpha)$ from iterative procedure only: (□) cyclohexane, 30°C.; (▽) bromobenzene, 30°C.; (○) phenol, 50.4°C.

the data for the three solvents do not converge to a common intercept, thus giving different values of the unperturbed dimensions. The dimensions for the bromobenzene data are about 5 to 10% lower than that obtained from the Θ solvent, and the value obtained in cyclohexane is considerably larger.

The data, therefore, do not completely agree with the predictions of the theory, but some rewarding internal consistencies are revealed. The unperturbed dimensions from the good solvent, bromobenzene, as determined exclusively by light-scattering measurements of the end-to-end distance or viscosity measurements and by combinations thereof and in comparison with the Fox-Flory dimensions in the Θ solvent, are remarkably consistent within the limits of our experimental error. This lends support to the use of a single function, of the K-S type, to describe the thermodynamic expansion of the chain in equilibrium or in dynamic viscosity measurements at low shear rates. Secondly, the values for the unperturbed dimensions from method 3, a and b in cyclohexane are reassuring even though the dimensions obtained are not the same as in phenetole at $T = \Theta$.

These inconsistencies result, in part, from experimental errors. First, in choosing our \bar{M}_w values as measured by light scattering rather than by using the determined Mark-Houwink expression to calculate a new \bar{M}_w from the measured viscosities, the disagreement between the three solvents was broadened. Calculations performed with the smoothed data show the intercepts, as in Figure 3, to be closer and the data to have less experimental scatter. Second, the temperatures for the measurements in the three solvents were not identical, and changes in the unperturbed dimensions with T can account for some of the deviations. Third, we note our failure to obtain $[\eta]$ as a function of shear and extrapolate to zero shear rate for a more accurate value of $[\eta]$, especially in cyclohexane. In attempting to unbiased our judgments completely, we subjected all of our light-scattering data to least-squares analysis. This improved certain aspects of the data; that is, our A_2 analysis fitted the theoretical requirements better, and our confidence in $\log \eta$ versus $\log \bar{M}_w$ increased, but there was no general improvement in the coincidence of the unperturbed dimensions as analyzed here. Thus, these data reflect some errors in judgment which are difficult to assess quantitatively. Finally, we note that all of the data recalculated by K-S from published results do not show a common intercept for all solvents,¹ in some cases, for many of these same reasons. However, real solvent effects on the unperturbed dimensions have been noted by two different techniques, and deviations here may be related similarly.^{8,9}

REMARKS AND CAUTIONS

Kurata and Stockmayer have provided an extensive method for analyzing the data from dilute solution studies of high polymers. It also provides a test for the adequacy of any two parameter theory which explains the non-ideal behavior of polymer solutions as measured by light scattering,

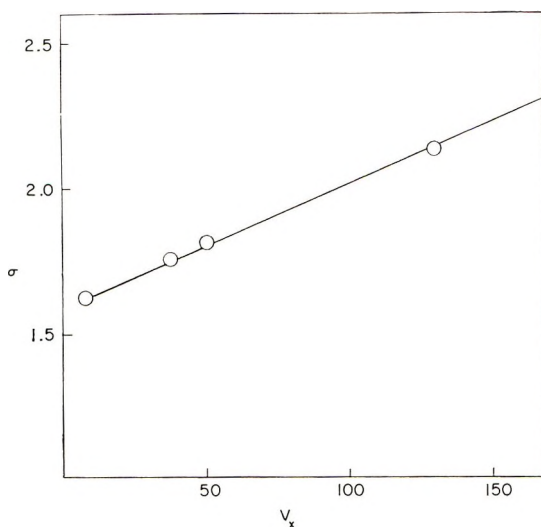


Fig. 4. Plot of $\sigma = (\bar{L}_{0f}^2)^{1/2}/(\bar{L}_{w0}^2)^{1/2}$ vs. V_x , molar volume of pendant group at $T = \theta$. First three points on left from Kurata and Stockmayer,¹ last point this work.

colligative property studies, and viscosity. It is our conviction that too few studies have been performed with enough care taken in all measurements to adequately accept the concept that all nonideal polymer solutions will be entirely describable by two parameters. In our own case, even though we have taken reasonable care with the experiments, the scatter of data is not sufficiently small for us to justify any criticism of the theory. Within our experimental limits, the theory adequately explains the data, and we agree that if Θ solvents are difficult to locate and measurements at the Θ temperature difficult to perform, that the Kurata-Stockmayer equations represent a useful method for determining or, at least, closely estimating the unperturbed dimensions of polymer chains.

Effect of the Pendant Group on the Unperturbed Dimensions

Kurata and Stockmayer have found a smooth correlation between σ , the ratio of the root-mean-square unperturbed dimensions to the root-mean-square freely rotating dimensions and the molar volume, V_x , of the pendant unit. For nonpolar polymers in the α -olefin class, this is a monotonically increasing curve in σ as V_x increases. The σ value obtained for polyoctene-1 of 2.14 is in excellent agreement with the extrapolated limiting curve for the nonpolar, linear poly- α -olefins (Fig. 4). That is, K-S draw several smooth curves for σ versus V_x for different homologous series of polar polymers. The poly- α -olefin's curve is in a sense limiting, in that chain dipole interactions are minimized. The K-S curve drawn smoothly through the experimental points from the lower n -alkyl series coincides at higher values of V_x (long pendant side groups) with the data obtained by Chinai² and co-workers with a large number of long side-chain n -alkyl methacrylates. Our new point falls directly on the K-S predicted curve

($V_z \cong 130$), supporting it as a limiting line, and also adds support to ideas on dipole interactions which produce a curve with a minimum in the polymethacrylate series.²

In partial fulfillment for the requirements for a Ph.D. in Chemistry. The financial assistance of the Petroleum Research Fund of the American Chemical Society is gratefully acknowledged.

References

1. Kurata, M., and W. H. Stockmayer, *Fortschr. Hochpolymer. Forsch.*, **3**, 196 (1963).
2. For instance, the large number of papers by S. N. Chinai, A. L. Resnick, and co-workers. See Reference 1 for a complete list.
3. Fox, T. G. and P. J. Flory, *J. Am. Chem. Soc.*, **73**, 1909 (1951).
4. Yanko, J. A., *J. Polymer Sci.*, **19**, 437 (1956).
5. Flory, P. J., *Principles of Polymer Chemistry*, Cornell University Press, Ithaca, New York, 1953, pp. 545.
6. Kirkwood, J. G., and J. Riseman, *J. Chem. Phys.*, **16**, 565 (1948).
7. Schulz, G. V., *Z. Physik. Chem.*, **B43**, 25 (1939).
8. Orofino, T. A., and J. W. Mickey, Jr., *J. Chem. Phys.*, **38**, 2512 (1963).
9. Ivin, K. J., and H. A. Ende, *J. Polymer Sci.*, **54**, 517 (1961).

Résumé

On a mesuré par diffusion lumineuse, osmométrie et viscosimétrie, les propriétés en solution diluée du polyoctène 1 et les expressions de Mark-Houwink ont été déterminées dans deux bons solvants du point de vue thermodynamique et dans un solvant à la température (Θ) de Flory. Les résultats ont été comparés et analysés par la technique de Kurata-Stockmayer et présentent une bonne concordance avec la théorie dans certains cas et moins bonne dans d'autres. Cependant les résultats ne sont pas suffisamment précis pour juger tous les aspects de la valeur d'une telle théorie à deux paramètres.

Zusammenfassung

Die Eigenschaften verdünnter Lösungen von Polyokten-1 wurden durch Lichtstreuung, Osmometrie und Viskosimetrie gemessen und die Mark-Houwink-Beziehung in zwei thermodynamisch guten Lösungsmitteln und in einem Lösungsmittel bei der Flory- Θ -Temperatur bestimmt. Die Versuchsdaten wurden nach der Methode von Kurata-Stockmayer zueinander in Beziehung gesetzt und analysiert und zeigen in manchen Fällen gute Übereinstimmung mit der Theorie und in anderen eine mässig schlechte. Die Daten sind aber nicht genau genug um alle Aspekte der Richtigkeit einer solchen Zwei-Parametertheorie beurteilen zu können.

Received October 2, 1964

Revised April 16, 1965

Prod. No. 4737A

NOTES

The Effect of Conversion on the Copolymerization of Ethylene and Dibutyl Fumarate

Recently, Ham and Brown¹ reported monomer reactivity ratio products (r_1r_2) for several ethylene copolymerizations to be considerably higher than unity. For example, the copolymerization of ethylene (M_1) and diethyl fumarate (M_2) gave $r_1 = 0.25$, $r_2 = 10$, and hence, $r_1r_2 = 2.5$, at 12,000 psi and 150°C.

A reactivity ratio product greater than unity implies that either substantial block copolymerization, or two independent homopolymerizations are occurring, a situation which never has proven to exist in free-radical copolymerizations. These results are especially surprising due to the reluctance of fumarate esters to homopolymerize. Moreover, recent work² has shown that ethylene copolymerizations with four different monosubstituted vinyl monomers of widely different reactivity approached ideality ($r_1r_2 \sim 1$).

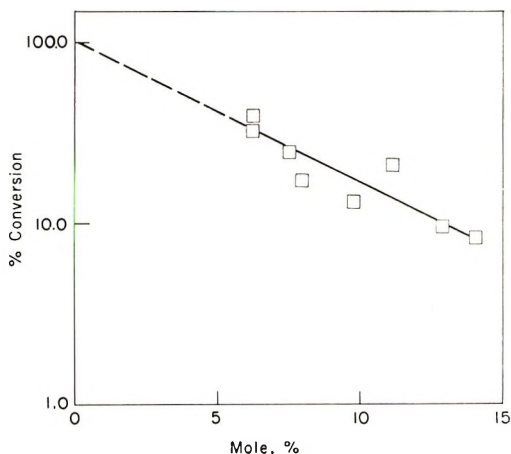


Fig. 1. Ethylene-dibutyl fumarate copolymerizations at an initial molar comonomer ratio of 99.5:0.5. Per cent conversion to copolymer plotted against ratio of mole-% dibutyl fumarate in resin to dibutyl fumarate in initial comonomer solution.

Our examination of the copolymerization of ethylene and dibutyl fumarate has suggested a possible solution to this apparent anomaly. When a solution of ethylene and dibutyl fumarate at a molar ratio of 99.5:0.5 was fed into a continuous tubular reactor at 35,000 \pm 5,000 psi and a jacket temperature of 185°C. in the presence of 60 ppm oxygen high molecular weight copolymer (melt indexes <100) was smoothly formed. Under these conditions it was found that the composition of the resin produced during these experiments changed dramatically with conversion, as shown in Figure 1. From these data it is apparent that the copolymer equation relating feed composition to copolymer composition would not be valid above very low conversions. Note, for example, that a reasonable line through the points in Figure 1 extrapolated to zero conversion leads to a ratio of dibutyl fumarate in the copolymer to dibutyl fumarate in the monomer solution of about 100, whereas at 10% conversion this value has decreased almost one order of

magnitude to about 17.0. It is also significant that extrapolation of the data in Figure 1 to zero conversion indicates that even at a molar monomer ratio of ethylene to dibutyl fumarate as low as 99.5:0.5 the initial copolymer is alternating in character.

It is apparent that reactivity ratio data obtained with systems such as ethylene-dibutyl fumarate, under the usual low conversions of 5–10%, do not describe the system under conditions where the copolymer equation is valid. Indeed, the data in Figure 1 indicate an initial alternating copolymer, and thus a reactivity ratio product close to zero.

References

1. Ham, G. E., and F. E. Brown, *J. Polymer Sci.*, **A2**, 3623 (1964).
2. Burkhart, R. D., and N. L. Zutty, *J. Polymer Sci.*, **A1**, 113 (1963).

R. ROBERTS
R. D. LUNDBERG
N. L. ZUTTY

Research and Development Department
Union Carbide Corporation, Plastics Division
South Charleston, West Virginia

Received May 25, 1965

Synthesis and Polymerization of Stereoisomeric 2-Methyl Cyclohexyl Methacrylates

In order to investigate the effect on polymer structures of stereoisomerism of 2-methyl cyclohexyl methacrylates, *cis*-2-methyl cyclohexyl methacrylate (1), *trans*-2-methyl cyclohexyl methacrylate (2) and mixed *cis* and *trans* 2-methyl cyclohexyl methacrylate (3) were synthesized by esterification of methacrylic acid with *cis*-2-methyl cyclohexanol, *trans*-2-methyl cyclohexanol, and mixed *cis* and *trans* 2-methyl cyclohexanol, respectively, in the presence of *p*-toluene sulfonic acid.

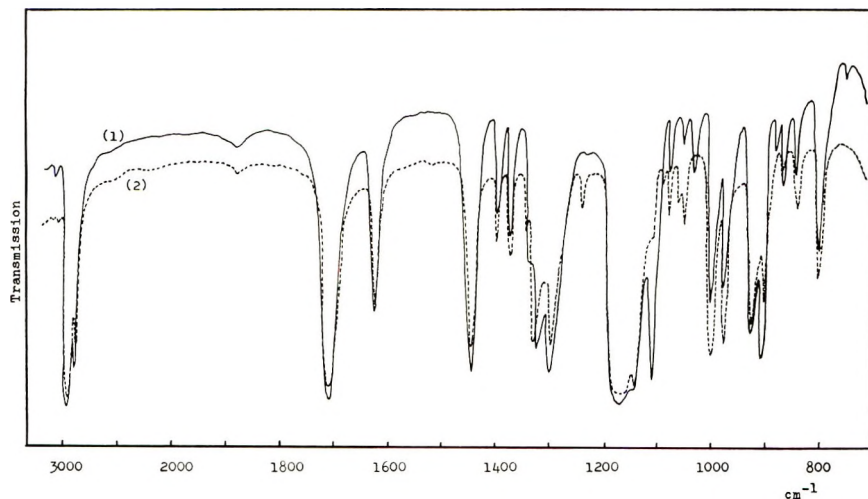


Fig. 1. Infrared spectra of *cis*-2-methyl cyclohexyl methacrylate (1) and *trans*-2-methyl cyclohexyl methacrylate (2) (liquid film).

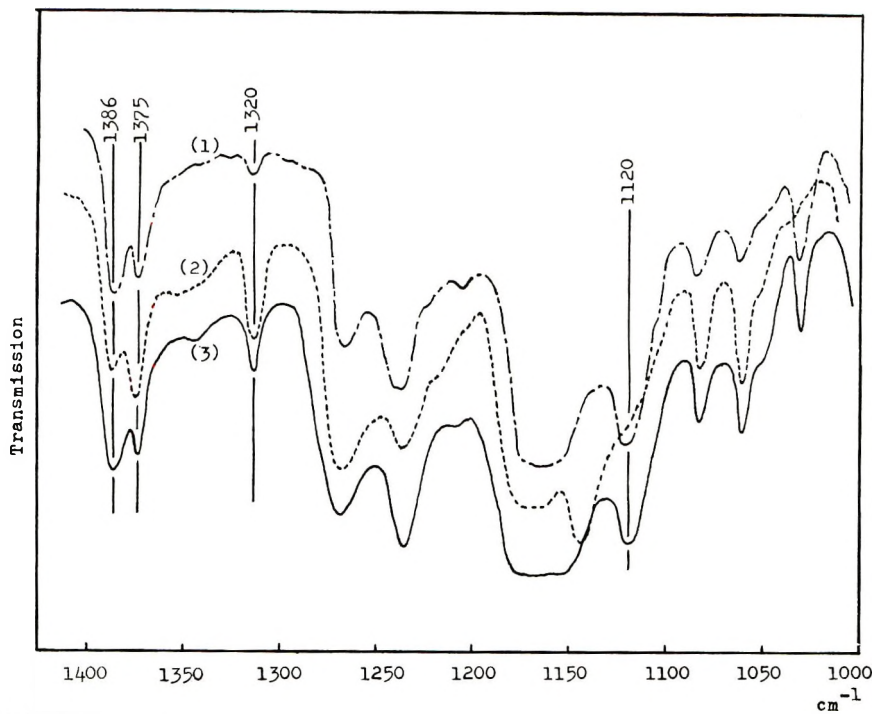


Fig. 2. Infrared spectra of poly-2-methyl cyclohexyl methacrylates obtained by using radical catalyst: (1) *cis* isomer, (2) *trans* isomer, (3) mixed *cis* and *trans*.

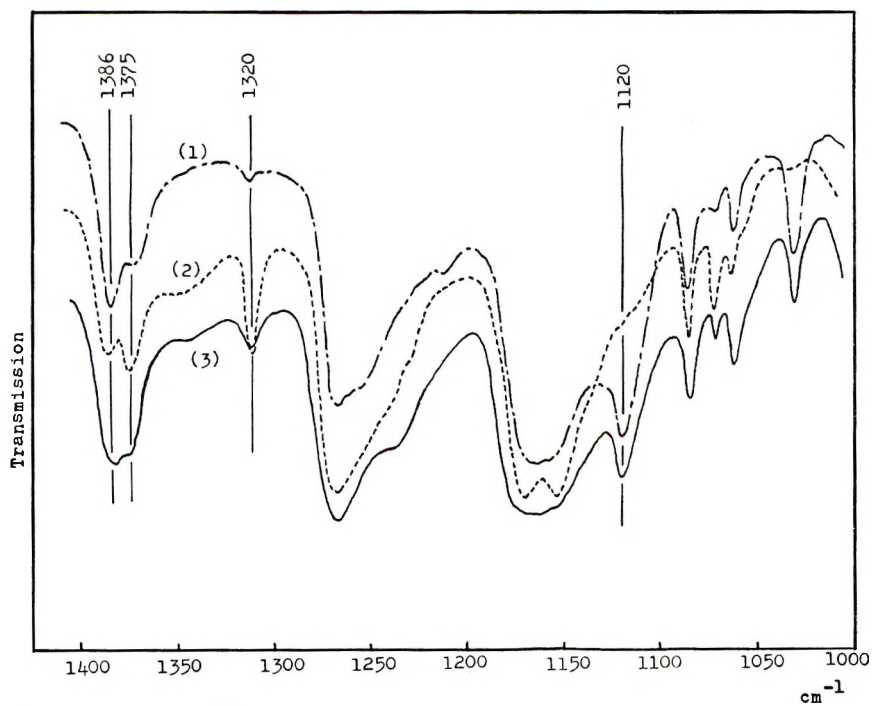


Fig. 3. Infrared spectra of poly-2-methyl cyclohexyl methacrylates obtained by using anionic catalyst: (1) *cis* isomer; (2) *trans* isomer; (3) mixed *cis* and *trans*.

Cis-2-methyl cyclohexanol was prepared by catalytic hydrogenation of 2-methyl cyclohexanone according to the method of Arnold, Smith, and Dodson.¹ *Trans*-2-methyl cyclohexanol was prepared by saponification of 2-methyl cyclohexyl-3,5-dinitrobenzoate and fractionated with recrystallization according to the method of Jackman, Macbeth, and Mills.² The *cis*-2-methyl cyclohexyl methacrylate and *trans*-2-methyl cyclohexyl methacrylate obtained were identified by infrared spectra and elementary analysis as shown in Figure 1 and Table I. These monomers showed the absorptions due to the double bond at 1630 cm^{-1} and the ester group at 1170 cm^{-1} .

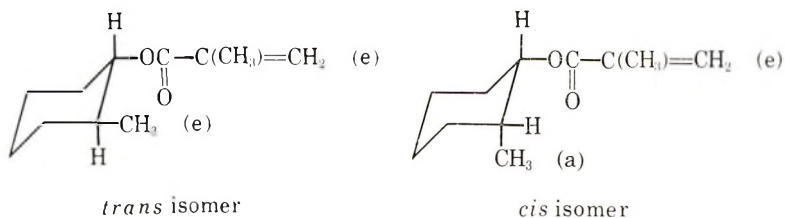


TABLE I
Boiling Point and Elementary Analysis of Stereoisomeric 2-Methyl Cyclohexyl Methacrylates

Monomers	Yield, %	Boiling point, °C./mm. Hg	Elementary analysis	
			Found	Calc.
(1) <i>cis</i>	30.5	68-70/3	C: 72.05 H: 10.05	C: 72.53 H: 9.9
(2) <i>trans</i>	44.0	80-81/4	C: 72.76 H: 10.00	C: 72.53 H: 9.9
(3) Mixed <i>cis</i> and <i>trans</i>	56.0	67-68/1-2	C: 72.39 H: 10.04	C: 72.53 H: 9.9

TABLE II
Polymerization of Stereoisomeric 2-Methyl Cyclohexyl Methacrylates Catalyzed by Benzoyl Peroxide^b

Monomers, cc.	Toluene, cc.	Benzoyl peroxide, mg.	Polymers, mg.	$[\eta]^a$
(1) <i>cis</i> 0.5	0.5	6.3	455.0	0.20
(2) <i>trans</i> 0.5	0.5	6.3	535.0	0.19
(3) Mixed <i>cis</i> and <i>trans</i>	0.5	6.3	455.0	0.21

^a The intrinsic viscosities were measured in chloroform at 20°C.

^b The monomers were polymerized at 75°C. for 17 hr.

The polymerizations of *cis*-2-methyl cyclohexyl, *trans*-2-methyl cyclohexyl, and mixed *cis* and *trans* 2-methyl cyclohexyl methacrylates were carried out by using radical (benzoyl peroxide) and anionic (*n*-butyllithium) catalysts.

The infrared spectra of these polymers are shown in Figures 2 and 3. The differences between *cis* and *trans* isomers are observed at 1120, 1320, 1375, and 1386 cm^{-1} , and the difference between polymers radically and anionically polymerized is evident at 1235 cm^{-1} . The effect of stereoisomeric configuration in 2-methyl cyclohexyl methacrylate was assumed from the differences in infrared spectra of the polymers.

TABLE III
Polymerization of Stereoisomeric 2-Methyl Cyclohexyl Methacrylates Catalyzed by *n*-Butyllithium^c

Monomers, cc.	Toluene, cc.	<i>n</i> -Butyllithium solution, ^a cc.	Polymers, g.	$[\eta]^b$
(1) <i>cis</i> 0.5	0.5	1.0	0.459	0.076
(2) <i>trans</i> 1.0	1.0	1.0	0.90	0.116
(3) Mixed <i>cis</i> and <i>trans</i> 2.0	2.0	2.0	1.982	0.154

^a The solution was prepared by reaction of 2.8 g. (0.03 mole) *n*-butylchloride with 0.24 g. (0.034 mole) lithium in 10 cc. *n*-hexane.

^b The intrinsic viscosities were measured in chloroform at 20°C.

^c The monomers were polymerized at -78°C. for 20 hr.

References

1. Arnold, R. T., G. G. Smith, and R. M. Dodson, *J. Org. Chem.*, **15**, 1256 (1950).
2. Jackman, I. M., A. K. Macbeth, and J. A. Mills, *J. Chem. Soc.*, **1949**, 1717.

WASABURO KAWAI

Government Industrial Research Institute
Osaka, Oyodo-cho, Oyodo-ku, Japan

Received March 10, 1965

Temperature Effects on Birefringence Intensity of Poly-3-Methyl-1-Pentene

Unusual temperature-dependent birefringence effects have been observed in the spherulites of crystalline poly-4-methyl-1-pentene. Saunders¹ has reported that the spherulitic structure birefringence changes sign (positive to negative) in the vicinity of 50°C. He suggested that the radial and tangential refractive index components of the index ellipsoid vary with temperature at different rates and cross at 50°C. This results in a change in the sign of birefringence.

Kirshenbaum et al.² in their study of this same phenomenon have shown that the change in sign of birefringence occurs at the same temperature as the amorphous-crystalline phase density inversion. That is, as the temperature is increased the density of the amorphous phase decreases faster than that of the crystalline phase, the two becoming equal at 50°C. It is known from the Lorenz equation that density (d) and refractive index (η) are related by the equation

$$(\eta^2 - 1)/(\eta^2 + 2) = kd,$$

where k is the specific refraction. It is expected from this relationship that the density and refractive index are interrelated. Kirshenbaum et al.² have noted this relationship. We have observed a similar phenomenon for poly-3-methyl-1-pentene (poly-MP-31). Both toluene-soluble and toluene-insoluble fractions were studied using the depolarized light intensity (DLI) technique.³

Experimental

Samples weighing approximately 0.2 mg. were sandwiched between strain-free cover slips and both heated and cooled on a Leitz hot stage. The optical system of a Zeiss Ultraphot II was adapted to measure the intensity of the light rotated by the sample by mounting a photoconductive cell at the secondary focus. The photoconductive cell was attached to a suitable bridge, the output of which drove the y -axis of a Moseley x - y recorder. The output of a platinum-10% platinum rhodium thermocouple mounted in contact with the cover slip in the hot stage powered the x -axis of the same recorder. The instrument was essentially identical in design to that given by Kirshenbaum et al.²

At the start of a heating cycle, the polarizers were crossed to extinction, the sample adjusted for maximum rotation of light, and a quartz correction plate interposed in the light path. The sample was heated from room temperature to 410°C. at 12°C./min. and subsequently cooled at the same rate. The DLI heating and cooling curves (loops) shown in Figures 1, 2, and 3 were obtained in this way. The hysteresis in the curves can be related to intrinsic viscosity. This will be the subject of a forthcoming publication.

Poly-MP-31 may be polymerized with a Ziegler catalyst as the optically active poly- d -MP-31 or as a racemic mixture, poly- d , l -MP-31. These materials have been prepared and were used in this study. Electron and x-ray diffraction show that both toluene-soluble and toluene-insoluble fractions are highly crystalline.

Discussion

The DLI-temperature loop for the toluene-insoluble, optically active poly- d -MP-31, Figure 1, shows that with increasing temperature the birefringence intensity minimum occurs at $\sim 250^\circ\text{C}$. At approximately 300°C . a high temperature maximum is recorded whose relative intensity is nearly equal to that observed at room temperature. A quartz compensator was used to determine the sign of the birefringence of the optically active poly- d -MP-31 fraction. Unlike poly-4-methyl-1-pentene, poly- d -MP-31 spherulites were found to have a negative birefringence below the 250°C . minimum and a positive birefringence above this temperature.

The DLI-temperature loop for poly-*d,l*-MP-31 (made from a *d*, *l*, or racemic mixture of the monomer) shows a birefringence intensity minimum at 300°C., Figure 2. However, spherulite birefringence was positive below 300°C. and became negative above this temperature.

The toluene-soluble poly-*d*-MP-31 fraction gave a DLI-temperature loop, Figure 3, showing a sharp birefringence decrease due to melting at 120°C. followed by a slow birefringence decrease to zero at 220°C. At room temperature, these two crystalline modifications appear as shown in Figure 4. At greater than 120°C. only the second crystal form is seen. *A* has melted and appears dark. The two crystal modifications are segregated upon recrystallization. Quartz compensation measurements for the sign of birefringence show that both modifications are negative.

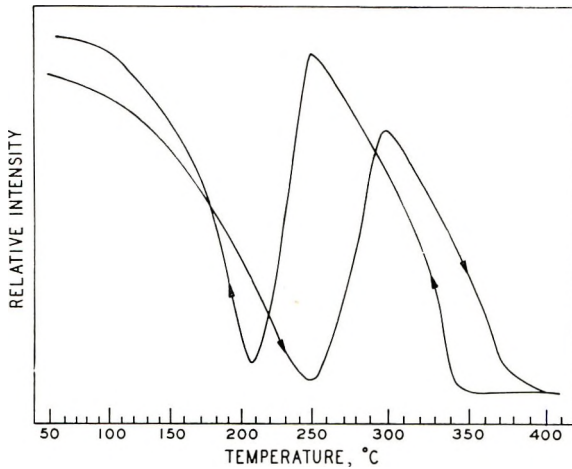


Fig. 1. DLI loop for poly-*d*-3-methyl-1-pentene: hot toluene-insoluble fraction.

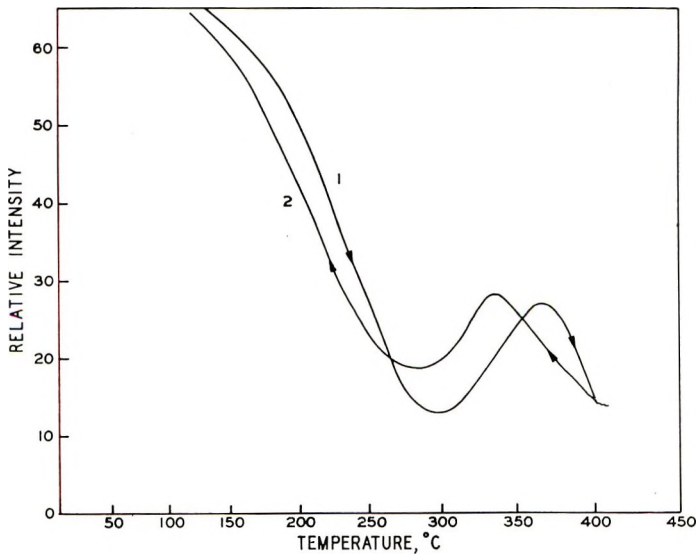


Fig. 2. DLI loop for poly-*d,l*-3-methyl-1-pentene: hot toluene-insoluble fraction.

X-ray diffraction patterns obtained for poly-*d,l*-MP-31 and poly-*d*-MP-31 toluene-insoluble fractions are identical. The x-ray diffraction pattern obtained for the poly-*d, l*-MP-31 toluene-soluble fraction is completely different from that obtained for the

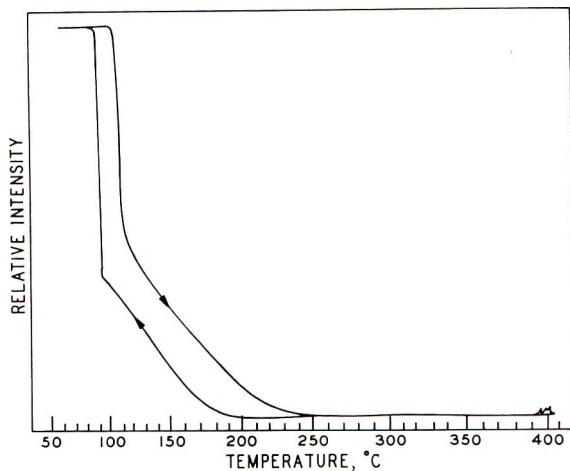
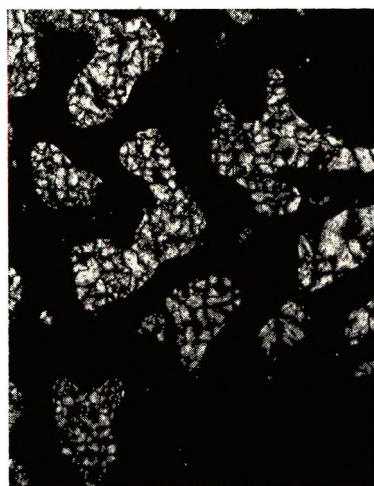
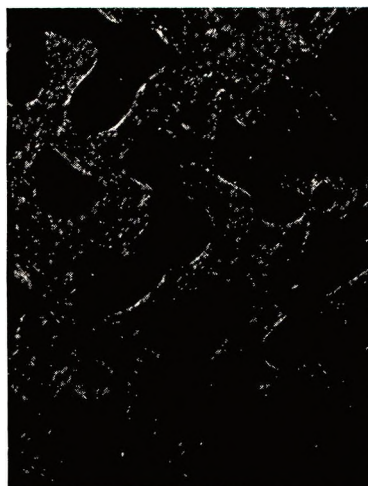


Fig. 3. DLI loop for poly-*d,l*-3-methyl-1-pentene: toluene-soluble fraction.



A and B

C_7 Soluble Poly-MP-31 Fraction
Temperature 25°C



B

Temperature 120-216°C

Fig. 4. Two modifications of the C_7 soluble poly-MP-31 fraction shown between crossed polarizers 47 \times .

toluene-insoluble fractions. This evidence, together with melting point data (120–210, and 389°C.), and the apparent interconvertibility of the birefringent forms suggest that there are three allotropic forms of poly-MP-31.

Single crystals of optically active poly-*d*-MP-31 were grown from dilute chloronaphthalene solutions at 160°C. for 12 hr. Rectangular lamellae are the primary crystal habit observed as shown in Figure 5.

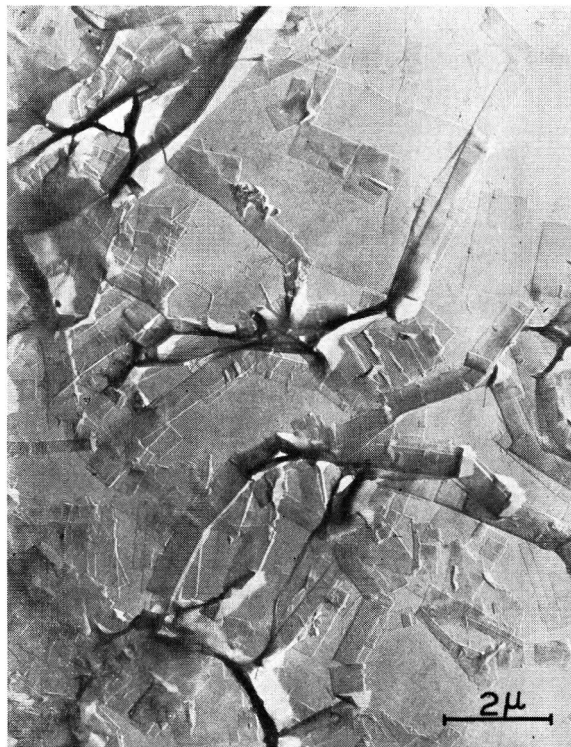


Fig. 5. Poly-*d*-3-methyl-1-pentene single crystals grown from a 0.01 wt.-% chloronaphthalene solution 7,000 \times .

Attempts to grow single crystals from the poly-*d*, *l*-MP-31 toluene-insoluble fraction resulted in fibrous and dendritic growth. Single crystal electron diffraction patterns obtained for the optically active toluene-insoluble fraction suggest a tetragonal structure with $a_0 = b_0 \sim 19.2$ Å, where c has not yet been determined.

Conclusions

Poly-3-methyl-1-pentene has a DLI curve showing a minimum similar to that reported for poly-4-methyl-1-pentene. The poly-*d*-MP-31 has an intensity minimum at 250°C. Unlike poly-4-methyl-1-pentene the spherulites have a negative birefringence at temperatures below the minimum. The racemic mixture, poly-*d,l*-MP-31 shows a DLI minimum at 300°C. with birefringence sign behavior reversed to that of poly-*d*-MP-31. The poly-*d,l*-MP-31 toluene-soluble fraction exhibits an unusual melting behavior with a sharp decrease in DLI at 120°C. followed by total extinction at 250°C. X-ray diffraction, melting point, and birefringence data indicate three allotropic forms of poly-MP-31.

The author wishes to thank Mr. R. Bacskai for the polymer samples and for helpful suggestions and Dr. Edward M. Barrall II for help in the preparation of the manuscript.

References

1. Saunders, F. L., *Polymer Sci.*, **B2**, 755 (1964).
2. Kirshenbaum, I., R. B. Isaacson, and W. F. Feist, *J. Polymer Sci.*, **B2**, 897 (1964).
3. Magill, J. H., *Polymer*, **2**, 221 (1961).

E. J. GALLEGOS

California Research Corporation
Richmond, California

Received January 29, 1965
Revised July 16, 1965

Point Imperfections and Dislocations: Proper Nomenclature

The nature of physical imperfections in polymers and their effect on properties have been studied increasingly during the past few years. Several types of point imperfections and dislocations have been postulated and observed.

In this new area of research however, an error in nomenclature has been compounded by invention of implausible names. Point defects have been referred to as dislocations and given at least six new names. A dislocation is defined as the boundary between slipped and unslipped regions in a crystal¹ and is therefore a *one-dimensional* or line imperfection. In contrast, a point imperfection is *zero-dimensional*. Thus, a point imperfection should never be referred to as a dislocation. I implore both authors and editors to insist upon correct terminology.

Reference

1. Taylor, G. I., *Proc. Roy. Soc. (London)*, **A145**, 362 (1934).

W. L. PHILLIPS, JR.

Engineering Materials Laboratory
Engineering Research Division
Engineering Department
E. I. du Pont de Nemours & Company, Inc.
Wilmington, Delaware

Received July 13, 1965

Dilute Solution Properties of Poly(*para*-Isopropylstyrene)

EXPERIMENTAL

Synthesis

1. The preparation of *para*-isopropylstyrene monomer was based on the method described by Matlack and co-workers.¹

2. Poly(*para*-isopropylstyrene) was prepared by a procedure similar to that reported by Browder and McCormick.² Samples of varying molecular weights were prepared as described by Szwarc and co-workers.³⁻⁵ The polymerization was conducted in tetrahydrofuran (THF) contained in an all-glass system under an atmosphere of nitrogen, at 25°C. Impurities in the nitrogen were removed by bubbling it through a suspension of a sodium-naphthalene complex in THF.

The monomer was purified by vacuum distillation from calcium carbide, followed by purging with nitrogen for several hours. THF was purified by distillation from a sodium-naphthalene complex. THF, monomer and a concentrated solution of the complex in THF, in this order, were added into the reaction vessel (the initiator was introduced by means of a hypodermic syringe). The polymerization was rapid, generally complete within 1/2 hr. The polyanions were destroyed by rapidly introducing oxygen-free water into the system. The polymer was precipitated in a ten-fold excess of methanol, and recovered by freeze drying from benzene solution.

Viscosity

Reduced viscosities were determined in toluene at 25°C. using a Ubbelohde suspended level dilution viscometer. Flow times were measured for each of five polymer concen-

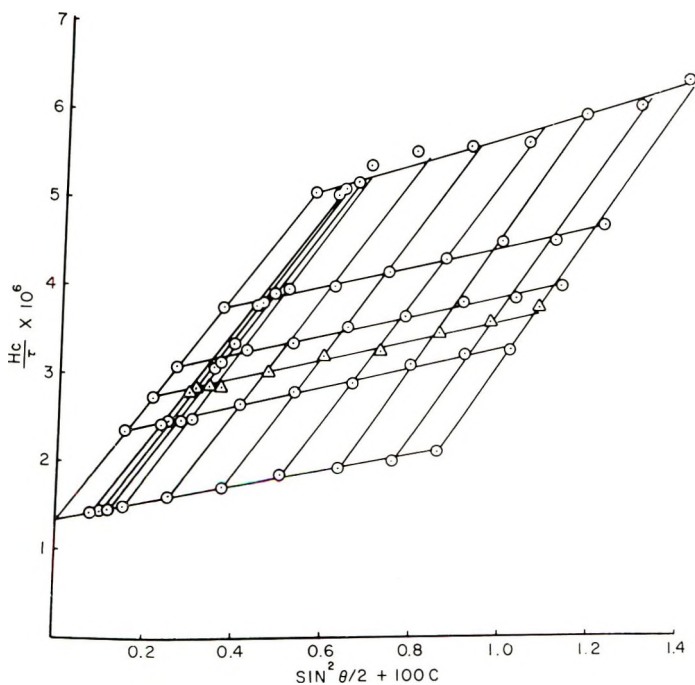


Fig. 1. Zimm plot of poly(*para*-isopropylstyrene) (B-62-2) in tetrahydrofuran at 4360 Å. and 25°C.

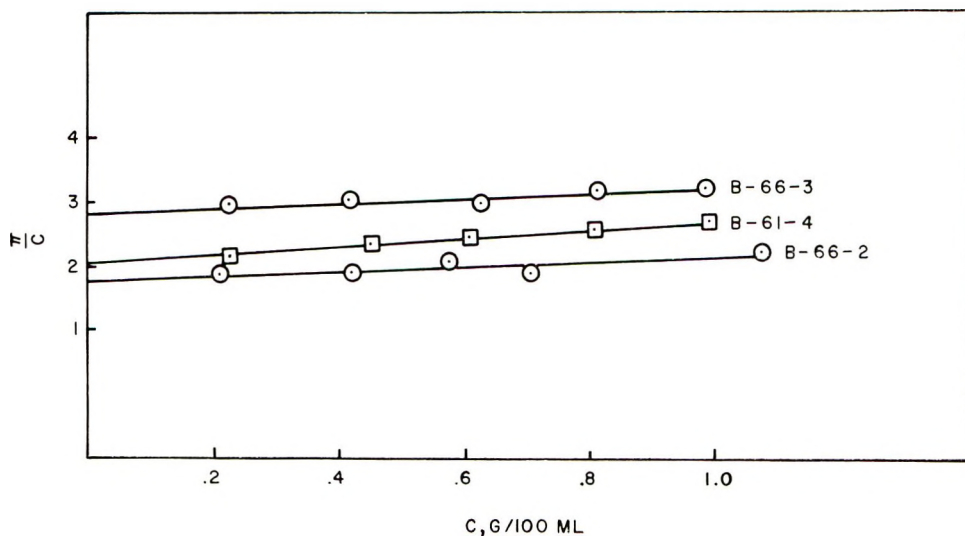


Fig. 2. Plot of π/c vs. concentration for poly(*para*-isopropylstyrene) polymers in methyl ethyl ketone at 25°C.

trations. No kinetic energy correction was applied since solvent flow times exceeded 100 sec.

Light Scattering

Light-scattering measurements were made in tetrahydrofuran at wavelengths 4360 and 5460 Å. at 25°C. using a Brice-Phoenix photometer. Polymer solutions were clarified by centrifugation at 52,000 *g* for 1 hr. in a Spinco Model L centrifuge. The calibration of the photometer was checked by determining the molecular weights of National Bureau of Standards' polymers nos. 705 and 706. The intensity of the scattered light was measured at ten angles between 32 and 135°C. to the primary beam for each of five concentrations of polymer. Refractive index increments, dn/dc , were measured with a Brice-Phoenix differential refractometer at 25°C. The dn/dc values for poly(*para*-isopropylstyrene) in THF at wavelengths 4360 and 5460 Å. were 0.177 and 0.167 ml./g., respectively.

Osmotic Pressure

Osmotic pressure measurements were made in methyl ethyl ketone (MEK) with a Stabin-Pinner osmometer at 25°C. using gel cellophane 600 membranes. Height measurements were made on each of five concentrations after equilibrating for 24 hr.

RESULTS AND DISCUSSION

The solution properties of five (unfractionated) preparations of *p*-isopropylstyrene polymers are shown in Table I. The table contains the weight-average molecular weight, \bar{M}_w , radius of gyration, $(s^2)^{1/2}$, and second virial coefficient, A_2 , from light scattering; number-average molecular weights, \bar{M}_n , from osmometry; and intrinsic viscosities, $[\eta]$, and the Huggins' constants, k' , from viscosity measurements. The \bar{M}_w , A_2 , and $(s^2)^{1/2}$ were obtained from Zimm plots. Figure 1 shows a Zimm plot of sample B-62-2. The osmometry results, used to determine \bar{M}_n , are given in Figure 2. The \bar{M}_n was obtained on three samples only, since the other two showed slight turbidity in the MEK solvent. However, these two samples were clear in THF. Sample B-66-3

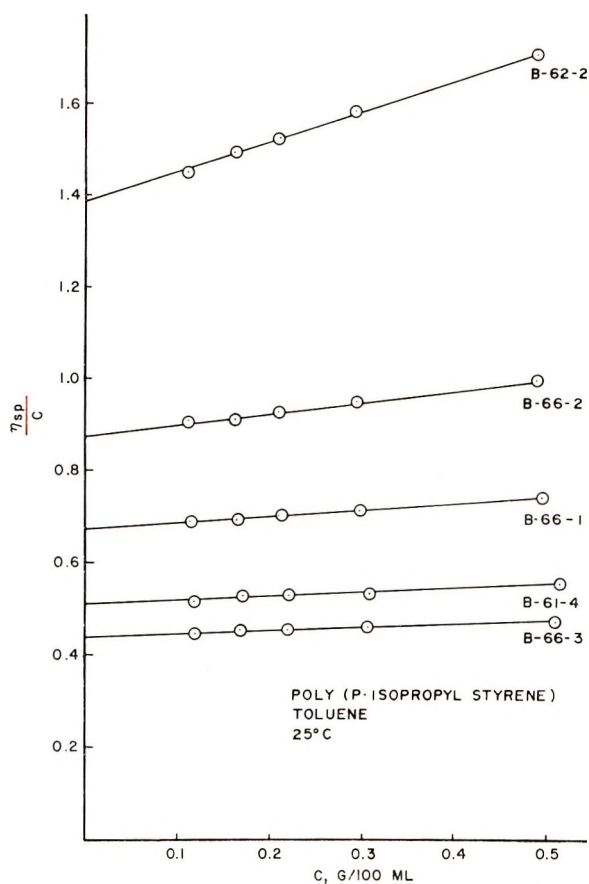


Fig. 3. Reduced viscosity vs. concentration for poly(*para*-isopropylstyrene) polymers in toluene at 25°C.

and B-61-4 have \bar{M}_w/\bar{M}_n ratios of 1.57 and 1.40, respectively. On the other hand, for sample B-66-2, the \bar{M}_w/\bar{M}_n is 2.76, showing a higher degree of polydispersity. This may be attributed to the presence of oxygen or water during the polymerization, causing premature termination of some of the growing polymer chains.

Figure 3 shows the reduced viscosities of the five samples plotted against concen-

TABLE I
Solution Properties of Poly(*p*-Isopropylstyrene)

Sample no.	\bar{M}_w	\bar{M}_n	\bar{M}_w/\bar{M}_n	$[\eta]$	$(s^2)^{1/2}$	$2A_2 \times$	k'
					A.	10^4	
B-66-3	140,000	89,000	1.57	0.439	128	9.61	0.38
B-61-4	180,000	123,000	1.40	0.513	149	7.68	0.33
B-66-1	282,000	—	—	0.675	182	10.11	0.31
B-66-2	392,000	141,000	2.76	0.880	250	7.45	0.31
B-62-2	741,000	—	—	1.39	394	6.89	0.34

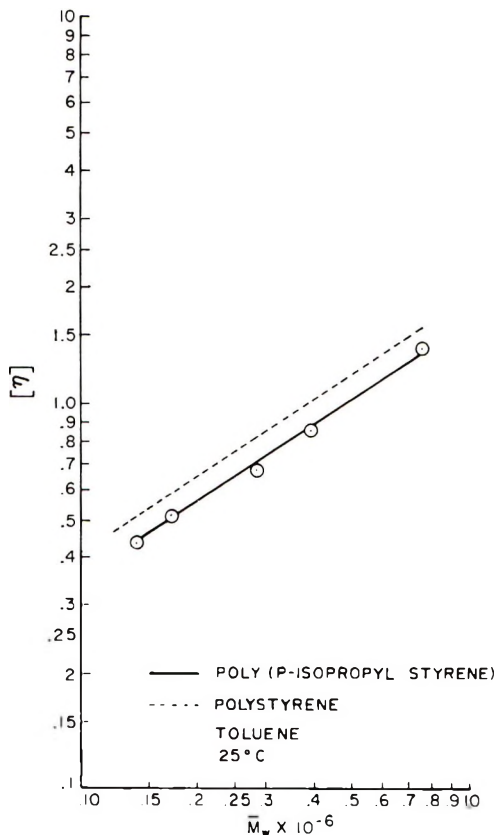


Fig. 4. Intrinsic viscosity vs. weight-average molecular weight for poly(*para*-isopropylstyrene) in toluene at 25°C.

tration. A log-log plot of $[\eta]$ versus \bar{M}_w is shown in Figure 4, from which the following relationship was obtained:

$$[\eta] = 1.23 \times 10^{-4} \bar{M}_w^{0.69} \quad (1)$$

The relationship is valid for poly(*para*-isopropylstyrene) in toluene at 25°C.

Figure 4 also includes a plot for anionically prepared polystyrene, constructed from the relationship reported by Morton and co-workers,⁶ namely:

$$[\eta] = 1.46 \times 10^{-4} \bar{M}_w^{0.69} \quad (2)$$

The two relationships are almost identical, as may be anticipated from the highly similar nature of the two polymers.

A log-log plot of $(s^2)^{1/2}$ versus \bar{M}_w is given in Figure 5. The equation relating $(s^2)^{1/2}$ to \bar{M}_w is:

$$(s^2)^{1/2} = 4 \times 10^{-2} \bar{M}_w^{0.68} \quad (3)$$

In general, the second virial coefficient, A_2 , decreases with increasing molecular weight. However, a plot of the data showed considerable scatter. The mathematical relationship between A_2 and \bar{M}_w in THF is:

$$2A_2 = 6 \times 10^{-3} \bar{M}_w^{(-0.16)} \quad (4)$$

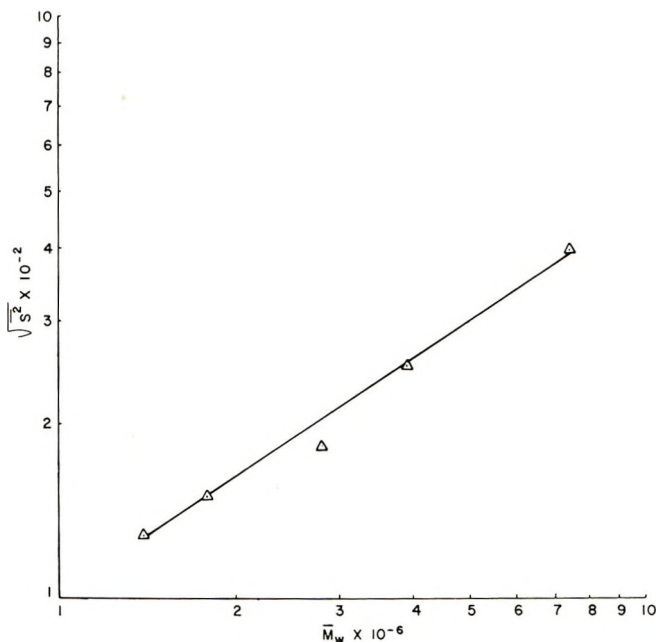


Fig. 5. Radius of gyration vs. weight-average molecular weight for poly(*para*-isopropylstyrene) in tetrahydrofuran at 25°C.

It is interesting to note that a similar relation for polystyrene in MEK was reported by Stacey:⁷

$$A_2 \sim M^{-0.16} \quad (5)$$

The similarity in these relationships is not surprising in view of the reported solubility parameters, δ , of 9.04 and 9.32 for MEK and THF, respectively.⁹

The values of k' , shown in Table I fall within a narrow range (0.31–0.38) and agree with those obtained for polystyrene in toluene by Chinai and co-workers.⁸

The findings as reported in this note strongly indicate that the solution properties of poly(*para*-isopropylstyrene) are very similar to those reported for polystyrene.

From a thesis submitted by F. S. Holahan in partial fulfillment of the requirements for the degree of Doctor of Philosophy in Chemistry at Stevens Institute of Technology.

References

1. Matlack, J. D., S. N. Chinai, R. A. Guzzi, and D. W. Levi, *J. Polymer Sci.*, **49**, 533 (1961).
2. Browder, F. M., and H. W. McCormick, *J. Polymer Sci.*, **A1**, 1749 (1963).
3. Szwarc, M., M. Levy, and R. Milkovitch, *J. Am. Chem. Soc.*, **78**, 1656 (1956).
4. Szwarc, M., and A. Rembaum, *J. Polymer Sci.*, **22**, 189 (1956).
5. Szwarc, M., *Proc. Roy. Soc.*, **A279**, 260 (1964).
6. Morton, M. T., E. Helminiak, S. D. Gadkary, and F. Bueche, *J. Polymer Sci.*, **57**, 471 (1962).
7. Stacey, K. A., *Light Scattering in Physical Chemistry*, Academic, New York, 1956, p. 121.
8. Chinai, S. N., P. C. Scherer, C. W. Bondurant, and D. W. Levi, *J. Polymer Sci.*, **22**, 527 (1956).

9. Allen, P. W., *Techniques of Polymer Characterization*, Butterworths, London, 1959, p. 8.

F. S. HOLAHAN*
S. S. STIVALA
D. W. LEVI*

Department of Chemistry and Chemical Engineering
Stevens Institute of Technology
Hoboken, New Jersey

Received April 19, 1965

Revised June 21, 1965

* Present address: Polymer Research Branch, Picatinny Arsenal, Dover, New Jersey.

Graft Copolymers of para-Isopropylstyrene and Ethyl Methacrylate†*

INTRODUCTION

The need for solution studies on polymers of nonuniform composition, e.g. block and graft copolymers, is well established.¹⁻⁴ The fact that Krause² has recently reported the behavior of block copolymers in solution to be considerably different than those of random copolymers should heighten the interest in the study of copolymeric systems.

Two of the major difficulties in studying graft copolymers are the lack of (a) suitable methods for estimating the amount of grafting and (b) assurance that the graft copolymer is free from homopolymer. As indicated in this paper, radioactive tracer techniques can be used effectively in determining composition of grafted samples and in insuring that isolation procedures are capable of separating graft from homopolymer.

EXPERIMENTAL

Synthesis

Benzene-C¹⁴ (1 mc.) (New England Nuclear Corp., Boston, Mass.) was diluted with unlabeled reagent grade benzene in a high vacuum manifold using standard techniques. It was then converted to cumene-C¹⁴ by reaction with isopropyl alcohol in the presence of sulfuric acid (80%). The cumene-C¹⁴ was distilled through a Vigreux column and the fraction boiling between 150-155°C. was collected.

The remainder of the syntheses of *para*-isopropylstyrene monomer, polymer, polymeric hydroperoxide, and graft copolymer were essentially the same as those reported by Matlack and co-workers.⁵

Ethyl methacrylate-C¹⁴ (450 μ c.) (New England Nuclear Corp.) was diluted with 12 g. of unlabeled monomer (Monomer-Polymer Corp.). The polymer was prepared using the procedure described by Chinai et al.⁶

Separation of Graft Copolymer

The product of the grafting reaction was a mixture of graft copolymer and poly(ethyl methacrylate) homopolymer. The homopolymer was removed by extracting the mixture with a 2:1 (volume) mixture of acetone/methanol. This solvent mixture dissolved the homopolymer. The colloidal dispersion of the graft copolymer was separated by centrifugation for 1 hr. at 25,000 rpm (52,000 *g*).

Viscosity

Viscosity measurements were made with an Ubbelohde suspended level dilution viscometer. Flow times were measured for five concentrations of each polymer. Since solvent flow times exceeded 100 sec. no kinetic energy correction was applied.

Light Scattering

Light-scattering measurements were made at 25°C. at wavelengths 4360 and 5460 Å. using a Brice-Phoenix photometer. Polymer solutions were clarified by centrifugation at 52,000 *g* for 1 hr. in a Spinco Model L centrifuge. The calibration of the photometer was checked by determining the molecular weights of National Bureau of Standards

* From a thesis submitted by F. S. Holahan in partial fulfillment of the requirements for the degree of Doctor of Philosophy in Chemistry at Stevens Institute of Technology.

† Presented at the Twelfth Canadian High Polymer Forum, St. Margarete Station, Canada, May 1964.

polymers nos. 705 and 706. The intensity of the scattered light was measured at 10 angles between 32 and 135° to the primary beam for each of five concentrations of polymer. Refractive index increments, dn/dc , were measured with a Brice-Phoenix differential refractometer at 25°C. The dn/dc values for both poly(*para*-isopropylstyrene) and the hydroperoxidized polymer in tetrahydrofuran at wavelengths 5460Å. and 4360Å. were 0.177 and 0.167 ml./g., respectively. For the graft copolymer the dn/dc values were 0.170 and 0.163 ml./g. respectively.

Osmotic Pressure

Osmotic pressure measurements were made at 25°C. with a Stabin-Pinner osmometer using gel cellophane 600 membranes. Each of five concentrations was allowed 24 hr. to come to equilibrium before height measurements were taken.

Spectra

NMR spectra were obtained with an HR60 spectrometer (Varian Associates) on polymer solutions using $CDCl_3$ (Merck, Sharpe, and Dohme of Canada, Ltd.) as the solvent. Tetramethylsilane (TMS) was used as an internal reference standard.

Infrared spectra were obtained with a Perkin-Elmer spectrometer (Model 21). The spectra were run on films which were cast directly on the salt plate from CCl_4 solutions of the polymer. Following evaporation of the CCl_4 , the salt plate was vacuum dried at 50°C. for 24 hr.

Radioactivity Measurements

Samples were radio assayed for C^{14} activity with a Tricarb Liquid Scintillation Spectrometer (Packard Instrument Co.). The scintillator solution consisted of toluene containing 2,5-diphenyloxazole (4 g./l.) and *para*-bis-2-(4-methyl-5-phenyloxazolyl) benzene (50 mg./l.).

Chemical Analysis

Carbon and hydrogen analysis, the neutralization equivalent, and the saponification equivalent were carried out by Schwarzkopf Microanalytical Laboratory, Woodside, New York.

RESULTS AND DISCUSSION

During the grafting reaction poly(ethyl methacrylate) homopolymer was formed. Previous work⁴ had indicated that selective extraction was effective in removing homopolymer of this type. The effectiveness of this extraction procedure in removing poly(ethyl methacrylate) homopolymer was checked by adding poly(ethyl methacrylate- C^{14}) to a solution of a nonradioactive graft-homopolymer mixture. The mixture was then isolated from the solution and extracted three times with an acetone-methanol mixture. The results of the radioactivity measurements on the extracts and residues is given in Table I.

TABLE I
Removal of Poly(ethyl methacrylate) Homopolymer by Extraction

Extraction no.	Specific activity, counts/min./100 mg.			Homopolymer content, %
	Initial mixture	Extract	Residue	
	229,500	—	—	—
1	—	326,000	6,400	2.0
2	—	—	1,200	0.4
3	—	—	400	0.1

TABLE II
Composition of Mixture from Grafting Reaction

Component	%
Soluble graft copolymer	19
Poly(ethyl methacrylate) homopolymer	57
Gel	24

The per cent carbon and the infrared spectrum of the polymer removed in the first extraction indicated that it was poly(ethyl methacrylate). This evidence and the data in Table I indicated that this extraction procedure was effective in removing homopolymer from the graft.

The amount of poly(ethyl methacrylate) homopolymer was determined by the isotope dilution⁷ technique. The gel content was determined gravimetrically and the graft copolymer content was determined by difference. The analysis of a typical mixture is reported in Table II.

The composition of the graft was determined from the decrease in specific activity which resulted from the addition of the nonradioactive side chains to the radioactive backbone. (No quenching effects were observed with a series of known mixtures of varying poly(*para*-isopropyl-styrene-C¹⁴)-poly(ethyl methacrylate) content). The amount of poly(*para*-isopropyl styrene) in the graft determined from per cent carbon measurements was consistently low. As will be discussed later, the low results probably were caused by the unexpectedly large value for the oxygen content of these polymers. Thus, small deviations from the expected composition can cause large errors in graft composition calculated from per cent carbon measurements.

Upon standing at room temperature for a period of months, graft copolymers showed turbidity when solutions were prepared in toluene. Both the graft and poly-(*para*-isopropylstyrene hydroperoxide) showed no such insoluble portion when stored for several months at 0°C. Both of these polymers became insoluble when heated at 75°C. under vacuum for 6 days. X-ray patterns of the backbone, graft, and gel portions indicated that the polymers were amorphous. The fact that the reaction is accelerated at elevated temperature and retarded at low temperature would seem to indicate that the hydroperoxide group is involved. It seems likely that free radicals produced upon the decomposition of the hydroperoxide groups were causing the polymer chains to join together producing crosslinked molecules.

Spectra of Polymers

The infrared spectrum of the graft copolymer is shown in Figure 1. A large absorption peak appears at 2.9 μ . The O—H stretching mode of the hydroperoxide group appears at this wavelength. This is an extremely strong absorption, considering the fact that the backbone polymer originally had approximately 3% hydroperoxide. In fact, the O—H peak at 2.9 μ in the spectrum of the backbone is barely discernible. The hydroperoxide group is also reported to give rise to an absorption band near 12 μ .^{8,9} Unfortunately, poly(*para*-isopropyl styrene) has a large absorption peak in this region which would mask that of the hydroperoxide group.

An interesting possibility is that the band at 2.9 μ is not due to the hydroperoxide group alone, but is due to both hydroperoxide and alcohol groups. When hydroperoxide groups are introduced into a molecule, the initial concentration very often acts autocatalytically, promoting further hydroperoxidation. The graft copolymer was stored at room temperature. Hydroperoxide groups are known to decompose at this temperature. One of the chief products from the thermal decomposition of cumene hydroperoxide is reported to be C₆H₅(CH₃)₂OH.¹⁰ If the hydroperoxide groups in the graft copolymer decompose in an analogous manner, a tertiary alcohol would be produced. Shreve and co-workers⁸ reported that there is no appreciable difference between the O—H

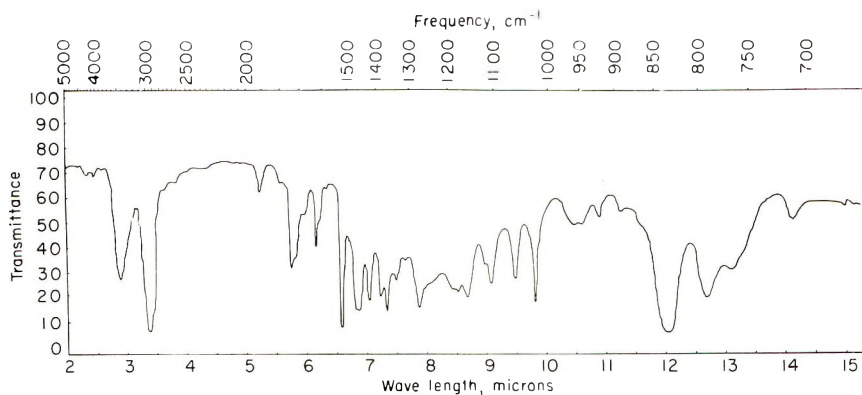


Fig. 1. Infrared spectrum of poly(*para*-isopropylstyrene)-ethyl methacrylate graft polymer.

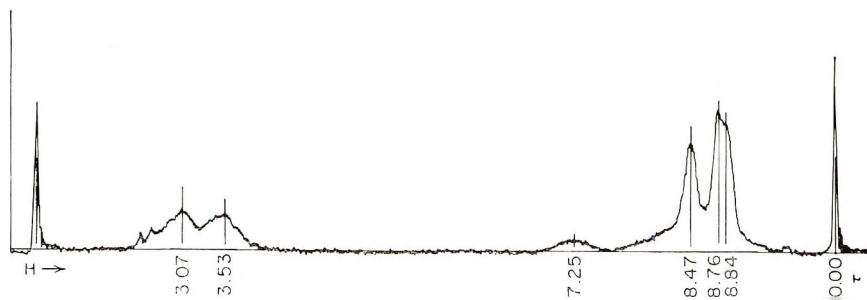


Fig. 2. NMR spectrum of poly(*para*-isopropylstyrene)-ethyl methacrylate graft polymer.

stretching frequency of a hydroperoxide and an alcohol. Therefore, the continuous formation and decomposition of hydroperoxide groups would account for the presence of the large absorption band at 2.9μ .

The fact that there are two types of groups containing oxygen present in the hydroperoxidized poly(*para*-isopropyl styrene) was recognized by Hahn and Lectenbohmer.¹¹ These authors distinguished between total oxygen and active oxygen where the active oxygen is hydroperoxide oxygen. Their hydroperoxidation experiments were run at 75°C . for 400 hr. The difference between active and total oxygen was attributed to hydroperoxide decomposition during the course of the oxidation reaction.

In the infrared spectrum of the graft copolymer, Figure 1, there are absorptions in the $5.71\text{--}5.75\mu$ region caused by the carbonyl group and also in the $7.75\text{--}8.75\mu$ region caused by $=\text{C}-\text{O}-\text{C}$ stretching. These regions are essentially blank in the poly(*para*-isopropyl styrene) backbone spectrum. Therefore, these absorptions are due to the presence of methacrylate. This is evidence for the formation of a graft copolymer.

The NMR spectrum of the graft copolymer is shown in Figure 2. The peak at the extreme right, 10.00τ , is due to the internal reference standard, TMS. The peak at the left-hand side of the spectrum is the TMS image. The spectrum of the graft is different from that of a mixture which is simply a superposition of the two homopolymer spectra.

One difference is that the quartet in the $5.78\text{--}6.11\tau$ region caused by the methylene protons of the ethyl methacrylate ester group does not appear. The possibility of ester hydrolysis during the grafting reaction was considered as a possible reason for the dis-

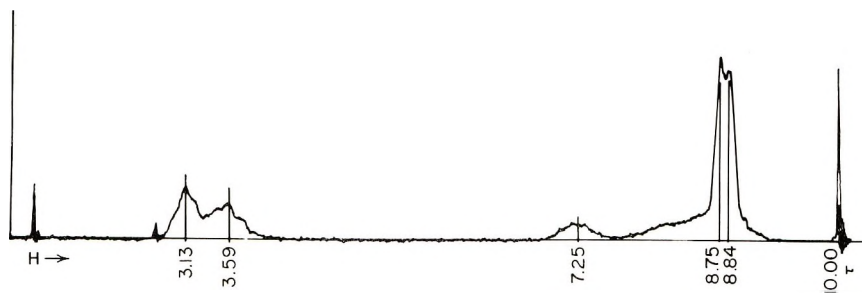


Fig. 3. NMR spectrum of poly(*para*-isopropylstyrene) homopolymer.

appearance of the methylene quartet. If this were the case, a carboxylic acid hydrogen should appear in the spectra. The peak for these protons is variable and sometimes occurs at negative τ values (e.g., the carboxylic proton of methacrylic acid monomer appears at $-1.57 \tau^{12}$). No peaks were observed in the graft copolymer spectra in the negative τ region. The carboxylic acid proton might be masked by appearing at the same τ value as some of the other protons. A good method for detecting such protons is to replace them, by exchange, with deuterium atoms. Deuterium does not absorb in this region. Therefore, if an exchangeable proton is present, the substitution of deuterium atoms causes the height of the original peak to diminish and it is sometimes possible to pick up the proton in HDO. There was no reduction in the intensity of any of the peaks. Also no new peaks appeared, even at negative τ values. This indicated that there was no detectable number of exchangeable protons in the graft copolymer, and thus no carboxylic acid groups.

The fact that there were no carboxylic acid groups was confirmed by titration of the graft dissolved in dimethylformamide. The neutralization equivalent was found to be zero.

The saponification equivalent was 1260. This corresponds to an approximate composition of 90% poly(*para*-isopropyl styrene) and 10% poly(ethyl methacrylate). This would seem to indicate that all of the ester groups are still in the polymer even though the peak in this region does not appear.

Additional evidence favoring the presence of the ester group is the presence of the ester group quartet in the spectrum of the extracted homopolymer. Since both the methacrylate in the graft and the homopolymer were subjected to the same reaction conditions, it is reasonable to assume that they would be affected in the same manner.

A possible way to bring out the ester group is to run the spectra at higher temperatures.¹³ As the temperature was raised, the ester group did begin to appear. However, at 130°C . the sample began to turn yellow, which indicated that the polymer was not stable at elevated temperature.

Another difference in the NMR spectrum of the graft copolymer is the peak at 8.47τ . This peak does not appear in the spectra of either of the homopolymers. Identification of this peak can be made by considering both NMR and infrared results. In the NMR spectrum of poly(*para*-isopropyl styrene), the methyl groups are located at 8.80τ (doublet). Evidence in support of this is obtained from the assignment for the methyl groups in *para*-cymene¹⁴ ($\tau = 8.78$) and cumene¹⁵ ($\tau = 8.75$).

The infrared spectrum of the graft indicates an OH band at 2.9μ probably resulting from hydroperoxide and alcohol structures as indicated above. Therefore, in some of the units along the polymer chain, oxygen atoms are attached to the same carbon atoms bonded to methyl groups. Since oxygen is more electronegative than hydrogen, it will tend to make these methyl protons appear at a lower field,¹⁶ (e.g., Tiers¹⁶ has reported that the methyl protons in cumene hydroperoxide appear at $\tau = 8.44$). In the graft copolymer spectrum, the intensity of the peaks in the 8.80τ region is reduced. Thus,

some of the methyl protons, now in the vicinity of oxygen, are probably responsible for the peak at 8.47 τ .

The position of the tertiary hydrogen atoms in the NMR spectrum of poly(*para*-isopropyl styrene) seems worthy of comment (Fig. 3). Previously Bovey et al.¹⁷ compared the τ -values of the tertiary hydrogen atoms in cumene and polystyrene. According to Bovey, these protons appear at approximately 7.2 τ in cumene but are shifted to higher field in polystyrene due to their spending more time on the average near the diamagnetic region of the benzene ring. In poly(*para*-isopropyl styrene), both types of tertiary protons are present, i.e., those in the isopropyl group as in cumene and those in the polymer chain as in polystyrene. The areas under the peaks indicate that the peak at 7.25 τ is due only to a single proton, most likely the tertiary proton of the isopropyl group, while the tertiary protons in the chain appear at higher field just as in the case of polystyrene. This is in agreement with Bovey's results. If the tertiary chain protons spend more time in the diamagnetic region, the tertiary isopropyl protons will spend more time away from this region. Therefore, they will appear at the normal position as in cumene.

Solution Properties

Table III summarizes viscosity, osmotic, and light scattering results for a whole backbone polymer, and a graft copolymer. The results in Table III show that, although \bar{M}_w of the graft shows the expected increase over the backbone polymer, \bar{M}_n is actually lower for the graft copolymer than for the backbone. Similar anomalous results have been reported by Smets and co-workers.^{18,19}

TABLE III
Solution Properties of Backbone and Graft Copolymers

	Backbone	Graft copolymer
\bar{M}_n	94,000	78,000
\bar{M}_w	382,000	870,000
$(\bar{S}^2)^{1/2}$	364	701
$A_2 \times 10^4$	6.85	3.15
$[\eta]$	0.36	0.46

Smets¹⁸ attributed his observation of a lower value for \bar{M}_n of the graft copolymer to degradation of the backbone polymer during the course of the grafting reaction. It is possible that such degradation has taken place during the preparation of the graft copolymer in this investigation. An attempt was made to study this by light scattering by finding a solvent that is isorefractive with the side chain of the graft. Benzene very closely met this condition. However, dn/dc for the graft copolymer was low enough so that the results were inconclusive. An attempt to carry out all of the reactions leading to the graft without adding ethyl methacrylate gave only crosslinked polymers.

Table III shows that the value of the radius of gyration, $(\bar{S}^2)^{1/2}$ for the graft copolymer is much larger than that of the backbone. The dimensions of the graft copolymer are higher than either poly(*para*-isopropyl styrene)²⁰ or poly(ethyl methacrylate)⁶ of comparable molecular weight. Stockmayer and co-workers²¹ have stated that the net effect of the interactions of the two species forming a copolymer will be repulsive, resulting in an expansion of the polymer coil, causing $(\bar{S}^2)^{1/2}$ to be larger. The value reported in Table III for the graft copolymer as well as the value for a similar graft copolymer reported by Matlack and co-workers⁵ show the radius of gyration of the graft copolymer to be greater than that of the homopolymer, consistent with the predictions of Stockmayer. Recently, Gallot and co-workers²² reported dimensions of a graft copolymer to be much closer to the dimensions of a homopolymer than those observed in this investigation. Since their work was with more homogeneous polymers, it appears reasonable to consider

dispersity as an important factor contributing to the larger difference in dimensions between the graft and homopolymer reported in Table III.

The second virial coefficient, A_2 , of the graft copolymer is approximately one-half that of the backbone polymer. According to polymer theory, A_2 should decrease with increasing molecular weight. The value of A_2 for linear poly(*para*-isopropyl styrene) having the same molecular weight as the graft, is approximately 6.9.²⁰ This value is still considerably higher than that of the graft. Since the graft polymer is a branched molecule, A_2 should be lower than that of a linear molecule. Thus the decrease in A_2 for the graft is as expected.

The higher intrinsic viscosity for the graft copolymer is also to be expected since \bar{M}_w is greater. The introduction of poly(ethyl methacrylate) into the molecule should also favor an increase in viscosity, since methyl ethyl ketone is a better solvent for this species than it is for poly(*para*-isopropyl styrene).

References

1. Casassa, E. F., *Unsolved Problems in Polymer Science*, National Academy of Sciences—National Research Council, Washington, D. C., 1962, p. 90.
2. Krause, S., *J. Phys. Chem.*, **68**, 1948 (1964).
3. Huggins, M. L., *J. Polymer Sci.*, **C4**, 445 (1963).
4. Ende, H. A., and V. Stannett, *J. Polymer Sci.*, **A2**, 4047 (1964).
5. Matlack, J. D., S. N. Chinai, R. A. Guzzi, and D. W. Levi, *J. Polymer Sci.*, **49**, 533 (1961).
6. Chinai, S. N., and R. J. Samuels, *J. Polymer Sci.*, **19**, 463 (1956).
7. Overman, R. T., and H. M. Clark, *Radioisotopic Techniques*, McGraw-Hill, New York, 1960.
8. Shreve, D., M. Heether, H. Knight, and D. Swern, *Anal. Chem.*, **23**, 282 (1951).
9. Philpotts, A., and W. Thain, *Anal. Chem.*, **24**, 638 (1952).
10. Tobolsky, A. V., and R. B. Mesrobian, *Organic Peroxides*, Interscience, New York, 1954, p. 90.
11. Hahn, W., and H. Lechtenbohmer, *Makromol. Chem.*, **16**, 50 (1955).
12. Bhacca, N. S., L. F. Johnson, and J. N. Shoolery, *Varian High Resolution Spectra Catalogue*, Varian Associates, Palo Alto, California, 1962 and 1963, Spectrum No. 62.
13. Bovey, F. A., private communication.
14. Varian Spectra Catalogue, *op. cit.*, Spectrum No. 268.
15. *Ibid*, Spectrum No. 240.
16. Tiers, G. V. D., *Characteristic Nuclear Magnetic Resonance (NMR) "Shielding Values" (Spectral Positions) for Hydrogen in Organic Structures*, Minnesota Mining and Manufacturing Co., St. Paul, Minnesota, 1958, p. 25.
17. Bovey, F. A., G. V. D. Tiers, and G. Filipovitch, *J. Polymer Sci.*, **38**, 73 (1959).
18. Smets, G., L. Convent, and X. Van der Borcht, *Makromol. Chem.*, **23**, 162 (1957).
19. Smets, G., and M. Claesen, *J. Polymer Sci.*, **8**, 289 (1952).
20. Holahan, F. S., Ph.D. Thesis, Stevens Institute of Technology, 1964.
21. Stockmayer, W. H., L. D. Moore, Jr., M. Fixman, and B. N. Epstein, *J. Polymer Sci.*, **22**, 527 (1956).
22. Gallot, Y., E. Franta, R. Rempp, and H. Benoit, *J. Polymer Sci.*, **C4**, 473 (1963).

F. S. HOLAHAN*

S. S. STIVALA

D. W. LEVI*

Department of Chemistry and Chemical Engineering
Stevens Institute of Technology
Hoboken, New Jersey

Received April 19, 1965

* Present address: Polymer Research Branch, Picatinny Arsenal, Dover, New Jersey.

ERRATUM**Dynamic Mechanical Properties of Poly(*n*-butyl Methacrylate)
near Its Glass Transition Temperature**

(*J. Polymer Sci.*, **A3**, 1785-1792, 1965)

By H. H. MEYER, P.-M. F. MANGIN, and JOHN D. FERRY
Department of Chemistry, University of Wisconsin, Madison, Wisconsin

On pages 1788 and 1790, the legends of Figures 3 and 6 should read as follows:

Fig. 3. Storage (J') and loss (J'') compliances reduced to 27°C. by shift factors calculated from eq. (1), pip up, measurements at 18.0°C.; successive 45° rotations clockwise correspond to 20.0, 22.0, 22.5, 25.0, 27.0, 28.5, 30.0, 31.5, and 33.0°C.; (---) data reduced from transducer measurements at higher temperatures⁵ on another sample of poly(*n*-butyl methacrylate).

Fig. 6. Storage compliance from data of Fig. 5, reduced to 27°C. and voluminal equilibrium by shift factors a_{T_i} calculated from free volume as described in text. Solid curve same as in Fig. 3; pip upper left, measurements, at 16.0°C.; successive 45° rotations clockwise correspond to 18.0, 20.0, 22.0, 22.5, and 25°C.